Postsynaptic molecular determinants of synapse specificity in the GABAergic neurotransmitter system

Dissertation

zur
Erlangung der naturwissenschaftlichen Doktorwürde
(Dr. sc. nat.)
vorgelegt der
Mathematisch-naturwissenschaftlichen Fakultät
der
Universität Zürich

von
Simon Früh

von
Neckertal, SG

Promotionskommission:
Prof. Dr. Jean-Marc Fritschy (Vorsitz)
Prof. Dr. Stephan Neuhauss
Prof. Dr. Peter Scheiffele

Zürich, 2016

ZUSAMMENFASSUNG

Die Direktionalität chemischer Synapsen sowie die Zelltyp-, Zelldomänen- und Neurotransmitter-spezifischen Innervierungsmuster neuronaler Netze im zentralen Nervensystem (ZNS) implizieren, dass Mechanismen existieren, die synaptische Spezifität gewährleisten. Die Erkenntnis, dass synaptische Proteine eine grosse molekulare Vielfalt aufweisen, hat zur Hypothese geführt, dass die Kombination synaptischer Proteine einen molekularen Code darstellt, der die Identität von Synapsen bestimmt. Diese Hypothese wurde in dieser Arbeit am Beispiel des GABAergen Neurotransmitter-Systems geprüft. Zwei synaptische Proteine, mit selektiv GABAerger und postsynaptischer Lokalisierung, wurden auf ihren Beitrag zur Spezifizierung GABAerger Synapsen in Bezug auf ihre präsynaptische Innervierung untersucht. Mittels Gen-Ablationsexperimenten in Mäusen wurde die Rolle des Dystrophin-Glykoprotein Komplexes (DGC) in der Bildung und im Unterhalt von Synapsen einer spezifischen Untergruppe GABAerger Interneuronen, der Cholecystokinin (CCK)-positiven Korbzellen, aufgedeckt. Der DGC hat folglich eine Funktion in der Spezifizierung von Synapsen innerhalb eines Neurotransmitter-Systems. Im Gegensatz dazu haben Ablations- und Überexpressionsexperimente des Dystrophin-Interaktionspartners synArfGEF in Primärneuronen gezeigt, dass dieses GABAerge postsynaptische Protein die Koordinierung von prä- und postsynaptischen GABAergen Strukturen kontrolliert. Somit trägt synArfGEF zur Spezifizierung von Synapsen zwischen Neurotransmitter-Systemen bei.

Durch die konditionelle Deletion des *Dag1* Gens, das für Dystroglycan (DG) kodiert, in Pyramidalzellen mittels der NEX-Cre-Linie, wurde die Ablation des neuronalen DGC erreicht. Dies hat die Untersuchung der Funktion des neuronalen DGC erlaubt, ohne begleitende Defizite in neuronaler Migration, die von der Beeinträchtigung der Funktion des DGC in Gliazellen ausgehen würde. Die immunhistochemische Analyse postsynaptischer GABAerger Proteine in Gewebe des Hippocampus und Neocortex von konditionellen knock-out (cKO)-Mäusen konnte nur geringe Abweichungen zu Kontrollmäusen nachweisen, weshalb eine obligatorische Rolle des DGC für die synaptische Aggregierung von Proteinen der postsynaptischen Dichte (PSD) ausgeschlossen werden konnte. Dieses Ergebnis steht schwerwiegenden Veränderungen der Immunoreaktivität präsynaptischer Markerproteinen gegenüber. DG-Ablation führte zum Verlust von immunhistochemischen Markern von Axonterminalen der CCK-positiven Korbzellen, aber nicht der Parvalbumin (PV)-positiven Korbzellen. Des Weiteren waren unspezifische Marker GABAerger Axonterminale nicht beeinträchtigt durch die Ablation von DG. Weil der spezifische Verlust der Epitope von CCK-positiven Axonterminalen nicht nur im Erwachsenenalter sondern auch in 21 Tage alten Mäusen beobachtet wurde, ist eine Funktion des DGC in der Bildung von Axonterminalen der CCK-positiven Korbzellen wahrscheinlich. Die Zufuhr von Cre mittels viralem Vektor in die Cornu ammonis 1 (CA1)-Region von Mäusen mit gefloxtem *Dag1* Gen ermöglichte die Ablation von DG im Erwachsenenalter. Der Verlust von DG lange nach dem entwicklungsbedingten ersten Schub der

Synaptogenese resultierte unerwarteterweise in einer Reduktion eines Axonterminal-Markers, der spezifisch ist für CCK-positive Korbzellen, was eine Funktion von DG in trans-synaptischer Signalübertragung nahelegt. Die physiologischen Konsequenzen des Verlustes der Axonterminale CCK-positiver Korbzellen wurden anhand von Patch-Clamp Messungen von spontanen inhibitorischen postsynaptischen Strömen (sIPSC) in DG-defizienten Pyramidalzellen untersucht. Eine Reduktion der sIPSC-Amplitude und -Frequenz deutete auf funktionelle Defizite in CCK-positiven Axonterminalen hin, was durch das Unvermögen von Carbachol, eine sIPSC-Frequenzerhöhung auszulösen, bestätigt wurde. Da DG an Neurexin bindet, abhängig von dessen alternativen Splice Inserts, wurde abschliessend die Erfordernis der Neurexinbindung für die Bildung der CCK-positiven Axonterminale anhand der Neurexin-bindungsunfähigen DG T190M Mutante geprüft. Die CCK-positiven Axonterminale waren nicht beeinträchtigt in DG T190M knock-in (KI) Mäusen, was nahelegt, dass ein neuartiger präsynaptischer DG Bindungspartner für die trans-synaptische Signalübertragung an CCK-positiven Axonterminalen verantwortlich ist. Insgesamt weisen diese Ergebnisse eine entscheidende Funktion des DGC in der Übertragung synaptischer Spezifität innerhalb des GABAergen Neurotransmitter-Systems nach und dienen als Ausgangspunkt für ätiologische Untersuchungen von Dystroglycanopathien mit geistiger Behinderung.

In einer Reihe von Zellkultur- und *in vitro*-Experimenten wurde die Rolle des GTP-Austauschfaktors (GEF) synArfGEF für die synaptische Spezifität analysiert. Obwohl synArfGEF ein Dystrophin-interagierendes Motiv enthält konnte eine Bindung an Gephyrin nachgewiesen werden, was auf eine allgemeinere Funktion im GABAergen System hindeutete. Deshalb wurde die Rolle von synArfGEF in der Koordinierung synaptischer Strukturen anhand von prä- und postsynaptischen Markern in Kulturen von hippocampalen Ratten-Primärneuronen untersucht. Ablation von synArfGEF mithilfe des Clustered Regularly Interspaced Short Palindromic Repeats (CRISPR) / Cas9-Systems führte zu einer Erhöhung des Anteils an Gephyrin-Clustern, die mit glutamatergen Axonterminalen fehlgepaart waren. Die spezifische Funktion von synArfGEF in fehlgepaarten GABAergen postsynaptischen Strukturen wurde bestätigt durch die Beobachtung dass die Gephyrin Cluster-Dichte insgesamt nicht durch die Ablation von synArfGEF beeinflusst wurde. Für eine genauere Betrachtung der Mechanismen, die dieser Regulierung zugrunde liegen, wurden synArfGEF-Konstrukte in Domänen mit bekannter Funktion mutiert und in primären hippocampalen Neuronen überexprimiert. Die Überexprimierung eines Konstrukts, das eine mutierte, für die GEF-Funktion wichtige, Sec7-Domäne enthielt, führte zu einer Erhöhung des Anteils an fehlgepaarten GABAergen PSD-Proteinen. Der Befund dass diese Mutante keinen Einfluss auf die Koordination des glutamatergen PSD-Proteins PSD-95 mit präsynaptischen Strukturen hatte, bestätigte, dass die Funktion von synArfGEF auf GABAerge PSD-Proteine beschränkt ist. Weil die Überexpression von Mutanten des potentiellen synArfGEF-Substrats Adenosyl-Ribosylierungs-Faktor 6 (Arf6) den Phänotyp der Sec7-Mutante widerspiegelte, könnte die Regulierung von fehlgepaarten GABAergen postsynaptischen Proteinen durch Arf6-Aktivierung vermittelt sein. Zudem deuteten die Bindung von Apocalmodulin an das IQ-

Motiv in synArfGEF, N-Methyl-D-Aspartat (NMDA)-verursachte Aggregierungsänderungen von dendritischem synArfGEF und die dendritische Lokalisierung von synArfGEF mRNA auf eine Abhängigkeit der Funktion von synArfGEF von neuronaler Aktivität hin. Diese Ergebnisse beschreiben insgesamt eine wichtige Funktion der katalytischen Aktivität von synArfGEF in der selektiven Regulierung von GABAergen postsynaptischen Proteinen, die mit glutamatergen präsynaptischen Strukturen fehlgepaart sind.

Zusammenfassend hat die Analyse zweier GABAerger PSD-Proteine mit selektiver Lokalisierung im ZNS gezeigt, dass postsynaptische Proteine an der Übertragung synaptischer Spezifität innerhalb von und zwischen Neurotransmitter-Systemen beteiligt sind. Die Ergebnisse dieser Arbeit legen eine funktionelle Beziehung zwischen der präsynaptischen Diversität und der postsynaptischen molekularen Vielfalt dar und tragen damit zur Hypothese eines molekularen Codes der synaptischen Spezifizierung bei.

ABSTRACT

The directionality of chemical synapses as well as the cell type-, subcellular domain- and neurotransmitter-specific innervation patterns of neuronal networks in the central nervous system (CNS) imply that mechanisms exist which ensure synapse specificity. The finding of a large molecular diversity of synaptic proteins gave rise to the hypothesis that the combination of synaptic proteins forms a molecular code, instructing the identity of synapses. This hypothesis was tested in this thesis at the example of the GABAergic neurotransmitter system. Two synaptic proteins, with selective GABAergic postsynaptic localization, were examined for their contribution to specification of GABAergic synapses in relation to their presynaptic innervation partners. Gene ablation experiments in mice revealed a role for the dystrophin-glycoprotein complex (DGC) in formation and maintenance of synapses from a specific subgroup of GABAergic interneurons, the cholecystokinin (CCK)-positive basket cells. Therefore, the DGC serves a function in synapse specification within the GABAergic neurotransmitter system. In contrast, ablation and overexpression experiments in primary neuron cultures, focusing on the dystrophin-interacting protein synArfGEF, demonstrated that this GABAergic postsynaptic protein controls pre- and postsynaptic alignment of GABAergic structures, thus regulating synaptic specificity between neurotransmitter systems.

Disruption of the neuronal DGC in mice was achieved by conditional deletion of *Dag1*, encoding dystroglycan (DG), in pyramidal cells using the NEX-Cre driver line. This allowed the study of the role of the DGC specifically in neurons, without interfering with glial DGC functions in neuronal migration. Immunohistochemical analysis of postsynaptic GABAergic proteins in DG conditional knock-out (cKO) hippocampal and neocortical tissue only identified minor alterations, excluding an obligatory role for the DGC in clustering of GABAergic postsynaptic density (PSD) proteins. This finding was contrasted by severe changes in immunoreactivity of presynaptic marker proteins. DG ablation led to the loss of immunohistochemical markers of axon terminals from CCK-positive but not from parvalbumin (PV)-positive basket cells. Furthermore, markers of GABAergic axon terminals not specific to a subgroup of GABAergic interneurons were not affected by DG ablation. The specific loss of CCK-positive terminal epitopes was observed in DG-deficient mice at postnatal day 21 as well as in adulthood, suggesting that formation of synapses of CCK-positive basket cells on pyramidal cells requires DG. Delivery of Cre to the cornu ammonis 1 (CA1) region of mice containing the floxed *Dag1* gene using a viral vector allowed ablation of DG during adulthood. Unexpectedly, loss of DG long after developmental synaptogenesis resulted in a reduction of a CCK-positive basket cell terminal marker, pointing towards a function of DG in continuous trans-synaptic signaling. The physiological consequences of CCK-positive basket cell terminal loss were assessed by patch-clamp recordings of spontaneous inhibitory postsynaptic currents (sIPSC) from DG-deficient pyramidal cells. The notion that loss of CCK-positive terminal markers was paralleled by functional deficits was suggested by a reduction of sIPSC amplitude and frequency and corroborated by the inefficiency of carbachol to

increase sIPSC frequency in DG cKO mice. Finally, since neurexin binds to DG in an alternative splice insert-dependent manner, knock-in (KI) mice containing the neurexin binding-deficient DG T190M were examined. CCK-positive terminals were not compromised in DG T190M KI mice, indicating that a novel presynaptic DG binding partner might be responsible for trans-synaptic signaling at CCK-positive basket cell terminals. Together, these findings demonstrate the crucial role of the DGC in conferring synaptic specificity within the GABAergic neurotransmitter system and provide a framework to explore the etiology of intellectual disability in dystroglycanopathy patients.

In a set of cell culture and *in vitro* experiments, the function of the guanine nucleotide exchange factor (GEF) synArfGEF in synapse specification was studied. Although synArfGEF contains a dystrophin-interacting motif, gephyrin was found to bind to synArfGEF, hinting at a more general function for the GABAergic system. Therefore, a role of synArfGEF in synaptic alignment was assessed by analysis of pre- and postsynaptic markers in rat primary hippocampal cultures. Clustered regularly interspaced short palindromic repeats (CRISPR) / Cas9-mediated ablation of synArfGEF uncovered that the fraction of gephyrin clusters mismatched to glutamatergic presynaptic axon terminals was increased in the absence of synArfGEF. Importantly, total gephyrin cluster density was not affected by synArfGEF ablation, demonstrating the specificity of synArfGEF function to mismatched GABAergic PSDs. To explore the mechanisms of this regulation, synArfGEF constructs were mutated in domains with known functions and overexpressed in primary hippocampal neurons. Overexpression of a construct containing a mutated Sec7 domain, essential for GEF function, led to an elevated proportion of mismatched GABAergic PSDs. The inability of this mutation to influence the presynaptic apposition of the glutamatergic PSD protein PSD-95 confirmed that synArfGEF function is restricted to GABAergic postsynaptic proteins. Because overexpression of mutations of the putative synArfGEF target ADP ribosylation factor 6 (Arf6) mirrored the Sec7 mutant phenotype, regulation of mismatched GABAergic PSDs might be mediated by Arf6 activation. In addition, the binding of apocalmodulin to the IQ motif in synArfGEF, changes in dendritic clustering of synArfGEF upon N-methyl-D-aspartate (NMDA) application and dendritically localized synArfGEF mRNA provided evidence of neuronal activity-dependence of synArfGEF function. Overall, these findings implicate the catalytic function of the GABAergic postsynaptic protein synArfGEF in the selective regulation of GABAergic PSDs mismatched to glutamatergic presynaptic terminals.

In conclusion, analysis of two GABAergic PSD proteins with selective distribution in the CNS revealed that postsynaptic proteins are involved in synapse specification within and between neurotransmitter systems. The findings of this thesis imply a functional relationship between the presynaptic diversity of innervation and the postsynaptic molecular heterogeneity, thereby providing evidence for a molecular code of synapse specification.

GENERAL INTRODUCTION

Synapses in the central nervous system

The nervous system enables animals to sense the environment and to appropriately react to it. For such interactions with the environment to be favored by natural selection, the fidelity and speed of information processing are of decisive importance. Noxious stimuli, for instance, have to be identified as harmful and avoidance behavior initiated rapidly. Some environments thus favor the development of a direct and fast connection between sensory and motor systems. However, adaptation to changing environments requires plasticity of the nervous system. This need drove the development of complex central nervous systems (CNS), containing central synaptic connections.

The requirement for fidelity and speed are seemingly best met by a syncytium, where sensory input and motor output are linked without being interrupted by intercellular connections. The existence of such a syncytium was posited by Camillo Golgi among others and became known as the reticular theory (Bock, 2013). However, visualization of individual neurons by Santiago Ramon y Cajal using the Golgi method later fortified the notion that the brain consists of interconnected individual cells (a notion that became the "neuron doctrine"). This first implied that synapses are abundant in the brain and that they are capable of mediating fast and precise communication between neurons. Indeed, an average neuron in the mouse neocortex forms several thousand synapses (Schuz and Palm, 1989).

The vast majority of CNS synapses are chemical synapses. Electrochemical gradients traveling along the plasma membrane have to be converted to chemical signals by the presynaptic terminal in order to transmit the signal to the postsynaptic cell. Pre- and postsynaptic structures are physically separated by the synaptic cleft, a narrow extracellular space filled with adhesion and signaling molecules. Under physiological conditions, a pool of neurotransmitter-containing synaptic vesicles is docked at the plasma membrane, allowing rapid release of neurotransmitters into the synaptic cleft. The process of neurotransmitter release is initiated by increasing intracellular calcium concentrations in response to an action potential, directly influencing the vesicle exocytosis machinery. Once released, neurotransmitters bind to specialized, mostly postsynaptic, receptors. The effect of this binding can be exerted on the postsynaptic cell directly, if the neurotransmitter receptor is an ion channel, by a change in ion permeability (ionotropic receptors). On the other hand, neurotransmitter receptors can act indirectly via activation of intracellular signaling pathways (e.g. metabotropic receptors). Finally, several mechanisms are employed to end neurotransmission, of which reuptake of the neurotransmitter into the presynaptic neuron or into surrounding glial cells is the most common.

Neurotransmission through chemical synapses thus relies on the coordinated action of a complex molecular machinery. Although this complexity leaves chemical synapses susceptible to dysfunctions, it provides several advantages over continuous intercellular connections. First, the nature of neurotransmitter release and receptor binding provides a clear directionality of neurotransmission

(even in reciprocal dendrodendritic synapses (Shepherd, 2009)). Secondly, the variety of neurotransmitter-receptor systems which can be employed offers a way to tune the kinetics with which postsynaptic membrane potential is impacted. Finally, the pre- and postsynaptic structures involved in chemical neurotransmission are amenable to molecular modifications, allowing neuronal activity-dependent and other plasticity mechanisms to change synaptic strength and properties.

Besides the directional neurotransmission of chemical synapses, which functions in an all-or-none fashion, the brain is capable of electrical neurotransmission between cells over gap junctions (Pereda, 2014). In these electrical synapses, transmembrane ion channels of the connexin family form a direct connection between neurons. Small molecules and ions (for example Ca^{2+} or cyclic AMP) are capable of diffusing through connexin channels, effectively building a partial syncytium between neurons connected by gap junctions. Still, neurotransmission at electrical synapses is not purely passive, since connexin channels can take open or closed conformations and are subject to molecular modifications. A change in membrane potential in one cell thus does not imply that a cell connected by gap junctions necessarily undergoes the same potential changes. However, if electrical synapses allow electrical conductance, such neurotransmission is bidirectional. Evidence has accumulated that electrical synapses, similar to chemical synapses, are dynamic. The connexin hemichannels are subject to endo- and exocytosis and their properties are under the control of neuromodulators. Furthermore, neuronal activity (at chemical synapses) can also induce plasticity at electrical synapses (Haas et al., 2016). Electrical synapses are likely to play a crucial role in coordinated network activity. For instance, parvalbumin (PV)-positive GABAergic interneurons in hippocampus and neocortex are interconnected via gap junctions (Katsumaru et al., 1988; Fukuda and Kosaka, 2000; Fukuda et al., 2006). Since the activity of PV-positive interneurons is coupled to, and in some brain regions crucial for, network oscillations, electrical synapses might coordinate firing properties between PV-positive interneurons in this process.

Challenging the absolute validity of the neuron doctrine, clonally related pyramidal cells in the neocortex transiently form electrical synapses between them (Yu et al., 2012). Formation of electrical synapses is necessary for later preferential chemical synapse formation between related cells. The importance for electrical neurotransmission for chemical synapse formation is also demonstrated by reduced chemical neurotransmission in mice lacking connexin 36 (Maher et al., 2009). Transient electrical coupling of clonally related pyramidal cells therefore determines the assembly of neocortical neuronal circuits. Electrical and chemical synapses are also interconnected in mature neurons. In "mixed synapses", electrical and chemical synaptic structures are in close proximity, influencing each other's properties. The strength of electrical synapses was shown to be modulated by activation of N-methyl-D-aspartate (NMDA) receptors in mixed glutamatergic / electrical synapses (Yang et al., 1990; Kothmann et al., 2012). Electrical and chemical synapses are thus interdependent during development and for plasticity in adulthood.

The abundance of glial cells in the brain highlights that the local environment of CNS synapses has to be considered in order to appreciate their complexity (Azevedo et al., 2009). Central synapses are exposed to the extracellular matrix (ECM) and perisynaptic astrocyte processes. These structures heavily impact the kinetics of neurotransmitter action. Astrocytes express a large variety of neurotransmitter transporters, which remove neurotransmitter molecules from the synaptic cleft. More indirectly, astrocytes influence neurotransmission by providing essential metabolites to neurons. Furthermore, the involvement of astrocytes and microglia in synapse elimination shows how intimately these cells are connected to synaptic plasticity and points towards a prominent role of glial cells in the pathological loss of synapses (Chung et al., 2013; Hong et al., 2016).

Neurotransmitter systems and their receptors

Even before the ultrastructural confirmation of physically separated contacts at chemical synapses, the molecular identity of some substances mediating neurotransmission in the peripheral nervous system (PNS) was elucidated. The relative ease of manipulation of peripheral nerves allowed the identification of epinephrine and acetylcholine as neurotransmitters, although the molecular mechanisms of their actions were still obscure (Elliott, 1905; Loewi, 1924). In the CNS, the search for neurotransmitters was advanced by experiments involving direct application of substances to the CNS and then probing the consequences for neurotransmission. In this manner, glutamate was identified as the main excitatory neurotransmitter in the brain. At present, several dozens of neurotransmitters are known, the exact number depending on the definition of neurotransmitters (Purves, 2012).

Since modulation of neurotransmission upon application of a substance is not conclusive evidence that a substance acts as a neurotransmitter, several criteria to classify a substance as a neurotransmitter were compiled (Cowan and Kandel, 2001). No binding definition has been agreed on, but the following criteria are generally accepted as the minimal requirements for classification as a neurotransmitter:

1. The substance is present in the presynaptic terminal and is released upon neuronal activity
2. The substance binds to postsynaptic receptors, affecting electrical and / or physiological properties of the postsynaptic cell
3. There exists a mechanism to degrade the substance or to remove the substance from the synaptic cleft, ending its action on the postsynaptic cell

Neurotransmitters are chemically heterogeneous and cover a wide range of molecular weights. For instance, amino acids, peptides, monoamines, adenosine triphosphate, nitric oxide and even protons are capable of acting as neurotransmitters (Du et al., 2014). Generally, a distinction between small-molecule neurotransmitters and peptide neurotransmitters (neuropeptides) is made. Neuropeptides have a slow, neuromodulatory effect on the postsynaptic cell and are released from large dense-core

synaptic vesicles (as opposed to small clear-core vesicles employed by most small-molecule neurotransmitters). Fast neurotransmission in the CNS is mediated by small-molecule neurotransmitters. Among them, most chemical synapses rely on neurotransmitters from the amino acid or the biogenic amine family. Catecholamines (dopamine, norepinephrine and epinephrine) are biogenic amine neurotransmitters which share tyrosine as the substrate for their biosynthesis. The two other biogenic amine neurotransmitters, serotonin (5-hydroxytryptamine) and histamine, depend on tryptophan and histidine for synthesis, respectively. The action of biogenic amine neurotransmitters on postsynaptic neurons is determined by specific, mostly metabotropic, receptors and can be excitatory as well as inhibitory.

Acetylcholine, although neither belonging to the group of amino acids or biogenic amines, is a small-molecule neurotransmitter essential for function of the PNS as well as the CNS. Named after the respective agonists, acetylcholine receptors are divided into two groups. The nicotinic acetylcholine receptors (nAChR) are ion channels permeable to Na^+ and K^+, therefore depolarizing the postsynaptic cell. Because nAChRs are responsible for the depolarization and therefore the contraction of muscle cells, they are among the best studied neurotransmitter receptors. However, nAChR-mediated neurotransmission also serves crucial roles in the autonomous nervous system and in the CNS. In contrast to nAChRs, muscarinic acetylcholine receptors (mAChR) are metabotropic receptors. Depending on the intracellular signaling cascade which is activated, acetylcholine binding to mAChRs can have excitatory or inhibitory effects on the postsynaptic cell. Besides their function in parasympathetic neurotransmission, mAChRs are also expressed in the CNS.

Four amino acids are known to act as neurotransmitters: Glutamate, aspartate, γ-aminobutyric acid (GABA) and glycine. In the mature mammalian brain, glutamate and GABA mediate the bulk of excitatory and inhibitory neurotransmission, respectively. As a nonessential amino acid, glutamate is metabolized from α-ketoglutarate, a product of the citric acid cycle. In addition, glutamine can be converted to glutamate, a reaction catalyzed by glutaminase. Although glutamate is abundant intracellularly, glutamate concentrations are kept low in the synaptic cleft through continual removal of glutamate by high-affinity excitatory amino acid transporters. It is estimated that glutamate concentrations in the synaptic cleft fluctuate from micro- to low millimolar concentrations during vesicular release (Clements et al., 1992). Glutamic acid decarboxylase (GAD) catalyzes the conversion of glutamate to GABA. Thus, the main excitatory and inhibitory neurotransmitters are only separated by a single catalytic step. Accordingly, GAD is localized almost exclusively at GABAergic axon terminals. Packing of glutamate and GABA into synaptic vesicles requires specific transporter proteins located on synaptic vesicles. Vesicular GABA transporter (VGAT) mediates active transport of GABA whereas glutamate accumulation in vesicles depends on vesicular glutamate transporters (VGluT).

Glutamate exerts its actions on postsynaptic cells by acting as a ligand for specific ionotropic and metabotropic receptors. α-Amino-3-hydroxy-5-methyl-4-isoxazolepropionic acid (AMPA) receptors

are the most abundant glutamate receptors in the CNS and together with kainate receptors are responsible for most fast excitatory neurotransmission. Ionotropic glutamatergic neurotransmission is also mediated by NMDA receptors, albeit with slower kinetics. Activation of NMDA receptors plays a crucial role in plasticity of glutamatergic synapses (Luscher and Malenka, 2012). The G-protein coupled metabotropic glutamate transporters (mGluR) are also involved in plasticity of the postsynaptic response to glutamate, in particular in long-term depression (LTD). In addition, a subset of mGluRs is localized presynaptically and modulates transmitter release. As in glutamatergic transmission, GABA acts as a ligand for both ionotropic and metabotropic receptors, which were named $GABA_A$ and $GABA_B$ receptors, respectively. Apart from the molecular mode of action, $GABA_A$ and $GABA_B$ receptors differ largely in kinetics of the postsynaptic potentials that they elicit. While activation of $GABA_B$ receptors produces slow and long-lasting inhibition, $GABA_A$ receptors mediate the vast majority of fast inhibitory neurotransmission in the adult mammalian brain (Hammond, 2008).

Molecular heterogeneity of the GABAergic postsynaptic density

$GABA_A$ receptors

$GABA_A$ receptors ($GABA_AR$) are pentameric GABA-gated anion channels. All of the individual subunits are members of the Cys-loop ligand-gated ion channel superfamily and as such are closely related to nAChRs, glycine receptors (GlyR) and ionotropic serotonin receptors. Based on sequence homology and pharmacological characterization, a total of 19 genes encoding $GABA_AR$ subunits were identified in mammals (Figure 1; (Olsen and Sieghart, 2008)).

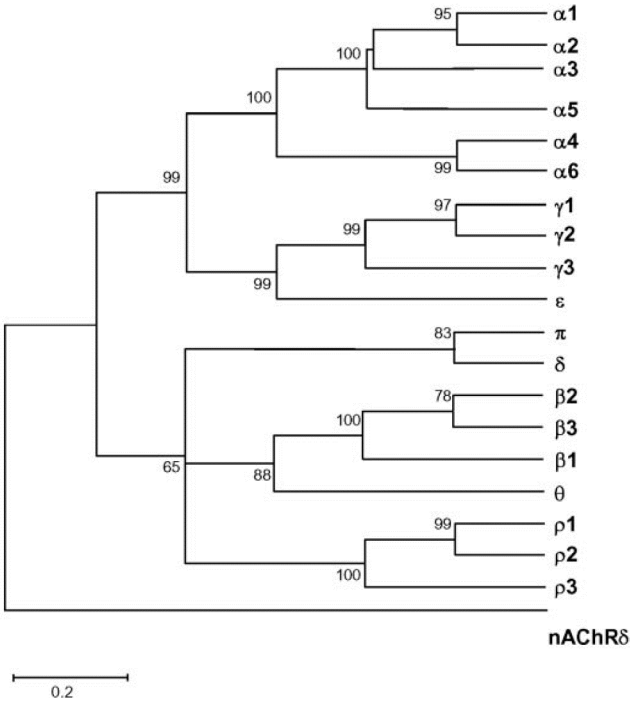

Figure 1. Dendrogram of the 19 human $GABA_AR$ subunit genes.
The length of horizontal branches represents the fractional divergence of any two $GABA_AR$ subunit amino acid sequences. To illustrate the close homology to nAChRs, the δ subunit of nAChRs was included. The scale bar represents 20% sequence divergence (Simon et al., 2004).

All subunits display a common secondary structure with an N-terminal extracellular tail including the eponymous Cys-loop, four transmembrane domains and an extracellular C-terminus (Figure 2). Also characteristic of $GABA_A$Rs, a large intracellular loop between transmembrane domain 3 and 4 is present in all subunits. Theoretically, thousands of $GABA_A$R combinations are possible by permutation of the 19 subunits in a pentameric receptor. However, the number of functional $GABA_A$R compositions is much lower, as suggested by experiments in heterologous cells overexpressing different subunit combinations. These experiments, together with biochemical and morphological studies, have revealed that the most abundant receptor composition in the forebrain consists of two α, two β and one γ subunit. In most synaptic $GABA_A$Rs in the forebrain the β2 and γ2 subunits are combined with the α1 subunit, but receptors containing α2 are also widespread, especially in the hippocampal formation (Fritschy and Panzanelli, 2014). Besides that, sufficient evidence has accumulated for the existence of several other subunit combinations, notably receptors containing α3-6 with β and γ subunits and receptors containing a δ subunit instead of the γ subunit. Major distinctions between $GABA_A$R combinations include kinetics, pharmacological properties and expression patterns. In addition, individual subunits have a major influence on subcellular localization of the receptor. β / γ -combinations together with the α5 subunit results in widespread extrasynaptic distribution whereas α1 and α2-containing receptors are clustered at GABAergic synapses (Serwanski et al., 2006; Kasugai et al., 2010). Similarly, α4 and the closely related α6 subunit can associate with either a single δ or γ2 subunit and are mostly present extrasynaptically. The existence of heterogeneous α or β subunit combinations in a single receptor was demonstrated (Li and De Blas, 1997; Benke et al., 2004; Balic et al., 2009). Furthermore, receptors containing ε, θ and π subunits were reported but these subunits show a limited distribution in the brain. ρ subunits (formerly $GABA_C$ receptors) are pharmacologically distinct from all other subunits and are thought to build homopentamers. Although association with other subunits cannot be excluded, their distinct pharmacological properties make an assembly with α or β subunits unlikely. Thus, among the 19 different subunit genes, the α to δ subunits make up most of the $GABA_A$R repertoire available to mediate GABA-induced fast inhibition in the brain.

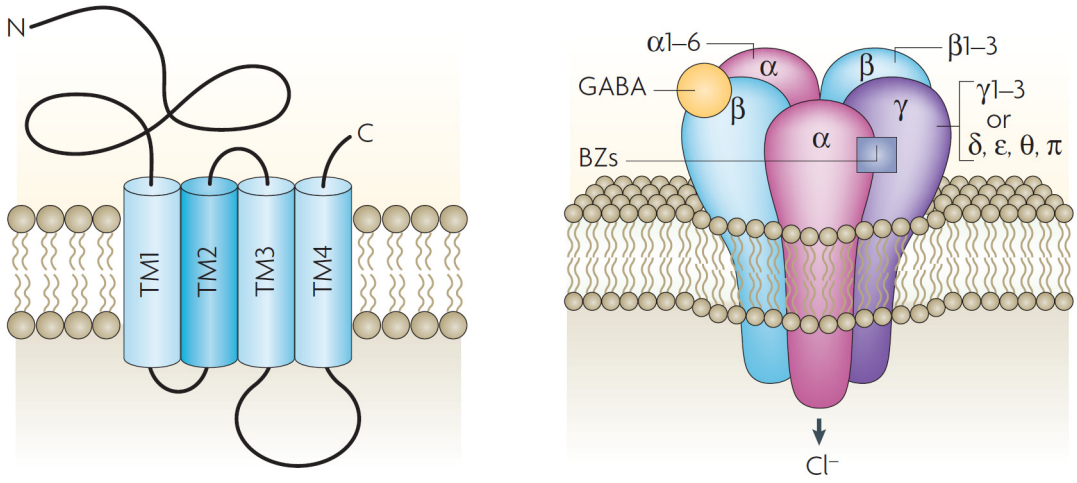

Figure 2. Domain structure and heteropentamerization of $GABA_AR$ subunits.
$GABA_AR$ subunits possess a characteristic domain structure containing four transmembrane domains, a large intracellular loop between transmembrane domains 3 and 4, and a large N-terminal region containing the Cys-loop (left). Functional receptors are pentameric, most commonly formed by two α, two β and one γ subunit (right). GABA binds at the interface of α and β subunits whereas benzodiazepines bind at the interface of α and γ subunits. BZ, benzodiazepines; TM, transmembrane domain (Jacob et al., 2008).

Heteropentameric $GABA_ARs$ possess two GABA binding sites, both at the interface between the α and β subunit. Binding of GABA induces a conformational change in the receptor, leading to the opening of the central pore. $GABA_ARs$ are selective anion channels with the highest permeability for Cl^- ions. Besides Cl^-, $GABA_ARs$ are known to be permeable to $HCO3^-$ ions, but the physiological importance of this conduction is unclear. The consequences of channel opening are primarily determined by the intra- and extracellular concentrations of Cl^-. Specific Cl^- co-transporters that mediate Cl^- influx (NKCC1) and efflux (KCC2) play a central role in controlling these concentrations. Since there is a developmental delay in KCC2 expression, intracellular Cl^- concentrations are high early in development. $GABA_AR$ activation during embryogenesis and around birth therefore leads to strong depolarization of the postsynaptic cell, exceeding the action potential threshold. Only in the adult CNS, when KCC2 expression surpasses NKCC1 expression, can an increase in Cl^- permeability cause hyperpolarization and therefore inhibition of the postsynaptic cell (Fiumelli and Woodin, 2007). $GABA_AR$ channel opening can also have an inhibitory effect by depolarization, if the Cl^- equilibrium potential is below the action potential threshold ("shunting inhibition"). Furthermore, because of local differences in subcellular KCC2 distribution, the impact of $GABA_AR$ activation is likely to be different in distinct subcellular compartments.

$GABA_ARs$ are the target of many drugs of pharmaceutical importance. Benzodiazepines, for instance, bind $GABA_ARs$ at the interface of α and γ subunits (Figure 2; (Rudolph and Knoflach, 2011)). Through allosteric modulation of the receptor, benzodiazepines increase the efficiency of GABA in activating $GABA_ARs$. The maximal response generated by GABA is not elevated by benzodiazepines,

reducing the danger of overdose substantially. Because of the anti-convulsive, anxiolytic, sedative and myorelaxant properties of benzodiazepines, their interaction with $GABA_AR$ subunits was studied extensively. In the study of the contribution of different $GABA_ARs$ to the clinical effects, the development of individual $GABA_AR$ subunit knock-out (KO) and knock-in (KI) mice was instrumental. The change of a single histidine residue in any α subunit is sufficient to abolish the effects of diazepam. Application of diazepam in KI mice containing histidine to arginine point mutations revealed a prominent role for α1 subunit-containing receptors for sedation (Rudolph et al., 1999; McKernan et al., 2000). Conversely, α2-containing receptors were shown to be necessary for the anxiolytic effects of diazepam (Low et al., 2000). KI mice harboring the homologous mutation in α3 or α5 subunits were also generated and revealed specific roles in myorelaxation (Crestani et al., 2001; Crestani et al., 2002). In addition, benzodiazepines can act as analgesics and anti-hyperalgesics, and experiments with triple KI mice demonstrated that these effects are mostly mediated by the α2 subunit (Ralvenius et al., 2015). These specific involvements in diazepam action exemplify the crucial importance of $GABA_AR$ heterogeneity for neuropharmacological studies but also for the physiological role of GABAergic neurotransmission.

In addition to subunit diversity, trafficking and post-translational modification (PTM) of $GABA_ARs$ add another layer of complexity by providing a dynamic regulation of GABAergic neurotransmission. The assembly of receptor subunits in the endoplasmic reticulum (ER) determines subunit composition of native receptors at the plasma membrane (Luscher et al., 2011). α / β / γ combinations have an obligatory directional arrangement regarding the positioning of the α to the γ subunit. Receptors exhibiting a different arrangement are degraded in the ER-associated protein degradation pathway. Expression of subunit combinations in heterologous cells demonstrated that, in contrast to α and β subunits, the γ subunit is not essential for the formation of functional receptors. However, assembly with the γ subunit is favored and necessary for synaptic targeting of $GABA_ARs$. Many of the subunit-specific modifications, which convey their distinct properties, target the large intracellular loop between transmembrane domains 3 and 4. The Golgi-specific DHHC zinc finger protein (GODZ) interacts specifically with γ2 intracellular loop and catalyzes palmitoylation of the γ2 subunit. This palmitoylation is essential for synaptic targeting of the receptor, as demonstrated by the loss of synaptic $GABA_ARs$ when GODZ is downregulated (Fang et al., 2006). As other transmembrane proteins, $GABA_ARs$ travel through the Golgi apparatus and are then present in secretory vesicles which are exocytosed. Integration into the plasma membrane is also controlled by interaction at the intracellular loop, by multiple proteins. $GABA_AR$-associated protein (GABARAP) was the first $GABA_AR$-interacting protein identified. Culture experiments provided evidence that GABARAP is involved in exocytosis of $GABA_ARs$ in response to potentiation of glutamatergic synapses (Marsden et al., 2007). However, the role of GABARAP and specificity in constitutive $GABA_AR$ trafficking is unclear, since GABARAP KO mice show normally clustered γ2 immunolabeling (O'Sullivan et al., 2005). The fact that GABARAP is not solely responsible for regulating $GABA_AR$ trafficking is

underlined by the finding of multiple GABARAP-interacting proteins which are involved in $GABA_AR$ exocytosis. These include the phospholipase C-related catalytically inactive proteins 1 and 2 (PRIP1/2). PRIP1/2 double KO mice exhibit a reduction in surface $GABA_AR$ abundance and in GABARAP interaction with $GABA_ARs$, indicating that PRIP and GABARAP form a complex to regulate receptor trafficking (Mizokami et al., 2007). $GABA_ARs$ in perisynaptic regions undergo endocytosis, a process which is also subject to activity-dependent regulation. Receptor endocytosis is clathrin-dependent and involves binding of the adaptor protein 2 (AP2) to β and γ subunits. AP2 binding is modulated by phosphorylation of serine residues in β1-3 subunits. Phosphorylation status of these residues, in turn, is controlled by protein kinase C (PKC), protein kinase A (PKA) and the protein phosphatases PP1α and PP2A. Interestingly, PRIP1/2 interact with these phosphatases and modulate their activity. Regulation of PP1α/PP2A through PRIP1/2 can thus lead to dephosphorylation of serine residues in β1-3, thereby facilitating their internalization. A substantial part of endosomes containing $GABA_ARs$ is exocytosed and therefore contributes to receptor recycling. However, $GABA_ARs$ can be degraded if the containing endosomes enter the lysosomal pathway. Receptor trafficking is both a constitutive process and a mechanism used to adjust synaptic strength through homeostatic plasticity. Excessive internalization of $GABA_ARs$ in response to flurazepam treatment was reported in cultured hippocampal neurons and is thought to represent one of the mechanisms underlying tolerance to benzodiazepines (Jacob et al., 2012).

Gephyrin

For proper GABAergic transmission, $GABA_ARs$ have to be concentrated opposite GABAergic axon terminals. Mechanisms to adapt this clustering on a short time-scale allow short-term plasticity of the strength of GABAergic transmission. The scaffolding protein gephyrin clusters $GABA_ARs$ at synaptic sites and provides a platform for fast regulation of the GABAergic postsynaptic density (PSD).

The capability of self-assembly is a feature of gephyrin that allows the formation of a lattice below synaptic $GABA_ARs$ (Tyagarajan and Fritschy, 2014). $GABA_ARs$ are trapped at synaptic sites by this lattice, making the gephyrin scaffold an important determinant of synaptic strength. Although most studies have focused on the clustered form of gephyrin (in association with receptors), gephyrin is present also in the cytosol (Specht et al., 2013). It is the dynamics of the equilibrium between the soluble and clustered form of gephyrin which determines the extent to which gephyrin acts as a scaffold for $GABA_ARs$.

Gephyrin was first isolated in conjunction with GlyRs from rat spinal cord (Pfeiffer et al., 1982). Binding of gephyrin to GlyRs occurs with nanomolar affinity, explaining the enrichment for gephyrin with purification of GlyRs (Schrader et al., 2004). Localization of gephyrin and receptors in the CNS by immunohistochemistry revealed that gephyrin is not only colocalized with glycine receptors but also with $GABA_ARs$ (Sassoe-Pognetto et al., 1995; Sassoe-Pognetto et al., 2000). As expected from sequence homology of GlyRs and $GABA_ARs$, gephyrin binds to $GABA_ARs$, albeit with lower affinity

(Maric et al., 2011). In addition, gephyrin interacts with tubulin, and thus connects the receptors to the cytoskeleton (Kirsch et al., 1991). Binding to β2 and β3 subunits was described, but the functional involvement of these interactions for gephyrin clustering is unclear (Kowalczyk et al., 2013). A direct binding to α2 subunit was mapped to the large intracellular loop between transmembrane domains 3 and 4 (Saiepour et al., 2010). The drastic reduction of gephyrin clusters in brains of $GABA_AR$ α2 subunit KO mice, despite compensatory upregulation of other subunits and intact clustering of other synaptic proteins, indicates and outstanding importance of α2 interaction for gephyrin synaptic clustering (Panzanelli et al., 2011).

Gephyrin consists of three domains: The N-terminal G domain, the C-terminal E domain and an intermediate C domain. The names of the G and E domains were derived from homology to the bacterial enzymes MogA and MoeA, respectively. These enzymes are essential for biosynthesis of molybdenum cofactor and gephyrin has retained this function. It is therefore not surprising that gephyrin expression in mammals is widespread throughout the body. Despite its crucial metabolic function, gephyrin has acquired novel features through the fusion of individual proteins during its evolutionary history. The quaternary structure of gephyrin homomultimers is still not fully elucidated. However, gephyrin G domain was shown to form trimers whereas the E domain assembles preferentially as dimers (Schwarz et al., 2001; Sola et al., 2001; Sola et al., 2004). Based on these interactions gephyrin was proposed to form a hexagonal lattice but the three-dimensional arrangement of gephyrin clusters is likely more complex and dynamic, involving interactions of the C-domain (Herweg and Schwarz, 2012). Gephyrin exists as multiple splice variants, some of which affect the capability of multimerization (Saiyed et al., 2007; Fritschy et al., 2008). In addition, gephyrin undergoes a large variety of PTMs. Many of these modifications control the propensity of gephyrin to self-assemble and thereby indirectly regulate $GABA_AR$ synaptic clustering and GABAergic transmission.

Most PTM target residues within gephyrin are located in the C domain. A large variety of PTMs were identified thus far: Gephyrin can be phosphorylated, acetylated, nitrosylated, ubiquitinated and SUMOylated (Tyagarajan and Fritschy, 2014). Although the exact conformational changes induced by PTMs are not understood in most cases, the consequences of PTM on gephyrin clustering are well described. For the serine residues 268, 270, 303 and 305 (all part of the C domain), the phosphorylating kinases as well as the downstream effectors and the impact on GABAergic neurotransmission were elucidated (Figure 3). The dephosphorylation-mimicking S268A mutant forms larger and more numerous clusters than wildtype gephyrin in primary hippocampal neurons (Tyagarajan et al., 2013). A corresponding increase in miniature inhibitory postsynaptic current (mIPSC) amplitude and frequency was observed in S268A-expressing neurons. Extracellular signal-regulated kinase 1 (ERK1) can phosphorylate gephyrin S268 and application of an ERK inhibitor recapitulated the morphological changes seen in S268A-expressing cells. Since the increase in gephyrin cluster size upon ERK inhibitor treatment was dependent on S268, ERK1 phosphorylation at

this site is likely to play a physiological role for modulating gephyrin cluster size. ERK1 activity, in turn, is regulated by neuronal activity, implicating this pathway in activity-dependent plasticity of GABAergic synapses. Interestingly, site-directed mutagenesis of the neighboring S270 revealed that phosphorylation state of this residue also plays a role in controlling gephyrin clustering (Tyagarajan et al., 2011). Compared to wildtype, S270A-mutated gephyrin overexpressed in primary hippocampal neurons shows primarily an elevated cluster density. This phenotype is obtained also by inhibition of glycogen synthase kinase 3β (GSK3β) in neurons overexpressing wildtype gephyrin. In gephyrin S270A-overexpressing neurons, however, application of GSK3β inhibitor does not affect cluster density. GSK3β, but not ERK1, can phosphorylate S270, and thus the phosphorylation state of the two nearby serine residues is controlled by two different pathways. Phosphorylation of S270 makes gephyrin prone to proteolytic cleavage by calpain. Yet, gephyrin is likely to be phosphorylated at S268 and S270 under basal conditions, and the phosphorylation state at both residues interacts to determine gephyrin cluster properties (Tyagarajan et al., 2013). The gephyrin monoclonal antibody 7a (mAb7a), which is most commonly used for immunofluorescent localization of gephyrin, requires phosphorylation at S270 for recognition of the epitope (Kuhse et al., 2012). This observation supports the notion that a large portion of clustered gephyrin is phosphorylated at this site and raises the concern of underrepresentation of non-phosphorylated gephyrin in immunofluorescence studies. Gephyrin residues S303 and S305 build another pair of serine phosphorylation sites which are under the control of an activity-dependent kinase (Flores et al., 2015). The homeostatic upregulation of inhibitory synapses in response to increased neuronal activity was shown to require Ca^{2+}/calmodulin-dependent protein kinase II (CaMKII), which phosphorylates S305. Serine to alanine mutation of both sites abolished the increase of gephyrin clustering normally seen after artificially stimulating neurons. These studies illustrate how the strength of GABAergic neurotransmission is regulated in response to neuronal activity by modifying single residues within the gephyrin C domain.

A multitude of gephyrin-interacting proteins have been identified. Intriguingly, most interactions were located to the C domain, the most heavily phosphorylated region in gephyrin (Tyagarajan and Fritschy, 2014). It is therefore likely that regulatory pathways converging on gephyrin not only modulate gephyrin conformation and self-assembly, but also influence its interactions with binding partners.

Other GABAergic postsynaptic density proteins

In the study of submembrane clustering mechanisms of gephyrin, collybistin has emerged as an essential protein promoting gephyrin clustering. When expressed in human embryonic kidney 293 (HEK293) cells, collybistin lacking its N-terminal Src homology 3 (SH3) domain induces gephyrin clustering near the plasma membrane (Kins et al., 2000; Harvey et al., 2004). In contrast, collybistin isoforms containing the SH3 domain localize together with gephyrin in large intracellular aggregates. The SH3 domain, assumed to exert an autoinhibitory effect on collybistin function, was shown to bind

to the intracellular region of neuroligin 2 (NL2) (Poulopoulos et al., 2009). Collybistin, NL2 and gephyrin co-expression in HEK293 cells leads to submembrane gephyrin clustering even with the SH3 domain present in collybistin. It was therefore proposed that collybistin binding to NL2 is an essential step in formation of the GABAergic PSD. Collybistin KO mice display a strong reduction of gephyrin as well as $GABA_AR$ clustering in major forebrain regions, confirming the essential role in gephyrin synaptic assembly (Papadopoulos et al., 2007; Papadopoulos et al., 2008). Because of the existence of several splice isoforms in the rat, either containing or lacking the SH3 domain and exhibiting variable C-termini, it is conceivable that collybistin differentially contributes to gephyrin clustering in different brain areas or subcellular compartments. Co-expression of collybistin isoforms with gephyrin in cultured neurons suggested that different isoforms promote gephyrin clustering to a similar degree (Korber et al., 2012). However, site-directed mutagenesis of the C-terminal region revealed that collybistin splice isoforms differ in ubiquitination sites, leading to distinct protein stabilities (De Groot-Ebeling, 2014). Furthermore, collybistin isoforms have different developmental expression patterns. Thus, it seems likely that collybistin isoforms take different functional roles and thereby provide another layer of complexity in regulation of the GABAergic PSD.

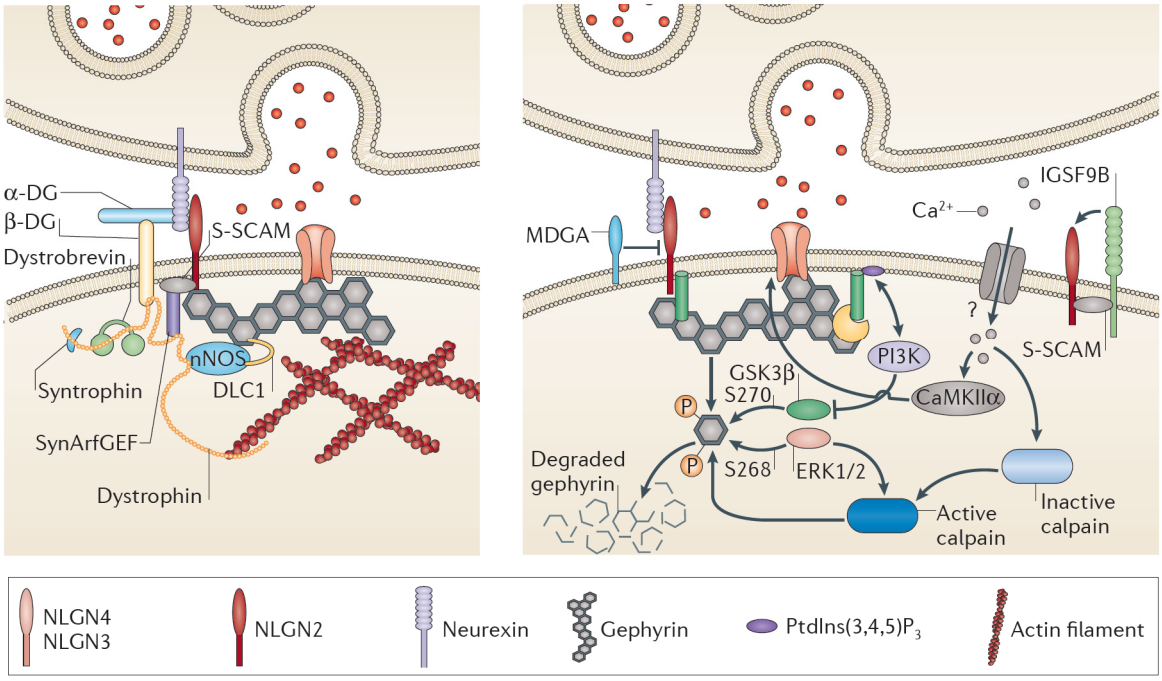

Figure 3. Schematic overview of the GABAergic PSD.
Protein interactions with the DGC, which is selectively localized in perisomatic regions in pyramidal cells, are depicted (left). The putative trans-synaptic interaction of α-DG with neurexin is illustrated. SynArfGEF is shown to interact with dystrophin and with S-SCAM, which in turn binds to NL2 and to β-DG. Various signaling pathways were found to act on gephyrin PTM, thereby regulating the strength of GABAergic neurotransmission (right). Gephyrin phosphorylation by the kinases GSK3β and ERK1/2 and the interconnection with calpain-mediated gephyrin degradation is shown. DLC1, dynein light chain 1; NLGN, neuroligin; nNOS, neuronal nitric oxide synthase; PI3K, phosphatidylinositol 3-kinase (Tyagarajan and Fritschy, 2014).

Among NLs, NL2 selectively interacts with the SH3-containing form of collybistin (Poulopoulos et al., 2009). This fits with the observation that NL2 is located preferentially at GABAergic synapses (Graf et al., 2004; Chih et al., 2005). NLs are the first postsynaptic molecules for which neurotransmitter-specific synaptogenic properties were described. Whereas NL1 and NL3 preferentially promote glutamatergic presynaptic differentiation, NL2 overexpression in heterologous cells induces glutamatergic and GABAergic differentiation in approximately equal amounts. These differences were later attributed to isoform-specific splice inserts in the extracellular esterase-homology domains (Chih et al., 2006). Splice insert "B", which is present in NL1 but not NL2, promotes differentiation of glutamatergic presynaptic terminals, even when artificially inserted in NL2. NLs form trans-synaptic complexes with presynaptic neurexins. Alternative splicing of the three mammalian neurexin genes generates an enormous diversity of neurexin isoforms (Baudouin and Scheiffele, 2010). Since the interaction of NLs with neurexins relies heavily on splice inserts, trans-synaptic signaling of NL-neurexin complexes is thought to underlie much of the specificity of synapse formation. Besides NL2, NL3 is localized at GABAergic synapses (Budreck and Scheiffele, 2007). NLs undergo both homo- and heterodimerization but the existence of NL2 / NL3 heterodimers was not yet conclusively demonstrated (Bemben et al., 2015). The inability of NL3 to interact with SH3-containing collybistin raises the question whether NL3 can fully compensate for the function of NL2. Finally, colocalization of NL4 with gephyrin and interaction with collybistin was shown (Hoon et al., 2011). NL4 has a limited distribution in the central nervous system with prominent expression in the brainstem and spinal cord, in contrast to the abundance of NL2 in the forebrain. The interaction of NLs with gephyrin and the selective interactions with collybistin, together with specific presynaptic interactions, suggest that NLs are important for validation of GABAergic synapses.

Although many proteins contribute to the molecular heterogeneity of the GABAergic PSD, few proteins are known that display a spatially restricted distribution in a subset of GABAergic synapses. Dystrophin and dystroglycan (DG), which together form the dystrophin-glycoprotein complex (DGC), are such sparsely localized GABAergic PSD proteins. In CNS neurons, the DGC is present mostly at perisomatic GABAergic synapses in pyramidal cells and in cerebellar Purkinje cells (Lidov et al., 1990; Knuesel et al., 1999). By interaction with synaptic scaffolding molecule (S-SCAM) and synArfGEF, the DGC seems to form an extended complex (Figure 3; (Sumita et al., 2007; Fukaya et al., 2011)). The physiological role of these biochemical interactions is unclear at present. Interestingly, an interaction of S-SCAM with NL2 was mapped to the NL2-gephyrin interaction region, raising the possibility that S-SCAM can interfere with gephyrin clustering at NL2-containing synapses (Sumita et al., 2007). Furthermore, similar to NL3, S-SCAM is also present at glutamatergic synapses, where its PDZ domains might bind to scaffolding molecules such as postsynaptic density protein 95 (PSD-95).

The repertoire of GABAergic PSD proteins was extended recently with two NL2-interacting proteins. Immunoglobulin superfamily member 9b (IgSF9b) binds to NL2 indirectly over S-SCAM, perhaps in analogy with putative indirect interactions with the DGC (Woo et al., 2013). Overexpression of

IgSF9b is not sufficient to drive GABAergic synapse formation, but through clustering of NL2 IgSF9b promotes the aggregation of the GABAergic PSD. Interestingly, IgSF9b shows a selective localization to GABAergic synapses in interneurons. Given the pyramidal cell-specific distribution of the DGC, S-SCAM might connect different proteins to NL2, depending on neuronal cell type. In contrast to IgSF9b, MAM domain-containing GPI anchor protein (MDGA) binds directly to the extracellular part of NL2 (Lee et al., 2013; Pettem et al., 2013). MDGA binding to NL2 inhibits the synaptic development-inducing properties of NL2, presumably by interfering with neurexin binding.

Synapse formation and differentiation

Formation of chemical synapses is a developmental process to first establish neuronal circuits but persists in adulthood as an important mechanism for learning and memory. The vast majority of synapses in the CNS are formed between subcellular domains which are specialized as either pre- or postsynaptic structures. Cell polarity in neurons is established before synapse formation, so that neurites are differentiated into dendrites or axons when intercellular contacts are first made.

The first step in synaptogenesis, cell adhesion, is common for all synapses, independent of which neurotransmitter system is employed (Missler et al., 2012). Cadherins and protocadherins are protein families which mediate homophilic cell adhesion during synaptogenesis. Although synaptic adhesion molecules are not necessarily inducing differentiation of pre- and postsynaptic structures, transmitter system-specificity might be primed already before contact is made, because factors secreted by neurons can have specific synaptogenic properties. For instance, neuronal activity-regulated pentraxin (Narp) is a presynaptically secreted factor which promotes the clustering of AMPA receptors but has no effect on GABAergic PSD proteins (O'Brien et al., 1999; O'Brien et al., 2002). Other factors such as Wnt proteins or fibroblast growth factors are secreted by target neurons and regulate axon morphology and differentiation (Krylova et al., 2002; Umemori et al., 2004). Thus, although initial cell adhesion might be mediated by the same protein families in synapses using different neurotransmitters, differentiation into specific pre- and postsynaptic structures begins already before contact formation. This is further illustrated by the finding that GABAergic synapse formation, in contrast to glutamatergic synapses, does not rely on dendritic protrusions (Wierenga et al., 2008). Still, at least in overexpression experiments, cell adhesion proteins can promote one type of synapse specifically. NLs, for instance, can change the ratio of excitatory to inhibitory synapses that contact the overexpressing neuron (Chih et al., 2006). The neurotransmitter specificity is mediated by selective trans-synaptic signaling, involving specific presynaptic neurexin isoforms. NLs are not required for synapse formation, as illustrated by the normal synapse number in NL triple KO mice (Varoqueaux et al., 2006). Therefore, although the pre- and postsynaptic side are primed to form a synapse of a specific neurotransmitter system, synapse validation by trans-synaptic complexes such as the NL-neurexin complex further drives differentiation.

The molecular diversity of trans-synaptic signaling complexes is thought to be instrumental in achieving the vastly heterogeneous composition of CNS synapses. Secreted morphogenic factors are essential for axon guidance and therefore for connectivity, especially with long-range projection neurons. However, given the diffuse nature of morphogenic signals, it is clear that in addition, trans-synaptic signaling must contribute to cell type-specific differentiation of synapses. A central role for the NL-neurexin complex in this process is suggested by the existence of thousands of neurexin alternative splice isoforms. Theoretically, this diversity in presynaptic binding partners could instruct differentiation of the PSD beyond the determination of the neurotransmitter used by the synapse. Instead, NL-neurexin interaction is hypothesized to represent a molecular "code" which defines the precise composition of synapses. With the help of Sam68-like mammalian protein 2 (SLM2) KO mice, evidence of such a code was recently found (Traunmuller et al., 2016). SLMs are splicing factors involved in regulation of alternative splicing of synaptic proteins, including neurexins. SLM2 KO mice showed a specific increase of the GluA1 subunit of AMPA receptors, minor alterations in excitatory neurotransmission and deficits in long-term potentiation (LTP). Heterozygotic deletion of neurexin 1 exon 21 was sufficient to rescue these changes, suggesting that alternative splicing of this exon by SLM2 is crucial for instructing specific synaptic properties.

The exact sequence in which proteins are recruited during synapse formation is not fully elucidated. Also, the minimally required set of proteins required for building functional synapses is still under debate. Insights into these questions was gained by overexpressing potentially synaptogenic proteins in heterologous cells. Besides NLs, synaptic cell adhesion molecule 1 (synCAM1) was found to promote synaptic structures when overexpressed in HEK cells (Biederer et al., 2002). The co-expression of GluA2 was sufficient to induce glutamatergic transmission onto HEK cells. Similarly, GABAergic currents can be detected in HEK cells which constitutively overexpress $GABA_A$Rs (Fuchs et al., 2013). $GABA_A$R contribute to trans-synaptic interactions directly over their N-terminal domains (Brown et al., 2016b). The relevance of these interactions *in vivo* is unclear, since co-expression of NL2 increased GABAergic transmission markedly (Fuchs et al., 2013).

The observation that neuronal activity is not necessary for developmental synapse formation supports the notion that trans-synaptic interactions are mainly driving synapse formation (Verhage et al., 2000). However, neurotransmission is required for the maintenance of synapses and membrane potential changes play a crucial role in neuronal differentiation and in maturation of synapses. The depolarizing action of GABAergic neurotransmission early after developmental synapse formation is critical for the functional development of silent glutamatergic synapses. By depolarizing the membrane, the Mg^{2+} block, which prevents the opening of NMDA receptors, is released (Ben-Ari et al., 2007). During adulthood, neuronal activity is an important factor in the elimination and formation of synapses (Caroni et al., 2014). For instance, growth of new spines is promoted by theta burst stimulation and hindered by low-frequency stimulation (Nagerl et al., 2004). Also, rearrangements of inhibitory

synapses assessed by gephyrin puncta dynamics *in vivo*, are induced when neuronal activity is blunted by monocular deprivation (Chen et al., 2012; van Versendaal et al., 2012).

Development and diversity of GABAergic interneurons

From a morphological, physiological and molecular perspective, GABAergic interneurons display a vast diversity in comparison to glutamatergic principal neurons. Different aspects of this heterogeneity partly coincide, giving rise to functionally distinct GABAergic cell types (Fishell and Rudy, 2011). Recently it has become clear that glutamatergic principal neurons are rivaling interneurons in regard to cell type diversity (Lodato et al., 2015). The obvious differences in appearance of GABAergic interneurons thus might have led to an overestimation of their functional diversity. However, GABAergic interneuron subtypes were implicated in many specific functions and have temporally unique firing properties. Understanding GABAergic interneuron diversity is thus important for understanding how their interaction with principal neurons impacts behavior (Klausberger and Somogyi, 2008).

GABAergic interneurons in the cerebrum are generated in the ganglionic eminences and the preoptic area, distantly from their target regions. The main bout of interneuron proliferation around E13 coincides with the generation of most pyramidal cells in the pallium (Le Magueresse and Monyer, 2013). Interneurons however, because they originate outside of the pallium, undergo tangential migration for several days before reaching the target destination. Differentiation of interneurons is on the one hand determined by the region in which they originate, equipping cells with a specific transcriptional program before migration. On the other hand, the effect of transcription factors on cell fate varies with time of development, so that transcription factors are essential for different cell types in different time windows. In addition, interneurons are exposed to a multitude of morphogenic factors during migration, which refines their differentiation along the way. All neocortical and hippocampal GABAergic interneurons originate in either the medial ganglionic eminence (MGE), the caudal ganglionic eminence (CGE) or the preoptic area (POA). Nkx2-1 is a transcription factor which is restricted to the MGE and POA and is essential for development of interneurons originating from these areas. Couptf2, in contrast, is specifically expressed in the CGE and essential for migration of CGE-derived interneurons (Kanatani et al., 2008). For differentiation of somatostatin (SST)-positive interneurons Nkx2-1 is required at E10.5 but not at E12.5 (Butt et al., 2008). Vasoactive intestinal polypeptide (VIP)-positive interneurons, in contrast, depend on Nkx2-1 expression at both time points, illustrating the importance of both temporal and spatial expression patterns for development of interneuron subtypes.

The tangential migration of GABAergic interneurons out of the subpallium into the pallium is guided by attractive and repulsive cues. For instance neuregulin-1 is a diffusible protein which acts in the pallium as a chemoattractant for interneurons (Flames et al., 2004). Regions which have to be avoided are thought to express chemorepulsive proteins. Class 3 semaphorins were identified as the molecules

responsible for mediating chemorepulsion of the striatum for interneurons targeted to the cortical regions (Marin et al., 2001). Although the response of interneurons to guidance cues depends on their expression profiles, the mechanisms of migration seem similar in all interneuron classes. Tangentially migrating GABAergic neurons share a common morphology with a prominent leading process, which is essential for sensing cues in the environment (Martini et al., 2009). Finally, ambient GABA and glutamate play an important role in migration of GABAergic neurons by activating $GABA_A$ and AMPA receptors which are diffusely located at the plasma membrane (Cuzon et al., 2006; Manent et al., 2006). The migration-inducing effect of GABA on GABAergic interneurons depends on depolarization of cells and therefore on the onset of KCC2 expression (Bortone and Polleux, 2009). In the developing cerebral cortex, interneurons migrate through the marginal zone, the subplate and the subventricular zone. Because they avoid the cortical plate, a tangential-to-radial switch is necessary to populate the newly formed neocortex with GABAergic neurons. Whether an intrinsic genetic program or external cues are responsible for the switch in direction is currently unclear.

GABAergic interneurons in the adult neocortex and hippocampus were classified according to morphological, transcriptional and electrophysiological criteria. Because of partial overlaps in expression profiles and smooth transitions between morphological classes it is difficult to clearly delineate all interneuron subtypes. Nevertheless, in the hippocampus at least 21 interneuron subgroups were clearly defined (Figure 4; (Klausberger and Somogyi, 2008)). Efforts to classify interneurons did not yet lead to a comprehensive list of GABAergic neuron subtypes. Common and objective criteria were therefore proposed to systematically classify interneurons in the cerebral cortex (Ascoli et al., 2008). Although GABAergic interneuron subtypes are not yet fully characterized, the use of molecular markers proved to be practical to bin interneurons into large classes. The expression of either PV, SST or 5-hydroxytryptamine 3a receptor (5-HT3aR) fully covers the range of GABAergic interneurons in the neocortex (Rudy et al., 2011). This classification partially correlates with developmental origin of cells, as PV-positive cells originate mostly in the MGE and 5-HT3aR-positive cells originate mostly in the CGE, for instance.

Importantly, glutamatergic principal neurons are targeted by GABAergic interneurons at distinct subcellular domains by different cell classes. In contrast to glutamatergic innervation which is restricted to dendritic spines, GABAergic axon terminals target the soma, dendrites and the axon initial segment of pyramidal cells. GABAergic interneurons innervating the soma and perisomatic region of pyramidal cells are called basket cells. All basket cells can be distinguished by the expression of either PV or cholecystokinin (CCK). However, axon initial segment-innervating chandelier cells are also PV-positive. Thus, although expression profiles reveal clues about neuronal function, morphology and electrophysiological properties have to be taken into account to describe the functional role of interneurons in network activity. During oscillatory activity in the hippocampus, interneuron classes were found to follow distinct patterns of activity (Klausberger and Somogyi, 2008). CCK-positive basket cells display maximal activity shortly before the peak of theta oscillations

in the hippocampus with respect to local field potential (LFP) activity. Bistratified cells, on the other hand, fire most at the trough of theta oscillations. Although PV-positive basket cells are similar in morphology and target region as CCK-positive basket cells, they show peak activity only after the peak of theta oscillations and also display distinct behavior from CCK-positive basket cells during other network activity. Molecular marker expression is thus indicative of neuronal function, albeit other criteria always have to be taken into account.

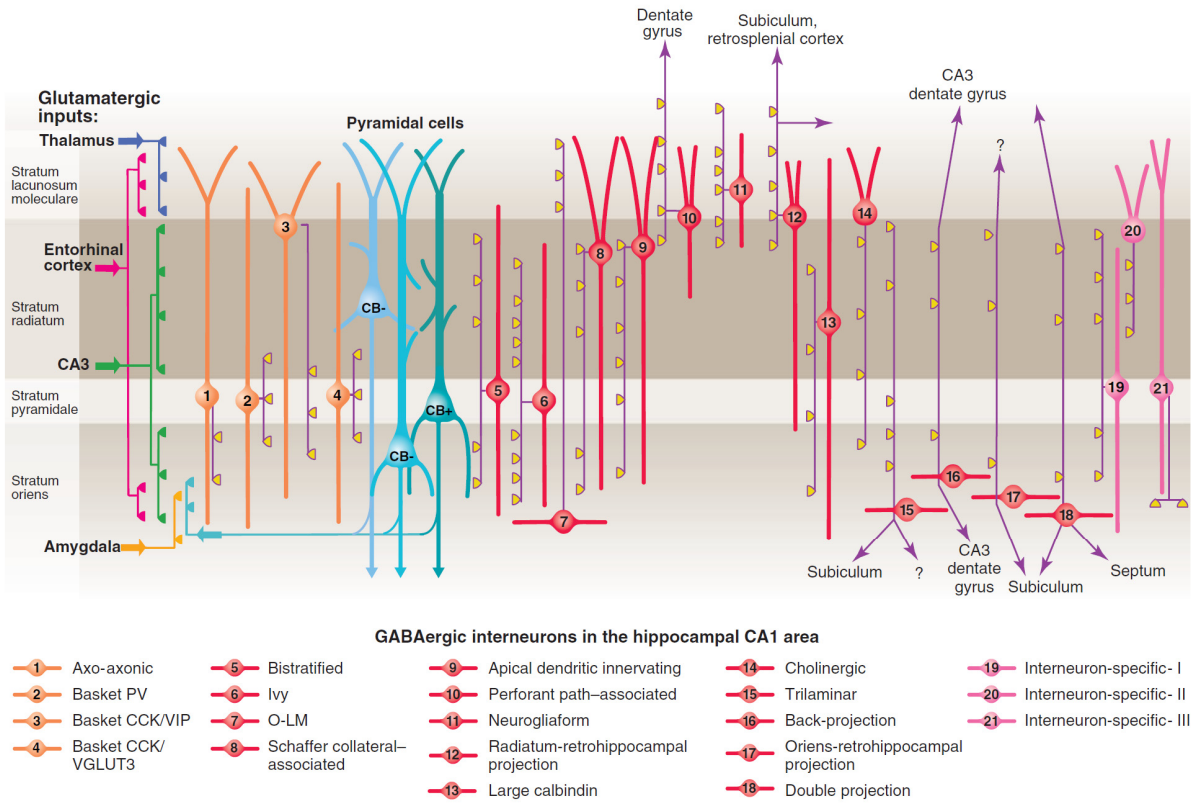

Figure 4. GABAergic interneuron diversity in the hippocampus CA1 region.
At least 21 distinct classes of interneurons were identified thus far. Orange cells represent interneuron classes which mainly innervate pyramidal cells (blue). The main synaptic terminations are shown in yellow. CA1, cornu ammonis 1; CCK, cholecystokinin; O-LM, oriens-lacunosum moleculare; PV, parvalbumin; VGLUT, vesicular glutamate transporter; VIP, vasoactive intestinal polypeptide (Klausberger and Somogyi, 2008).

PV- and CCK-positive cells build two non-overlapping groups of basket cells and together comprise all cells of this interneuron class. Besides spiking properties during network activity, the two groups also differ in expression profiles, membrane properties and the physiology of input and output synapses (Bartos and Elgueta, 2012). Firing patterns in response to current injection are accommodating for CCK-positive basket cells and non-accommodating for PV-positive cells. The majority of PV-positive cells also displays a higher firing frequency upon current injection. Synaptic terminals formed by the two groups of basket cells are equipped with a different set of receptors and other synaptic proteins. Cannabinoid receptor 1 (CB1) is exclusively located at CCK-positive terminals whereas the μ-opioid receptor (MOR) is mostly present at PV-positive terminals. Both CB1

and MOR activation can lead to suppression of GABA release from terminals. However, receptor agonists are released under different circumstances, implicating CB1- and MOR-containing terminals in different processes. Endocannabinoids are synthesized in response to strong glutamatergic transmission and are released to activate presynaptic CB1 receptors. This retrograde signaling underlies the process of depolarization-induced suppression of inhibition (DSI), which was first described electrophysiologically at a subset of inhibitory synapses. Along with CB1, vesicular glutamate transporter 3 (VGluT3) is also exclusive to CCK-positive basket cells among GABAergic interneurons. The presence of VGluT3 in VGAT-containing synaptic vesicles of CCK-positive basket cells indicates that glutamate is coreleased from these synapses together with GABA (Stensrud et al., 2013; Stensrud et al., 2015). Some CCK-positive basket cells express VIP instead of VGluT3, illustrating that subtypes of interneuron classes can be defined by the combination of molecular marker expression.

The dystrophin-glycoprotein complex

In the light of GABAergic molecular diversity, the DGC is of special interest for three reasons. First, this complex is restricted to a subset of GABAergic synapses, most prominently on pyramidal cells in the forebrain and in cerebellar Purkinje cells. Secondly, multiple proteins were shown to associate with the DGC. These interactions may impart a role of a molecular hub to the DCG, on which several signaling pathways could converge. Finally, through its interactions with presynaptic binding partners, the DGC might be involved in trans-synaptic signaling. The selective distribution of the DGC suggests that such trans-synaptic signaling might be specific to certain interneurons classes.

Dystrophin

The core of the DGC is formed by the proteins dystrophin and DG, of which β-DG builds the transmembrane and α-DG the extracellular part of the complex (Figure 3). Dystrophin is a large cytosolic protein and builds the connection of the DGC to intracellular binding partners. Its domain structure reveals clues about the function of dystrophin in the DGC. On the N-terminal end an actin-binding domain is located whereas the C-terminal end contains domains which interact with DG and the associated proteins syntrophin and dystrobrevin (Anderson et al., 2012). The N-terminal actin-binding domain is separated from the C-terminus by the rod domain, named after the tubular structure that is formed by its spectrin-like repeats. Interestingly, the crucial interaction of dystrophin with β-DG is mediated in part by WW domains in dystrophin, the same domains which are necessary for binding the signaling protein synArfGEF (Fukaya et al., 2011). S-SCAM, in turn, interacts with β-DG and NL2 over its WW domains (Sumita et al., 2007). The observation that the same modular domain structure serves to build the DGC and associated interactions points towards a common regulation of this extended protein complex.

Because the dystrophin gene (*DMD*) contains several internal promoters, shorter protein isoforms exist which lack the actin-binding domain. The DMD gene is, due to extensive intronic regions, one of the largest genes in the human genome, spanning around 2.4 megabases (Koenig et al., 1987; Love et al., 1990). The large size of the DMD gene makes dystrophin susceptible to mutations. This underlies the relatively high incidence of muscular dystrophies, one of the clinical manifestations of dystrophin mutations.

Dystroglycan

Several glycoproteins were isolated in conjunction with dystrophin (Campbell and Kahl, 1989; Ervasti et al., 1990). Among these, a 43 kilodalton (kDa) protein was found to be directly linked to dystrophin and was later renamed β-DG (Ervasti and Campbell, 1991). On the basis of biochemical interactions of glycoproteins, it was concluded that the large glycoprotein α-DG is located on the extracellular side of the DGC. Other glycoproteins associated with dystrophin turned out to bind to DG but not directly to dystrophin (Ozawa et al., 2005). These proteins were named sarcoglycans, in line with their prominent expression in muscle.

α- and β-DG are encoded by a single gene (*Dag1*) and generated by proteolytic cleavage of a precursor protein (Ibraghimov-Beskrovnaya et al., 1992). The two mature proteins remain non-covalently attached and the function of proteolytic cleavage is still unclear. However, mutation of the cleavage site in DG leads to glycosylation defects and muscular dystrophy (Jayasinha et al., 2003). α-DG is more extensively glycosylated than β-DG, making up more than half of its molecular weight (Barresi and Campbell, 2006). By far most glycosylation sites in α-DG lie in the mucin-like domain and undergo O-mannosylation. The sequence of catalytic steps involved in α-DG is not fully elucidated but can be broadly divided into two processes. First, there is the attachment of mannose, which is in turn linked to other glycans and phosphorylated. This modification depends in part on protein-O-mannosyl-transferase 1 and 2 (POMT1/2). Secondly, further glycans are attached to the phosphate group in the process of post-phosphoryl-glycosylation. Several enzymes are putatively involved in this modification but only the role of like-acetylglucosaminyltransferase (LARGE) is established so far (Waite et al., 2012).

Glycosylation of α-DG is essential for interaction with extracellular binding partners. Both proteins secreted into the ECM and located presynaptically were found to interact with α-DG. The presence of a laminin G-domain is common to most α-DG-binding proteins such as laminin, agrin and neurexin. Interaction with laminin and agrin is important for structural integrity of the sarcolemma and clustering of receptors at the neuromuscular junction (NMJ), respectively. The finding that neurexin binds α-DG in a splice isoform-specific manner fueled speculations about a trans-synaptic function of DG in the brain (Sugita et al., 2001).

Distribution of the dystrophin-glycoprotein complex in the brain

Because of the prominent involvement of the DGC in muscular dystrophies and the strong expression in muscle, the function of the DGC in this tissue is well studied. However, DGC components are widely expressed throughout the body, albeit in different subcompositions (Chamberlain et al., 1988; Chelly et al., 1988; Hoffman et al., 1988). In the brain, the strongest expression of dystrophin and DG is found in astrocytes, where the DGC is located at the end-feet surrounding blood vessels (Tian et al., 1996). The neuronal DGC displays a punctate distribution, which is due to the clustering of the complex in GABAergic PSDs (Miike et al., 1989; Lidov et al., 1990; Lidov et al., 1993; Knuesel et al., 1999). Neuronal DGC expression is widespread in the CNS, ranging from the spinal cord to the brain stem and cortical areas (Gorecki et al., 1992; Zaccaria et al., 2001; Wright et al., 2012). By far the most prominent immunolabeling, however, was described in forebrain pyramidal cells and in cerebellar Purkinje cells. On these cells, DGC components can be detected in characteristic large clusters that are restricted to the perisomatic subcellular compartment. The reason for this limited distribution is unknown thus far, but the compartment-specific innervation of some interneuron classes in the cerebral cortex suggests a function of the DGC specifically in basket cell synapses.

Functions of the dystrophin-glycoprotein complex in the central nervous system

Depending on cell type and developmental stage, DG serves various functions in the CNS. Constitutive ablation of DG is lethal early in embryonic development (Williamson et al., 1997). Therefore, conditional KO (cKO) strategies were employed to study the function of the DGC in the brain. Crossing DG floxed mice with mice expressing glial fibrillary acidic protein (GFAP)-driven Cre recombinase efficiently led to the ablation of DG in astrocytes (Moore et al., 2002). This resulted in gross structural brain abnormalities, including defects in the layering of the cerebral cortex and macrocephaly. The absence of the DGC from the glia limitans likely underlies these structural deficits. The DGC, however, is also expressed in radial glial cells (RGC), and Nestin-Cre / DG null mice display a similar layering phenotype (Satz et al., 2010). Neuronal migration in the cerebral cortex is thus likely controlled by DG expressed in astrocytes and in RGCs. In addition, mice expressing a mutated DG glycosyl transferase exhibit abnormal layering of the cerebral cortex, stressing the importance of DG glycosylation for this function. In another subcellular compartment of astrocytes, the end-feet surrounding blood vessels, the DGC serves an unrelated function. In this context, the DGC is involved in clustering aquaporin-4 channels (Waite et al., 2012).

Because intellectual disability is a common finding in patients with Duchenne's muscular dystrophy (DMD), mice lacking the largest form of dystrophin (mdx mice) were examined extensively for neurological abnormalities. The finding that clustering of $GABA_AR$ subunits, but not of gephyrin, is reduced in mdx mice, indicated that the DGC is involved in clustering GABAergic PSD proteins (Knuesel et al., 1999; Vaillend et al., 2010). However, DG is not necessary for synaptic clustering of $GABA_AR$ subunits in primary hippocampal neurons (Levi et al., 2002). Also, the observation that

DGC components are always apposed to GABAergic presynaptic terminals in primary cultures suggests a trans-synaptic, rather than a purely postsynaptic function of the DGC (Brunig et al., 2002). Multiple other alterations in brain morphology and physiology of mdx mice were reported (Cohen et al., 2015). Yet, because mdx mice carry a constitutive mutation which also affects muscle and other tissue, it is not clear whether these changes are due to indirect compensatory effects or whether they represent the physiological function of dystrophin in the brain.

Brain involvement in muscular dystrophies

Already in the earliest descriptions of DMD, intellectual disability (ID) was noted as a hallmark of the disease (Duchenne de Boulogne, 1861). The degree of neurological involvement in muscular dystrophies ranges from severe brain malformations in congenital muscular dystrophies (CMD) to very mild ID in dystrophinopathies. It is well established that the mean intelligence quotient of DMD patients lies around one standard deviation below average (Cotton et al., 2001; Cotton et al., 2005). The severity of ID correlates with the position of the mutation in the DMD gene, presumably because more downstream mutations cause more dystrophin isoforms to be lost (Taylor et al., 2010). In contrast to CMDs, dystrophinopathies are not associated with lissencephaly or other severe brain abnormalities, hinting towards a crucial role of synaptic dystrophin for cognitive function. Moreover, severe ID is common in rare forms of limb girdle muscular dystrophy without structural brain abnormalities, further supporting the notion that the neuronal DGC is essential for normal cognition (Dincer et al., 2003; Hara et al., 2011).

SynArfGEF

SynArfGEF was first described as a protein-coding complementary DNA isolated from human brain (Kikuno et al., 1999). The initial finding that this gene is expressed most abundantly in brain was confirmed by Northern and Western blot analyses as well as by immunohistochemical stainings (Inaba et al., 2004). Furthermore, biochemical and immunolocalization experiments suggested that synArfGEF is enriched in the glutamatergic PSD, giving rise to the “syn” prefix. Based on sequence homology, the presence of a Sec7 domain in synArfGEF was identified early on, suggesting a function as a guanine nucleotide exchange factor (GEF) (Osada et al., 2001). Indeed, synArfGEF (brefeldin A-resistant Arf-GEF 3 [BRAG3]; IQ motif and Sec7 domain 3 [IQSEC3]) belongs to the group of Sec7 domain-containing ADP ribosylation factor (Arf) nucleotide exchangers (Cox et al., 2004). Later, it was described as a dystrophin-interacting protein present in the GABAergic PSD (Fukaya et al., 2011; Sakagami et al., 2013). In the light of the gephyrin clustering-inducing properties of collybistin, another GEF protein in the GABAergic PSD, speculations about the involvement of synArfGEF in GABAergic PSD regulation arose.

Conflicting results were reported about Arf selectivity of synArfGEF catalytic function. The human isoform was shown to activate Arf1 whereas the rat isoform seems to act specifically as an Arf6 GEF

(Hattori et al., 2007; Fukaya et al., 2011). Arf6 exhibits a wide-spread distribution in the CNS and serves various functions, most notably as a modulator of neuronal morphology (Jaworski, 2007). It is a membrane-bound small GTPase, and, in contrast to Arf1-5, cycles between the plasma membrane and endocytic compartments. The synaptic localization of synArfGEF is therefore in line with activation of Arf6 rather than Arf1. Cell morphology is controlled by Arf6 through two mechanisms. Arf6 activation affects actin dynamics by increasing Ras-related C3 botulinum toxin substrate 1 (Rac1) activity. On the other hand, Arf6 activation can induce both clathrin-dependent and -independent endocytosis. The use of Arf6 constitutively active (CA) and dominant negative (DN) mutants in overexpression experiments in cultured neurons elucidated the crucial role of this GTPase in regulation of neuronal morphology. Axonal and dendritic branching as well as the abundance of dendritic spines are impacted by Arf6 activity (Hernandez-Deviez et al., 2002; Hernandez-Deviez et al., 2004; Miyazaki et al., 2005). Under physiological conditions, however, Arf6 activity is controlled by a multitude of GEFs and GTPase activating proteins (GAP), so that Arf6 function is determined by the nanodomain distribution of these regulatory proteins (Jaworski, 2007).

The synArfGEF homologs IQSEC1 and IQSEC2 are both present at glutamatergic PSDs and regulate internalization of GluA2 and GluA1-containing AMPA receptors, respectively (Scholz et al., 2010; Myers et al., 2012). In the case of GluA1 internalization, unbinding of calmodulin from IQSEC2 precedes the activation of Arf6 by IQSEC2. The IQ motif binds to calmodulin preferably in low Ca^{2+} concentrations (apocalmodulin), so that an influx of Ca^{2+} might trigger the release of calmodulin from IQSEC2. Like its close homologs, synArfGEF also contains an IQ motif N-terminally to the Sec7 domain. Functions of synArfGEF in the GABAergic PSD are therefore likely to be modulated by neuronal activity. In line with this hypothesis, synArfGEF transcription is induced by increased neuronal activity or enriched environment through the transcription factor neuronal PAS domain protein 4 (NPAS4) (Bloodgood et al., 2013). Strikingly, NPAS4 regulates GABAergic synapses in a layer-specific manner in the hippocampus, correlating with the association of synArfGEF with the mostly perisomatically localized DGC.

AIMS OF THE THESIS

Since the identification of GABA as a neurotransmitter, advances in molecular genetics, pharmacology, electrophysiology and optical imaging have revealed an enormous molecular diversity of GABAergic postsynaptic proteins. This molecular complexity is mirrored by the morphological and physiological heterogeneity of GABAergic interneurons. On the other hand, the molecular mechanisms of cell- and compartment-selectivity of GABAergic innervation are still unclear. This thesis aims to uncover a relationship between the molecular heterogeneity of GABAergic synaptic proteins and the specificity of GABAergic synapse formation, maintenance and elimination. Two levels will be considered in the investigation of the dependence of synapse specificity on PSD protein heterogeneity: The interplay of these factors within and between neurotransmitter systems.

The presence of the DGC at synaptic sites in CNS neurons and its role in the development and function of GABAergic synapses are largely unexplored scientific issues. Due to its restricted localization in a subset of GABAergic synapses and its potential post- as well as trans-synaptic functions, the DGC represents an ideal candidate to explore whether GABAergic PSD composition and the specificity of GABAergic innervation are interconnected. The preferred perisomatic localization of this complex in forebrain pyramidal neurons implies that the DGC is essential specifically for GABAergic basket cell function, if a direct structure-to-function relationship exists. In the first study, this hypothesis is tested mainly by disrupting the complex *in vivo*, using conditional deletion of DG. A role in postsynaptic clustering of GABAergic PSD proteins was assigned to the DGC on the basis of studies that examined mice deficient in a single dystrophin isoform. However, unveiling potential trans-synaptic functions of the DGC requires disrupting the complex, and therefore any specific signaling, completely. Nevertheless, the conditional deletion approach also offers the possibility to examine whether GABAergic PSD components require the DGC for postsynaptic clustering, without the issue of residual DGC formed by other dystrophin isoforms. The dependence of GABAergic PSD proteins, in particular NL2, on the DGC for postsynaptic clustering is therefore tested in DG-deficient mice as well. Finally, elucidation of the neuronal networks which depend on DGC signaling might facilitate the development of novel strategies to alleviate some of the neurological symptoms many muscular dystrophy patients suffer from.

In order to characterize the mechanisms that convey neurotransmitter-specificity of synapse formation and function, the second study focuses on the DGC-associated protein synArfGEF. This protein, due to its initial characterization in glutamatergic as well as GABAergic PSDs, its function as an activator of Arf GTPases and the potential activity-dependence of its function, lends itself to study postsynaptic regulatory processes that convey neurotransmitter-specificity. The purpose of this study is to characterize the biochemical interactions, the functions of individual synArfGEF domains and the neuronal activity-dependence of these functions. These aspects are examined primarily by using an ablation and an overexpression approach in primary neuronal cultures, combined with the targeted

mutagenesis of synArfGEF. With an emphasis on the processes that promote the alignment of pre- and postsynaptic structures, a function of synArfGEF in conferring glutamatergic or GABAergic synaptic specificity is considered. The occurrence of “mismatched” synapses in primary cultures offers the opportunity to study the sorting mechanisms that ensure targeting of PSD proteins to appropriate synapses. Neurotransmitter specificity of synArfGEF function is studied in this context, in order to uncover processes which are not amenable to study under physiological conditions *in vivo*.

RESULTS

STUDY I: NEURONAL DYSTROGLYCAN IS NECESSARY FOR FORMATION AND MAINTENANCE OF FUNCTIONAL CCK-POSITIVE BASKET CELL TERMINALS ON PYRAMIDAL CELLS

Simon Früh[1,5], Jennifer Romanos[1,5], Patrizia Panzanelli[2], Daniela Bürgisser[3], Shiva K. Tyagarajan[1,5], Kevin P. Campbell[4], Mirko Santello[1,5], Jean-Marc Fritschy[1,5]

[1]Institute of Pharmacology and Toxicology, University of Zurich, 8057 Zurich, Switzerland
[2]Department of Neuroscience Rita Levi Montalcini, University of Turin, 10124 Turin, Italy
[3]ETH Zurich, 8092 Zurich, Switzerland
[4]Howard Hughes Medical Institute, Department of Molecular Physiology and Biophysics, Department of Neurology, The University of Iowa Roy J. and Lucille A. Carver College of Medicine, Iowa City, Iowa 52242, USA
[5]Neuroscience Center Zurich, University of Zurich and ETH Zurich, 8057 Zurich, Switzerland

Author contributions: S.F., M.S. and J.-M.F. designed research; S.F., J.R., P.P., D.B. and M.S. performed research; K.P.C. contributed unpublished reagents; S.F., J.R., P.P., D.B., S.K.T., M.S. and J.-M.F. analyzed data; S.F. and J.-M.F. wrote the paper.

Part of this study was published as a Master thesis in Pharmaceutical Sciences (ETH) by Daniela Bürgisser under the title *Role of the dystrophin-glycoprotein complex for regulation of GABAergic synapses in the mouse hippocampus*.

Abstract

Distinct types of GABAergic interneurons target different subcellular domains of pyramidal cells, thereby shaping pyramidal cell activity patterns. Whether the presynaptic heterogeneity of GABAergic innervation is mirrored by specific postsynaptic factors is largely unexplored. Here we show that dystroglycan, a protein responsible for the majority of congenital muscular dystrophies when dysfunctional, has a function at postsynaptic sites restricted to a subset of GABAergic interneurons. Conditional deletion of Dag1, encoding dystroglycan, in pyramidal cells caused loss of CCK-positive basket cell terminals in hippocampus and neocortex. PV-positive basket cell terminals were unaffected in mutant mice, demonstrating interneuron subtype-specific function of dystroglycan. Loss of dystroglycan in pyramidal cells had little influence on clustering of other GABAergic postsynaptic proteins and of glutamatergic synaptic proteins. CCK-positive terminals were not established at P21 in the absence of dystroglycan and were markedly reduced when dystroglycan was ablated in adult mice, suggesting a role for dystroglycan in both formation and maintenance of CCK-positive terminals. The necessity of neuronal dystroglycan for functional innervation by CCK-positive basket cell axon terminals was confirmed by reduced frequency of inhibitory events in pyramidal cells of dystroglycan-deficient mice and further corroborated by the inefficiency of carbachol to increase IPSC frequency in these cells. Finally, neurexin binding seems dispensable for dystroglycan function since knock-in mice expressing binding-deficient T190M dystroglycan displayed normal CCK-positive terminals. Taken together, we describe a novel function of dystroglycan in interneuron subtype-specific trans-synaptic signaling, revealing correlation of pre- and postsynaptic molecular diversity.

Introduction

GABAergic interneurons, which provide the main source of inhibitory drive in the adult mammalian brain, form several distinct classes according to morphological, molecular and functional criteria (Fishell and Rudy, 2011). This specialization allows interneurons to adapt to different demands of postsynaptic targets and thereby control membrane excitability in a spatially and temporally precise manner (Klausberger and Somogyi, 2008). Most interneuron classes innervate only a specific subcellular domain of target cells, for example the axon initial segment, the cell soma or dendritic regions. Synaptic transmission from different interneuron subtypes has thus fundamentally different impact on the activity of postsynaptic cells. It might be advantageous to account for this diversity of GABAergic innervation with postsynaptic specializations matching the specific properties and plasticity mechanisms of synaptic terminals they are contacted from. Indeed, the GABAergic postsynaptic density (PSD) is characterized by a large molecular heterogeneity (Tyagarajan and Fritschy, 2014). However, little is known about such subtype-specific postsynaptic GABAergic adaptations.

Basket cells are GABAergic interneurons that specifically target the perisomatic region of principal neurons. In cerebral cortex and hippocampus, expression of parvalbumin (PV) or cholecystokinin (CCK) identifies basket cells as belonging to one of two non-overlapping groups (Freund and Katona, 2007). Although these two interneuron subtypes innervate the same subcellular domain, they are distinguished by various traits (Bartos and Elgueta, 2012). Only CCK-positive basket cells express presynaptic cannabinoid receptors, enabling retrograde signaling of endocannabinoids to suppress GABA release. Different firing patterns, expression profiles and developmental origins further set the two subtypes apart. Therefore, it is conceivable that the two types of basket cells use different mechanisms for synapse formation and require a different set of postsynaptic proteins to exert their vastly different functions.

Dystroglycan (DG) is the central component of the dystrophin-glycoprotein complex (DGC). The extracellular α-DG and transmembrane β-DG, generated by proteolytic cleavage of a single gene product, bind the large cytoplasmic protein dystrophin, which in turn can interact with actin filaments. α-DG, through its glycosyl side chains, can bind to extracellular matrix components. The crucial role of the DGC in muscle tissue was revealed by mutations affecting DGC components that lead to muscular dystrophies (McNally and Pytel, 2007). The DGC, albeit differing slightly in its molecular composition, is also expressed in the central nervous system by glial cells and neurons (Waite et al., 2012). Developmental brain malformations and intellectual disability, observed frequently in muscular dystrophies caused by DGC dysfunction, testify to the importance of this complex for brain function. The finding that the DGC is present in pyramidal cells as large, mostly perisomatic clusters postsynaptic to GABAergic terminals spurred interest in the synaptic function of the DGC (Lidov et al., 1990). Because reduced $GABA_AR$ immunoreactivity was found in a mouse model of Duchenne's

muscular dystrophy (DMD), a function for the DGC in clustering of PSD components was posited (Knuesel et al., 1999; Vaillend et al., 2010). Despite the selective DGC subcellular distribution, biochemical interaction with presynaptic neurexins and the obligatory association of DG with GABAergic presynaptic terminals in neuronal cultures, the role of the DGC in trans-synaptic signaling was never systematically assessed (Sugita et al., 2001; Brunig et al., 2002).

We hypothesized that the diversity of GABAergic PSD composition is functionally related to the heterogeneity of GABAergic innervation. Due to its restricted distribution and known role as a transmembrane complex, DG seemed ideally suited to address this issue. Ablation of DG specifically in pyramidal neurons allowed us to study the synaptic function of the DGC without confounding deficits in neuronal migration associated with loss of DG in other tissues. Using this approach, we demonstrate that the neuronal DGC plays an essential role in trans-synaptic signaling necessary for formation and maintenance of functional axon terminals from CCK-positive basket cells. Since the neuronal circuits depending on this signaling have been shown to be involved in major cognitive functions, our findings open new avenues in identifying the causes of intellectual disability in muscular dystrophies.

Materials and methods

Animals

All mice were bred on C57BL/6 background at the Laboratory Animal Service Center (Schlieren, Zurich, Switzerland) and kept in standard housing with food and water provided *ad libitum*. Mice harboring loxP sites in exon 2 of *Dag1* were obtained from The Jackson Laboratory (Bar Harbor, ME). NEX-Cre transgenic mice were used to achieve selective ablation of neuronal DG (Goebbels et al., 2006) and were provided by Dr. Sandra Goebbels (Max-Planck-Institute of Experimental Medicine, Goettingen, Germany). *Dag1* T190M knock-in mice were provided by Dr. Kevin P. Campbell (Howard Hughes Medical Institute, Iowa City, IA). *Dag1* floxed mice were genotyped by PCR analysis using primers 5'-GGAGAGGATCAATCATGG-3' and 5'-CAACTGCTGCATCTCTAC-3'. Genotyping of NEX-Cre transgenic mice was performed as described (Goebbels et al., 2006). To obtain DG cKO and control mice, NEX-Cre$^{tg/+}$ / *Dag1*$^{loxP/+}$ mice were bred to NEX-Cre$^{+/+}$ / *Dag1*$^{loxP/loxP}$ mice. All experiments were approved by the veterinary office of the Canton of Zurich.

Western blotting

Adult DG cKO and control mice of both sexes were anaesthetized with pentobarbital (Nembutal; 50 mg/kg intraperitoneally) and sacrificed by decapitation. Cheek muscle was dissected on ice and transferred to lysis buffer (50 mM Tris (pH 7.6), 150 mM NaCl, 1% Triton X-100, Complete Mini Protease Inhibitor Cocktail [Roche, Rotkreuz, Switzerland]). Tissue was Dounce homogenized, sonicated and incubated on ice for 1h. Lysates were centrifuged at 50'000 RPM for 1h at 4 °C and supernatants were stored at -80 °C. For anti-α-DG blots, glycosylated proteins were enriched by incubating lysates with wheat germ agglutinin (WGA) agarose beads (Vector Labs, Burlingame, CA) at 4 °C overnight (ON). Proteins were eluted with 300 mM N-Acetyl-glucosamine and stored at -20 °C. Laemmli buffer was added to WGA-enriched and non-enriched lysates (for loading control) and samples were run on 8% tris-glycine polyacrylamide gels. Proteins were transferred to polyvinylidene fluoride (PVDF) membranes. Mouse anti-α-DG (11H6C4; Millipore; 1:1000) and rabbit anti-actin (Sigma; 1:5000) antibodies were incubated in tris-buffered saline with 0.05% Tween 20 (TBST) including 5% Western Blocking Solution (Roche) ON at 4 °C. Membranes were washed 5 times in TBST. Horseradish peroxidase-coupled donkey secondary antibodies (1:20'000) were incubated for 1h at room temperature (RT) and membranes were washed again 5 times in TBST. SuperSignal West Pico Chemiluminescent Substrate (Thermo Fisher Scientific, Waltham, MA) was applied and membranes were developed on X-ray film (Fujifilm, Tokyo, Japan).

Tissue preparation for immunohistochemistry

DG cKO and control mice of both sexes at the age of 8 to 12 weeks were anaesthetized by intraperitoneal pentobarbital injection (Nembutal; 50 mg/kg) and perfused transcardially with ice-cold oxygenated artificial cerebrospinal fluid (ACSF; pH 7.4) for 2 min, as described (Notter et al., 2014).

Brains were immediately dissected and fixed in 4% paraformaldehyde (PFA) for 100 min on ice. After rinsing in phosphate-buffered saline (PBS), brains were incubated in 30% sucrose (in PBS) at 4 °C ON. 50 µm thick coronal sections were cut from frozen blocks using a sliding microtome (HM400; Microm, Walldorf, Germany) and stored at -20 °C in antifreeze solution. Tissue preparation from P21 mice followed the same protocol with the following modifications: Mice were perfused with 4% PFA (after brief perfusion with PBS to rinse blood) and brains were post-fixed for 3h.

Target	Host species	Dilution	Cat. no.	Company / origin
α-Dystroglycan (VIA4-1)	Mouse	1:100	05-298	EMD Millipore
α-Dystroglycan (11H6C4)	Mouse	1:100	05-593	EMD Millipore
β-Dystroglycan	Mouse	1:100	ab49515	Abcam
Bassoon	Mouse	1:2000	VAM-PS003	StressGen
Cannabinoid receptor 1	Rabbit	1:3000	258 003	Synaptic Systems
Cholecystokinin 8	Mouse	1:1000	ab37274	Abcam
Cre recombinase	Rabbit	1:1000	PRB-106C	Covance
Dystrophin (C-terminal)	Mouse	1:100	BT39-9050-05	Biotrend
$GABA_AR$ α1 subunit	Guinea pig	1:20‘000	-	(Fritschy and Mohler, 1995)
$GABA_AR$ α2 subunit	Guinea pig	1:6000	-	(Fritschy and Mohler, 1995)
$GABA_AR$ γ2 subunit	Guinea pig	1:10‘000	-	(Fritschy and Mohler, 1995)
GAD65/67	Rabbit	1:2000	GC 3008	Biomol
Gephyrin	Mouse	1:1000	147 021	Synaptic Systems
NeuN	Mouse	1:1000	MAB377	Chemicon
Neuroligin 2	Rabbit	1:10‘000	-	Gift from Dr. Peter Scheiffele
Parvalbumin	Rabbit	1:1000	24428	ImmunoStar
PSD-95	Mouse	1:1000	MA1-045	ABR
Synaptotagmin 2	Rabbit	1:1000	105 123	Synaptic Systems
synArfGEF	Guinea pig	1:3000	-	Gift from Dr. Hiroyuki Sakagami (Fukaya et al., 2011)
VGAT	Rabbit	1:3000	131 003	Synaptic Systems
VGluT1	Guinea pig	1:1000	135 304	Synaptic Systems
VGluT3	Guinea pig	1:4000	AB5421	Merck Millipore

Table 1. Antibodies used for immunohistochemical stainings.
If not otherwise stated, antibody VIA4-1 was used to label α-dystroglycan. For secondary antibodies see materials and methods.

Immunohistochemistry

After rinsing once in PBS, sections were incubated in primary antibody solution (50 mM Tris, 150 mM NaCl, 0.2% Triton X-100, 2% normal goat serum (NGS), pH 7.4) with antibodies listed in Table 1. Primary antibodies were incubated at 4 °C ON, or for 3 days if DG or dystrophin was labelled. Sections were washed 3 times for 10 min in PBS and incubated in secondary antibody solution (50 mM Tris, 150 mM NaCl, 0.05% Triton X-100, 2% NGS, pH 7.4) for 30 min at RT with secondary antibodies raised in goat. Antibodies conjugated to Alexa Fluor 488 and Alexa Fluor 647 (Invitrogen, La Jolla, CA) were diluted 1:1000 whereas antibodies conjugated to Cy3 (Jackson ImmunoResearch, West Grove, PA) were diluted 1:500. Sections were washed 3 times for 10 min in PBS and mounted on gelatin-coated slides using Fluorescence Mounting Medium (Dako, Carpinteria, CA). For immunoperoxidase stainings, biotinylated secondary antibodies were diluted 1:300. After washing 3 times for 10 min in PBS, sections were incubated with avidin-peroxidase-complex solution (Vector

Labs) for 30 min at RT and washed again 3 times for 10 min in PBS. Sections were pre-incubated in diaminobenzidine (DAB) solution (50 mM Tris, 150 mM NaCl, 0.05% Triton X-100, 0.5 g/L DAB, pH 7.7) for 5 min under agitation and DAB solution containing 0.01% H_2O_2 was added to sections. The reaction was stopped by washing in ice-cold PBS several times. Sections were mounted on gelatinized slides and dried ON. After dehydration by immersion in increasingly concentrated ethanol solutions and clearing in xylene, slides were coverslipped with Eukitt (Merck, Darmstadt, Germany).

Stereology

Immunoreactive cells were counted and the size of the dorsal hippocampus estimated with the help of Mercator software (Explora Nova, La Rochelle, France). 4 equidistant coronal sections per mouse were used to count cells in all layers of the hippocampus proper. The volume was estimated using Mercator software and cell density was calculated.

Image acquisition and statistical analysis

Z-stack images (3 optical sections, 0.5 µm step size) were recorded of all specimens using confocal laser scanning microscopy (LSM 700, Carl Zeiss, Oberkochen, Germany). Images were taken using a 40x objective with a numerical aperture of 1.4 and had a pixel size of 112 x 112 nm^2. To reduce variability, 3-4 sections were imaged per mouse and cluster density values were averaged from these sections. All imaging parameters were kept constant between genotypes. For cluster analysis, maximum intensity projections were created from z-stacks and analyzed using ImageJ (NIH, Bethesda, MD). Representative example images were processed with Imaris (Bitplane, Belfast, UK). Statistical tests were performed using Prism software (GraphPad, La Jolla, CA). A minimum of 4 mice per group were used and statistical tests were performed using data points from individual mice for density values and using pooled cluster data from all mice per group for size (see Table 2).

Stereotactic injections

8 to 10 weeks old mice transgenic for loxP in exon 2 of *Dag1* were anaesthetized with isoflurane (Attane; Piramal, Mumbai, India). After mice were head-fixed on a stereotactic frame (David Kopf Instruments, Tujunga, CA), a small longitudinal incision was made under continuous administration of isoflurane to reveal the skull. Bregma was identified and the skull was perforated unilaterally using a surgical drill at the following coordinates relative to Bregma: x = -1.9 mm, y = 1.6 mm. A glass pipette filled with virus solution was inserted into the brain to z = 1.5 mm. A total of 1 µL virus solution was injected using an automated injection pump in increments of 70 nL over 10 min. The pipette was removed and the incision sutured. Mice were injected intraperitoneally with 1 mg/kg buprenorphine (Temgesic; Essex Chemicals, Lucerne, Switzerland) and placed on a warm pad for recovery before returning to the home cage.

Virus

AAV8-CaMKIIa-mCherry-Cre (dot blot titer $4.7x10^{12}$ VG/mL) was purchased from the University of North Carolina Vector Core (Chapel Hill, NC).

Acute brain slice preparation

5 to 6 weeks old DG cKO and control mice were briefly anaesthetized with isoflurane and decapitated. The brain was quickly removed and transferred to ice-cold solution containing 65 mM NaCl, 2.5 mM KCl, 1.25 mM NaH_2PO_4, 25 mM $NaHCO_3$, 7 mM $MgCl_2$, 0.5 mM $CaCl_2$, 25 mM glucose and 105 mM sucrose saturated with 95% O_2 and 5% CO_2. 350 μm-thick transverse slices containing the hippocampus were cut from the tissue block with a vibratome (Microm HM 650V, Thermo Scientific, Waltham, MA) and kept in oxygenated ACSF (315 mOsm) containing 125 mM NaCl, 2.5 mM KCl, 1.25 mM NaH_2PO_4, 25 mM $NaHCO_3$, 1 mM $MgCl_2$, 2 mM $CaCl_2$ and 25 mM glucose at 34 °C for 25 min and then at room temperature until use.

Electrophysiology and data analysis

For recording, individual slices were transferred to a recording chamber perfused with oxygenated ACSF solution (same as above) at a flow rate of 1 to 2 mL/min. Whole-cell recordings were made from hippocampal cornu ammonis 1 (CA1) pyramidal neurons. Cells were first selected using oblique IR illumination with a BX51 microscope (40x water-immersion objective; Olympus, Tokyo, Japan). Subsequently, neurons were anatomically identified using a fluorescent dye (Alexa 488, 10 μM) included in the intracellular solution. The dye was excited with wLS broad-band LED illumination (488 nm) and images were acquired with Retiga R1 camera using Ocular software (Qimaging, Surrey, Canada). The cells were patched with borosilicate glass pipettes (2-5 MΩ) containing: 135 mM KCl, 10 mM HEPES, 10 mM sodium phosphocreatine, 4 mM Mg-ATP, 0.3 mM Na-GTP, pH 7.3 with KOH. Recordings were performed using Multiclamp 700B amplifier and data were acquired with a Digidata 1550A 16-bit board (all from Molecular Devices, Sunnyvale, CA). All experiments were performed at room temperature. Spontaneous inhibitory postsynaptic currents (sIPSC) were recorded from CA1 pyramidal cells clamped at a membrane voltage of -70 mV in the presence of 10 μM NBQX to block excitatory transmission. Recordings with unstable baseline or greater than -400 pA were rejected. Currents were filtered off-line using a Butterworth low-pass filter (2 kHz) and analyzed in 1 or 2 min bins using the Mini-Analysis Program 6.0.7 (Synaptosoft, Decatur, GA). For pharmacology, baseline was analyzed 2 minutes before the application of carbachol (CCh, 10 μM). To study the effect of CCh, 1-2 min bins were analyzed at least 8 minutes following the arrival of CCh into the bath. Recordings with leak increasing more than 100 pA and access resistance changing more than 30% between the beginning and the end of the recording were discarded. At least 100 events were analyzed for any condition in any experiment. Events were identified as sIPSC by setting the event detection threshold at least 2-fold the baseline noise level and by checking that events had (i) rise times faster

than the decay time, (ii) rise times greater than 0.5 ms and (iii) decay times greater than 1.5 ms. Events not fitting the above parameters were rejected. Event amplitudes, inter-event intervals, rise and decay times were first averaged within each experiment and regrouped by condition. The frequencies were calculated from the inter-event intervals and the resulting means were averaged between experiments. Single cell properties (access resistance, membrane capacitance, etc.) were analyzed with Clampfit 10.5 (Axon instruments, Union City, CA). Graphs were done using Igor 6.37 software (Wavemetrics, Tigard, OR) and Illustrator 15.1.0 (Adobe, San José, CA).

Results

Use of NEX-Cre driver line for pyramidal cell-specific DG ablation

To study the role of neuronal DGC in the brain without gross morphological alterations, it is necessary to target DG in neurons but spare glial DG. For this reason, mice harboring loxP sites in *Dag1* were crossed to the NEX-Cre driver line, which exhibits an exclusively neuronal Cre recombinase expression pattern (Goebbels et al., 2006; Satz et al., 2010). In hippocampus and neocortex, NEX promoter-mediated Cre expression is restricted to pyramidal cells, the cell type displaying most prominent DG expression in the forebrain. DG conditional knockout mice (cKO; NEX-Cre$^{Tg/+}$, *Dag1*$^{loxP/loxP}$) showed reduced size compared to control mice (NEX-Cre$^{Tg/+}$, *Dag1*$^{loxP/+}$; Figure 1A). The smaller size was reflected in reduced body and brain weight (Figure 1B and C; 25.3 ± 1.0 g [mean ± SEM] versus 18.7 ± 1.0 g, t_{28}=4.670, $p<0.001$ and 473.1 ± 5.4 mg versus 436.4 ± 6.5 mg, t_{28}=4.381, $p<0.001$, unpaired t-tests). Although cKO mice were born in Mendelian proportions, in adulthood less than the expected 25% cKO were observed due to higher lethality of cKO mice (Figure 1D). To exclude a contribution of muscular dystrophy to this phenotype because of Cre leakage in muscle cells, α-DG levels were examined by Western blotting of WGA-enriched muscle proteins. cKO mice showed similar levels of muscle α-DG as control mice (Figure 1E). As reported before, DG cKO mice retained proper lamination of hippocampus (Figure 1F) and neocortex (Figure 1G) according to NeuN and DAPI labeling (Satz et al., 2010). Cre expression was restricted to pyramidal cells in hippocampus and neocortex and was not detected in dentate gyrus granule cells of adult mice (Figure 1F and G) (Goebbels et al., 2006).

Efficiency and specificity of DG ablation was examined immunohistochemically in relevant brain regions. α-DG, β-DG and dystrophin can be detected immunohistochemically in large perisomatic clusters in CA1 pyramidal cells (Figure 2A) (Lidov et al., 1990; Knuesel et al., 1999). This characteristic immunolabeling was absent in DG cKO mice for DG and to the same extent for dystrophin, showing that dystrophin needs DG for synaptic clustering *in vivo*. In neocortex, perisomatic distribution of α-DG, β-DG and dystrophin was replaced by diffuse unspecific staining in neuropil in DG cKO mice (Figure 2B). Astrocyte endfeet are labeled prominently by antibodies to β-DG and dystrophin and this labeling was preserved in DG cKO mice, as expected from neuron-specific Cre expression (asterisks in Figure 2A and B). α-DG immunolabeling in dentate gyrus granule cells showed the same clustered distribution in both genotypes (Figure 2C). The transient NEX promoter activity in these cells during early postnatal development might not be sufficient to achieve recombination (Goebbels et al., 2006). Alternatively, loss of DG during early development might be of little consequence in adulthood because of DG expression by granule cells that were born later. To further demonstrate specificity of NEX-induced DG ablation, striatum was selected as a control region. As expected, the characteristic sparse α-DG labeling persisted in striatum of DG cKO mice (Figure 2D).

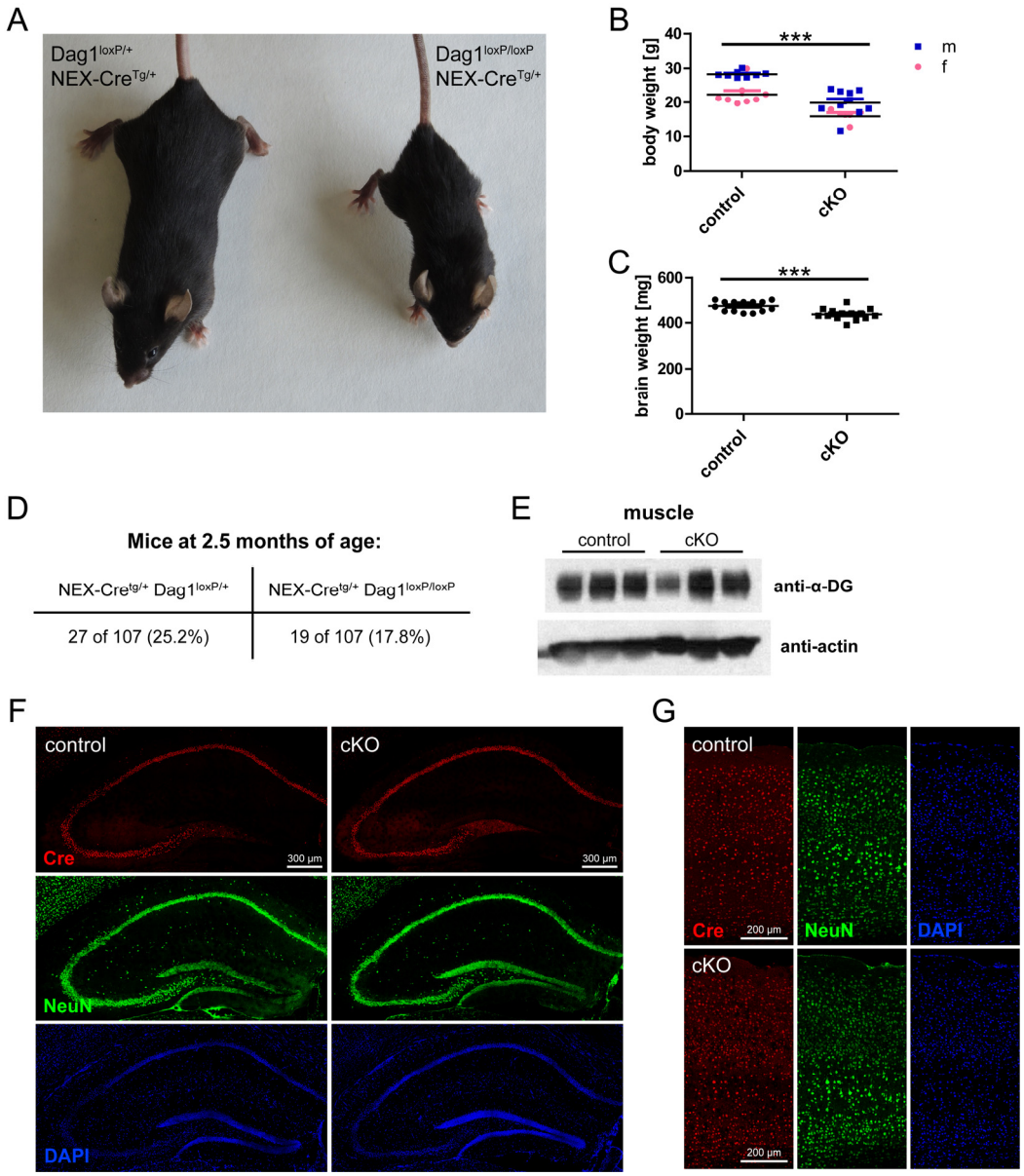

Figure 1. Characterization of NEX-Cre / Dag1 conditional KO mice.
A, Representative examples of NEX-CreTg/+ / Dag1loxP/+ (control) and NEX-CreTg/+ / Dag1loxP/loxP (cKO) mice (4 months of age, siblings, both female). B, cKO mice exhibit reduced body weight compared to sibling control mice. C, Wet brain weight was lower in cKO mice than in controls. D, cKO mice exhibited a higher mortality rate than control mice, resulting in a frequency of cKO mice lower than the expected 25% at the age of 10 weeks. E, Similar levels of α-DG isolated from cheek muscle were found for cKO and control mice. F, Cre expression was restricted to pyramidal cells in the hippocampus of cKO and control mice. In adult mice, dentate gyrus granule cells were not immunoreactive for Cre recombinase. NeuN and DAPI labeling show intact neuronal migration when NEX-Cre is used as driver line to ablate Dag1. G, In primary somatosensory cortex Cre expression was also restricted to pyramidal cells. No migratory deficits were found in the neocortex in cKO mice. ***p<0.001.

Epitope	Conditions	Unpaired t-test (density)	Kolmogorov-Smirnov test (size)
$GABA_AR$ α1 subunit	DG cKO / adult / CA1	t_6=0.920, p=0.393	n=33385, D=12.662, p<0.001
$GABA_AR$ α2 subunit	DG cKO / adult / CA1	t_{15}=3.816, p=0.002	n=18495, D=3.484, p<0.001
$GABA_AR$ γ2 subunit	DG cKO / adult / CA1	t_7=1.607, p=0.152	n=31807, D=3.692, p<0.001
Gephyrin	DG cKO / adult / CA1	t_7=1.252, p=0.251	n=39289, D=0.720, p=0.677
Neuroligin 2	DG cKO / adult / CA1	t_6=0.979, p=0.366	n=32217, D=5.476, p<0.001
synArfGEF	DG cKO / adult / CA1	t_6=1.093, p=0.316	n=22737, D=3.850, p<0.001
VGAT	DG cKO / adult / CA1	t_{15}=0.646, p=0.528	n=20569, D=0.528, p=0.943
	DG cKO / adult / neocortex	t_9=1.309, p=0.223	n=24713, D=1.107, p=0.172
Parvalbumin	DG cKO / adult / CA1	t_7=0.198, p=0.849	n=24929, D=1.068, p=0.204
	DG cKO / adult / neocortex	t_9=0.454, p=0.661	n=20534, D=4.845, p<0.001
	DG cKO / P21 / CA1	t_8=0.869, p=0.410	n=8010, D=1.037, p=0.233
Cannabinoid receptor 1	DG cKO / adult / CA1	t_6=16.869, p<0.001	n=4654, D=4.325, p<0.001
	DG cKO / adult / neocortex	t_{11}=7.117, p<0.001	n=8067, D=6.960, p<0.001
	T190M / adult / CA1	t_8=0.681, p=0.515	n=9152, D=0.881, p=0.420
Synaptotagmin 2	DG cKO / adult / CA1	t_9=1.456, p=0.179	n=3397, D=1.977, p=0.001
Cholecystokinin 8	DG cKO / adult / CA1	t_{17}=6.292, p<0.001	n=5111, D=4.133, p<0.001
	DG cKO / adult / neocortex	t_6=4.475, p=0.004	n=1387, D=1.874, p=0.002
PSD-95	DG cKO / adult / CA1 / SP	t_6=1.106, p=0.311	n=16281, D=1.554, p=0.016
	DG cKO / adult / CA1 / SR	t_6=0.243, p=0.817	-
Bassoon	DG cKO / adult / CA1 / SP	t_{10}=0.767, p=0.461	n=32489, D=2.275, p<0.001
	DG cKO / adult / CA1 / SR	t_{10}=0.871, p=0.404	-
VGluT1	DG cKO / adult / CA1	t_6=0.094, p=0.928	n=12776, D=0.492, p=0.969
VGluT3	DG cKO / adult / CA1	t_{21}=13.213, p<0.001	n=5975, D=8.273, p<0.001
	DG cKO / adult / neocortex	t_9=0.456, p=0.659	n=6523, D=2.054, p<0.001
	DG cKO / P21 / CA1	t_8=13.437, p<0.001	n=1830, D=8.270, p<0.001
	T190M / adult / CA1	t_8=0.494, p=0.634	n=4763, D=0.702, p=0.708

Table 2. Results of statistical tests performed for immunohistochemical stainings.
Numbers in subscript in t-tests represent degrees of freedom. D represents test statistics for Kolmogorov-Smirnov tests.

Epitope	Conditions	t-test (unpaired between genotypes, paired between hemispheres; density)	Kruskal-Wallis test (size)	Dunn's multiple comparison test (size)
VGluT3	28dpi / loxP/+	t_3=0.520, p=0.639	n=13610	y=283.498, p<0.05
	28dpi / loxP/loxP	t_4=2.895, p=0.044	H=55.796	y=539.294, p<0.001
	28dpi / contralateral	t_7=1.032, p=0.336	p<0.001	y=136.188, p>0.05
	28dpi / ipsilateral	t_7=2.894, p=0.023		y=391.984, p<0.001
	42dpi / loxP/+	t_4=0.870, p=0.434	n=9915	y=93.906, p>0.05
	42dpi / loxP/loxP	t_4=3.478, p=0.025	H=87.162	y=693.091, p<0.001
	42dpi / contralateral	t_8=1.040, p=0.329	p<0.001	y=82.049, p>0.05
	42dpi / ipsilateral	t_8=4.059, p=0.004		y=681.234, p<0.001
	84dpi / loxP/+	t_5=1.843, p=0.125	n=7378	y=16.550, p>0.05
	84dpi / loxP/loxP	t_3=8.578, p=0.003	H=52.415	y=466.868, p<0.001
	84dpi / contralateral	t_8=0.682, p=0.515	P<0.001	y=143.428, p>0.05
	84dpi / ipsilateral	t_8=3.495, p=0.008		y=593.745, p<0.001

Table 3. Results of statistical tests performed for immunohistochemical stainings of injected tissue.
Numbers in subscript in t-tests represent degrees of freedom. H and y represent test statistics for Kruskal-Wallis tests and Dunn's multiple comparison tests, respectively.

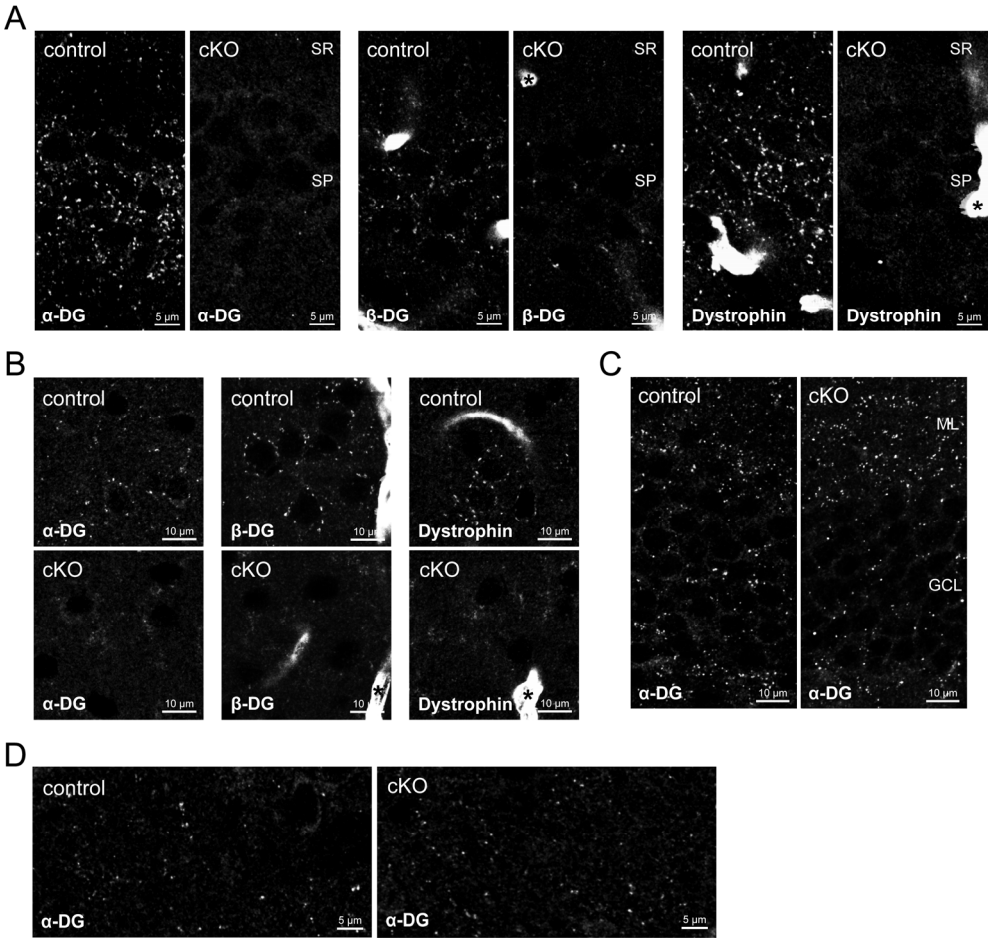

Figure 2. NEX-Cre-mediated ablation of dystroglycan leads to specific loss of dystrophin-glycoprotein complex in pyramidal cells.
A, Characteristic staining of α- and β-DG and dystrophin around CA1 pyramidal layer is lost in cKO mice. Labeling of β-DG and dystrophin in astrocyte end-feet is retained in cKO mice (asterisks). B, In primary somatosensory cortex layer 2/3, clustered labeling of DGC components around pyramidal cells is replaced by diffuse staining in the neuropil. Astrocyte end-feet labeling of β-DG and dystrophin is retained in cKO mice (asterisks). C, α-DG immunofluorescence in dentate gyrus is unaffected by NEX-Cre-mediated ablation of DG.

(Figure legend continued) D, α-DG expression in striatum is unaffected in cKO mice, confirming specificity of NEX-Cre expression to pyramidal cells. SR, stratum radiatum; SP, stratum pyramidale; ML, molecular layer; GCL, granule cell layer.

Loss of neuronal DG results in minor alterations in GABAergic PSD protein clustering

Dependence of GABAergic postsynaptic density (PSD) proteins on the DGC for synaptic clustering was suggested because of the subcellular localization of the DGC, its molecular interactions and because a reduction in $GABA_AR$ clustering was observed in mice lacking full-length dystrophin (Knuesel et al., 1999; Sumita et al., 2007; Waite et al., 2012). However, requirement of DG for clustering of GABAergic postsynaptic proteins was never systematically tested *in vivo*. We hypothesized that loss of neuronal DG affects neuroligin 2 (NL2) clustering, which might be important for clustering of $GABA_ARs$ at perisomatic synapses through its interaction with gephyrin (Poulopoulos et al., 2009; Panzanelli et al., 2011). DG cKO and control mice were analyzed for changes in clustering of these markers in CA1 pyramidal layer. As previously reported (Knuesel et al., 1999; Brunig et al., 2002; Levi et al., 2002), extensive colocalization of α-DG and dystrophin was observed with GABAergic markers, with a minority of DGC clusters showing no colocalization (Figure 3A and B; arrowheads and arrows, respectively). Visual examination of GABAergic markers revealed no obvious differences between genotypes (Figure 3A-C). However, quantification of cluster density and size showed a significant decrease of $GABA_AR$ α1 subunit size in cKO accompanied by an increase of $GABA_AR$ α2 subunit density (Figure 3D and F). No changes were observed in $GABA_AR$ γ2 subunit and gephyrin clustering (Figure 3E and H), indicating that total synaptic $GABA_AR$ content might be unchanged whereas α subunit composition is altered by loss of DG. Surprisingly, NL2 clustering was barely affected in cKO mice, showing no difference in density and only a slight but significant reduction in cluster size (Figure 3G). Neuronal DGC is also dispensable for normal colocalization of $GABA_AR$ γ2 subunit with gephyrin and of α1 subunit with NL2 (Figure 3I). Furthermore, dystrophin was suggested to be important for anchoring synArfGEF at GABAergic PSDs (Fukaya et al., 2011). Although dystrophin clustering is lost in DG cKO mice, synArfGEF distribution remained almost unchanged in CA1 pyramidal layer of cKO mice (Figure 3J).

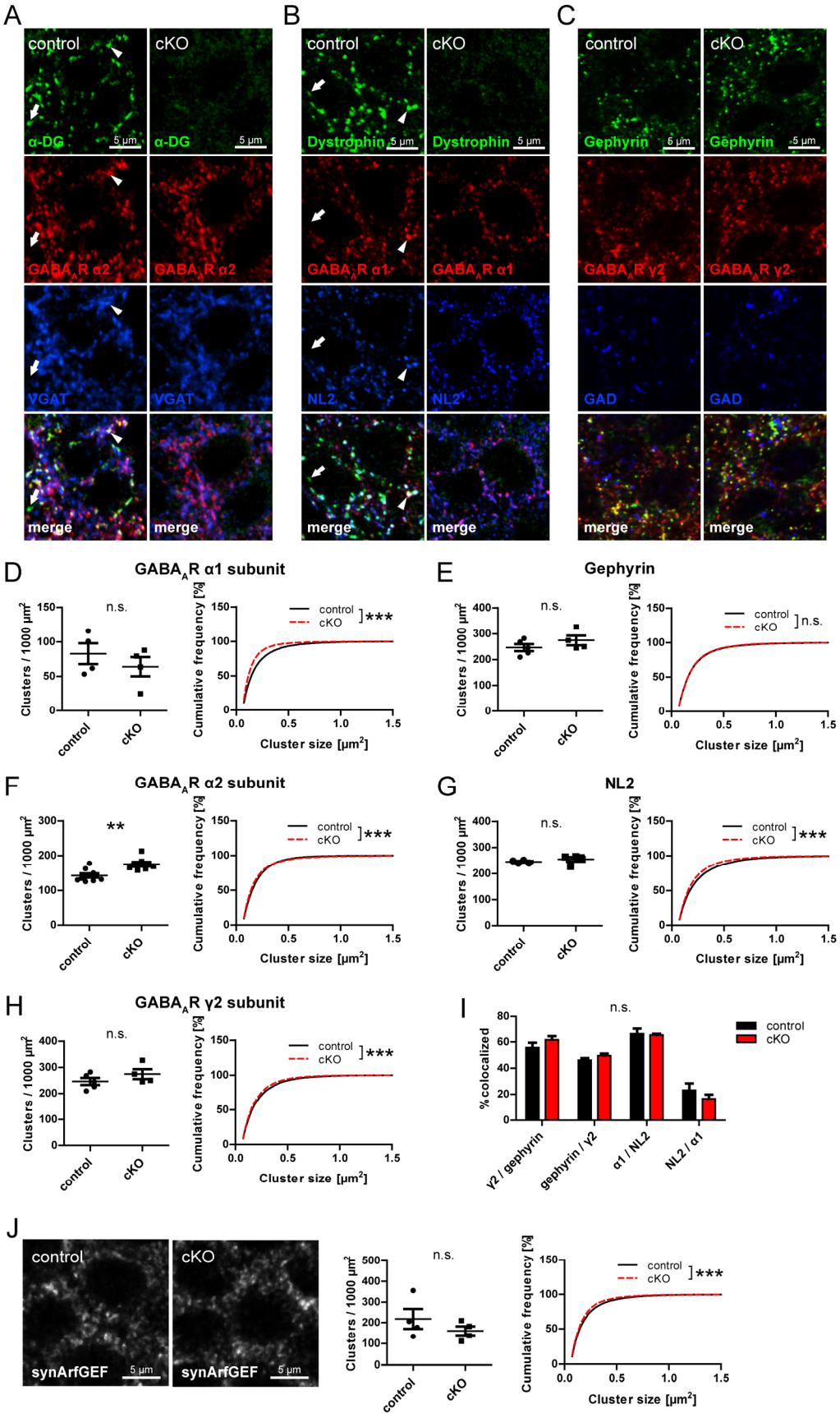

Figure 3. Loss of neuronal dystroglycan does not prohibit formation of GABAergic PSD but leads to minor changes in GABA$_A$R subunit clustering.

(Figure legend continued) A-C, Triple immunofluorescence labeling of GABAergic postsynaptic markers in pyramidal layer of hippocampus CA1 area. The DGC is largely colocalized with α2 subunit and VGAT (A; arrowheads) but also with α1 subunit and NL2 (B; arrowheads). A minority of DGC clusters is not associated with GABAergic markers (A and B; arrows). D-H, Quantification of postsynaptic GABAergic markers in CA1 pyramidal cell layer. Cluster density and size are shown for $GABA_AR$ α1 (D), α2 (F) and γ2 (H) subunits and for gephyrin (E) and NL2 (G). A decrease of α1 subunit cluster size was accompanied by an increased α2 subunit cluster density. I, Colocalization of postsynaptic GABAergic markers was analyzed in cKO and control mice. Data represent the number of colocalized clusters as percentage of first mentioned marker. No significant differences in colocalization were found between genotypes. J, Clustering of synArfGEF was analyzed in CA1 pyramidal layer of DG cKO and control mice. Data points represent individual mice. **p<0.01, ***p<0.001 (see Table 2 for statistical tests).

Neuronal DG ablation leads to selective loss of markers of CCK-positive basket cell terminals

Many binding partners of α-DG have been identified, among them the presynaptic neurexins (Sugita et al., 2001). Taken together with the observation that DG is always apposed to GABAergic presynaptic terminals in primary neuronal culture, a trans-synaptic function for DG seemed probable (Brunig et al., 2002). We therefore probed DG cKO and control brains tissue with antibodies to presynaptic GABAergic markers. Perisomatic GABAergic terminals can be attributed to parvalbumin (PV)- or cholecystokinin (CCK)-positive interneurons, which are labeled by PV / synaptotagmin 2 (Syt2) and CCK8 / VGluT3 / cannabinoid receptor 1 (CB1), respectively. We found that markers for presynaptic terminals from CCK-positive interneurons were virtually absent in CA1 pyramidal layer of DG cKO mice (Figure 4A-D, G, I and K). Still, like in control mice, CCK-positive cell somata were occasionally observed in cKO CA1 pyramidal layer, and these were often covered with VGluT3-positive boutons (arrowheads in Figure 4A). Syt2 and PV immunolabeling were still present in typical punctate distribution in the pyramidal layer of cKO mice (Figure 4A-D, H and J), demonstrating specific requirement of DG for formation of presynaptic terminals from CCK-positive interneurons. Preferential apposition of DG to CCK-positive interneuron terminals might be expected from this finding. However, apposition of DG to VGluT3 as well as to PV suggests no such distinction, at least at the resolution of conventional confocal laser scanning microscopy (arrowheads in C). Still, as percentage of presynaptic immunofluorescence apposed to DG, VGluT3 showed more complete overlap with DG, indicating PV apposition to DG might be caused by mere abundance of PV immunofluorescence in the pyramidal layer (data not shown). Loss of CCK-positive interneuron terminals extended from CA3 to CA1 (Figure 4E). Surprisingly, no corresponding reduction in VGAT puncta was observed (Figure 4F). To test if sprouting of PV-positive axons compensates for the loss of CCK-positive terminals, the portion of VGAT-positive terminals containing PV was assessed. No significant difference was found in the fraction of VGAT puncta colocalized with PV between genotypes (31.05 ± 2.05 % for control versus 33.24 ± 1.57 % for cKO, t_8=0.847, p=0.422, unpaired t-test), suggesting that PV-positive axon terminal sprouting does not account for the persisting VGAT immunolabeling.

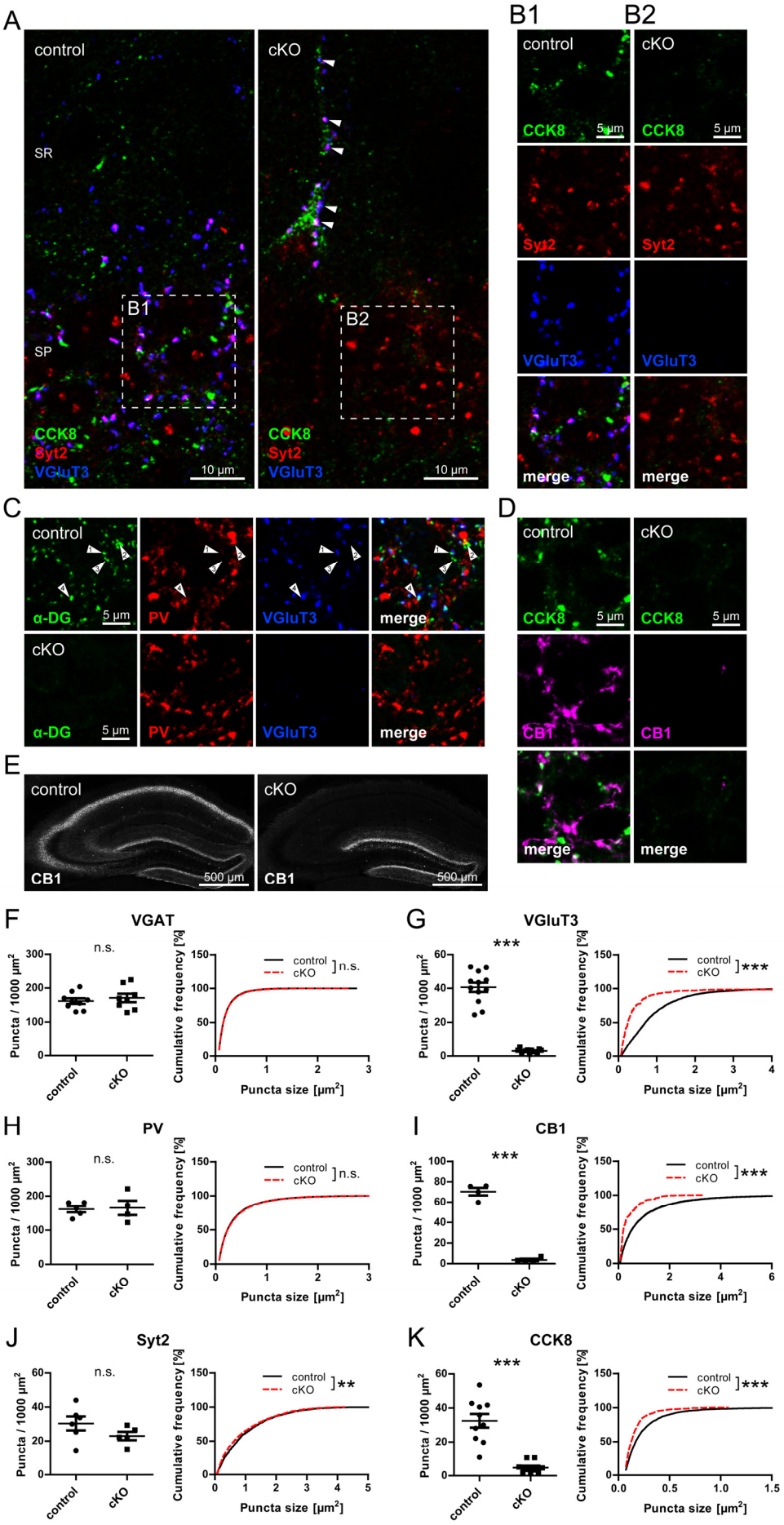
A
control
cKO
SR
SP
B1
B2
CCK8
Syt2
VGluT3
10 µm
B1
B2
control
cKO
CCK8
5 µm
Syt2
VGluT3
merge
C
control
cKO
α-DG
5 µm
PV
VGluT3
merge
D
control
cKO
CCK8
5 µm
CB1
merge
E
control
cKO
CB1
500 µm
F
VGAT
n.s.
Puncta / 1000 µm²
control
cKO
Cumulative frequency [%]
Puncta size [µm²]
G
VGluT3
***
H
PV
I
CB1
J
Syt2
**
K
CCK8

Figure 4. Neuronal dystroglycan ablation leads to specific loss of terminals from CCK-positive basket cells on hippocampal pyramidal cells.
A-D, Triple immunofluorescence labeling of presynaptic GABAergic markers in hippocampus CA1 area. A, In pyramidal layer, markers labeling CCK-positive basket cell terminals (CCK8, VGluT3) are missing around pyramidal cell bodies, but are still present on CCK-positive cell somata occasionally observed near the pyramidal layer (arrows). These VGluT3-positive boutons on CCK-positive somata were often immunopositive for synaptotagmin 2. In the pyramidal layer, immunostaining for synaptotagmin 2 remained in cKO mice. B1 and B2 show separated channels of insets in A. C, PV immunolabeling in CA1 pyramidal layer of DG cKO mice is indistinguishable from control. In CA1 pyramidal layer of control mice, the majority of α-DG clusters is either apposed to VGluT3 (arrow 1) or PV (arrow 2), but some clusters are not apposed to either marker (arrow 3). A minority of α-DG clusters showed apposition to both VGluT3 and PV (arrow 4). D, Along with CCK8 and VGluT3, CB1 staining is strongly reduced in CA1 pyramidal layer of DG cKO mice. E, Loss of CB1 immunofluorescence in DG cKO mice was observed from CA1 to CA3. F-K, Quantification of presynaptic GABAergic markers in CA1 pyramidal layer. No changes were found for VGAT (F) and PV-positive basket cell markers (H, J) between genotypes but cluster density and size of markers of CCK-positive basket cell terminals (G, I, K) were strongly reduced in DG cKO mice. Data points represent individual mice. ***$p<0.001$ (see Table 2 for statistical tests). SR, stratum radiatum; SP, stratum pyramidale.

Despite the drastic loss of CCK-positive terminals, somata exhibiting CCK immunofluorescence were observed in cKO hippocampi (Figure 4A). In order to characterize the distribution and abundance of CCK-positive interneurons, sections of cKO and control dorsal hippocampus were immunoperoxidase-stained and CCK-positive cell density quantified using stereology. CCK-positive cell somata in cKO mice were reduced to less than half the density observed in control mice (816.77 ± 28.38 mm^{-3} versus 368.51 ± 4.88 mm^{-3}, t_8=15.566, $p<0.001$, unpaired t-test). Along with cell density, immunoperoxidase staining intensity of CCK-positive cells was diminished in CA1 to CA3 region in DG cKO mice.

Because the DGC is prominently expressed by pyramidal cells in the neocortex, it seemed likely that CCK-positive interneuron terminals in neocortex are also compromised by loss of neuronal DG. Indeed, CCK8 and CB1 immunolabeling was strongly reduced in primary somatosensory cortex (S1) of DG cKO mice whereas PV staining was unchanged (apart from a minute difference in size; Figure 5). VGluT3 puncta density was not decreased in neocortex of DG cKO mice, in agreement with histological studies showing VGluT3 is present mostly in serotonergic fibers in this brain area (Figure 5B and G)(Schafer et al., 2002). As in hippocampus, reduction of CCK-positive terminals was not paralleled by a decrease of VGAT puncta (Figure 5A and E). Markers for CCK-positive terminals were reduced uniformly across all cortical layers and in all regions of the neocortex which were examined (Figure 5D).

Satz et al. (2010) have reported blunted long-term potentiation in CA1 pyramidal cells of mice with NEX-Cre-mediated DG ablation. To exclude that loss of CCK-positive interneuron terminals represents compensatory changes to large glutamatergic alterations, glutamatergic markers were examined as a proxy for integrity of glutamatergic synapses (Figure 6). Clustering of the postsynaptic glutamatergic markers PSD-95 and bassoon did not differ significantly between genotypes (Figure 6A and B) and neither did VGluT1 immunolabeling (Figure 6C). Furthermore, the portion of PSD-95 clusters apposed to VGluT1 was similar in both genotypes (Figure 6D).

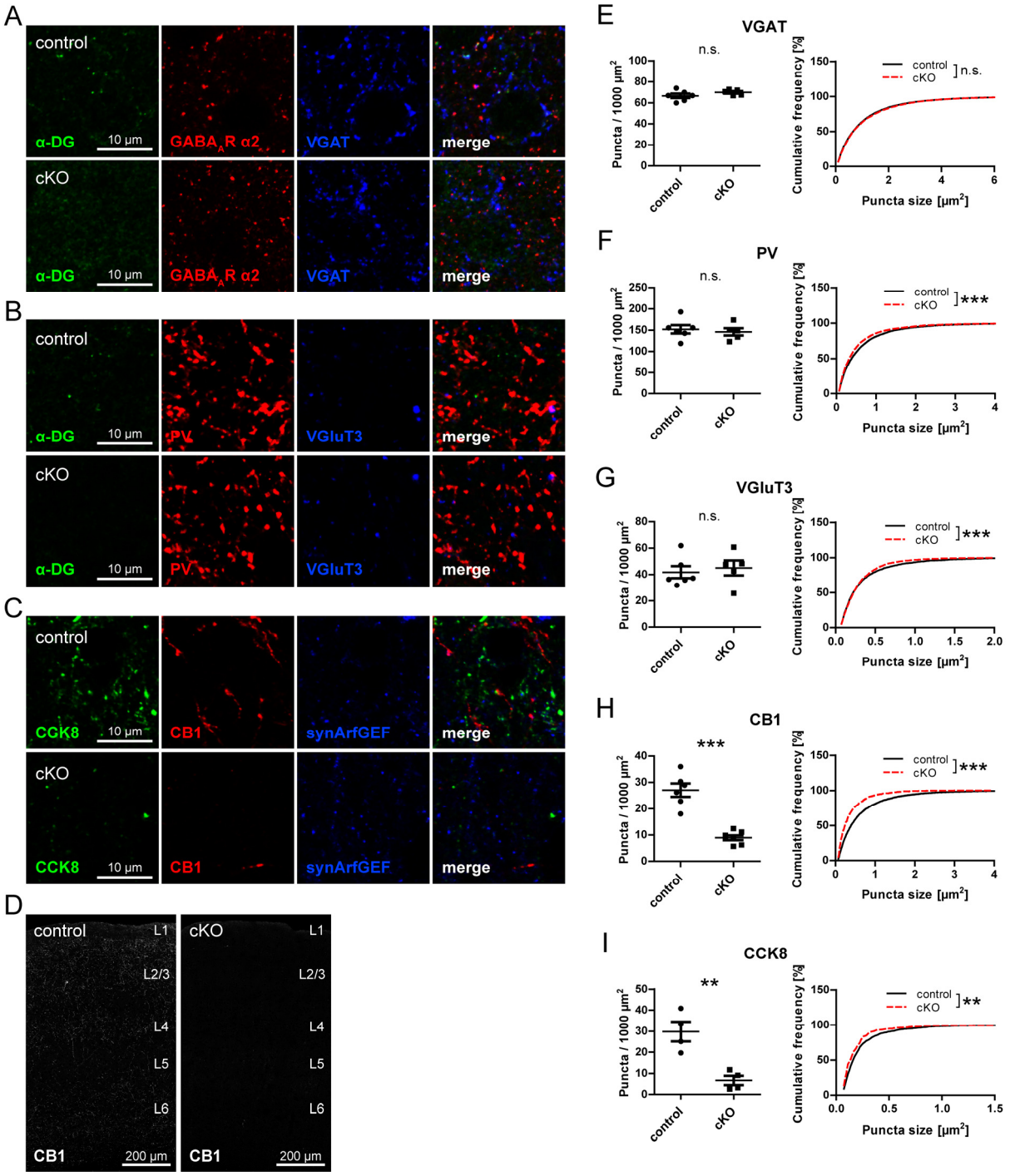

Figure 5. Neuronal dystroglycan ablation leads to specific loss of terminals from CCK-positive basket cells on pyramidal cells in neocortex.
A-C, Triple immunofluorescence labeling of GABAergic markers in layer 2/3 of primary somatosensory cortex (S1) of DG cKO and control mice. A, As in hippocampus, the majority of DG clusters is colocalized with pre- and postsynaptic GABAergic markers in neocortex. B, Neocortical PV and VGluT3 immunolabeling is not affected by loss of neuronal DG. C, CCK8 and CB1 immunofluorescence is strongly reduced in neocortex of DG cKO mice. Immunolabeling of synArfGEF showed clustered distribution and did not differ between genotypes. D, Overview of S1 of DG cKO and control mice. Typical punctate CB1 immunofluorescence was lost across all layers of the cortex in DG cKO mice. E-I, Quantification of presynaptic GABAergic markers in S1 layer 2/3. VGAT and PV, and in contrast to hippocampus, also VGluT3 were not reduced in density and size in mice lacking neuronal DG (E, F, G). However, CB1 and CCK8 showed a similar reduction as in hippocampus in DG cKO mice compared to control mice (H and I). Data points represent individual mice. **p<0.01, ***p<0.001 (see Table 2 for statistical tests).

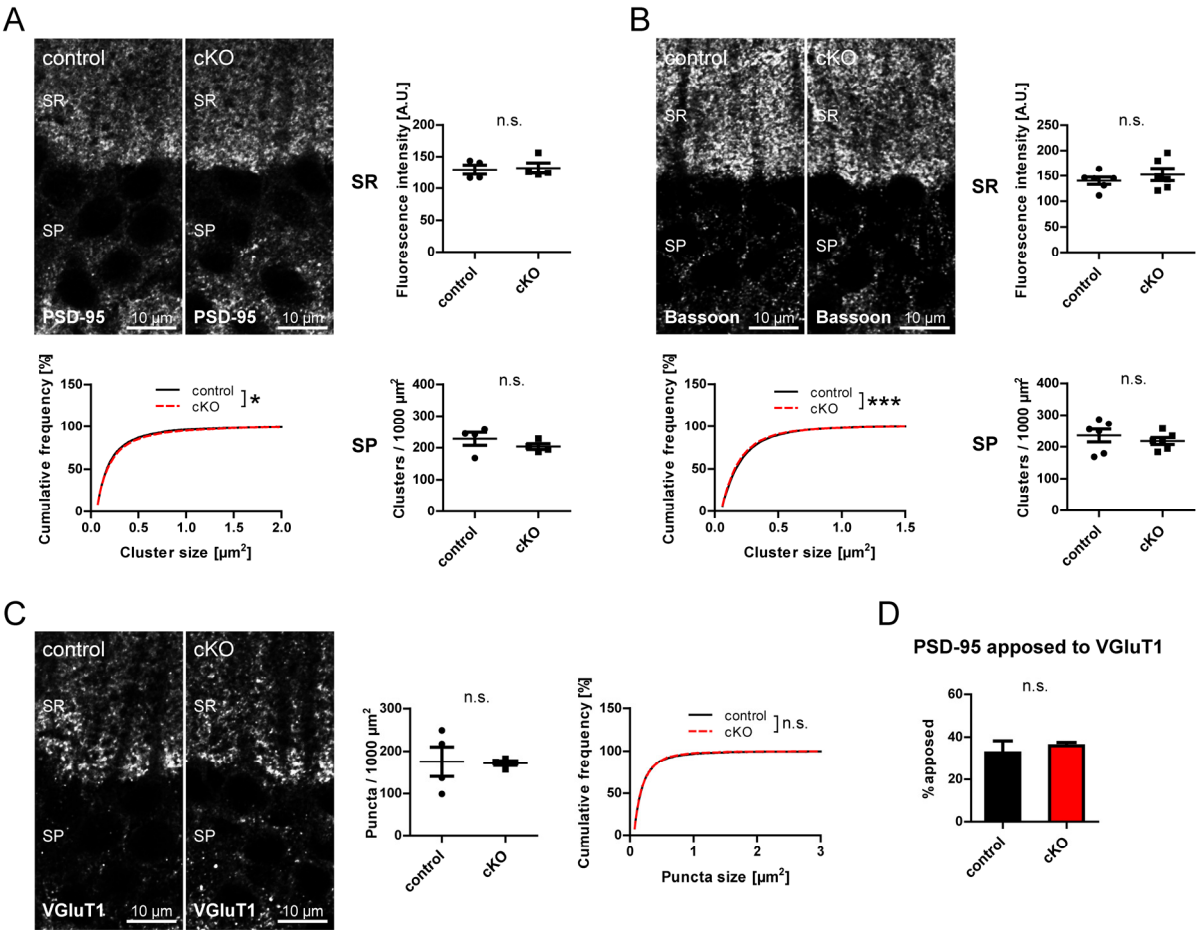

Figure 6. Neuronal dystroglycan is not necessary for clustering of glutamatergic synaptic proteins.
A and B, To assess integrity of glutamatergic postsynaptic structures, antibodies to PSD-95 and bassoon were used and immunofluorescence quantified in stratum pyramidale and stratum radiatum. Cluster density and size was analyzed in stratum pyramidale and fluorescence intensity in stratum radiatum. All parameters analyzed did not differ between genotypes. C, VGluT1 was used as a marker of glutamatergic presynaptic terminals and puncta density and size in stratum pyramidale was quantified. No changes in VGluT1 puncta density and size were found between genotypes. D, PSD-95 apposition to VGluT1 was examined in stratum pyramidale and represented as percent PSD-95 clusters apposed to VGluT1 puncta. The apposition of PSD-95 to VGluT1 did not differ between genotypes. Data points represent individual mice. *p<0.05, ***p<0.001 (see Table 2 for statistical tests).

Formation and maintenance of CCK-positive basket cell terminals require neuronal DG

DG expressed by pyramidal cells might have a function in synapse formation or in guidance of a subset of axons, similar to its role in the spinal cord (Wright et al., 2012). Alternatively, a function in maintenance of synapses through continuous trans-synaptic signaling is conceivable. If neuronal DG is crucial for synapse formation of CCK-positive terminals, these boutons should be reduced to the same degree as in adults at a time point right after initial synaptogenesis. Following this reasoning, we examined CCK-positive terminals of 21-day-old DG cKO and control mice in CA1 pyramidal layer. Indeed, VGluT3 puncta were largely missing also at this stage of development whereas immunostaining of PV-positive terminals was not significantly different between genotypes (Figure 7).

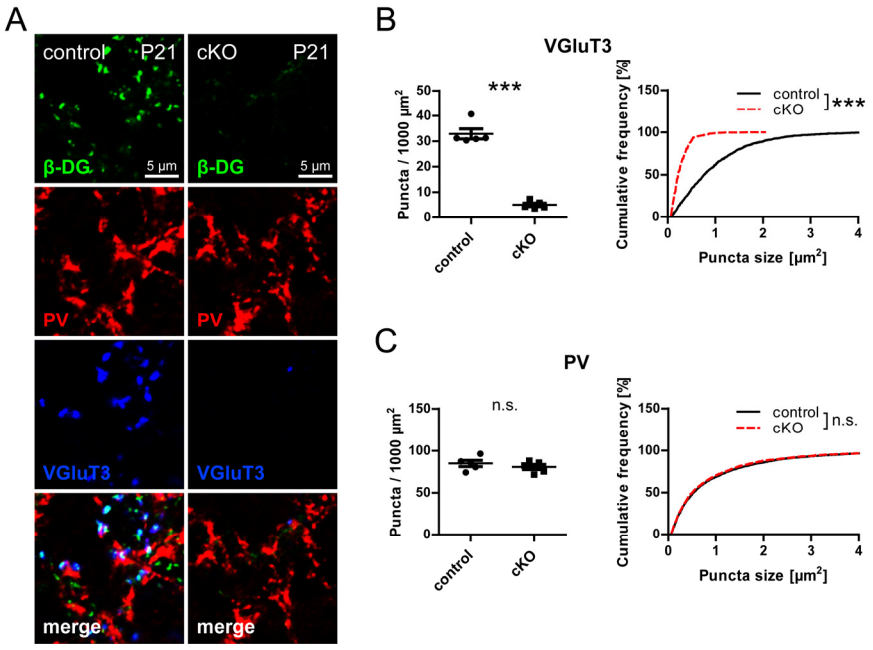

Figure 7. CCK-positive terminals are not established in the absence of neuronal dystroglycan.
A, Triple immunofluorescence labeling of DG cKO and control CA1 pyramidal layer at postnatal day 21. B and C, Quantification of puncta density and size reveals loss of VGluT3 puncta in DG cKO tissue to the same degree as in adult mice (B) but unchanged PV immunolabeling (C). Data points represent individual mice. ***p<0.001 (see Table 2 for statistical tests).

Although this finding indicates that synapse formation of functional CCK-positive terminals depends on DG, it does not rule out a role for DG in maintaining already formed connections. In order to assess this putative function of DG in synapse maintenance, we ablated DG long after developmental synapse formation, by viral delivery of Cre to adult mice carrying one or both floxed *Dag1* alleles. AAV8-CaMKII-mCherry-Cre was stereotactically injected unilaterally into the CA1 region and mice sacrificed at 14, 28, 42 or 84 days post injection (dpi; Figure 8A and C). At 14 dpi, Cre as well as mCherry fluorescence were clearly visible (Figure 8B). Loss of β-DG staining at 28 dpi in homozygously floxed mice indicated efficient recombination of loxP sites (Figure 8D). In heterozygously floxed mice only a moderate reduction of β-DG labeling was observed, suggesting one wildtype allele is sufficient to sustain the bulk of DG expression. Because dystrophin immunostaining revealed a reduction that mirrored β-DG, and in addition showed lower background, dystrophin was used to assess DGC loss at subsequent time points (Figure 8E-G). Examination of VGluT3-positive terminals at 28 dpi in Cre-expressing regions of CA1 pyramidal layer revealed a moderate but significant reduction of VGluT3 puncta density and size in homozygously floxed mice compared to contralateral side as well as compared to the ipsilateral side of heterozygously floxed mice (Figure 8H). VGluT3-positive terminals in heterozygous mice were not affected. Compromised VGluT3 immunolabeling was also found at later time points in homozygous mice, and the effect became more prominent with increased time after injection (Figure 8I and J). Together, these results provide strong evidence for a role of DG both in synapse formation and in retrograde trans-synaptic signaling for maintenance of CCK-positive terminals.

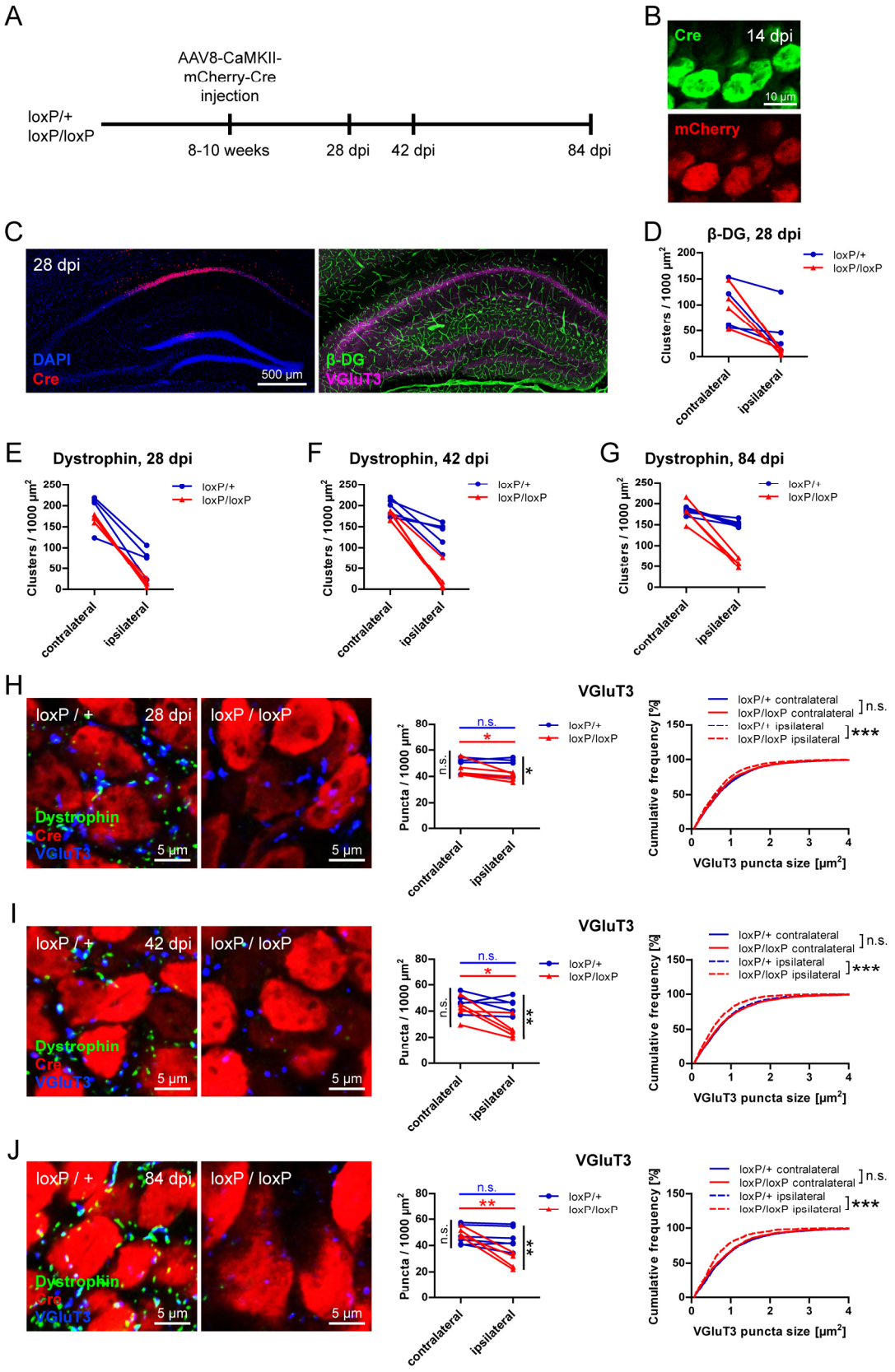

Figure 8. Maintenance of CCK-positive basket terminals requires dystroglycan.
A, Overview of experimental design. Virus was stereotactically injected unilaterally into CA1 region in adult mice heterozygous or homozygous for loxP sites flanking Dag1 gene. B, After 14 dpi, Cre recombinase immunolabeling as well as mCherry fluorescence was clearly visible in pyramidal cell somata. C, Example of injection site at 28 dpi. Cre expression was mostly restricted to CA1 pyramidal cell layer. VGluT3 and

(Figure legend continued) dystrophin or DG immunofluorescence was analyzed in the same sections. D, In mice containing homozygously floxed *Dag1*, β-DG immunostaining was markedly reduced in CA1 pyramidal layer at 28 dpi. Heterozygous mice showed a moderate reduction in β-DG immunofluorescence. E-G, As observed for β-DG, Cre expression lead to loss of dystrophin in homozygously floxed mice whereas only a slight decrease was observed in heterzygous mice. Reduction of dystrophin labeling was similar at 28 dpi (E), 42 dpi (F) and 84 dpi (G). H-J, Representative example images and quantifications of VGluT3 immunostaining in CA1 pyramidal layer at 28 dpi (H), 42 dpi (I) and 84 dpi (J). Ipsilateral VGluT3 size and density in homozygously floxed mice was significantly reduced compared to both contralateral side and ipsilateral side of heterozygously floxed mice. With increased time after injection this reduction of VGluT3 puncta became more prominent. Data points represent individual mice. *p<0.05, **p<0.01, ***p<0.001 (see Table 3 for statistical tests).

Absence of CCK-positive basket cell terminals due to DG ablation impacts pyramidal cell inhibitory input and response to cholinergic activation

If axon terminals from CCK-positive basket cells are indeed lost in DG ablated mice, this should be reflected by functional changes of pyramidal cell inhibitory input. To test this hypothesis, acute slices were prepared from adult DG cKO and control brains and used for patch-clamp electrophysiological recordings from morphologically identified CA1 pyramidal cells (Figure 9). With inhibitors of glutamatergic transmission present in the bath, occurrence of sIPSCs was probed in both genotypes. As anticipated from immunohistological changes, sIPSC frequency in DG cKO was reduced to about half of that in control slices (Figure 9; 8.71 ± 1.52 Hz versus 4.46 ± 0.90 Hz, t_{26}=2.214, p=0.036, unpaired t-test). Furthermore, DG cKO pyramidal cells were marked by a significantly smaller sIPSC amplitude than that of control cells (61.49 ± 7.90 pA versus 39.18 ± 2.39 pA, t_{26}=2.374, p=0.025, unpaired t-test). No significant differences were found between genotypes in sIPSC rise and decay times (rise time 1.73 ± 0.09 ms versus 1.63 ± 0.12 ms, t_{26}=0.664, p=0.512, unpaired t-test; decay time 14.84 ± 0.64 ms versus 14.21 ± 0.53 ms, t_{26}=0.717, p=0.480, unpaired t-test).

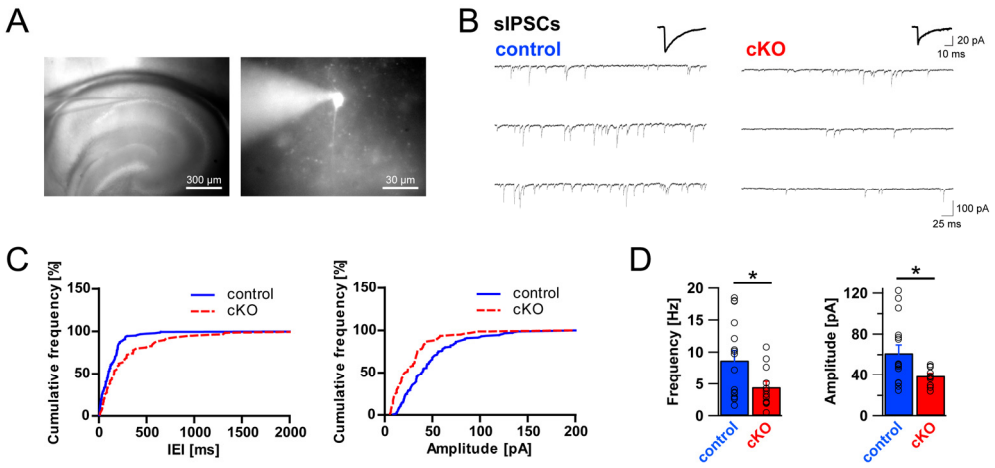

Figure 9. Frequency and amplitude of sIPSCs are reduced in dystroglycan cKO pyramidal cells.
A, Image showing the position of the recording pipette in the hippocampal CA1 region (left, 4x), and an example image of a typical CA1 pyramidal cell identified using LED illumination (Alexa Fluor 488, right, 40x). B, Representative example traces of whole-cell sIPSC recordings from control mice (left trace) and DG cKO mice (right trace). Average sIPSCs are shown above the traces. C, Cumulative frequency plot of inter-event intervals of sIPSCs from control (blue line) and DG cKO cell (red line) from the traces in B (left panel) and cumulative frequency plot of sIPSC amplitudes from the same cells (right panel). D, Comparison of average sIPSC

(Figure legend continued) frequency and amplitude between control and DG cKO slices. DG cKO mice exhibit significantly lower sIPSC frequency and amplitude than control mice. Data points represent individual cells. *p<0.05.

The differences observed in baseline sIPSCs could be due to a general reduction of inhibitory transmission instead of interneuron subtype-specific loss of terminals. In order to gain insight into the origin of reduced inhibitory transmission in DG cKO pyramidal cells, we examined the effect of the acetylcholine receptor agonist carbachol on inhibitory currents. In slices, carbachol exposure leads to an increase of perisomatic inhibitory transmission in pyramidal cells, which is mediated by direct excitation of CCK-positive interneurons (Nagode et al., 2014). Given that CB1 receptor-containing terminals are required for increased inhibitory transmission after application of carbachol, this effect should be absent in DG cKO mice, if CCK-positive basket terminals are indeed non-functional in these mice. Carbachol was bath-applied to DG cKO and control acute slices from which sIPSCs were recorded in CA1 pyramidal cells. In control slices, carbachol led to a robust increase in sIPSC frequency within minutes after application (Figure 10A-C; frequency: 6.15 ± 1.45 Hz versus 10.53 ± 2.47 Hz, t_7=3.522, p=0.010; amplitude: 63.36 ± 8.84 pA versus 70.35 ± 12.59 pA, t_7=0.943, p=0.377; paired t-tests). However, no statistically significant effect of carbachol was observed in DG cKO pyramidal cells (Figure 10D-F; frequency: 3.45 ± 0.75 Hz versus 4.47 ± 1.56 Hz, t_6=0.797, p=0.456; amplitude: 45.70 ± 4.17 pA versus 53.03 ± 5.00 pA, t_6=1.239, p=0.262; paired t-tests). Together with the results from baseline recordings and immunohistochemical analysis, these findings strongly argue that functional connectivity between CCK-containing basket cells and pyramidal cells is lost in DG-ablated mice.

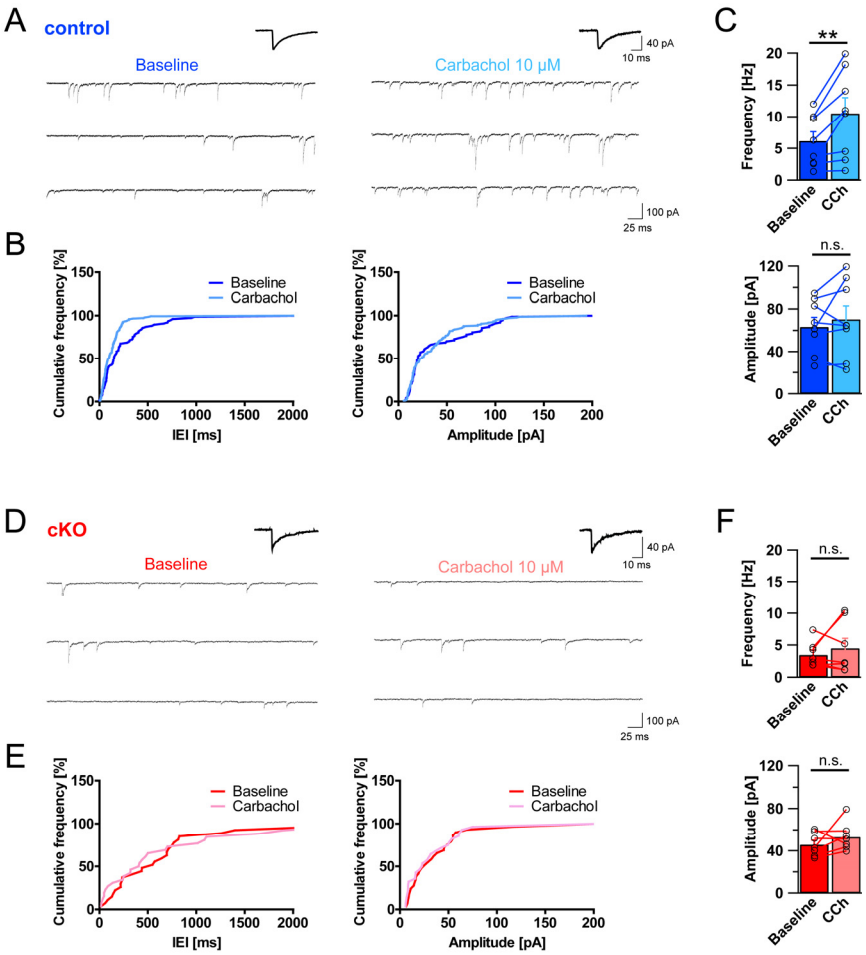

Figure 10. Dystroglycan is necessary for carbachol-induced increase of inhibitory currents in pyramidal cells.
A, Representative example traces of sIPSC recordings before (baseline, left trace) and after the application of carbachol (CCh, right trace) in control mice. Average sIPSCs are shown above the traces. B, Cumulative frequency plots of inter-event intervals (IEI) and amplitudes of sIPSCs from traces in A. C, Comparison of average sIPSC frequency and amplitude before and after application of CCh in control slices. Application of CCh resulted in typical increase of IPSC frequency in control pyramidal cells but amplitude was not affected by CCh. D, Representative example traces of sIPSC recordings before (baseline, left trace) and after the application of CCh (right trace) in DG cKO mice. Average sIPSCs are shown above the traces. E, Cumulative frequency plots of inter-event intervals (IEI) and amplitudes of sIPSCs from traces in D. F, Comparison of average sIPSC frequency and amplitude before and after application of CCh in DG cKO slices. In contrast to control slices, application of CCh did not lead to a significant increase of sIPSC frequency in DG cKO pyramidal cells. Data points represent individual cells. **p<0.01.

Persistence of CCK-positive terminals in DG T190M knock-in mice suggests trans-synaptic DG function is independent of neurexin binding

The intriguing finding that DG is required for formation and maintenance of CCK-positive terminals calls for an assessment of the clinical significance of this observation. In a subgroup of dystroglycanopathies, intellectual disability, although severe, is not accompanied by neuronal migration deficits (Godfrey et al., 2007). *Dag1* T190M knock-in mice are a model of one such form of dystroglycanopathy and resemble the symptoms found in patients with the corresponding mutation (Dincer et al., 2003; Hara et al., 2011). Interestingly, this mutation abolishes binding of DG to

neurexin, a putative presynaptic DG binding partner. We compared markers of CCK-positive terminals in CA1 pyramidal layer of homozygous *Dag1* T190M mice to wildtype mice (Figure 11). Surprisingly, both VGluT3 and CB1 puncta were indistinguishable between *Dag1* T190M and wildtype mice. Weaker and more diffuse labeling in *Dag1* T190M mice using the α-DG glycosylation-specific antibody 11H6 confirmed that this mutation affects glycosylation of neuronal DG (Figure 11B). Apposition of β-DG to PV or VGluT3-positive terminals was not changed by T190M mutation (Figure 11E). Therefore, DG function for CCK-positive terminals is likely neurexin-independent, which suggests a novel presynaptic receptor might be involved in this trans-synaptic connection.

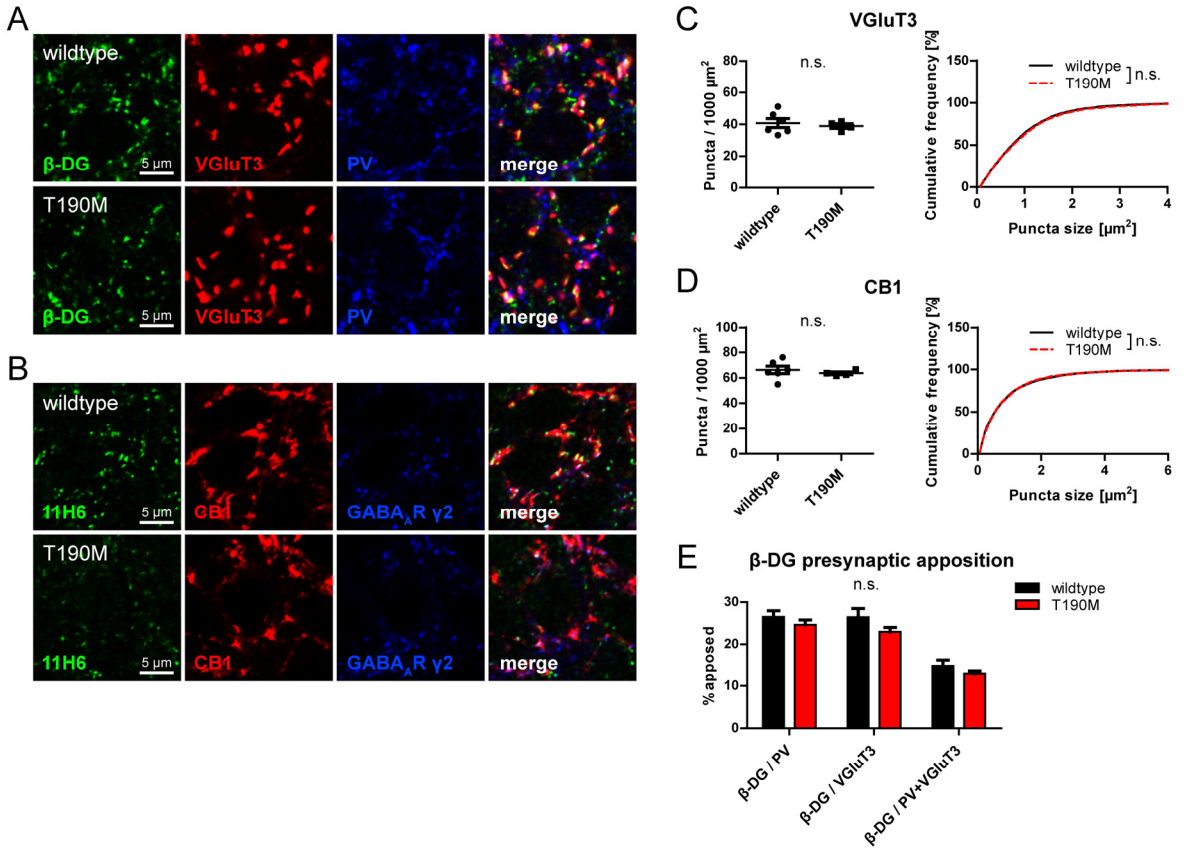

Figure 11. Neurexin- and laminin-binding of α-dystroglycan is not essential for formation of CCK-positive basket terminals on pyramidal cells.
A and B, Triple immunofluorescence labeling of GABAergic markers in CA1 pyramidal layer of *Dag1* T190M and wildtype mice. A, Antibody to β-DG revealed typical clustered distribution in *Dag1* T190M mice. VGluT3 and PV immunofluorescence was indistinguishable between genotypes. B, Intensity of DG clusters was markedly reduced and background staining increased using the α-DG glycosylation-specific antibody 11H6, confirming glycosylation deficits of synaptic DG in T190M mice. CB1 and GABA$_A$R γ2 subunit immunofluorescence was indistinguishable between genotypes. C and D, Quantification of density and size of VGluT3 (C) and CB1 (D) puncta in CA1 pyramidal layer of *Dag1* T190M and wildtype mice. Density and size of puncta did not differ significantly between genotypes. E, Quantification of β-DG apposition to PV and/or VGluT3 in CA1 pyramidal layer. Data represent number of β-DG clusters apposed to PV or VGluT3 or both (triple colocalized) as percentage of total β-DG clusters. Apposition of β-DG to presynaptic markers did not differ significantly between genotypes. Data points represent individual mice. See Table 2 for statistical tests.

Discussion

Our experiments have yielded five main findings about the synaptic function of DG. Ablation of neuronal DG, which also hindered synaptic clustering of dystrophin, led only to minor changes in clustering of GABAergic PSD proteins. These alterations might reflect compensatory changes to the massive presynaptic defects found in DG-deficient mice. Importantly, DG synaptic function is interneuron subtype-specific since loss of synaptic markers was restricted to CCK-expressing basket cell terminals. Formation and maintenance of these synapses required neuronal DG, indicating that trans-synaptic signaling is important both at the time of developmental synaptogenesis and continuously during adulthood. Function of CCK-positive basket cell terminals was likely compromised along with specific marker expression, since loss of DG resulted in a reduced baseline spontaneous inhibitory activity in pyramidal cells that could not be increased by carbachol. Finally, post-phosphorylation glycosylation of DG is not necessary for CCK-positive synapse formation because *Dag1* T190M knock-in mice showed normal CCK-positive terminals, suggesting that presynaptic receptors other than neurexins might be involved in DG trans-synaptic function.

Postsynaptic GABAergic alterations ascribed to DGC deficits may be secondary to innervation defects

Ablation of DG in primary hippocampal culture has revealed that DG is not necessary for GABAergic synapse formation and for clustering of main GABAergic PSD proteins, including $GABA_A$Rs (Levi et al., 2002). Yet, involvement of the DGC in clustering of GABAergic postsynaptic proteins was supported by several lines of evidence. Mdx mice, used as a DMD model because of their lack of full-length dystrophin, were shown to have reduced $GABA_A$R (but not gephyrin) clustering in the hippocampus CA1 region (Knuesel et al., 1999). Overexpression of a shorter dystrophin construct *in vivo* rescued the decrease of $GABA_A$R cluster density and size, adding to the notion that dystrophin loss directly caused $GABA_A$R clustering defects (Vaillend et al., 2010). Neuroligin 2 (NL2) was shown to biochemically interact with dystrophin over the intracellular synaptic scaffolding molecule S-SCAM (Sumita et al., 2007). Furthermore, a functional connection between the DGC and NL2 is suggested by the observation that in $GABA_A$R α2 subunit KO mice NL2 clustering is only compromised in dendritic but not in perisomatic areas (Panzanelli et al., 2011). The modest increase in $GABA_A$R α2 subunit density and decrease in $GABA_A$R α1 subunit size found in the present study does not correspond to the findings in mdx mice, in which both subunits cluster less efficiently than in wildtype mice (Knuesel et al., 1999; Vaillend et al., 2010). Rather, these alterations might reflect a subunit composition change because $GABA_A$R γ2 subunit clusters were not affected by ablation of DG (except for a minute reduction in cluster size, which might be a reflection of reduced $GABA_A$R α1 subunit cluster size). The finding that gephyrin clustering was unchanged in DG cKO mice further supports the conclusion that overall clustering of synaptic $GABA_A$R subunits was not influenced by neuronal DG loss. The discrepancy between our results and published data from mdx mice might be

explained by different roles of dystrophin isoforms at the GABAergic PSD. Short dystrophin isoforms still present in the mdx model might, by binding to DG, cause the reduction in synaptic $GABA_AR$ clustering. It is worth noting that the α2 subunit of $GABA_ARs$, which is localized preferentially at CCK-positive synapses (Nyiri et al., 2001), does not require the DGC or CCK-positive terminals for clustering. The DGC is thus likely involved in targeting the α2 subunit to synapses apposed to CCK-positive terminals but clustering mechanisms seem to be DGC-independent. NL2 clustering was intact in DG cKO mice, apart from a slight decrease in cluster size. Therefore, the notion of the DGC as an obligatory stabilizer of postsynaptic NL2 clustering by mutual interaction with S-SCAM does not hold. Similarly, a role for the DGC in clustering the dystrophin-interacting protein synArfGEF at GABAergic synapses was suggested (Fukaya et al., 2011). Not excluding a contribution of the DGC to synArfGEF function by clustering additional signaling proteins, synArfGEF does not rely on the DGC to form clustered, presumably synaptic structures.

In the light of the dramatic changes in GABAergic innervation due to DG loss, an indirect presynaptic contribution to reduced postsynaptic clustering in dystrophin-deficient models should be considered. This hypothesis is supported also by the finding of reduced CCK-positive basket cell markers in mdx mice, suggesting that dystrophin plays part in trans-synaptic signaling (Krasowska et al., 2014). The role of dystrophin in clustering signaling proteins at CCK-positive terminals is still unexplored, but might include retrograde signaling by nitric oxide synthase. Resolution of conventional confocal laser scanning microscopy is not sufficient to conclusively answer whether the DGC is restricted to synapses from CCK-positive basket cells. Although apposition of DG to PV- and CCK-positive terminals was found with approximately equal frequency (Figure 11E), the percentage of CCK-positive terminals apposed to DG was higher than that of PV-positive terminals (data not shown; Figure 4C and 7A). Therefore, it seems likely that the DGC localizes preferentially postsynaptic to CCK-positive terminals to regulate synapse formation and function.

Basket cell type specificity of DG function implies specificity of trans-synaptic interaction with presynaptic binding partner

The selective dependence of the CCK-containing subtype of basket cells on neuronal DG for innervating target cells is a major finding of our study and has far-reaching implications. The DGC indeed acts as a trans-synaptic complex in central synapses, suggesting that presynaptic, rather than extracellular binding partners, enable DGC function in this context. Any such presynaptic adhesion molecule would have to be specifically localized at CCK-positive terminals. Interestingly, differential splicing of neurexins in PV- and CCK-expressing basket cells was recently reported (Fuccillo et al., 2015). Transcripts lacking neurexin1α alternative splice inserts 2 and 4, which prevent α-DG binding to LSM domains 2 and 6, respectively, were only found in CCK-positive basket cells (Sugita et al., 2001; Reissner et al., 2014; Fuccillo et al., 2015). This neurexin isoform-specificity of basket cell subtypes would provide a mechanism for selective dependence of CCK-positive basket terminals on

DG. However, we found terminals from CCK-positive basket cells to be intact in *Dag1* T190M knock-in mice. DG containing the T190M mutation was found to lose neurexin binding capacity (Hara et al., 2011). This finding thus suggests that a novel presynaptic DG binding partner might be specifically localized at CCK-positive terminals. But because the diversity of neurexin isoforms was not considered in DG T190M binding assays, the possibility of a specific neurexin-DG trans-synaptic complex at CCK-positive terminals remains.

Continuous trans-synaptic signaling required for maintenance of CCK-positive terminals might reflect novel plasticity mechanism

Stopping trans-synaptic signaling mediated by the DGC by ablating DG in adulthood led to a decrease of CCK-positive terminals within weeks. This unexpected result implies that DG function goes beyond a potential role in validating newly formed synapses from CCK-positive basket cells. In addition to clustering signaling molecules at these synapses, our findings open the possibility that the DGC, by forming a trans-synaptic complex, is a direct target to regulate abundance of CCK-positive terminals. β-DG is a substrate of MMP-9 in a neuronal activity-dependent manner (Yamada et al., 2001; Kaczmarek et al., 2002; Michaluk et al., 2007). Cleavage of DG might therefore represent a physiological interneuron subtype-specific plasticity mechanism. In striking agreement with this hypothesis, CCK-positive terminals are selectively lost in a model of temporal lobe epilepsy (Wyeth et al., 2010).

Decreased inhibitory input to pyramidal cells in DG-ablated cells confirms functional significance of DG signaling for CCK-positive terminals

The possibility that loss of CCK-specific markers in DG cKO mice is only due to inability of terminals to differentiate was ruled out by the finding that DG-ablated pyramidal cells receive reduced inhibitory drive. Along with sIPSC frequency, amplitude was markedly reduced, possibly reflecting mistargeting of $GABA_A$Rs in the absence of the DGC. Genesis of carbachol-induced increase of inhibitory currents is not fully understood but involves Gad2-positive rather than PV-positive interneurons in the CA1 region (Nagode et al., 2014). Since the group of Gad2-expressing interneurons includes CCK-positive basket cells and carbachol-induced currents are sensitive to depolarization-induced suppression of inhibition, our results add to the notion that CCK-positive basket cells play a crucial role in carbachol-induced activity. Activity patterns elicited by carbachol correlate with behaviorally relevant theta oscillations. Mechanisms of theta oscillation generation should thus be considered in future investigations of the etiology of intellectual disability associated with muscular dystrophies.

Conclusions

Our investigation of the role of neuronal DG in GABAergic synapses has revealed a surprising interneuron type-specific function of DG in trans-synaptic signaling. It has shown that GABAergic

postsynaptic diversity is functionally related to interneuron subtype heterogeneity and supports the emerging notion of a cell type-specific molecular code of synapse formation. Future studies will have to further characterize signaling and plasticity enabled by the DGC and delineate its behavioral consequences. Taking the interneuron-specific role of DG into consideration will help elucidate the mechanisms underlying intellectual disability observed in muscular dystrophies without developmental brain malformations.

Acknowledgements

This work was supported by a University of Zurich Forschungskredit grant to SF, the Swiss National Science Foundation (grant 310030_146120 to JMF) and a Paul D. Wellstone Muscular Dystrophy Cooperative Research Center grant (1U54NS053672 to KPC). KPC is an investigator of the Howard Hughes Medical Institute. We thank Prof. Peter Scheiffele and Prof. Stephan Neuhauss for scientific discussion and Dr. Tatjana Haenggi and Cornelia Schwerdel for genotyping.

STUDY II: THE CATALYTIC FUNCTION OF THE GEPHYRIN-BINDING PROTEIN SYNARFGEF REGULATES NEUROTRANSMITTER-SPECIFIC MATCHING OF PRE- AND POSTSYNAPTIC STRUCTURES IN PRIMARY HIPPOCAMPAL CULTURES

Simon Früh[1,2], Shiva K. Tyagarajan[1,2], Giovanna Bosshard[1], Jean-Marc Fritschy[1,2]

[1]Institute of Pharmacology and Toxicology, University of Zurich, 8057 Zurich, Switzerland
[2]Neuroscience Center Zurich, University of Zurich and ETH Zurich, 8057 Zurich, Switzerland

Author contributions: S.F., S.K.T. and J.-M.F. designed research; S.F. and G.B. performed research; S.F., S.K.T. and J.-M.F. analyzed data; S.F. and J.-M.F. wrote the paper.

Abstract

Correct neurotransmitter-receptor matching is of fundamental importance for the function of chemical synapses. *In vivo*, temporal and spatial cues as well as trans-synaptic signaling ensure that pre- and postsynaptic specializations are appropriately matched. In dissociated neuronal cultures the absence of spatial and temporal cues causes the emergence of mismatched synapses, where GABAergic postsynaptic structures are in part apposed to glutamatergic presynaptic terminals and vice versa. This mismatch offers an opportunity to study the mechanisms that regulate correct synaptic apposition. We report here that the IQ motif and Sec7 domain-containing postsynaptic protein synArfGEF (IQSEC3; BRAG3) is specifically involved in the regulation of mismatched GABAergic PSD proteins. CRISPR-mediated ablation of synArfGEF in rat primary hippocampal neurons caused an increase in the proportion of eGFP-gephyrin clusters apposed to VGluT-positive presynaptic terminals. Overexpression of synArfGEF constructs harboring mutations that ablate Sec7 domain or IQ motif function revealed that synArfGEF catalytic activity suppresses GABAergic PSD apposition to glutamatergic terminals. Neurons co-expressing eGFP-gephyrin with synArfGEF Sec7 mutant displayed a dramatically increased fraction of mismatched eGFP-gephyrin clusters compared to other constructs. Along with eGFP-gephyrin, endogenous $GABA_A$ receptor cluster mismatching was also increased by synArfGEF Sec7 mutant overexpression. Conversely, GFP-PSD-95 clusters were unaffected by overexpression of any of the synArfGEF constructs. GABAergic PSD mismatch phenotype was recapitulated by Arf6 mutant overexpression, suggesting that Arf6 is a substrate for synArfGEF in this process. In addition, we demonstrate binding of gephyrin to synArfGEF near the IQ motif, which in turn binds calmodulin at low Ca^{2+} concentrations. N-terminal coiled-coil domain in synArfGEF was necessary for gephyrin binding and affected efficiency of calmodulin binding, indicating that synArfGEF is present in different conformational states. Dendritic aggregation of synArfGEF upon NMDA application and the presence of dendritically localized synArfGEF mRNA further suggested that synArfGEF function is activity-dependent. Taken together, these findings provide the first description of a postsynaptic protein which specifically regulates correct apposition of the GABAergic PSD.

Introduction

Alignment of presynaptic terminals of each neurotransmitter with postsynaptic densities (PSD) containing the corresponding postsynaptic receptors is a fundamental requirement for neurotransmission at chemical synapses. Most neurons in the mammalian central nervous system (CNS) are innervated by axon terminals with a wide range of neurochemical compositions and synapses employing different neurotransmitter systems are often in close proximity. Yet, mismatched pre- and postsynaptic structures are virtually absent *in vivo*. Temporal differences in synapse formation between neurotransmitter systems do not fully account for correct apposition since synapse formation and elimination are life-long processes (Tyzio et al., 1999; Khazipov et al., 2001; Caroni et al., 2014). Molecular mechanisms must therefore contribute to the fidelity of neurotransmitter-specific synaptic apposition.

Synapse formation is initiated by cell adhesion through homophilic trans-synaptic adhesion complexes, which are not neurotransmitter-specific (Missler et al., 2012). Differentiation of postsynaptic structures into specializations suited for a given presynaptic neurotransmitter is achieved after initial contact formation by signaling molecules, of which only few are known to date. One of the best described mechanisms of neurotransmitter-specific induction of postsynaptic differentiation is dependent on alternative splicing of neurexin and neuroligin (NL). For instance, isoform-specific splice inserts in NL extracellular domains interact with neurexins, promoting neurotransmitter-specific presynaptic differentiation. Thus, splice insert “B” is only present in the glutamatergic-selective NL1 and promotes glutamatergic presynaptic development (Chih et al., 2006). Likewise, the presence of neurexin splice insert 4 determines the type of postsynaptic differentiation that is promoted by neurexins. Beyond their interaction with neurexins, neuroligins are also instructive in the assembly of postsynaptic proteins. The cytoplasmic tail of NL2, which is localized mostly at GABAergic synapses, binds to gephyrin in GABAergic PSDs whereas NL1 clusters N-methyl-D-aspartate (NMDA) receptors in glutamatergic synapses (Poulopoulos et al., 2009). While other trans-synaptic molecules are known to be involved in promotion of neurotransmitter-specific differentiation, factors responsible for suppressing mismatched synaptic structures are not known thus far.

Although *in vivo* misalignment of pre- and postsynaptic structures is very rare, formation of mismatched synapses is common in dissociated neuronal cultures (Rao et al., 2000; Brunig et al., 2002; Christie et al., 2002). Both $GABA_A$ receptors ($GABA_AR$) and AMPA receptors are found opposed to inappropriate axon terminals. Appearance of mismatched synapses in dissociated cultures is a consequence of the lack of spatial and temporal cues that guide synapse formation *in vivo*. However, although the altered situation in dissociated neurons does not directly correspond to the situation *in vivo*, the presence of mismatched synapses in neuronal cultures provides an opportunity to study the molecular underlinings of synapse validation. The observation that the fraction of mismatched synapses in primary neurons is reduced with time in culture suggests that correction

mechanisms ensure appropriate apposition after synapse formation. Since drugs affecting synaptic transmission have a strong influence on the abundance of mismatched synapses, such mechanisms are likely activity-dependent (Anderson et al., 2004).

SynArfGEF (IQSEC3; BRAG3) is a guanine nucleotide exchange factor (GEF) for small GTPases of the ADP-ribosylation factor (Arf) family and is strongly expressed in the brain (Kikuno et al., 1999). The protein was first described as part of the glutamatergic PSD because of immunoreactivity in the PSD fraction and the presence of a C-terminal PDZ-domain binding motif (Inaba et al., 2004). Later investigations concluded that synArfGEF is principally located at GABAergic postsynaptic sites, on the basis of immunohistochemical analyses on light and electron microscopy levels and due to its binding to dystrophin (Fukaya et al., 2011; Sakagami et al., 2013). As all Arf GEFs, synArfGEF contains a catalytic Sec7 domain. The specificity of its GEF function is still unclear, since rat synArfGEF showed activity for Arf6 but not Arf1 whereas the opposite was reported for the human homolog (Hattori et al., 2007; Fukaya et al., 2011). Interestingly, the close synArfGEF homologs IQSEC1 and IQSEC2 are located in the glutamatergic PSD and regulate endocytosis of GluA2- and GluA1-containing AMPA receptors, respectively (Scholz et al., 2010; Myers et al., 2012). SynArfGEF functions at the synapse were not yet described but the nearly identical domain structure of synArfGEF suggests parallels in its role at the GABAergic PSD.

Here, we explored the molecular mechanisms governing the correct alignment of pre- and postsynaptic structures in primary neuronal cultures. In particular, we addressed the question whether a postsynaptic protein like synArfGEF is capable of regulating mismatched postsynaptic proteins and whether such regulation is neurotransmitter-specific. Because it is well established that neuronal activity plays a crucial role in synapse formation, the involvement of activity-dependent processes in regulation of mismatched synapses was considered. By taking an overexpression approach using various mutated and truncated forms of synArfGEF, we demonstrate that the catalytic function of synArfGEF specifically controls misalignment of GABAergic PSD proteins with glutamatergic axon terminals. Similar alterations in mismatched synapses were found with overexpression of Arf6 mutants, suggesting that activation of Arf6 by synArfGEF is an essential step in this pathway. Colocalization and biochemical interaction with gephyrin validated the proximity of synArfGEF to GABAergic postsynaptic structures. Furthermore, the findings of Ca^{2+}-dependent calmodulin binding to synArfGEF and alterations in synArfGEF distribution upon NMDA treatment confirmed the notion that regulation of mismatched synapses is an activity-dependent process. Taken together, our experiments uncovered a neurotransmitter-specific process aimed at controlling mismatched GABAergic postsynaptic proteins in primary neuronal cultures.

Materials and methods

Constructs

pCIneo-FLAG-synArfGEF plasmid was provided by Dr. Hiroyuki Sakagami and encodes FLAG-tagged rat synArfGEF (IQSEC3; NCBI NM_207617.1). The insert was PCR amplified and subcloned into the same vector using restriction sites EcoRI and NotI to avoid double insertion and remove part of synArfGEF 3'-UTR which was present in the original plasmid. Site-directed mutagenesis of the resulting plasmid was achieved through whole-plasmid amplification using point-mutated primers with Pfu Ultra Hotstart DNA Polymerase (Agilent, Santa Clara, CA). Template was digested with DpnI, DNA purified with GenElute PCR Clean-up kit (Merck, Darmstadt, Germany) and electrocompetent *E. coli* were transformed with purified mutated plasmids. Inserts were validated by control digestion and by sequencing. ΔPH deletion construct was created by whole-plasmid amplification with Pfu Ultra Hotstart DNA polymerase using 5'-phosphorylated primers on either side of PH domain. Truncations were created by PCR amplification synArfGEF regions and subcloning into pCIneo-FLAG vector using restriction sites EcoRI and NotI. For mCherry-synArfGEF fusion constructs, FLAG sequence was removed in pCIneo-FLAG-synArfGEF constructs using restriction sites NheI and EcoRI and replaced by directional cloning of PCR-amplified mCherry containing restriction sites NheI at 5'-end and EcoRI at 3'-end. For targeting synArfGEF by CRISPR-mediated gene modification, pCMV-Cas9-RFP all-in-one plasmids were purchased from Merck. These plasmids allow the combined expression of Cas9 and RFP under the control of the CMV promoter and the expression of the following gRNA under the control of the U6 promoter: gRNA 1 5'-CGTCTAGACGAGCTGAGCGCGG-3', gRNA 2 5'-GCGGCCCAGGAACCGCTTCAGG-3'. Both gRNAs target exon 1 of IQSEC3 and exhibit 100% homology between rat and mouse. The identical pCMV-Cas9-RFP plasmid without gRNA expression was used as a control plasmid.

HEK cell transfection

HEK293T cells were kept in Dulbecco's Modified Eagle Medium (DMEM; Thermo Fisher Scientific, Waltham, MA) containing 10% fetal calf serum (FCS) at 37 °C in 5% CO_2. Prior to transfection, HEK cells were passaged and grown to approximately 60% confluency. Medium was replaced with fresh DMEM containing 10% FCS 2 h before transfection. A total of 3 µg of DNA was mixed with polyethylenimine (PEI) in 150 mM NaCl solution to a final PEI concentration of 75 µg/mL. After a 30 min incubation at room temperature (RT), the mix was added dropwise to HEK cells. HEK cells were kept in culture for 24 h before lysis.

Western blotting

HEK cells were rinsed carefully with ice-cold PBS and lysed in 50 mM Tris (pH 7.6), 120 mM NaCl, 0.5% NP-40 containing protease inhibitors (Complete Mini Protease Inhibitor Cocktail [Roche, Basel, Switzerland]) by shaking on a compensator for 20 min at 4 °C. Lysates were centrifuged at 20'000

RPM for 20 min at 4 °C and supernatants were stored at -80 °C. Samples were mixed with Laemmli buffer, boiled at 90 °C and run on tris-glycine polyacrylamide gels. Proteins were transferred to polyvinylidene fluoride (PVDF) membranes. Primary antibodies were incubated in tris-buffered saline with 0.05% Tween 20 (TBST) including 5% Western Blocking Solution (Roche) ON at 4 °C. Membranes were washed 5 times in TBST. Horseradish peroxidase-coupled donkey secondary antibodies (1:20'000) were incubated for 1h at RT and membranes were washed again 5 times in TBST. SuperSignal West Pico Chemiluminescent Substrate (Thermo Fisher Scientific, Waltham, MA) was applied and membranes were developed on X-ray film (Fujifilm, Tokyo, Japan).

Immunoprecipitation

HEK cell lysates were incubated with 1 µg of immunoprecipitation antibody on a rotator for 3 h at 4 °C. Protein G-agarose (for immunoprecipitation antibodies raised in mouse) or protein A-agarose (for immunoprecipitation antibodies raised in rabbit) beads in EBC buffer (50 mM Tris, 120 mM NaCl, 0.5% NP-40) were added to lysates and the samples rotated again for 1 h at 4 °C. After a wash in high salt buffer (50 mM Tris, 500 mM NaCl, 1% NP-40), the beads were washed twice with EBC buffer. Immunoprecipitates were eluted from beads by heating to 90 °C in Laemmli buffer for 3 min.

Primary hippocampal cultures

Pregnant Wistar rats were anaesthetized at E18 with isoflurane (Attane; Piramal, Mumbai, India) and sacrificed by cervical dislocation. Embryonic hippocampi were dissected on ice. Care was taken not to contaminate hippocampi with neocortical cells. After digestion of tissue with 0.5 mg/mL papain and 10 µg/mL DNase I for 15 min at 37 °C, cells were dissociated by gently mixing with a Pasteur pipette. Cells were diluted in DMEM + GlutaMAX-I (Thermo Fisher Scientific) including 10% FCS, 2 mM L-glutamine, 0.1 mg/mL gentamicin and 2.5 µg/mL fungizone and plated on poly-L-lysine-coated coverslips at a density of approximately 35'000 cells per coverslip. After 2 h incubation at 37 °C / 5% CO_2, coverslips were transferred to 12-well dishes containing cell culture medium (15 mM HEPES, 15% NU serum [Corning Incorporated, Corning, NY], 0.45% glucose, 1 mM Na-pyruvate, 2 mM L-glutamine and B27 [1x; Thermo Fisher Scientific] in Minimum Essential Medium [Thermo Fisher Scientific]) and returned to the incubator until use.

Transfection of cultured neurons

Opti-MEM medium (Thermo Fisher Scientific) was mixed with 500 ng of endotoxin-free DNA per plasmid and coverslip to be transfected. After a 5 min incubation of lipofectamine 2000 (Oz Biosciences, Marseille, France) in Opti-MEM, the mix was added to the DNA solution for a final dilution of 1:30. Magnetofection reagent (Oz Biosciences) was added at a final dilution of 1:300 to the DNA / lipofectamine 2000 mixture and the solution was incubated at RT for 15 min. The transfection solution was added dropwise to coverslips in 1 mL of cell culture medium and cells incubated at 37 °C

/ 5% CO_2 for 40 min. Coverslips were transferred to 1 mL of conditioned medium and returned to the incubator until use.

Treatments of cell cultures

Compounds were added to cell culture medium and cells returned to the incubator until fixation for the following durations: Ionomycin (5 μM) for 3 min, N-methyl-D-aspartate (NMDA; 30 μM) for 30 min, (2*R*)-amino-5-phosphonopentanoate (AP5; 50 μM) for 30 min, (S)-3,5-dihydroxyphenylglycine (DHPG; 100 μM) for 30 min, tetrodotoxin (TTX; 1 μM) for 24h.

Immunocytochemistry

Following a quick rinse in PBS to remove residual cell culture medium, cells were fixed immediately in 4% PFA in PBS for 10 min at RT. Coverslips were rinsed again in PBS and cells permeabilized in PBS containing 10% normal goat serum (NGS) and 0.15% Triton X-100 for 5 min. Cells were incubated with primary antibodies diluted in PBS containing 10% NGS for 90 min at RT. After washing coverslips 3 times in PBS for 5 min under agitation, cells were incubated with secondary antibodies diluted in PBS for 45 min. Secondary antibodies were raised in goat and were coupled to the following fluorophores: Alexa Fluor 488 (1:1000; Jackson ImmunoResearch, West Grove, PA), Cy3 (1:500; Jackson ImmunoResearch), Alexa Fluor 647 (1:1000; Jackson ImmunoResearch). Coverslips were washed 3 times in PBS for 5 min under agitation, dried and mounted with Fluorescence Mounting Medium (Dako, Carpinteria, CA).

Image acquisition and analysis

All specimens were imaged using confocal laser scanning microscopy (LSM 700 and LSM 710, Carl Zeiss, Oberkochen, Germany). Images were taken using a 40x objective with a numerical aperture of 1.4 and had a pixel size of 112 x 112 nm^2. For quantification of synaptic markers, individual dendrites were framed by a region of interest with 2.5 μm thickness and clusters quantified by an automated macro in ImageJ (NIH, Bethesda, MD). To determine apposition of pre- and postsynaptic clusters, presynaptic marker size was enlarged by 1 pixel and colocalization with postsynaptic marker sampled. All imaging and quantification parameters were kept constant between conditions.

Antibodies

Primary antibodies used in Western blots: Mouse anti-FLAG (1:5000; clone M2; Merck), rabbit anti-GFP (1:5000; Synaptic Systems, Göttingen, Germany), rabbit anti-mCherry (1:1000; Abcam, Cambridge, UK). Primary antibodies used for immunocytochemistry: Mouse anti-FLAG (1:5000; clone M2; Merck), rat anti-hemagglutinin (HA; 1:2000; clone 3F10; Roche), mouse anti-gephyrin (1:1000; Synaptic Systems), guinea pig anti-$GABA_AR$ α2 subunit (1:5000; (Fritschy and Mohler, 1995)), guinea pig anti-$GABA_AR$ γ2 subunit (1:5000; (Fritschy and Mohler, 1995)), rabbit and guinea pig anti-synArfGEF (both 1:1000; gift from Dr. Hiroyuki Sakagami (Fukaya et al., 2011)), rabbit anti-

VGAT (1:3000; Synaptic Systems), rabbit anti-VGluT1 (1:5000; Synaptic Systems), rabbit anti-VGluT2 (1:5000; Synaptic Systems).

Calmodulin binding assay

HEK cells transfected with FLAG-tagged synArfGEF constructs were lysed in the presence of either 2 mM $CaCl_2$ or 2 mM EGTA. To avoid decreasing $CaCl_2$ or EGTA concentrations in further steps in the assay, all solutions before elution contained either 2 mM $CaCl_2$ or 2 mM EGTA. After sparing a sample of each lysate as loading control, lysates were mixed with Calmodulin Sepharose beads (GE Healthcare, Little Chalfont, UK) and incubated on a rotator for 3 h at 4 °C. Beads were washed 3 times in 50 mM Tris, 150 mM NaCl, 1% Triton X-100 containing protease inhibitors (Complete Mini Protease Inhibitor Cocktail [Roche]). For elution, beads were incubated in 50 mM Tris, 150 mM NaCl containing high concentration of the opposite condition (10 mM EGTA or 10 mM $CaCl_2$) for 30 min at RT on a rotator. Supernatant containing pull-down proteins was mixed with Laemmli buffer, heated to 90 °C for 3 min and used for Western blot analysis.

Fluorescence *in situ* hybridization

Primary hippocampal cultures were transfected with plasmids encoding FLAG-tagged synArfGEF and a GFP marker at days *in vitro* (DIV) 12. At DIV 19, cells were fixed with 4% PFA in PBS for 15 min at RT. The following steps were performed using QuantiGene ViewRNA ISH Cell Assay (Affymetrix, Santa Clara, CA) according to the manufacturer's instructions. Cells were permeabilized using "Detergent Solution QC" for 5 min at RT. IQSEC3 transcripts were detected with Type 1 probes, whereas NLGN2, GPHN and ARHGEF9 probes were Type 6 probes. This allowed detection of IQSEC3 signal with peak intensity at 550 nm together with detection of other probes at 650 nm. Probes were incubated for 3 h at 40 °C and PreAmplifier, Amplifier as well as Label Probe Mix were incubated for 40 min at 40 °C. Coverslips were mounted with Fluorescence Mounting Medium (Dako).

Results

Gephyrin interacts with synArfGEF near its IQ motif

SynArfGEF was described as a dystrophin-interacting protein because of its capability to bind dystrophin WW domains and due to the colocalization of both proteins in primary hippocampal neurons (Fukaya et al., 2011). Immunohistochemical analyses of brain and retina sections, however, have revealed a distribution pattern reminiscent of more broadly distributed GABAergic postsynaptic proteins, such as gephyrin (Fukaya et al., 2011; Sakagami et al., 2013). For this reason, we probed synArfGEF-gephyrin interaction in heterologous cells. According to known functions of domains found in synArfGEF homologs, mutations and truncations of synArfGEF were generated (Figure 1A). First, synArfGEF interaction with gephyrin domains was assessed. Full-length synArfGEF was expressed together with full-length gephyrin, gephyrin GC- or E-domain in HEK293T cells and lysates used for co-immunoprecipitation assays. Full length gephyrin and its GC-domain but not E-domain were found to co-immunoprecipitate with synArfGEF (Figure 1B). To gain insight into the site of gephyrin interaction on synArfGEF, synArfGEF constructs were used in interaction assays together with enhanced green fluorescent protein (eGFP)-tagged full-length gephyrin (Figure 1C-F). Mutation of the IQ motif (I318A/Q319A/R323A), a serine residue undergoing phosphorylation (S348), the catalytically essential glutamate residue in Sec7 domain (E749K) or the dystrophin-interacting PP motif (P1165A/P1166A/Y1168A) had no effect on gephyrin binding efficiency (Figure 1C-D)(Cherfils et al., 1998; Trinidad et al., 2006; Fukaya et al., 2011; Myers et al., 2012). Interaction with gephyrin was also retained when using a synArfGEF construct lacking the pleckstrin homology (PH) domain. However, deletion of the first N-terminal 181 amino acids in synArfGEF caused a drastic reduction of eGFP-gephyrin detected in the immunoprecipitate (Figure 1D). In order to determine the minimal domain requirement of synArfGEF for gephyrin interaction, synArfGEF truncations were made and their binding assessed. Surprisingly, the domain containing the IQ motif was sufficient for gephyrin binding but the coiled coil (CC)-containing N-terminal part alone was not able to bind gephyrin (Figure 1E-F). Within the IQ motif containing domain, the region close to the IQ motif was found to bind gephyrin whereas the region close to the Sec7 domain did not. Expression of an intermediate region (IQ fragment 2; Figure 1A) and of the isolated Sec7 domain was not strong enough to assess binding capability to gephyrin. Together, these results show that synArfGEF binds to gephyrin near the IQ motif and that the N-terminal CC domain is required for efficient binding.

Figure 1. SynArfGEF interacts with gephyrin G- or C-domain near the IQ motif.
A, Schematic overview of synArfGEF constructs and summary of gephyrin interaction results. Binding to gephyrin is indicated by "+", "(+)" indicates weaker binding compared to wildtype synArfGEF and "-" indicates absence of binding. B-F, Representative Western blots of co-immunoprecipitation (co-IP) experiments performed to assess synArfGEF interaction with gephyrin. In all experiments constructs were expressed in HEK293T cells and lysates used for co-IP using mouse anti-FLAG antibody bound to agarose beads. Two negative controls were employed to exclude unspecific binding. Anti-FLAG antibody was replaced by unspecific mouse IgG but both constructs were expressed. In addition, the construct to be immunoprecipitated was not expressed but immunoprecipitation antibody was present. B, GFP-tagged full-length gephyrin as well as gephyrin CG-domain was co-immunoprecipitated with FLAG-tagged synArfGEF. For gephyrin E-domain, no

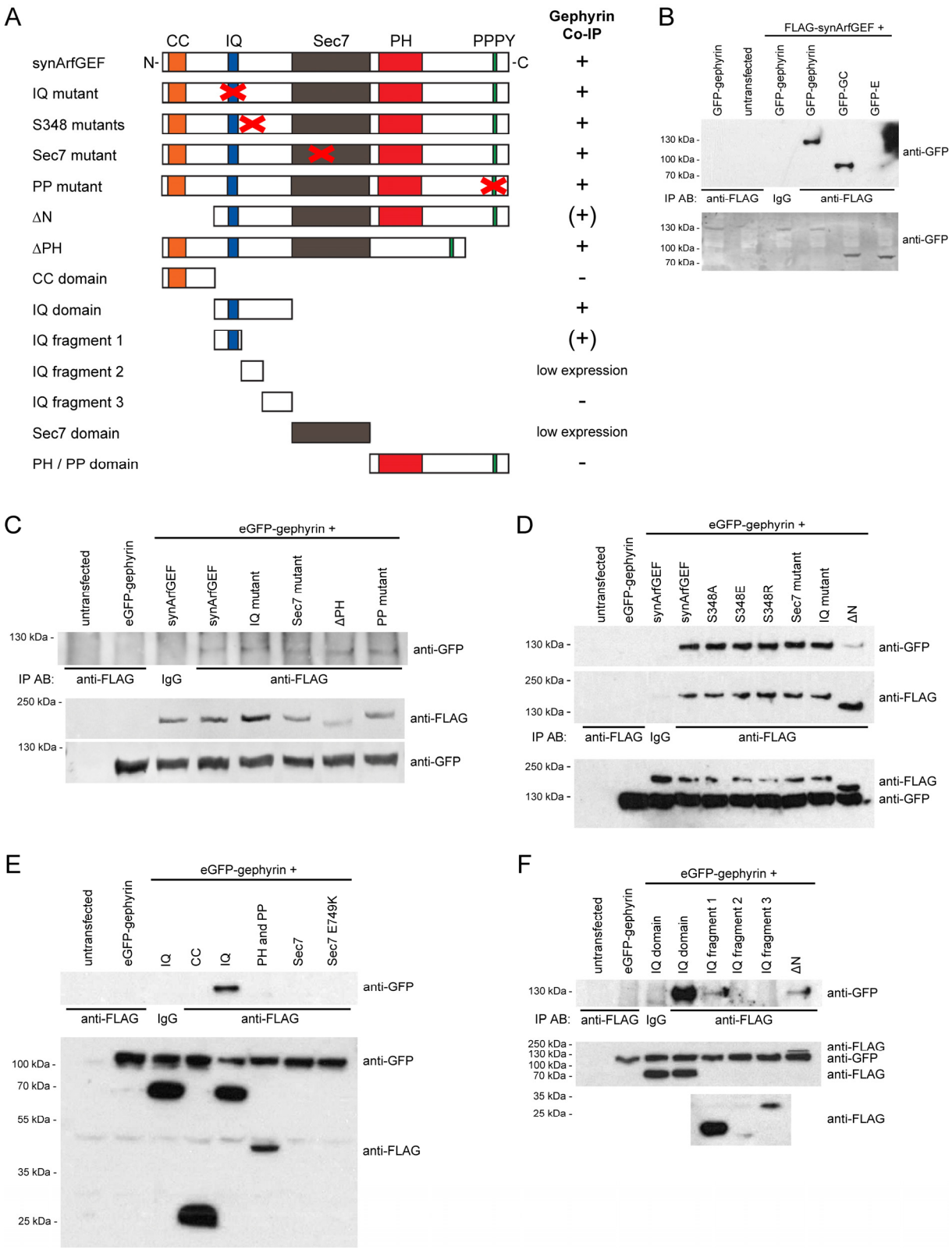

(Figure legend continued) GFP-immunoreactive band was found after immunoprecipitation. C, Mutation of IQ motif, Sec7 catalytic domain and PP motif as well as deletion of PH domain do not hinder binding of synArfGEF to gephyrin. D, Mutation of synArfGEF S348 does not affect binding to gephyrin but N-terminal CC domain is necessary for efficient interaction with gephyrin. E, IQ domain is sufficient for gephyrin binding and CC domain, which is missing in N-terminal deletion, itself does not bind gephyrin. For constructs encoding Sec7 domain and Sec7 domain containing E749K mutation expression in HEK293T cells was too week to assess interaction by co-IP. F, Gephyrin binds to region near IQ motif in synArfGEF. Only IQ fragment 1 was detected in immunoprecipitates but not IQ fragment 3. Expression of IQ fragment 2 in HEK293T cells was too weak to assess binding to gephyrin.

CRISPR-mediated gene ablation reveals a role of synArfGEF in regulation of gephyrin presynaptic apposition

The extensive colocalization with GABAergic PSD proteins, biochemical interaction with gephyrin and the function as an Arf6 GEF suggested an important role for synArfGEF in regulation of the GABAergic PSD. Strategies to ablate synArfGEF function were thus explored. Downregulation of synArfGEF levels through RNA interference (RNAi) was not successful, despite testing of multiple published and unpublished shRNA sequences (Bloodgood et al., 2013). For this reason, synArfGEF was targeted at the genomic level through clustered regularly interspersed short palindromic repeats (CRISPR)-mediated gene modification. Two guide RNA (gRNA) sequences were designed, targeting exon 1 of the IQSEC3 (synArfGEF) gene to maximize chances of ablation of a functional gene product. Together with Cas9 and RFP, gRNAs were expressed from single plasmids transfected in rat primary hippocampal neurons at DIV 8. To allow sufficient time for functional consequences of potential gene ablation, cultures were analyzed at DIV 22 (Incontro et al., 2014).

Figure 2. CRISPR-mediated synArfGEF ablation reveals a role in regulation of gephyrin apposition.
A-B, Validation of CRISPR-mediated synArfGEF ablation in primary hippocampal neurons. Cells were transfected at DIV 8 and analyzed at DIV 22. A, Representative images of neuronal somata transfected with plasmids expressing Cas9, RFP and synArfGEF-specific gRNAs or Cas9 and RFP only (control). Two validated anti-synArfGEF antibodies were used to assess synArfGEF expression level of transfected cells. Most control-transfected cells were marked by bright somatic synArfGEF immunolabeling whereas synArfGEF-specific gRNA-expressing cells showed similar immunofluorescence levels as background. B, Quantification of anti-synArfGEF immunofluorescence intensities of transfected neuronal somata and surrounding untransfected area. With both synArfGEF antibodies (raised in rabbit and guinea pig, respectively), drastically reduced somatic immunofluorescence intensity was found for both gRNAs compared to cells expressing control plasmid. No statistically significant differences were found in background immunofluorescence levels surrounding transfected cells. Bars represent means and whiskers represent standard errors of the mean. C-G, Analysis of eGFP-gephyrin clustering and apposition to presynaptic markers in primary hippocampal neurons co-expressing CRISPR plasmids and eGFP-gephyrin. Cells were transfected at DIV 8 and analyzed at DIV 22. C, Representative images of dendrites of co-transfected neurons labelled either with anti-VGAT or with anti-VGluT1 and anti-VGluT2 antibodies. In control conditions, around half of eGFP-gephyrin clusters are not apposed to VGAT (arrowhead). eGFP-gephyrin clusters misapposed to VGluT1+2 puncta constitute around one third of all clusters in control cells (arrow). Such mismatched eGFP-gephyrin clusters are more abundant in cells co-expressing synArfGEF-specific gRNAs. D, Quantification of total dendritic eGFP-gephyrin cluster densities revealed no statistically significant changes between transfected constructs. E, Quantification of absolute VGAT-apposed and -nonapposed eGFP-gephyrin cluster densities and fraction of VGAT-apposed clusters as percent of total clusters. VGAT apposition was unchanged by co-expression of synArfGEF-targeting gRNAs. F, Quantification of VGluT1+2 apposition showed that the fraction of VGluT1+2-apposed eGFP-gephyrin clusters was increased in synArfGEF-ablated cells, mirrored by corresponding changes in absolute VGluT1+2-apposed and -nonapposed eGFP-gephyrin cluster densities. G, Quantification of overall eGFP-gephyrin cluster size and intensity in synArfGEF-ablated and control dendrites. Expression of synArfGEF-targeting gRNAs led to a small but statistically significant increase in both cluster size and intensity. In box plots, lines, crosses, boxes and whiskers represent median, mean, 25-75 percentile and 10-90 percentile, respectively. Data points represent individual cells. *$p<0.05$, ***$p<0.001$.

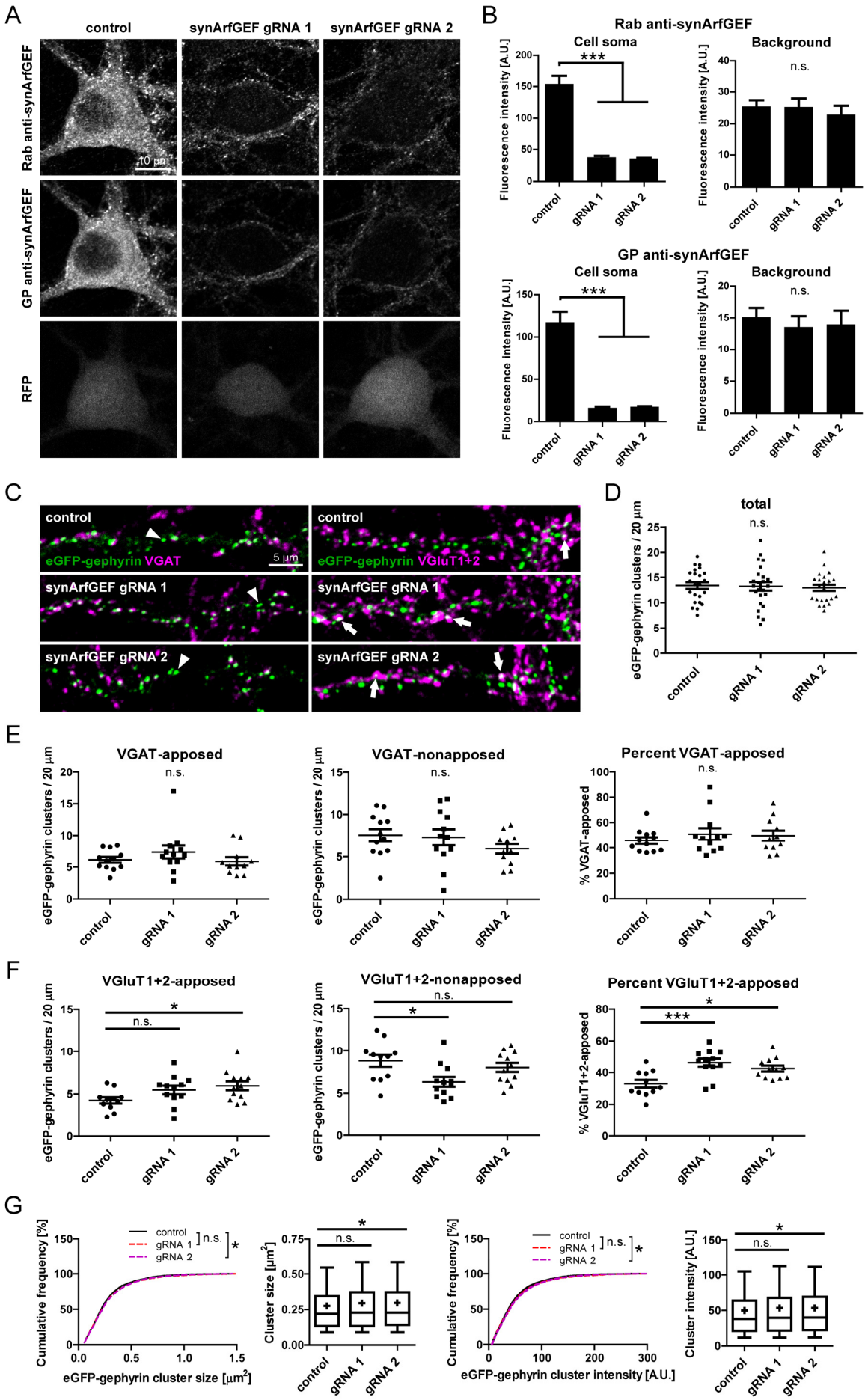
A
control
synArfGEF gRNA 1
synArfGEF gRNA 2
Rab anti-synArfGEF
GP anti-synArfGEF
RFP
10 µm
B
Rab anti-synArfGEF
Cell soma
Background
Fluorescence intensity [A.U.]
***
n.s.
control
gRNA 1
gRNA 2
GP anti-synArfGEF
C
control
eGFP-gephyrin VGAT
5 µm
eGFP-gephyrin VGluT1+2
synArfGEF gRNA 1
synArfGEF gRNA 2
D
total
eGFP-gephyrin clusters / 20 µm
E
VGAT-apposed
VGAT-nonapposed
Percent VGAT-apposed
% VGAT-apposed
F
VGluT1+2-apposed
VGluT1+2-nonapposed
Percent VGluT1+2-apposed
% VGluT1+2-apposed
G
Cumulative frequency [%]
eGFP-gephyrin cluster size [µm²]
Cluster size [µm²]
eGFP-gephyrin cluster intensity [A.U.]
Cluster intensity [A.U.]

Two validated anti-synArfGEF antibodies were used to determine synArfGEF levels in neurons transfected with plasmids containing one of the synArfGEF-targeting gRNAs or Cas9 and RFP only (Figure 2A)(Fukaya et al., 2011). Strong immunolabeling was observed frequently in cells overexpressing control plasmid. Cells expressing synArfGEF-targeting gRNAs, on the other hand, showed background level immunofluorescence intensity. Immunofluorescence intensity in the surrounding area of transfected cells was similar between conditions (Figure 2B). These findings strongly suggest that CRISPR-mediated gene modification led to ablation of synArfGEF in a majority of gRNA-expressing cells and that 14 DIV after transfection synArfGEF protein levels were strongly reduced.

As a readout of the consequences of synArfGEF ablation for the GABAergic PSD, eGFP-gephyrin was co-expressed with CRISPR plasmids. Overall eGFP-gephyrin cluster density was not affected by co-expression of gRNAs (Figure 2 C-D). However, when GABAergic and glutamatergic presynaptic terminals were visualized separately with VGAT and VGluT1+2 immunolabeling, respectively, differences in the frequency of apposition of gephyrin clusters to the two classes of presynaptic terminals were unveiled between synArfGEF-ablated and control cells. Specifically, eGFP-gephyrin clusters apposed to VGluT1+2-positive terminals (mismatched synapses), which constitute around one third of clusters in control cells, were increased to around 50% in cells expressing either of the two gRNAs (arrows in Figure 2C and Figure 2F). Yet, the fraction of gephyrin clusters apposed to VGAT-positive terminals was not affected by CRISPR-mediated synArfGEF ablation. These findings suggest that the mechanisms ensuring appropriate matching between presynaptic GABAergic / glutamatergic terminals and the corresponding postsynaptic density are regulated by SynArfGEF. Interestingly, loss of synArfGEF led to a minute increase of eGFP-gephyrin cluster size and intensity, suggesting a function for synArfGEF in aggregation or degradation of gephyrin (Figure 2G).

Figure	Conditions	One-way ANOVA	Bonferroni's multiple comparison test
2B	Rab anti-synArfGEF, cell soma	F=38.773, p<0.001	Control vs gRNA 1, t=7.186 Control vs gRNA 2, t=7.519
	Rab anti-synArfGEF, background	F=0.263, p=0.770	-
	GP anti-synArfGEF, cell soma	F=32.697, p<0.001	Control vs gRNA 1, t=6.704 Control vs gRNA 2, t=6.807
	GP anti-synArfGEF, background	F=0.192, p=0.826	-
2D	Total cluster density	F=0.095, p=0.909	-
2E	VGAT-apposed	F=1.117, p=0.340	-
	VGAT-nonapposed	F=1.224, p=0.308	-
	Percent VGAT-apposed	F=0.501, p=0.611	-
2F	VGluT1+2-apposed	F=3.43, p=0.045	Control vs gRNA 1, t=1.820 Control vs gRNA 2, t=2.557
	VGluT1+2-nonapposed	F=4.350, p=0.021	Control vs gRNA 1, t=2.869 Control vs gRNA 2, t=0.914
	Percent VGluT1+2-apposed	F=8.707, p=0.001	Control vs gRNA 1, t=4.065 Control vs gRNA 2, t=2.927
3B	Total cluster density	F=12.461, p<0.001	Empty vector vs synArfGEF, t=1.305 Empty vector vs Sec7 mut., t=4.748 Empty vector vs IQ mut., t=0.043
3C	VGAT-apposed	F=0.406, p=0.749	-
	VGAT-nonapposed	F=28.295, p<0.001	Empty vector vs synArfGEF, t=1.468 Empty vector vs Sec7 mut., t=7.363 Empty vector vs IQ mut., t=0.222
	Percent VGAT-apposed	F=14.635, p<0.001	Empty vector vs synArfGEF, t=1.447 Empty vector vs Sec7 mut., t=5.022 Empty vector vs IQ mut., t=0.496
3D	VGluT1+2-apposed	F=15.525, p<0.001	Empty vector vs synArfGEF, t=0.944 Empty vector vs Sec7 mut., t=5.662 Empty vector vs IQ mut., t=0.741
	VGluT1+2-nonapposed	F=0.447, p=0.720	-
	Percent VGluT1+2-apposed	F=16.203, p<0.001	Empty vector vs synArfGEF, t=0.931 Empty vector vs Sec7 mut., t=5.815 Empty vector vs IQ mut., t=1.217
4B	Total cluster density	F=2.775, p=0.042	Empty vector vs synArfGEF, t=0.094 Empty vector vs Sec7 mut., t=0.541 Empty vector vs IQ mut., t=2.579
4C	VGAT-apposed	F=2.281, p=0.084	-
	VGAT-nonapposed	F=2.498, p=0.064	-
	Percent VGAT-apposed	F=1.604, p=0.193	-
4D	VGluT1+2-apposed	F=2.597, p=0.056	-
	VGluT1+2-nonapposed	F=0.486, p=0.693	-
	Percent VGluT1+2-apposed	F=1.165, p=0.327	-
5A	VGAT density	F=0.678, p=0.566	-
	VGAT apposed to eGFP-gephyrin	F=0.378, p=0.769	-
5B	VGluT1+2 density	F=2.282, p=0.080	-
	VGluT1+2 apposed to eGFP-gephyrin	F=12.803, p<0.001	Empty vector vs synArfGEF, t=0.079 Empty vector vs Sec7 mut., t=5.597 Empty vector vs IQ mut., t=1.008
6B	VGAT-apposed	F=1.674, p=0.181	-
	VGAT-nonapposed	F=7.558, p<0.001	Neighb. untr. vs synArfGEF, t=0.106 Neighb. untr. vs Sec7 mut., t=3.698 SynArfGEF vs Sec7 mut., t=3.888
	Percent VGAT-apposed	F=7.164, p<0.001	Neighb. untr. vs synArfGEF, t=0.130 Neighb. untr. vs Sec7 mut., t=4.146 SynArfGEF vs Sec7 mut., t=3.314
6D	VGluT1+2-apposed	F=5.117, p=0.005	Neighb. untr. vs synArfGEF, t=0.935 Neighb. untr. vs Sec7 mut., t=3.148 SynArfGEF vs Sec7 mut., t=2.569
	VGluT1+2-nonapposed	F=1.057, p=0.379	-
	Percent VGluT1+2-apposed	F=8.243, p<0.001	Neighb. untr. vs synArfGEF, t=0.961 Neighb. untr. vs Sec7 mut., t=3.862 SynArfGEF vs Sec7 mut., t=3.501
7B	Total cluster density	F=2.543, p=0.059	-

7C	VGAT-apposed	F=1.779, p=0.159	-
	VGAT-nonapposed	F=4.159, p=0.009	Untr. vs Arf6 CA, t=1.105 Untr. vs Arf6 DN, t=2.452 Arf6 CA vs Arf6 DN, t=3.371
	Percent VGAT-apposed	F=6.523, p<0.001	Untr. vs Arf6 CA, t=1.088 Untr. vs Arf6 DN, t=3.284 Arf6 CA vs Arf6 DN, t=4.119
7D	VGluT1+2-apposed	F=6.625, p<0.001	Untr. vs Arf6 CA, t=0.283 Untr. vs Arf6 DN, t=3.382 Arf6 CA vs Arf6 DN, t=4.115
	VGluT1+2-nonapposed	F=0.809, p=0.493	-
	Percent VGluT1+2-apposed	F=6.106, p<0.001	Untr. vs Arf6 CA, t=0.979 Untr. vs Arf6 DN, t=2.866 Arf6 CA vs Arf6 DN, t=3.808
8A	Total cluster density	F=1.125, p=0.330	-
8B	VGAT-apposed	F=0.528, p=0.593	-
	VGAT-nonapposed	F=4.606, p=0.015	Arf6 vs Arf6 CA, t=1.244 Arf6 vs Arf6 DN, t=1.833 Arf6 CA vs Arf6 DN, t=3.011
	Percent VGAT-apposed	F=5.372, p=0.008	Arf6 vs Arf6 CA, t=2.077 Arf6 vs Arf6 DN, t=1.230 Arf6 CA vs Arf6 DN, t=3.246
8C	VGluT1+2-apposed	F=0.203, p=0.817	-
	VGluT1+2-nonapposed	F=0.149, p=0.862	-
	Percent VGluT1+2-apposed	F=1.253, p=0.301	-
Unpaired t-test			
10D	SynArfGEF	t_{18}=3.067, p=0.007	
	Sec7 mutant	t_{20}=2.912, p=0.009	
	IQ mutant	t_{19}=3.981, p<0.001	
10E	% VGluT1+2-apposed, synArfGEF	t_{18}=0.782, p=0.445	
	% VGluT1+2-apposed, Sec7 mutant	t_{20}=0.646, p=0.526	
	% VGluT1+2-apposed, IQ mutant	t_{19}=0.679, p=0.506	
	% Gephyrin-colocalized, synArfGEF	t_{18}=0.548, p=0.590	
	% Gephyrin-colocalized, Sec7 mutant	t_{20}=0.718, p=0.481	
	% Gephyrin-colocalized, IQ mutant	t_{19}=1.786, p=0.090	

Table 1. Results of statistical tests performed on cluster density values.
F and t represent test statistics for one-way ANOVA and Bonferroni's multiple comparison test / unpaired t-test, respectively.

Figure	Conditions	Kruskal-Wallis test	Dunn's multiple comparison test
2G	eGFP-gephyrin cluster size	n=9632, H=7.526, p=0.023	Control vs gRNA 1, y=-132.474, p>0.05 Control vs gRNA 2, y=-181.828, p<0.05
	eGFP-gephyrin cluster intensity	n=9632, H=8.254, p=0.016	Control vs gRNA 1, y=-135.565, p>0.05 Control vs gRNA 2, y=-191.465, p<0.05
3E	eGFP-gephyrin cluster size	n=7027, H=30.161, p<0.001	E. v. vs synArfGEF, y=213.368, p<0.01 E. v. vs Sec7 mut., y=317.373, p<0.001 E. v. vs IQ mut., y=316.009, p<0.001
4E	GFP-PSD-95 cluster size	n=9707, H=2.866, p=0.413	-

Table 2. Results of statistical tests performed on cluster size values.
H and y represent test statistics for Kruskal-Wallis test and Dunn's multiple comparison test, respectively.

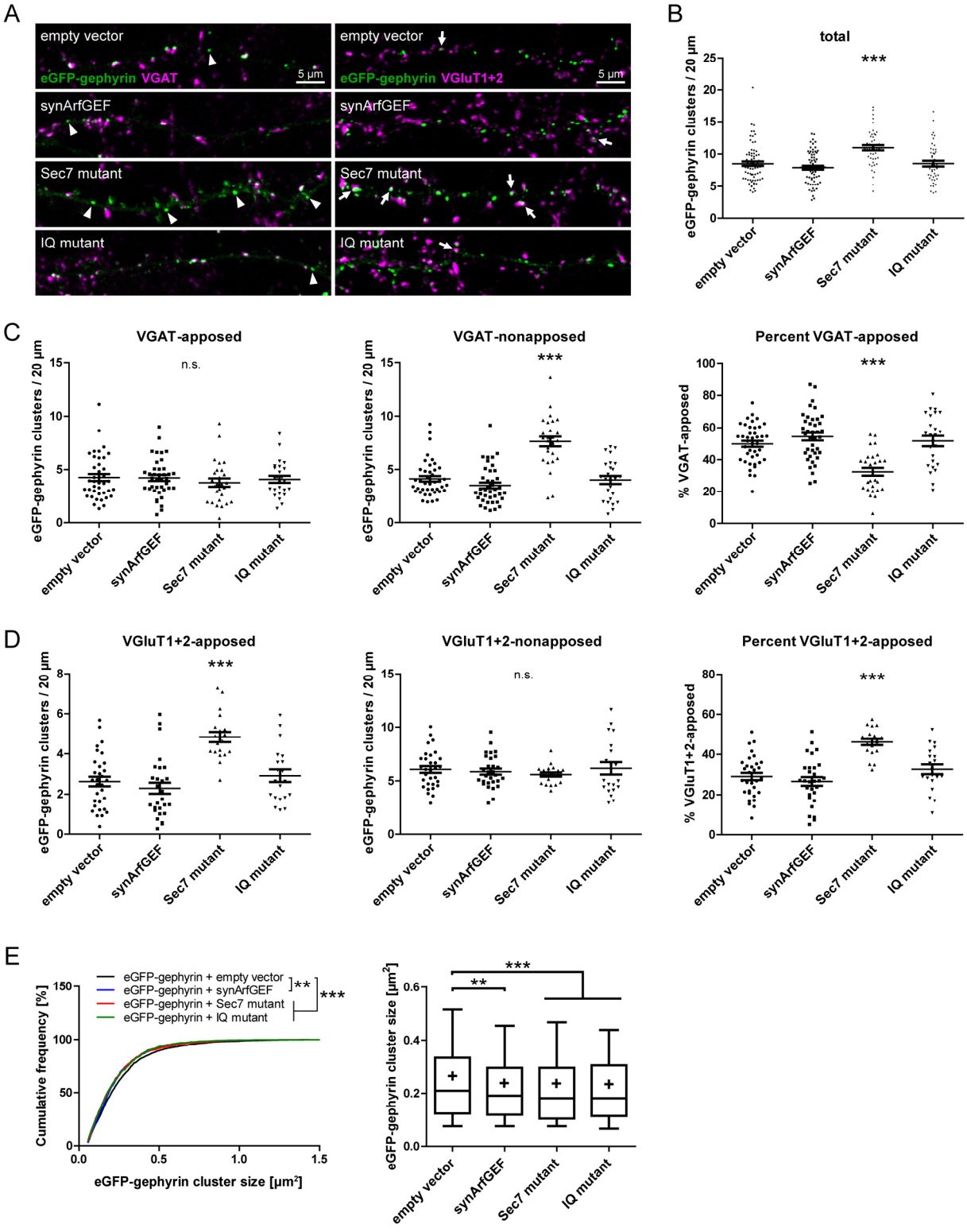

Figure 3. Catalytic function of synArfGEF selectively regulates mismatched gephyrin cluster density. FLAG-tagged synArfGEF constructs or empty vector was co-expressed with eGFP-gephyrin in primary hippocampal neurons at DIV 8 and apposition to VGAT or VGluT1+2 immunofluorescent puncta assessed at DIV 15. A, Representative images of dendrites of transfected cells. SynArfGEF Sec7 mutant-overexpressing cells exhibit an increased amount of VGAT-nonapposed eGFP-gephyrin clusters (arrowheads) in comparison to all other constructs. VGluT1+2-apposed eGFP-gephyrin clusters (arrows) are also more abundant in cells overexpressing Sec7 mutant. B, Quantification of total dendritic eGFP-gephyrin cluster densities. Overexpression of synArfGEF Sec7 mutant led to an increase in eGFP-gephyrin cluster density whereas synArfGEF wildtype or IQ mutant did not significantly change eGFP-gephyrin cluster density. C, Quantification

(Figure legend continued) of eGFP-gephyrin VGAT apposition. VGAT-apposed eGFP-gephyrin cluster density showed no significant differences between constructs. In contrast, VGAT-nonapposed eGFP-gephyrin clusters displayed an increased density in Sec7 mutant-expressing cells compared to all other constructs, resulting in a decreased percentage of VGAT-apposed eGFP-gephyrin clusters. D, Quantification of eGFP-gephyrin VGluT1+2 apposition. VGluT1+2-apposed eGFP-gephyrin cluster density was increased by overexpression of Sec7 mutant but in VGluT1+2-nonapposed eGFP-gephyrin clusters no significant differences were found between groups. The increase of VGluT1+2-apposed eGFP-gephyrin cluster density in Sec7 mutant-expressing neurons is reflected in a higher percentage of VGluT1+2-apposed eGFP-gephyrin clusters. E, Quantification of overall eGFP-gephyrin cluster size in cells co-expressing synArfGEF constructs. Compared to empty vector, all synArfGEF constructs caused a small but statistically significant reduction of cluster size when co-expressed with eGFP-gephyrin. In box plots, lines, crosses, boxes and whiskers represent median, mean, 25-75 percentile and 10-90 percentile, respectively. Data points represent individual cells. **p<0.01, ***p<0.001.

Regulation of mismatched PSD proteins by synArfGEF depends on its catalytic function and is restricted to GABAergic postsynaptic proteins

Similar to glutamate receptor regulation by synArfGEF homologs, the role of synArfGEF in regulation of gephyrin presynaptic apposition might depend on its catalytic function (Scholz et al., 2010; Myers et al., 2012). To test this possibility, FLAG-tagged synArfGEF constructs were overexpressed in primary hippocampal neurons together with eGFP-gephyrin at DIV 8 and analyzed at DIV 15. Again, cultures were labeled with anti-VGAT or anti-VGluT1+2 antibodies to distinguish between GABAergic synapses and mismatched synapses (gephyrin clusters apposed to glutamatergic terminals). This approach revealed a dramatic elevation of eGFP-gephyrin clusters nonapposed to VGAT-positive terminals in cells overexpressing synArfGEF Sec7 mutant in comparison to cells transfected with empty vector or with other synArfGEF constructs (Figure 3A and C). A reduction of the percentage of VGAT-apposed gephyrin clusters paralleled the cluster density results in Sec7 mutant-overexpressing cells. VGluT1+2-apposed eGFP-gephyrin cluster density was increased to a similar extent as VGAT-nonapposed cluster density, demonstrating that many VGAT-nonapposed clusters are mismatched (Figure 3D). Sec7 mutant-transfected cells were also marked by an increase in overall eGFP-gephyrin cluster density, consistent with the notion that Sec7 mutant overexpression promotes mismatched gephyrin clustering (Figure 3B). Surprisingly, overexpression of wildtype synArfGEF and IQ motif mutant did not lead to changes in overall eGFP-gephyrin cluster density or in apposition of eGFP-gephyrin clusters. Finally, eGFP-gephyrin cluster size was reduced in cells transfected with any of the synArfGEF constructs, indicating that this reduction is caused by binding of constructs to gephyrin and not by synArfGEF catalytic activity (Figure 3E).

Figure 4. SynArfGEF catalytic function is not involved in regulation of presynaptic apposition of glutamatergic postsynaptic density.
FLAG-tagged synArfGEF constructs were co-expressed with GFP-PSD-95 in primary hippocampal neurons at DIV 8 and apposition to presynaptic markers analyzed at DIV 15. A, Representative images of dendrites of transfected cells immunolabeled either for VGAT or VGluT1+2. The majority of GFP-PSD-95 clusters is apposed to VGluT1+2 puncta but a minor fraction of clusters is misapposed to VGAT (arrows) or is not apposed to VGluT1+2 (arrowheads). B-E, Quantification of clustering and apposition parameters of GFP-PSD95. In all analyses, there were no statistically significant differences found between constructs. B, Quantification of total dendritic GFP-PSD-95 cluster densities. C, Quantification of VGAT apposition of GFP-PSD-95. D, Quantification of VGluT1+2 apposition of GFP-PSD-95. E, Quantification of overall GFP-PSD-95 cluster size.

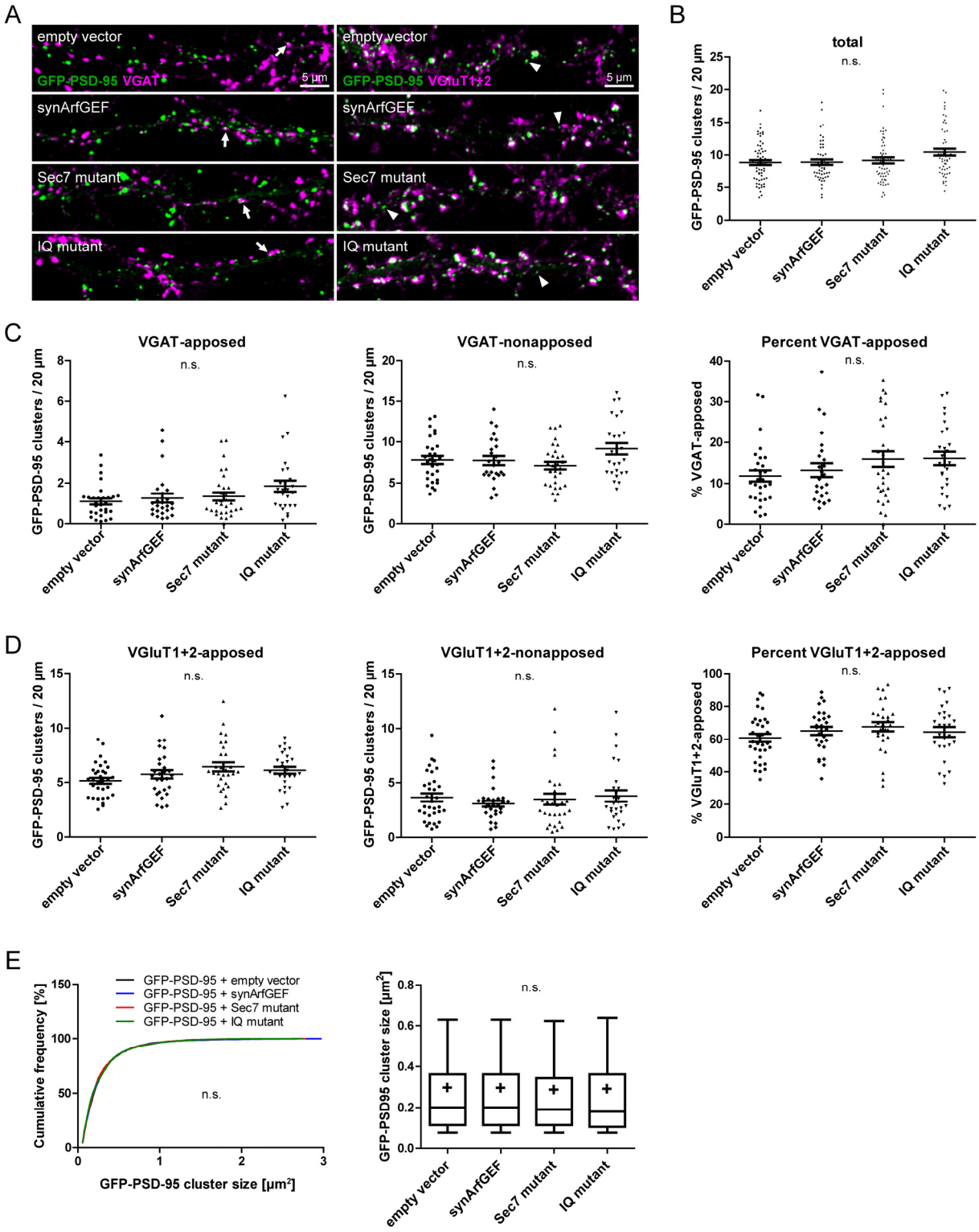

(Figure legend continued) In box plots, lines, crosses, boxes and whiskers represent median, mean, 25-75 percentile and 10-90 percentile, respectively. Data points represent individual cells.

SynArfGEF exhibits a PDZ domain-binding motif at the C-terminal end and was first described as a glutamatergic PSD protein (Inaba et al., 2004). The observed phenotype could be a manifestation of a more general function of synArfGEF in synapse validation, both for GABAergic and glutamatergic

PSD proteins. For this reason, we co-expressed synArfGEF constructs with GFP-PSD-95 and examined apposition to presynaptic markers (Figure 4). In these experiments, synArfGEF catalytic function did not affect the density of mismatched (VGAT-apposed) PSD-95 clusters. Instead, GFP-PSD-95 clusters were about 5 times more frequently apposed to VGluT1+2- than to VGAT-positive terminals in all conditions (Figure 4A-D). In addition, GFP-PSD-95 cluster size was not affected by overexpression of synArfGEF constructs (Figure 4E). SynArfGEF catalytic function thus seems to be specifically required for regulation of presynaptic terminal apposition to the GABAergic PSD.

Regulation of gephyrin presynaptic apposition by synArfGEF raises the question whether such control is exerted through trans-synaptic signaling or whether purely postsynaptic mechanisms are involved. Quantification of presynaptic marker density reveals that innervation density is not affected by synArfGEF overexpression (Figure 5). In terms of fraction of presynaptic markers misapposed to eGFP-gephyrin, only VGluT1+2 puncta exhibit an increase upon Sec7 mutant overexpression. This is consistent with the notion that synArfGEF has a postsynaptic role in regulation of GABAergic PSD apposition.

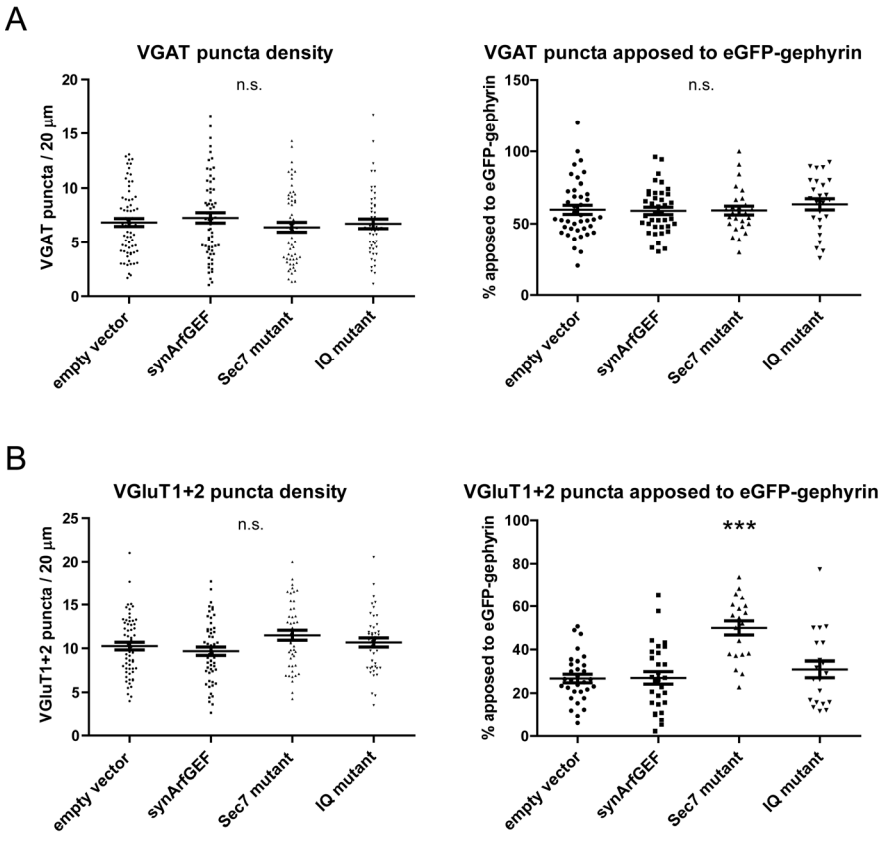

Figure 5. Fraction of mismatched glutamatergic presynaptic terminals but not innervation density is affected by synArfGEF catalytic function.
A, Quantification of VGAT puncta densities and percentage of VGAT puncta apposed to eGFP-gephyrin. Co-expression of synArfGEF constructs had no statistically significant effect on puncta density or percentage of apposition to eGFP-gephyrin. B, Quantification of VGluT1+2 puncta densities and percentage of VGluT1+2 puncta apposed to eGFP-gephyrin. Percentage of VGluT1+2 puncta apposed to eGFP-gephyrin was increased in Sec7 mutant-overexpressing cells compared to all other groups but absolute VGluT1+2 densities were unaffected by synArfGEF construct co-expression. Data points represent individual cells. ***$p<0.001$.

To exclude the possibility that synArfGEF function is restricted to downregulation of gephyrin at mismatched sites, overexpression experiments were repeated without eGFP-gephyrin co-expression. Instead, $GABA_AR$ γ2 subunit was immunolabeled in these cultures to assess consequences of synArfGEF wildtype and Sec7 mutant overexpression for $GABA_AR$ apposition (Figure 6). Neighboring non-transfected dendrites were used in both conditions as internal controls. As with eGFP-gephyrin co-expression, Sec7 mutant-transfected cells exhibited higher proportion of mismatched γ2 subunit clusters (apposed to VGluT1+2-positive terminals) than untransfected dendrites. Along with gephyrin apposition, synArfGEF catalytic function thus contributes to regulate the apposition of $GABA_AR$ clusters to neurotransmitter-specific presynaptic terminals.

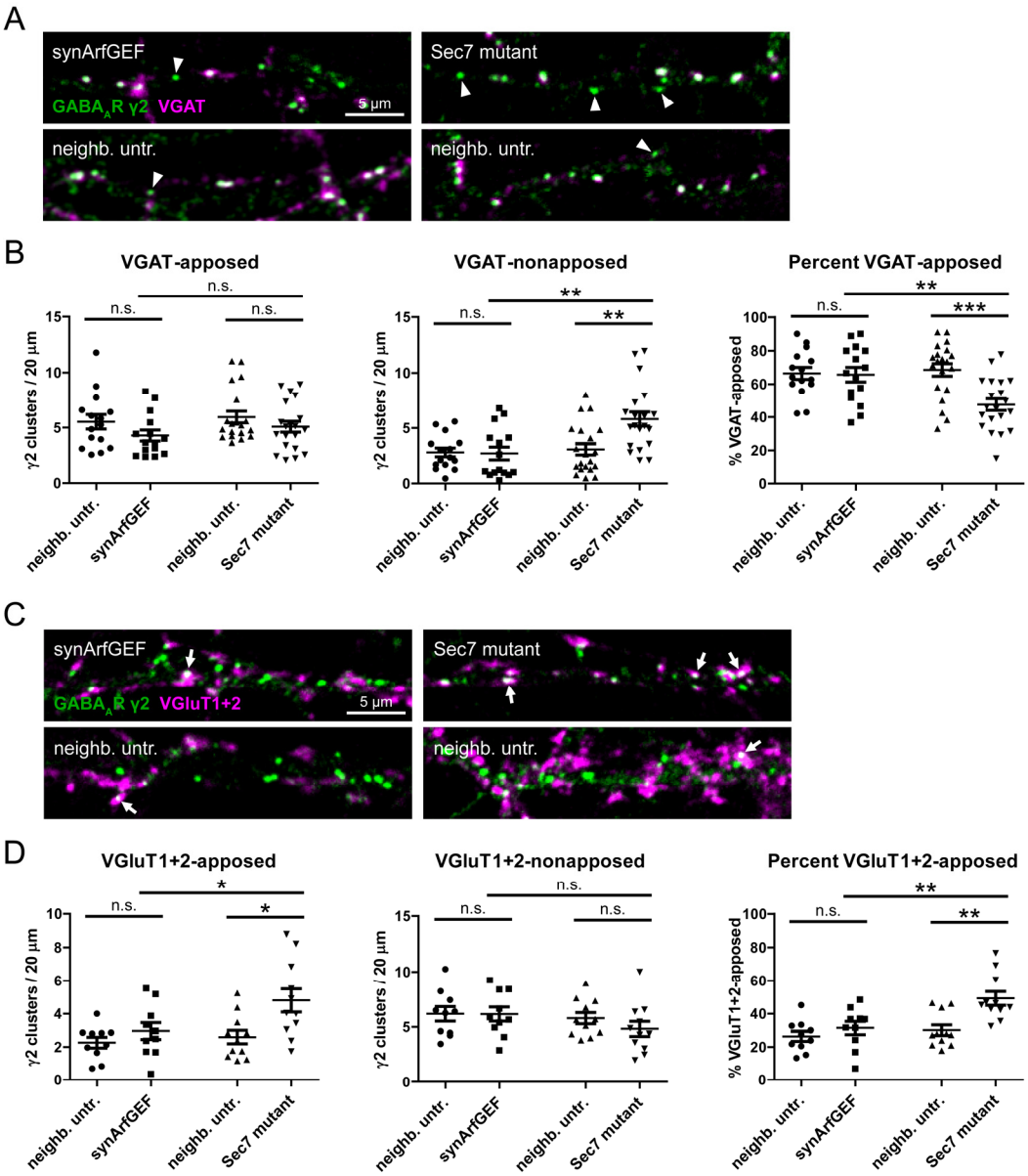

Figure 6. Presynaptic apposition of $GABA_A$ receptors is regulated by synArfGEF catalytic function.

(Figure legend continued) Primary hippocampal neurons were transfected with synArfGEF wildtype or Sec7 mutant constructs at DIV 8 and presynaptic apposition of $GABA_AR$ γ2 subunit clusters analyzed at DIV 15. Untransfected dendrites neighboring transfected cells served as control. A, Representative images of dendrites of cells transfected with synArfGEF constructs (upper panels) and untransfected neighboring dendrites (lower panels) immunolabeled for VGAT. Note the high abundance of $GABA_AR$ γ2 subunit clusters not apposed to VGAT (arrowheads) in dendrites of cells transfected with Sec7 mutant. B, Quantification of $GABA_AR$ γ2 subunit cluster VGAT apposition. Compared to untransfected neighboring dendrites and to cells overexpressing wildtype synArfGEF, cells overexpressing Sec7 mutant show elevated VGAT-nonapposed cluster densities, reflected in a lower percentage of VGAT-apposed clusters. C, Representative images of dendrites of cells transfected with synArfGEF constructs (upper panels) and untransfected neighboring dendrites (lower panels) immunolabeled for VGluT1+2. Note the high abundance of $GABA_AR$ γ2 subunit clusters apposed to VGluT1+2 puncta (arrows) in dendrites of cells overexpressing Sec7 mutant. D, Quantification of $GABA_AR$ γ2 subunit cluster VGluT1+2 apposition. Sec7 mutant-transfected cells showed significantly higher density of VGluT1+2-apposed $GABA_AR$ γ2 subunit clusters compared to untransfected cells and to cells transfected with wildtype synArfGEF. The increase in VGluT1+2-apposed cluster density is mirrored by a higher percentage of VGluT1+2-apposed clusters. Data points represent individual cells. *$p<0.05$, **$p<0.01$, ***$p<0.001$.

Recapitulation of synArfGEF phenotype by Arf6 mutant overexpression suggests regulation of mismatched GABAergic PSDs might be mediated by Arf6 activation

If Arf6 is the target of synArfGEF catalytic activity for regulation of GABAergic PSD apposition, abolition of Arf6 activity alone should replicate the apposition phenotype of the Sec7 mutant. Overexpression of Arf6 in its wildtype form, and to a larger extent overexpression of constitutively active (CA; Q67L) or dominant negative (DN; T27N) Arf6 mutants, affects neuronal morphology (Hernandez-Deviez et al., 2002; Miyazaki et al., 2005). Neurite and spine outgrowth seem to be regulated by Arf6, since these processes are promoted by Arf6 DN and inhibited by Arf6 CA overexpression, respectively. For this reason, primary hippocampal neurons overexpressing HA-tagged Arf6 variants were probed with antibodies to $GABA_AR$ α2 subunit to assure that formation of the GABAergic PSD is not affected by morphology changes. Indeed, $GABA_AR$ α2 subunit clusters were observed on dendrites of Arf6-expressing neurons to the same extent as on non-transfected neurons (Figure 7A). To facilitate the assessment of GABAergic PSD abundance and apposition, eGFP-gephyrin was co-expressed with Arf6 constructs. As expected from observations of $GABA_AR$ α2 subunit clustering, eGFP-gephyrin overall density did not exhibit a statistically significant change with Arf6 construct overexpression (Figure 7B). Analysis of presynaptic apposition, however, uncovered that in Arf6 DN-expressing cells a smaller fraction of eGFP-gephyrin clusters is correctly apposed and a larger fraction present in mismatched synapses, both compared to Arf6 CA-expressing cells and to cells expressing eGFP-gephyrin only (Figure 7C-D). Similar to results from synArfGEF overexpression experiments, these alterations were caused by an increase in the proportion of mismatched gephyrin clusters apposed to VGluT1+2-positive terminals. Therefore, Arf6 activity is sufficient for regulation of GABAergic PSD presynaptic apposition, indicating that Arf6 is a likely target of synArfGEF in this process.

To corroborate the finding that Arf6 activation controls matching of the GABAergic PSD with presynaptic structures, $GABA_AR$ γ2 subunit was immunolabeled and apposition assessed in Arf6-overexpressing neurons (Figure 8). As with co-expression of eGFP-gephyrin, total γ2 subunit cluster

density was not affected by Arf6 construct overexpression. However, apposition to VGAT-positive terminals was again reduced in Arf6 DN- compared to Arf6 CA-overexpressing cells whereas an increased proportion of mismatched clusters was observed. Unexpectedly, although mean percentage of mismatched clusters was higher in Arf6 DN- than in Arf6 CA-expressing cells, no statistically significant difference was found in the fraction of γ2 subunit clusters apposed to VGluT1+2-positive terminals.

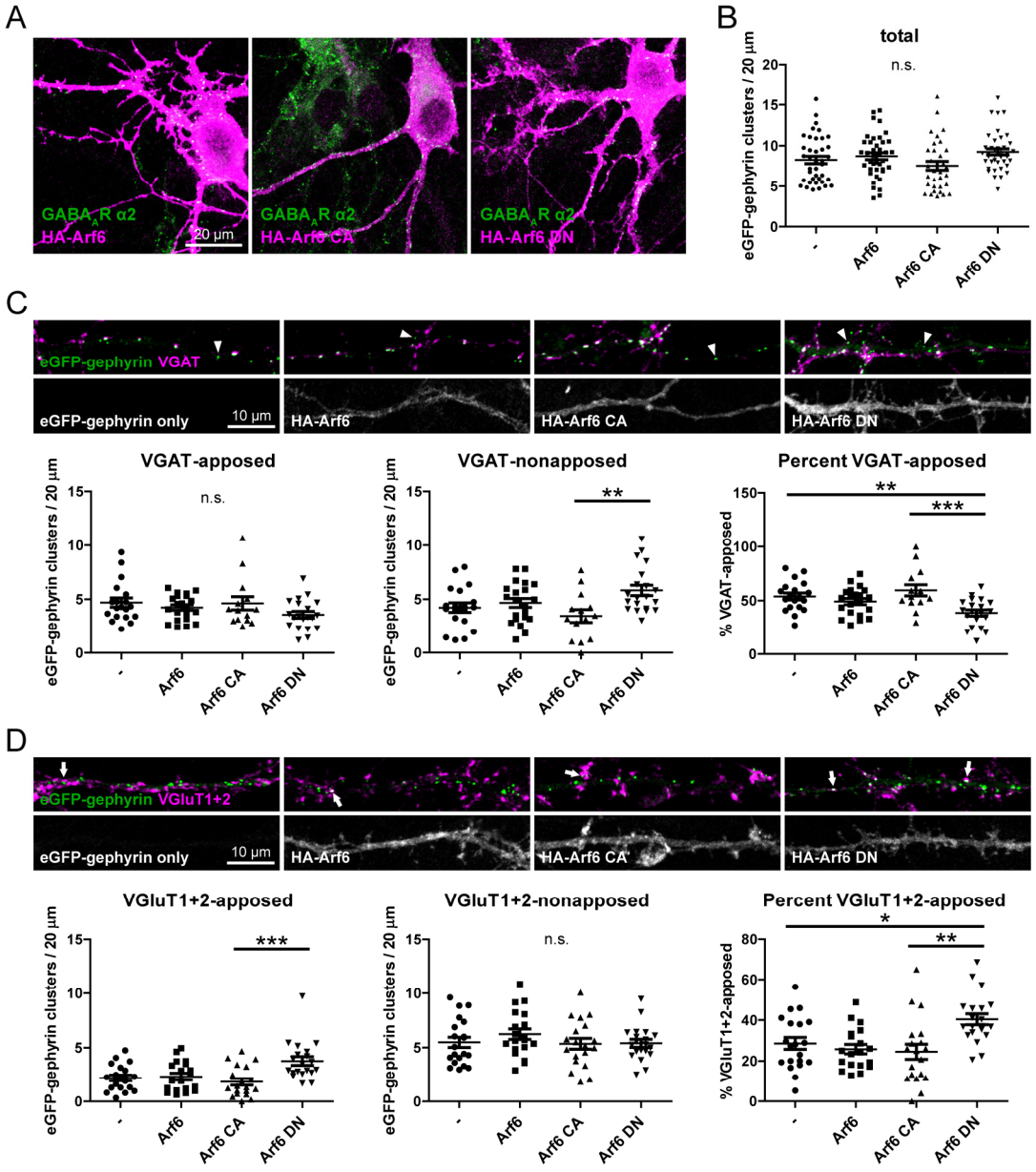

Figure 7. Arf6 is involved in regulation of gephyrin presynaptic apposition.
A, $GABA_AR$ clusters are present on neurons overexpressing Arf6 constructs. Primary hippocampal neurons were transfected with HA-tagged Arf6 wildtype, constitutively active (CA) mutant or dominant negative (DN) mutant and $GABA_AR$ clustering assessed by α2 subunit immunolabeling. B, Quantification of total eGFP-gephyrin cluster densities in cells co-expressing Arf6 constructs or expressing eGFP-gephyrin alone. Primary hippocampal cultures were transfected at DIV 8 and cells analyzed at DIV 15. Co-expression of Arf6 constructs had no effect on eGFP-gephyrin cluster density. C, Representative images and quantifications of eGFP-gephyrin apposition to VGAT. Cells co-expressing HA-Arf6 DN displayed a higher density of VGAT-nonapposed clusters and a lower percentage of VGAT-apposed clusters than cells co-expressing HA-Arf6 CA. Arrowheads

(Figure legend continued) indicate eGFP-gephyrin cluster not apposed to VGAT. D, Representative images and quantifications of eGFP-gephyrin apposition to VGluT1+2. Cells co-expressing HA-Arf6 DN displayed a higher density and percentage of eGFP-gephyrin clusters apposed to VGluT1+2 than cells co-expressing HA-Arf6 CA. Arrows indicate eGFP-gephyrin clusters apposed to VGluT1+2. Data points represent individual cells. **p<0.01, ***p<0.001.

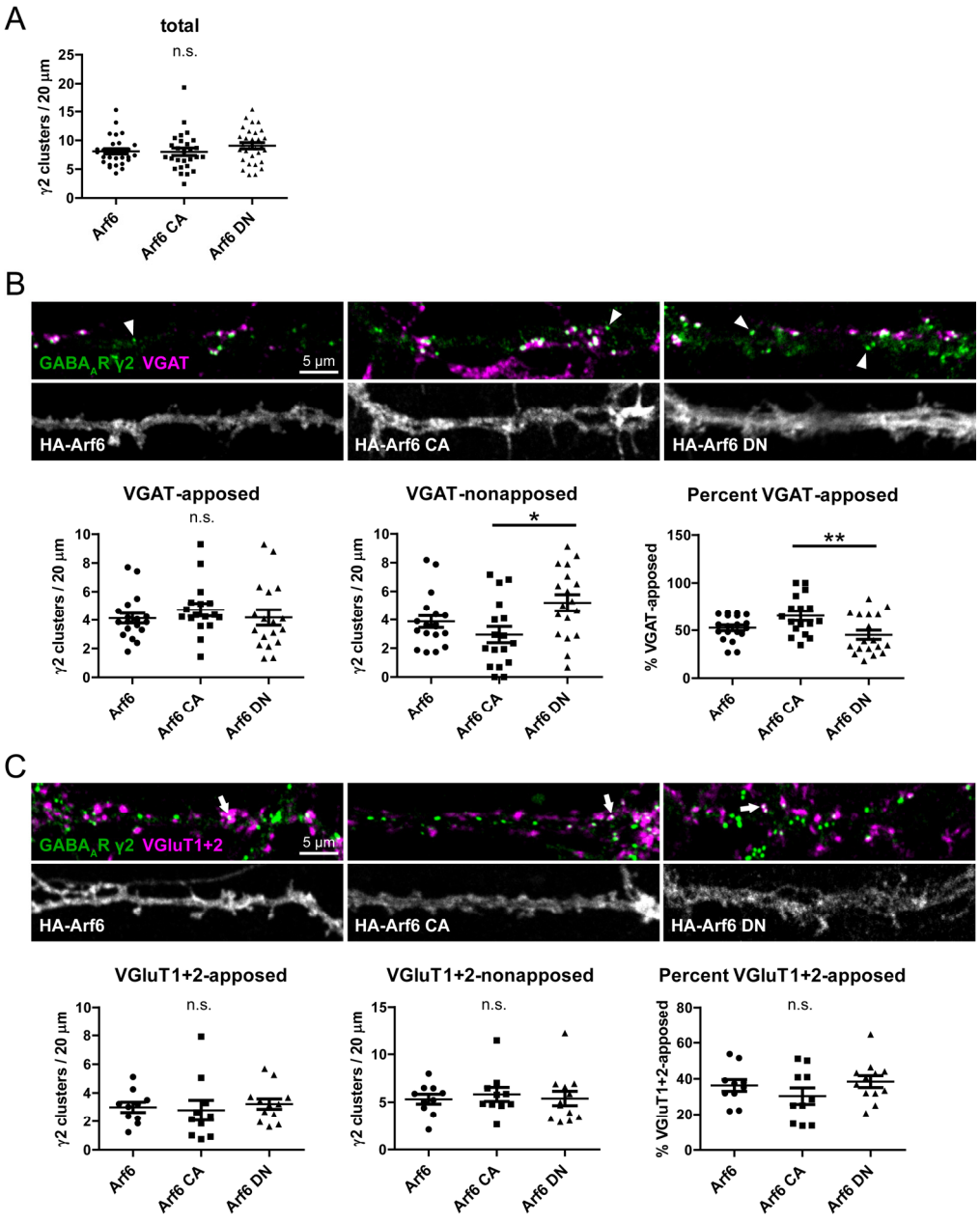

Figure 8. Arf6 is involved in regulation of GABA$_A$ receptor presynaptic apposition.
Primary hippocampal neurons were transfected at DIV 8 with Arf6 constructs and GABA$_A$R clustering assessed at DIV 15 by immunolabeling of γ2 subunit. A, Quantification of total dendritic GABA$_A$R γ2 subunit cluster densities in cells transfected with Arf6 constructs. No significant differences were found between groups. B, Representative images and quantifications of GABA$_A$R γ2 subunit VGAT apposition in cells overexpressing Arf6 constructs. HA-Arf6 CA and HA-Arf6 DN-transfected cells differed significantly in apposition, with DN mutant showing higher VGAT-nonapposed γ2 subunit density and lower percentage of VGAT-apposed γ2 subunit clusters. Arrowheads indicate GABA$_A$R γ2 subunit clusters not apposed to VGAT. C, Representative images and quantifications of GABA$_A$R γ2 subunit VGluT1+2 apposition in cells overexpressing Arf6 constructs. No significant differences were found between groups. Arrows indicate GABA$_A$R γ2 subunit clusters apposed to VGluT1+2. Data points represent individual cells. *p<0.05, **p<0.01.

The N-terminal coiled-coil domain and the IQ motif are involved in synArfGEF aggregation

Our findings demonstrated a role for synArfGEF catalytic function specifically in regulating the correct apposition of the GABAergic PSD to GABAergic terminals. On the other hand, co-IP results point to a direct binding of gephyrin with synArfGEF near its IQ motif. This interaction is also supported by extensive colocalization of eGFP-gephyrin and synArfGEF when co-expressed in neurons (data not shown). The N-terminal CC-domain necessary for this interaction has been demonstrated to be essential for homomultimerization (Myers et al., 2012). This line of evidence suggests a relationship between synArfGEF homomultimerization and gephyrin interaction. FLAG-tagged synArfGEF constructs overexpressed in primary hippocampal neurons formed large somatic aggregates, reminiscent of aggregates formed by overexpressed gephyrin (Figure 9A). Somatic synArfGEF aggregates were consistently immunopositive for endogenous gephyrin. Strikingly, deletion of the N-terminus abolished the majority of somatic aggregates and so did mutation of the IQ motif. The remaining somatic aggregates, however, consisted of small aggregates for ΔN construct and of large aggregates in the case of the IQ mutant. Mutation of S348, the catalytic glutamate residue in the Sec7 domain, the PP motif or deletion of the PH domain did not influence somatic synArfGEF aggregation. Since individual domains overexpressed in neurons did not form somatic aggregates, large somatic aggregates might be formed only by synArfGEF constructs that retain the ability of gephyrin interaction as well as homodimerization capability. The importance of N-terminal CC-domain for homomultimerization is further stressed by a lower propensity of mCherry-tagged synArfGEF to co-immunoprecipitate with ΔN construct than with other constructs (Figure 9B). To clarify whether synArfGEF aggregates would be formed in heterologous cells, FLAG-tagged synArfGEF or IQ mutant was overexpressed in HEK293T cells (Figure 9C). FLAG immunolabeling revealed a granular distribution of synArfGEF constructs that was unaffected by application of the ionophore ionomycin. Together, these results suggest that synArfGEF homomultimerization is connected to gephyrin interaction and depends on neuron-specific factors.

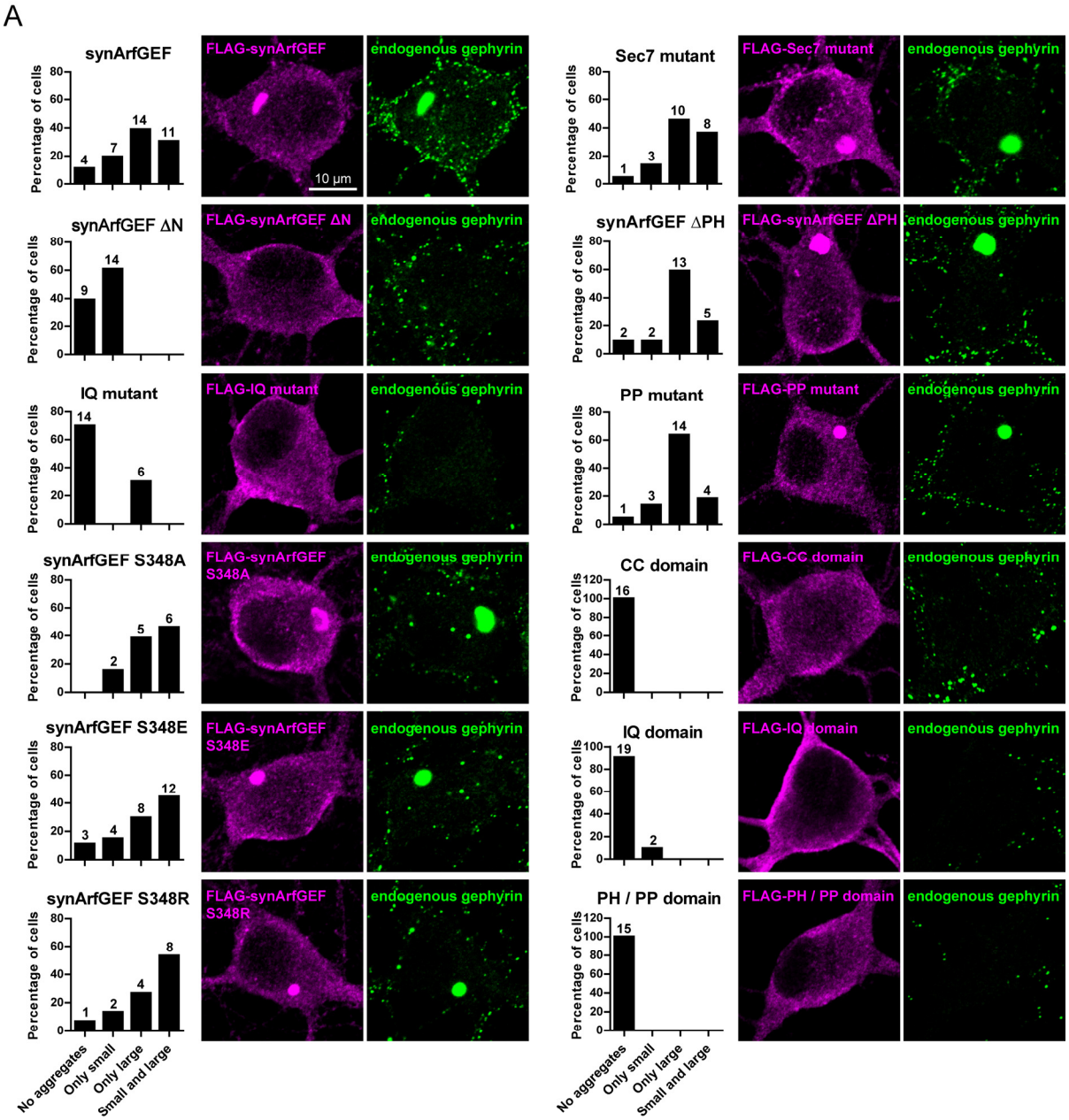
A
synArfGEF
FLAG-synArfGEF
endogenous gephyrin
10 µm
synArfGEF ΔN
FLAG-synArfGEF ΔN
IQ mutant
FLAG-IQ mutant
synArfGEF S348A
FLAG-synArfGEF S348A
synArfGEF S348E
FLAG-synArfGEF S348E
synArfGEF S348R
FLAG-synArfGEF S348R
Sec7 mutant
FLAG-Sec7 mutant
synArfGEF ΔPH
FLAG-synArfGEF ΔPH
PP mutant
FLAG-PP mutant
CC domain
FLAG-CC domain
IQ domain
FLAG-IQ domain
PH / PP domain
FLAG-PH / PP domain
Percentage of cells
No aggregates
Only small
Only large
Small and large

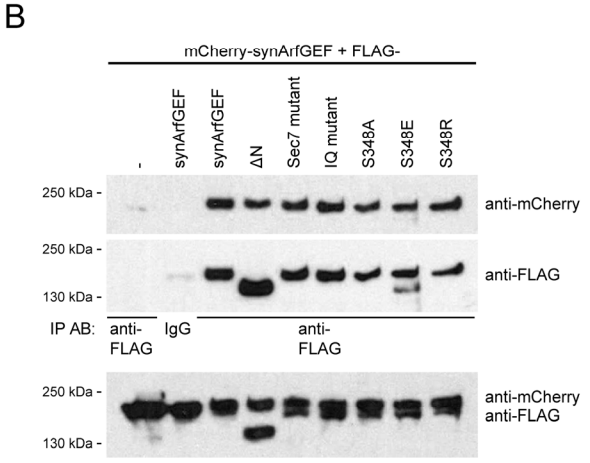
B
mCherry-synArfGEF + FLAG-
-
synArfGEF
synArfGEF
ΔN
Sec7 mutant
IQ mutant
S348A
S348E
S348R
250 kDa
anti-mCherry
anti-FLAG
130 kDa
IP AB:
anti-FLAG
IgG
anti-FLAG
anti-mCherry
anti-FLAG

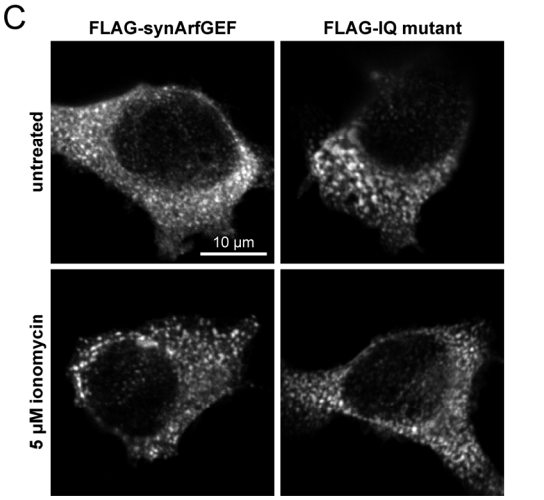
C
FLAG-synArfGEF
FLAG-IQ mutant
untreated
5 µM ionomycin
10 µm

Figure 9. SynArfGEF builds somatic aggregates immunopositive for gephyrin which depend on N-terminus and IQ motif when overexpressed in primary hippocampal neurons.
A, Representative images and quantifications of somatic aggregates of FLAG-tagged synArfGEF constructs. Neuronal somata were blindly divided into cells containing small aggregates, large aggregates or both. Most cells overexpressing wildtype synArfGEF contain small or large aggregates. Deletion of CC-domain containing N-terminus or mutation of IQ motif results in diffuse somatic distribution of synArfGEF in most transfected cells. Small aggregates remain in synArfGEF ΔN and large aggregates remain in IQ mutant. Overexpression of individual synArfGEF domains is not sufficient for formation of somatic aggregates. B, Ability of synArfGEF multimerization was assessed by co-IP of mCherry-tagged synArfGEF with FLAG-tagged synArfGEF constructs. mCherry-synArfGEF was co-immunoprecipitated with all FLAG-synArfGEF constructs. C, Overexpression of synArfGEF constructs in HEK293T cells does not result in formation of aggregates but in granular distribution throughout cells. Application of 5 µM ionomycin for 3 min before fixation had no effect on granular synArfGEF distribution.

SynArfGEF interactions, response to NMDA and dendritically localized mRNA point towards the dependence of synArfGEF function on neuronal activity

Because gephyrin binding was localized to the region near the IQ motif and due to altered somatic aggregation of synArfGEF IQ mutant, the functional importance of the IQ motif in synArfGEF was examined using calmodulin binding assays. This motif is present in multiple proteins that bind calmodulin at low Ca^{2+} concentrations (apocalmodulin). SynArfGEF constructs were expressed in HEK cells and lysates incubated with calmodulin-bound beads either in the presence of 2 mM Ca^{2+} or 2 mM EGTA. Indeed, binding of synArfGEF to calmodulin was observed in low Ca^{2+} conditions (Figure 10A). This interaction was completely abolished with synArfGEF IQ mutant, confirming that binding takes place at the IQ motif. Interestingly, in the case of synArfGEF ΔN, a strongly increased pull-down efficiency was observed, indicating that synArfGEF multimerization is linked to calmodulin binding. To address whether Ca^{2+}-dependent calmodulin binding might play part in a physiological process to control synArfGEF conformation, the impact of various drugs on FLAG-synArfGEF distribution was tested (Figure 10B). Dendritic synArfGEF distribution was altered by NMDA, but not by the application of AP5, DHPG or TTX. NMDA treatment of neurons transfected with mCherry-tagged synArfGEF constructs also induced distribution changes, in particular increased dendritic aggregation (Figure 10C-D). IQ mutant synArfGEF showed a similar increase in aggregation as wildtype and Sec7 mutant synArfGEF, ruling out the possibility that aggregation changes are directly caused by calmodulin interactions. Aggregation changes might be dependent on gephyrin interaction or be restricted to sites of glutamatergic innervation. Therefore, synArfGEF colocalization with gephyrin and apposition to VGluT1+2 was analyzed in NMDA-treated or sham-treated cultures. In both cases, no statistically significant differences were found between treatment conditions (Figure 10E).

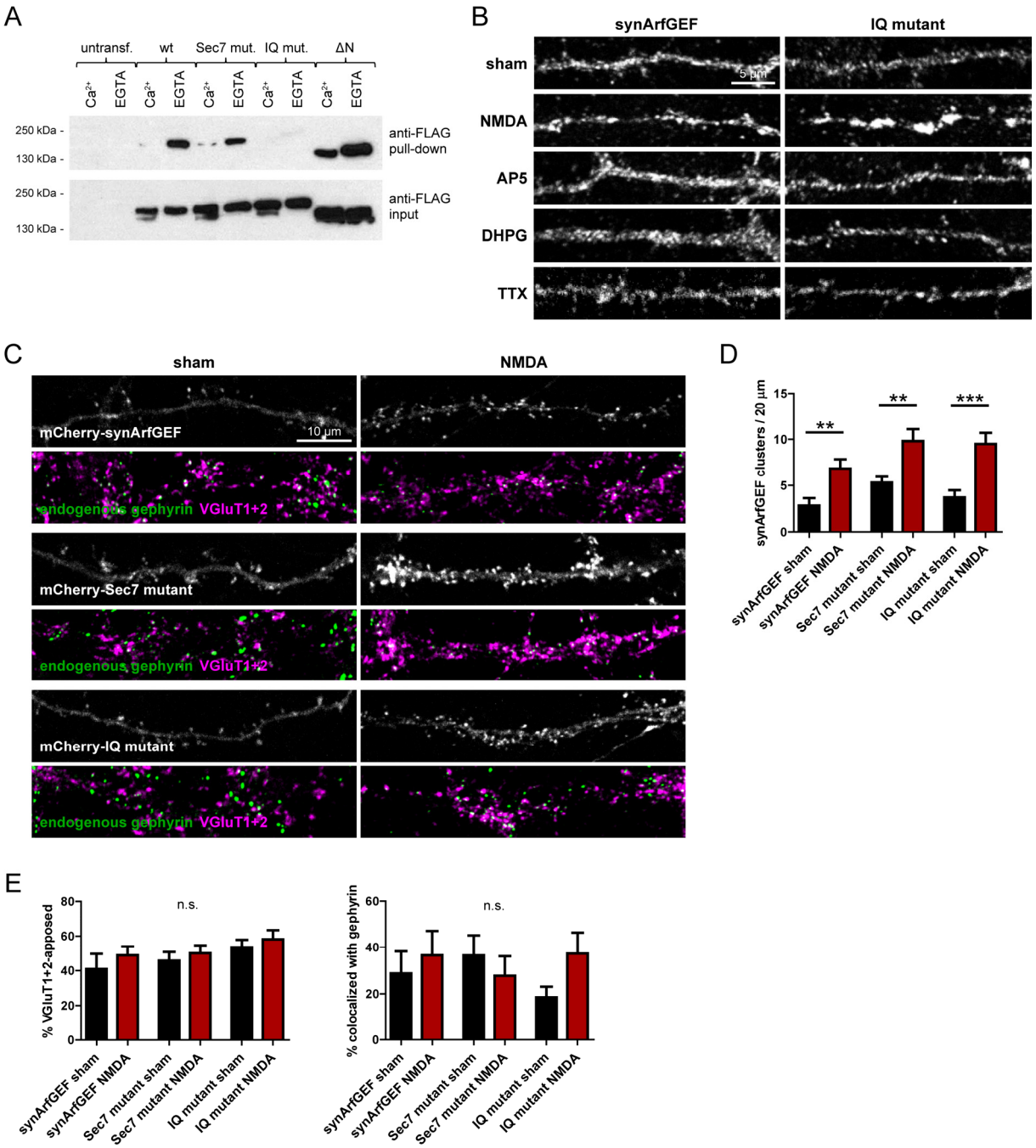

Figure 10. Apocalmodulin binds to synArfGEF IQ motif and NMDA receptor activity promotes synArfGEF dendritic aggregation.
A, Representative Western blot of calmodulin pull-down of synArfGEF constructs in high and low Ca^{2+} conditions. SynArfGEF binds to calmodulin more efficiently in low Ca2+ conditions and requires IQ motif for interaction. SynArfGEF constructs were overexpressed in HEK293T cells and lysates used for calmodulin pull-down assay in the presence of 2 mM $CaCl_2$ or 2 mM EGTA. B, Representative images of FLAG-tagged synArfGEF in dendrites of transfected primary hippocampal neurons in the presence of the indicated compounds. Application of NMDA (30 µM, 30 min) promoted aggregation of dendritic synArfGEF. No change in synArfGEF immunolabeling was observed after application of AP5 (50 µM, 30 min), DHPG (100 µM, 30 min) or TTX (1 µM, 24 h). C, Representative images of primary hippocampal neurons transfected with mCherry-tagged synArfGEF constructs and treated with NMDA (30 µM, 30 min) or sham treated. D, Quantification of mCherry-synArfGEF dendritic aggregates revealed an approximately two-fold increase of aggregate density after NMDA treatment compared to sham treated cells. E, Quantification of VGluT1+2 apposition and gephyrin colocalization of mCherry-synArfGEF aggregates. No significant differences were found between treatment conditions. **p<0.01, ***p<0.001.

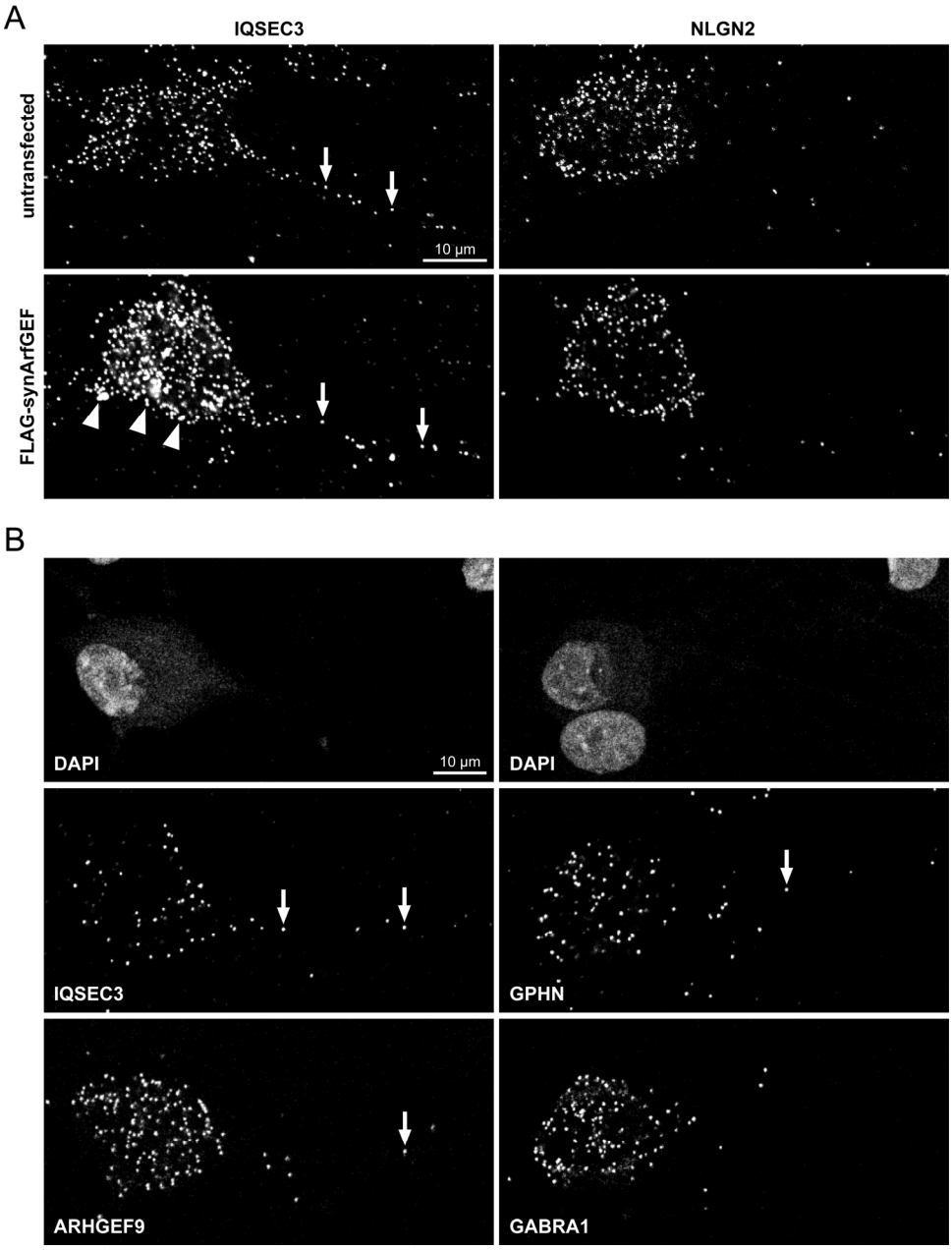

Figure 11. Fluorescence *in situ* hybridization confirms the presence of dendritically located synArfGEF mRNA.
A, Validation of IQSEC3 (synArfGEF) probe specificity. Primary hippocampal neurons were transfected with FLAG-tagged synArfGEF construct at DIV 12 and processed for fluorescence *in situ* hybridization at DIV 19. A massive increase in signal intensity in transfected cells (arrowheads) with IQSEC3 probe but not with NLGN2 probe confirmed IQSEC3 probe specificity to synArfGEF mRNA. Dendritically located IQSEC3 signal is highlighted by arrows. B, Comparison of synArfGEF mRNA localization with other transcripts of GABAergic PSD proteins in untransfected primary hippocampal cultures at DIV 19. In relation to somatic signal intensity, dendritic localization of transcripts (arrows) was more prominent for synArfGEF (IQSEC3) than for collybistin (ARHGEF9), gephyrin (GPHN) and $GABA_AR$ α1 subunit (GABRA1) transcripts.

Ca^{2+}-dependent calmodulin binding and distribution changes upon NMDA treatment suggests activity-dependence of synArfGEF function. As a target of NPAS4, synArfGEF transcription was shown to depend on neuronal activity (Bloodgood et al., 2013). Local translation of synArfGEF transcripts would provide an additional level of activity-dependent regulation. Therefore, synArfGEF messenger

RNA (mRNA) cellular distribution was examined by the use of fluorescence *in situ* hybridization (FISH). Primary hippocampal neurons at DIV 19 displayed strong synArfGEF (IQSEC3) signal (Figure 11A). SynArfGEF but not neuroligin 2 (NLGN2) signal intensity was markedly higher in neurons transfected at DIV 11 with FLAG-synArfGEF, confirming specificity of synArfGEF probes. Importantly, synArfGEF signal was abundant in dendrites (arrows in Figure 11B). Dendritically localized signal was less frequently observed using collybistin (ARHGEF9) or gephyrin (GPHN) probes and virtually absent using $GABA_AR$ α1 subunit (GABRA1) probes. These results confirm that synArfGEF mRNA is localized in dendrites and open the possibility of activity-dependent synArfGEF translation.

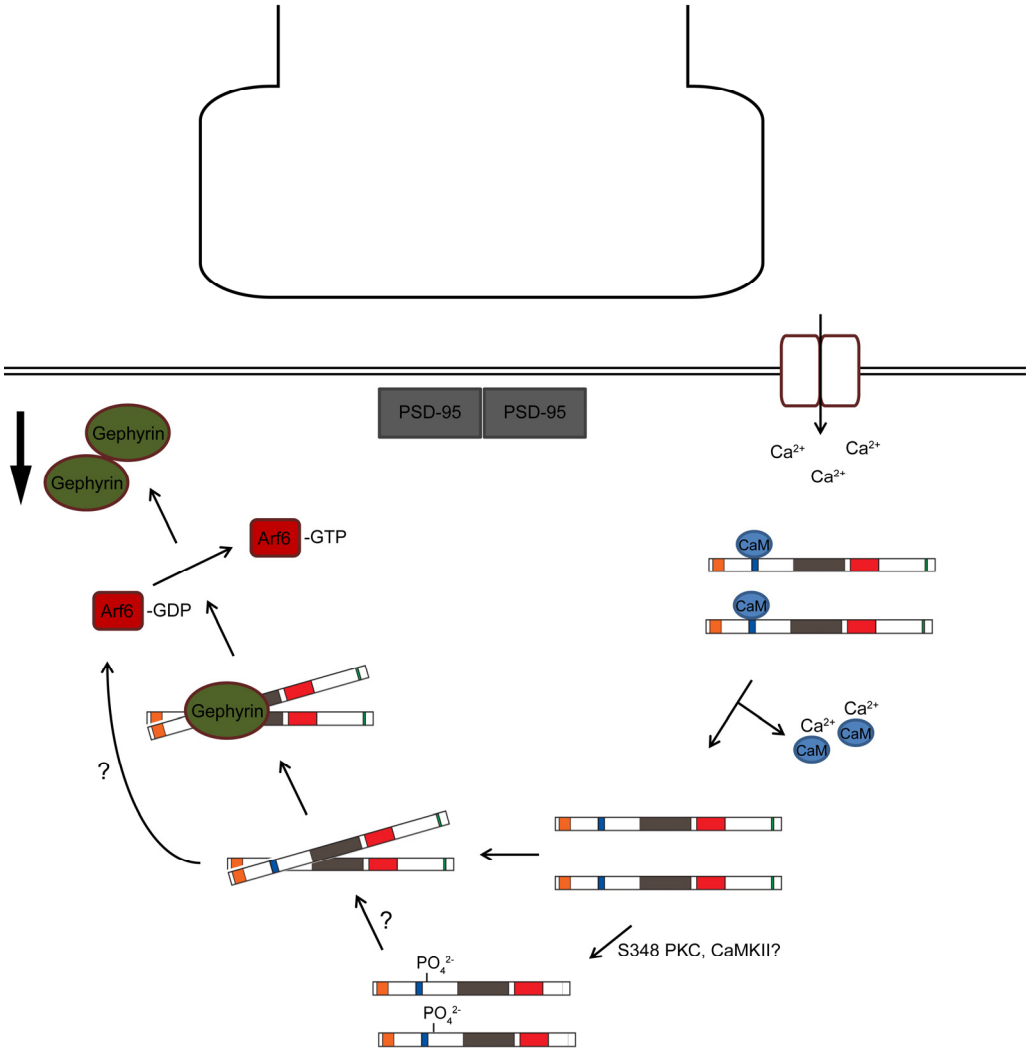

Figure 12. Model of synArfGEF function at mismatched GABAergic postsynaptic structures.

Discussion

Our study of synArfGEF function in primary hippocampal neurons provides evidence of activity-dependent control of mismatched GABAergic postsynaptic proteins by synArfGEF. Catalytic activity is implicated in this regulation by the strong effect of Sec7 domain mutation as well as the recapitulation of the misapposition phenotype by Arf6 overexpression. SynArfGEF function is restricted to misapposed GABAergic PSDs since PSD-95 apposition to GABAergic or glutamatergic terminals was not affected. However, NMDA-induced synArfGEF distribution changes, Ca^{2+}-dependent calmodulin binding and the finding that correctly matched GABAergic PSDs were unaffected in all experiments strongly suggests that proximity to glutamatergic structures enables synArfGEF function. Gephyrin binding was found to be near the calmodulin binding site and dependent on an N-terminal CC domain involved in synArfGEF homomultimerization. This points to a mechanism by which synArfGEF undergoes conformational changes upon neuronal activity to regulate mismatched GABAergic postsynaptic proteins (Figure 12).

SynArfGEF interaction with gephyrin is likely to be essential for regulation of mismatched GABAergic PSDs

A physiologically relevant interaction of synArfGEF with gephyrin is suggested by several findings. First, co-IP experiments in heterologous cells revealed binding that depended on domains with known functions. Secondly, co-expression of both proteins in primary neurons leads to extensive colocalization in all subcellular domains. Thirdly, somatic synArfGEF aggregates formed upon overexpression are immunopositive for endogenous gephyrin. These observations are in line with large overlap of other GABAergic markers reported in various parts of the CNS (Fukaya et al., 2011; Sakagami et al., 2013). Dystrophin interaction may be involved in accumulating synArfGEF at dystrophin-containing synapses. However, the restricted dystrophin distribution in cortical areas excludes an obligatory role for dystrophin in synArfGEF clustering (Lidov et al., 1990; Knuesel et al., 1999). Along the same lines, localization of synArfGEF containing mutated PP motif necessary for dystrophin interaction did not differ from wildtype and synArfGEF clustering was unaffected in cerebral cortex of mice with pyramidal cell-specific loss of the DGC. Gephyrin binding to synArfGEF was recently reported on the basis of yeast-two-hybrid and co-IP experiments and also identified the IQ motif area as the minimally-required area for interaction (Um et al., 2016). Furthermore, gephyrin downregulation in primary neurons caused a reduction in synArfGEF clustering, arguing that this interaction is necessary for synArfGEF synaptic localization. Substantial evidence has thus accumulated that synArfGEF is present in the GABAergic PSD due to specific gephyrin interaction near the IQ motif.

Paradoxically, Um et al. (2016) have found an overall increase of gephyrin and GAD67 puncta density upon synArfGEF overexpression, an effect which was dependent on gephyrin binding as well as on synArfGEF catalytic activity. The reasons for the discrepancy to our results are not clear, since the

same isoform of rat synArfGEF was used in primary hippocampal cultures. Still, the use of the chicken beta-actin enhancer and the resulting massive overexpression of synArfGEF in their experiments might explain some of these differences. None of our ablation and overexpression experiments have yielded results that implicate synArfGEF in the regulation of correctly apposed GABAergic proteins, despite the preferential GABAergic localization of synArfGEF. Even the increase in overall eGFP-gephyrin cluster density upon Sec7 mutant overexpression is a reflection of elevated density of mismatched GABAergic synapses. Further experiments will have to clarify whether synArfGEF can contribute to overall GABAergic synapse development, and under what conditions.

Mechanisms underlying the selectivity of synArfGEF function to mismatched GABAergic PSDs

Interaction with gephyrin might reflect a mechanism to target synArfGEF to the GABAergic PSD rather than an interaction implicating direct gephyrin regulation. Indeed, gephyrin binding might even have an inhibitory effect on synArfGEF catalytic activity, since the multimeric form of synArfGEF (containing the N-terminus) bound to gephyrin seems to be catalytically inactive in correctly apposed gephyrin clusters. Other factors must be present at mismatched sites, allowing their suppression through synArfGEF activity. Calmodulin is a likely candidate to take this role, because of the binding near the gephyrin-binding site in low Ca^{2+} conditions. Binding of calmodulin was also enhanced in the ΔN truncation, further suggesting that this interaction competes with gephyrin binding and represents a monomeric inactive state (Myers et al., 2012). The cycling of calmodulin-synArfGEF interaction with different Ca^{2+} concentrations might enable an active conformational state which allows activation of Arf6 in the mismatched GABAergic PSD. Involvement of calmodulin in formation of such an active state would also account for the fact that neuronal activity was implicated in the fidelity of GABAergic apposition (Anderson et al., 2004). Two conditions, both of which are given in the mismatched GABAergic PSD, would therefore have to be fulfilled for synArfGEF activity: Abundance of synArfGEF clustered by gephyrin and unbinding of calmodulin from synArfGEF through neuronal activity. Increased dendritic aggregation caused by NMDA is in agreement with such a model. Unexpectedly, however, IQ mutant synArfGEF also responded to NMDA with increased dendritic aggregation. This suggests that aggregation is not a direct consequence of calmodulin release from synArfGEF but might be caused by modification of synArfGEF through other activity-dependent factors. NMDA experiments should be repeated with ΔN and S348 mutant constructs to further characterize mechanism of these aggregation changes. S348 was identified as a target of protein kinase C (PKC) and would be well suited to modulate synArfGEF conformation or gephyrin binding because of its proximity to the IQ motif (Trinidad et al., 2006). Alternatively, activity-dependent translation of dendritically localized synArfGEF mRNA might underlie the altered immunolabeling after NMDA treatment.

The fact that Arf6 catalytic mutants replicated the misapposition phenotype of the Sec7 mutant strongly suggests that Arf6 acts as a substrate of synArfGEF in this context. Arf6 is also the target of IQSEC1 and IQSEC2, leading to the internalization of GluA2 and GluA1 subunits, respectively. In order for synArfGEF to achieve GABAergic PSD-specific regulation, activation of Arf6 would have to be restricted to GABAergic PSD-containing nanodomains. It is unclear how this specificity is ensured in mismatched synapses presumably containing glutamatergic PSD proteins close to GABAergic proteins, but spatial restriction of synArfGEF to GABAergic elements might be one level of control. Arf6 is a membrane-bound GTPase which has diverse functions in neurons and is controlled by a multitude of GEF and GTPase-activating proteins (GAPs) (Jaworski, 2007). Downstream effectors of Arf6 regulate actin dynamics and both clathrin-dependent and -independent plasma membrane endocytosis. Therefore, direct regulation of gephyrin clustering as well as regulation of GABAergic PSD proteins through internalization of $GABA_A$Rs are possible consequences of synArfGEF-mediated activation of Arf6.

Putative *in vivo* functions of synArfGEF

The absence of spatial and temporal cues is likely the main underlying cause for the formation of mismatched synapses in primary neuronal cultures. Therefore, it is unclear whether the regulation of misapposition by synArfGEF has a physiological relevance *in vivo*. However, it is conceivable that formation of mismatched synapses by loss of guidance cues follows different principles than what was uncovered by loss of synArfGEF or overexpression of the Sec7 mutant. This notion is supported by the observation that overexpression of wildtype synArfGEF did not lead to a statistically significant reduction of mismatched synapses, since mismatched synapses caused by other mechanisms might not be under the influence of synArfGEF regulation. *In vivo*, synArfGEF function might be restricted to synapses that are closely apposed to synapses employing a different neurotransmitter system. GABAergic synapses that are located on dendritic spines are often in close proximity to glutamatergic synapses and therefore synArfGEF might be involved in the regulation of PSD spine nanodomains (Chen et al., 2012; van Versendaal et al., 2012). Although complicated by high synaptic density *in vivo*, increased focus on synaptic mismatch in intact tissue might thus lead to a better understanding of the mechanisms underlying neurotransmitter-specific PSD regulation. On the one hand, synArfGEF knockout mice will be instrumental in the elucidation of the physiological roles of synArfGEF. On the other hand, the development of *in vivo* models of synaptic mismatch would allow to probe the involvement of genes required to correct misapposition, by design of rescue experiments. This might be achievable through blockade of neuronal activity, as mismatch of GABAergic terminals with glutamatergic postsynaptic structures was observed in Purkinje cells of TTX-infused cerebella (Cesa et al., 2008). However, to the best of our knowledge, occurrence of postsynaptic GABAergic structures misapposed to glutamatergic axon terminals was not yet demonstrated *in vivo*.

Conclusions

Strikingly, in a recent transcriptomic analysis, synArfGEF was found to be the gene which is most strongly downregulated in schizophrenia, autism and bipolar disorder (Ellis et al., 2016). Major issues that have to be addressed on the path to potential translational applications of our findings include the question of Arf subtype activation of human synArfGEF and the uncertainty of mismatch-regulating mechanisms *in vivo*. So far, the physiological and behavioral consequences of receptor-transmitter mismatch *in vivo* are unexplored. However, in the light of association of synArfGEF expression levels with major synaptic disorders in humans, a role for synaptic mismatch in the etiology of these disorders should be considered in future investigations.

Acknowledgements

Acknowledgements: This work was supported by an UZH Forschungskredit grant to S.F. and by the Swiss National Science Foundation (SNSF). We thank Dr. Hiroyuki Sakagami for providing reagents and Prof. Peter Scheiffele and Prof. Stephan Neuhauss for scientific discussions.

GENERAL DISCUSSION

The studies carried out in this thesis aimed to characterize the relationship between interneuron cell type diversity and variations of postsynaptic GABAergic molecular composition in the context of specificity of synapse formation. In particular, the main findings of the two studies relate the molecular heterogeneity of GABAergic PSDs to the selectivity of synapse formation and maintenance within neurotransmitter systems and to the sorting mechanisms that assure segregated assembly of postsynaptic proteins between neurotransmitter systems. The unsuspected roles of postsynaptic GABAergic PSD components in subsets of synapses defined by their presynaptic cellular partners, demonstrate that presynaptic diversity is mirrored by a functional postsynaptic diversity in GABAergic synapses.

Two GABAergic PSD proteins with unknown function and a restricted distribution within GABAergic synapses were selected to approach the research question. Although there is evidence suggesting that DG and synArfGEF are present in a molecular complex, the results of the present studies point towards distinct roles in determining specificity of GABAergic synapses.

The ablation of neuronal DG in the forebrain revealed that the DGC is essential for the formation of functional GABAergic axon terminals from the group of CCK-positive basket cells, but not from other GABAergic interneurons. Postsynaptic proteins were only marginally affected by loss of DG in their capacity to cluster opposite GABAergic terminals, contrary to results from previous studies, which hinted at a crucial role for the DGC in clustering of $GABA_A$Rs or NL2. The absence of CCK-positive terminals was mirrored by a decrease of sIPSCs in pyramidal cells and the inability of CCh to induce such inhibitory events, demonstrating that the lack of immunohistochemical markers correlated with a functional loss of terminals. Importantly, the finding that CCK-positive terminals were also compromised by ablation of DG during adulthood implied that continuous trans-synaptic signaling is necessary for GABAergic axon terminal function. Finally, CCK-positive terminals persisted in DG T190M KI mice, opening the possibility that presynaptic receptors other than neurexins might bind to DG to enable its trans-synaptic function. This study is the first to show that GABAergic postsynaptic proteins can mediate continuous trans-synaptic and subtype-specific signaling, which is essential for the function of GABAergic presynaptic terminals.

Biochemical interaction experiments as well as ablation and overexpression experiments in primary neuronal cultures uncovered a specific role of synArfGEF in regulation of mismatched GABAergic PSD proteins. This function depended on the Sec7 domain and the phenotype of synArfGEF ablation and overexpression experiments was recapitulated by overexpression of Arf6 mutants, making a strong argument for an involvement of synArfGEF catalytic function in control of misapposed GABAergic postsynaptic proteins. The specificity of this regulation is underlined by the finding that synArfGEF overexpression did not affect PSD-95 apposition and by binding of synArfGEF to gephyrin in co-IP experiments. Furthermore, several observations indicated that synArfGEF function

is controlled by neuronal activity. Calmodulin interaction with synArfGEF depended on Ca^{2+} concentrations, synArfGEF aggregation in dendrites was modulated by NMDA application in primary neurons, and FISH revealed synArfGEF transcripts in dendrites. Together, these results demonstrate that synArfGEF serves a specific function in regulating GABAergic PSD proteins which are mismatched to glutamatergic presynaptic structures, which may underlie the fidelity of GABAergic synapse formation *in vivo*.

Interneuron subtype-selectivity of DG function suggests that a molecular code underlies specificity of GABAergic synapse formation

A key finding from *in vivo* DG conditional ablation is the selective requirement of DG for basket cells of the CCK-containing but not of the PV-containing type. Indeed, innervation from other GABAergic interneuron classes seemed unaffected, judging from the unaltered VGAT and GAD immunostainings. The finding that glutamatergic pre- and postsynaptic markers were also essentially unchanged by loss of DG further confirms the specificity of DG function. These findings have far-reaching implications, since the DGC is the first postsynaptic GABAergic complex found to be essential for the function of only one subtype of GABAergic interneurons.

The diversity of presynaptically located transmembrane proteins became evident with the description of neurexin alternative splice variants and drove speculations that this diversity might underlie a molecular code, which ensures that postsynaptic targets are innervated by appropriate cell types or brain regions (Boucard et al., 2005; Krueger et al., 2012). Considering that the total number of splice isoforms is 12 for NLs but amounts to several thousand for neurexins, it is clear that other postsynaptic proteins have to be involved, possibly in a combinatorial manner together with NLs, to account for the specificity of the vast amount of neuronal circuits in the brain (Baudouin and Scheiffele, 2010). In order for DG to be part of a molecular code which coordinates the specificity of synapse formation, two requirements have to be met, apart from the observed synapse specificity of DG itself. First, presynaptic binding partners have to show a selective, cell type-specific distribution. These binding partners might be neurexins or other laminin-alpha, neurexin and sex hormone-binding globulin (LNS)-domain containing proteins such as agrin or pikachurin. The second requirement is that DG exhibits selective interactions with presynaptic binding partners. Studies which have addressed these issues allow for an assessment whether the two criteria are met. The hypothesis of interneuron-specific expression of neurexin splice variants was recently tested using single cell quantitative PCR (qPCR) (Fuccillo et al., 2015). Overall, neurexin1α and neurexin3 levels were found to be much more abundant in CCK-positive than in PV-positive cells, suggesting a larger dependence of CCK-positive basket cells on neurexin for synapse specification. Among neurexin1 mRNA, only CCK-positive basket cells exhibited substantial amounts of neurexin1 transcripts that lack splice inserts 2, 3 and 4. This finding is in striking accordance with the biochemical investigation of DG-neurexin interaction,

which revealed that LNS domains 2 and 6 in neurexin1 are DG binding partners only in the absence of inserts at splice sites (SS) 2 and 4, respectively (Sugita et al., 2001). If neurexin1 is indeed the presynaptic DG binding partner in this context, the cell type-specific alternative splice programs of basket cells might be sufficient to ensure that DG trans-synaptic signaling is restricted to CCK-positive cells. Together with the perisomatic distribution of the DGC in pyramidal cells, this mechanism might hinder axon terminals from other interneuron classes to form or maintain synapses containing the DGC. Alternatively, other interneuron classes might employ an active mechanism to avoid interaction of neurexin1 lacking inserts at SS2 and SS4 with DG. Neurexophilin is a neurexin-interacting protein that binds to neurexin1 at SS2, thereby inhibiting the interaction of neurexin1 with DG at SS2 (Missler et al., 1998; Reissner et al., 2014). The expression pattern of neurexophilin is in agreement with a limited distribution in a subset of interneurons in the hippocampus and cerebral cortex (Petrenko et al., 1996). Furthermore, neurexophilin displays the domain structure and PTMs typical of a secreted protein (Petrenko et al., 1996; Missler and Sudhof, 1998). It is therefore conceivable that locally secreted neurexophilin acts as an inhibitor of DG-neurexin1 trans-synaptic signaling.

Based on the interneuron subtype-specific distribution of neurexin isoforms, matching DG binding preferences, and the interneuronal expression of neurexophilin, it is tempting to posit that this diversity underlies subtype-selectivity of DG function. However, in the light of the unaltered CCK-positive terminals in DG T190M KI mice, the notion of a combinatorial code arising from these molecules remains speculative. Hara et al. (2011) demonstrated that neurexin (and laminin) binding capacity of DG T190M is dramatically reduced, both in DG isolated from brain and from muscle. Still, only neurexin1α was tested in these assays (Kevin P. Campbell, personal communication). This leaves open the possibility that the interactions with neurexin2 and neurexin3, which bind to wildtype DG, are not affected by the T190M mutation (Sugita et al., 2001). It is also not clear whether residual binding of neurexin1α to DG T190M might be sufficient for DG function at CCK-positive terminals.

Still, results from T190M KI mice call for the consideration of other molecules as presynaptic receptors of DG to mediate its trans-synaptic function. Only few other DG binding partners were described to date, including laminin, perlecan, pikachurin and agrin, all of which primarily act as secreted proteins in the ECM (Sato et al., 2008; Waite et al., 2012). Although laminin and perlecan were found to serve important functions in the nervous system, their distribution and mode of action make these ligands unlikely to mediate trans-synaptic signaling (Jucker et al., 1996; Farach-Carson et al., 2014; Yao et al., 2014). In contrast, pikachurin is the first DG ligand for which a function in CNS synapses was described (Sato et al., 2008; Omori et al., 2012). Both DG and pikachurin are necessary for normal development and function of ribbon photoreceptor synapses in the retina. However, in the ribbon synapse, DG is localized presynaptically and pikachurin is released into the ECM, where it binds to α-DG. It is therefore likely, that in addition, a postsynaptic receptor is required for this function. Together with the observation that pikachurin expression in the brain is almost undetectable

in the brain, these findings do not suggest a function of pikachurin as a presynaptic receptor in the forebrain.

Several lines of evidence render agrin a better candidate for the role of DG presynaptic receptor. Agrin binds to DG and is important for postsynaptic differentiation and maturation at the NMJ (Sugiyama et al., 1994; Shi et al., 2012). Furthermore, a transmembrane form of agrin is highly expressed in the brain, which might serve functions for which its secreted counterpart might not be suited (Daniels, 2012). On the basis of experiments using recombinant agrin in primary hippocampal cultures, agrin was reported to induce homeostatic upscaling of GABAergic synapses through DG (Pribiag et al., 2014). Whether these results reflect a physiological plasticity mechanism for synaptic scaling *in vivo* is not clear, especially because the interneuron subtype-specific innervation central to DG trans-synaptic function is lost in dissociated cultures. Furthermore, a function of DG in homeostatic plasticity of postsynaptic GABAergic proteins is in stark contrast with the present finding that clustering of GABAergic PSD proteins in DG-ablated mice is almost unaffected. The increased synaptic localization of DG upon agrin application is, however, consistent with an interdependence of both factors for trans-synaptic signaling. Examination of markers specific for CCK-positive terminals in brain tissue deficient in agrin will elucidate the role of agrin in GABAergic synapses on pyramidal cells.

The wealth of DG binding partners, serving different tasks in different tissues, highlights that molecules that were not yet described as DG interactors should not be excluded as potential DG receptors in CCK-positive basket cell synapses. The Roundabout (Robo) receptor Slit was added to the list of DG interacting proteins when mutations in DG glycosyl transferases revealed the involvement of DG in aggregating Slit in the spinal cord floor plate (Wright et al., 2012). Mice carrying the same mutations also have deficits in axon guidance in the forebrain, as axons of the internal capsule show abnormal trajectories (Wright et al., 2015). Because these deficits resemble the phenotype of mice lacking Cadherin EGF LAG seven-pass G-type receptor 3 (Celsr3), and because Celsr3 contains two LNS domains, Celsr3 might act as a presynaptic DG receptor in this context (Tissir et al., 2005). Similarly, Celsr3 is a candidate DG receptor at CCK-positive terminals to mediate trans-synaptic signaling. The availability of Celsr3 floxed and CCK-Cre mouse lines allows the conditional ablation of Celsr3 in CCK-positive interneurons to test this hypothesis (Zhou et al., 2008; Taniguchi et al., 2011).

The integrity of CCK-positive terminals in DG T190M KI mice implies that post-phosphorylation glycosylation is not essential for DG function at CCK-positive terminals. On the other hand, these mice display muscle weakness and reduced NMJ size (Hara et al., 2011). This illustrates that distinct glycosyl modifications on α-DG are required for different functions. Considering the diversity of DG glycosyl transferases and the complexity of DG glycosylation, these modifications might themselves contribute to synaptic diversity. By cell type-selective expression of glycosyltransferases,

glycosylation of DG and other postsynaptic proteins such as NLs might thus generate postsynaptic molecular heterogeneity, matching the diversity of presynaptic adhesion molecules.

DG requirement for functional innervation by CCK-positive basket cells in adulthood points towards continuous trans-synaptic signaling

Ablation of neuronal DG in adult mice led to the unsuspected finding that DG is necessary after initial synapse formation for synapse maintenance. Two mechanisms (or a combination of both) may underlie the continuous requirement of DG during adulthood. The DGC may mediate continuous trans-synaptic, retrograde signaling which is essential for the function of CCK-positive axon terminals. Alternatively, the DGC could serve a structural function, ensuring CCK-positive terminals are aligned properly with GABAergic PSDs. Because of continuous synapse turnover in adulthood, the latter hypothesis may involve a structural role in maintenance of synapses or only in formation of synapses. Deficits in formation of new synapses during adulthood thus may be sufficient for loss of functional innervation by CCK-positive basket cells, due to an imbalance of synapse formation and elimination.

The results of several independent experiments point towards a role of the DGC in trans-synaptic signaling rather than in structural integrity of CCK-positive basket cell synapses. Although markers for CCK-positive terminals, which constitute a substantial part of GABAergic terminals in the pyramidal layer of the hippocampus (Nyiri et al., 2001), were almost completely lost in DG cKO mice, general markers of GABAergic terminals were not affected. VGAT and GAD showed neither a reduction in puncta size not density, which would be expected from the structural loss of CCK-positive terminals. Furthermore, the idea that PV-positive axons sprout and compensate for the lack of CCK-positive terminals does not hold, since PV immunolabeling as well as the fraction of PV puncta colocalized with VGAT was unaltered by DG ablation. Mdx mice display a reduction of CB1 and VGluT3 immunoreactivity in CA1 pyramidal layer, indicating that dystrophin is part of trans-synaptic signaling through DG (Krasowska et al., 2014). Again, PV immunolabeling in CA1 pyramidal layer was unaltered in these mice. There is evidence to suggest that PV-positive somata are more abundant in the hippocampus of mdx mice (Del Tongo et al., 2009; Krasowska et al., 2014). However, since also interneurons other than basket cells express PV and because no changes were seen in PV immunolabeling in the pyramidal layer, whether this increase represents a compensatory upregulation of PV-positive basket cells is questionable. Furthermore, no major differences were found in density of symmetric synapses between mdx and wildtype mice on the ultrastructural level, reinforcing the notion that reduction of CCK-positive terminals is not accompanied by a structural loss of synapses (Graciotti et al., 2008; Miranda et al., 2009). Finally, no alterations of PV or GAD immunolabeling in CA1 pyramidal layer were found in an epilepsy model, despite the loss of CCK-positive terminals (Wyeth et al., 2010).

If the absence of CCK-positive terminal markers does not imply synapse loss, then the compromised function of these synapses represents a conundrum. Electrophysiological recordings from pyramidal cells established that inhibitory drive is blunted in DG-ablated cells, and the inefficiency of CCh to elevate IPSC frequency suggested that this reduction is due to dysfunction of CCK-positive terminals. Under the assumption that loss of CCK-positive terminals is not paralleled by structural synaptic changes, trans-synaptic signaling through the DGC must thus be essential for normal synaptic transmission at these terminals. All interneuron subtype-specific markers analyzed for CCK-positive cells (CCK, CB1, VGluT3) were drastically reduced in hippocampus pyramidal layer of DG cKO mice. Also, an increase of immunolabeling of these markers in other areas was not evident, arguing that mislocalization of these proteins is not the cause for the absence of immunolabeling in the pyramidal layer. Even more surprisingly, the amount of CCK-positive somata in the hippocampus of DG cKO mice was reduced to around half the density found in control mice, and the staining intensity of immunopositive cells in cKO mice was decreased. Assuming that ablation of DG does not lead to synapse or cell loss, these results suggest that DG trans-synaptic signaling is involved in maintaining a specific expression profile in CCK-positive cells, aimed to uphold transcription of synaptic proteins essential for function of CCK-positive terminals.

Testing of this hypothesis is hindered by several difficulties. First, it would require to conclusively demonstrate that neuronal DG ablation does not lead to morphological changes in axon terminals and somata of CCK-positive basket cells. This might be approached in DG cKO mice by ultrastructural analysis of inhibitory synapses and ectopic expression of a marker protein in CCK-positive basket cells. However, untangling structural from transcriptional changes represents a challenge because the expression of marker proteins by promoters specific for CCK-positive cells might be blunted in DG-ablated mice due to the loss of DG trans-synaptic signaling. Thus, it would be difficult to distinguish whether the reduction in a CCK-driven fluorescent protein in DG cKO mice is due to reduced transcription or due to cell loss. Therefore, this approach would require the expression of a marker protein in CCK-positive basket cells under the control of a constitutive promoter, for instance with the help of a CCK-driven Cre recombining a floxed stop cassette. Combined with the concurrent ablation of DG in pyramidal cells, this approach might faithfully visualize morphology of (formerly) CCK-positive basket cells. Secondly, expression profiles of CCK-positive cells would have to be analyzed to demonstrate that genes specific for this interneuron class are downregulated. Using the same technique of ectopic expression of a marker protein, fluorescence-assisted cell sorting followed by qPCR or RNA sequencing could be employed to characterize expression profiles of CCK-positive cells. Finally, the mechanism of retrograde signaling from CCK-positive terminals to transcriptional regulators in the cell soma would have to be elucidated. For this, the presynaptic binding partner of DG and the associated signaling pathway would have to be identified.

The involvement of GABAergic PSD proteins in synaptic maintenance was only recently addressed by ablation of NL2 in the prefrontal cortex of adult mice (Liang et al., 2015). Similar to loss of DG, NL2

ablation in adulthood caused a reduction of a presynaptic marker over several weeks. However, the decrease of GAD65 puncta density indicates that NL2 is necessary for the maintenance of all GABAergic terminals, and does not exhibit the interneuron subtype-specific function found for DG.

General phenotype of DG cKO mice and potential off-target effects

The use of the NEX-Cre driver line for ablation of neuronal DG resulted in cKO mice with a compromised physical constitution. DG cKO mice were smaller and displayed reduced body and brain weight compared to control mice. Furthermore, an increased mortality rate was noted for DG-deficient mice.

The occurrence of this systemic phenotype was unexpected because of the specificity of the NEX promoter. NEX expression is restricted to the CNS, and is specific to principal neurons within cerebral hemispheres (Bartholoma and Nave, 1994; Schwab et al., 1998). Replacement of the coding region of NEX with the Cre recombinase expression cassette did not change the limited expression of this locus (Goebbels et al., 2006). Western blot analysis revealed similar DG levels in muscle of DG cKO and control mice, providing evidence that muscle DG was indeed not affected by NEX-Cre mediated ablation of DG. However, to rule out subtle anatomical changes due to residual NEX expression in muscle, histological and immunohistochemical analysis of muscle tissue should be performed.

Close examination of NEX-Cre expression pattern using mice harboring a floxed β-Galactosidase as a reporter line reveals that weak NEX expression is present in brain areas outside the cerebral cortex (Goebbels et al., 2006). These areas include small cell populations in the olfactory bulb, amygdala, cerebellum and in the brainstem. Since DG expression partly overlaps with these areas, it is conceivable that weak Cre expression leads to ablation of DG in these cells. For instance, DG was localized to the mitral cell layer in the olfactory bulb, and to the pontine nucleus, where Cre expression was detected (Zaccaria et al., 2001; Goebbels et al., 2006). NEX expression was further demonstrated in the amygdala, a region where dystrophin and thus presumably also DG is expressed (Sekiguchi et al., 2009). The function of the DGC in these brain areas is unknown at the moment, and the consequences of the putative ablation of DG therefore remain elusive. However, it is possible that the use of the NEX-Cre driver line leads to cognitive and behavioral deficits which are caused by DG ablation in brain neurons outside of the cerebral hemispheres.

NEX expression was further demonstrated in the developing and adult spinal cord (Goebbels et al., 2006). The essential role of DG in binding Slit, an essential axon guidance protein for midline crossing of commissural axons, suggests that this function might be compromised in DG cKO mice. However, DG is localized mostly in the floor plate, in contrast to the diffuse distribution of NEX primarily in the dorsal horn. Therefore, it seems unlikely that ablation of DG in the spinal cord is the cause of the deficits in physical constitution of DG cKO mice.

In the light of the reduced size of DG cKO mice and of the crucial role of DG for CCK-positive interneurons, it is striking that CCK is a regulator of satiety. CCK is released in the small intestine in

response to food intake and acts as a satiety signal and to increase the release of digestive enzymes. However, in the CNS, CCK acts locally over activation of CCK_B receptors, in contrast to CCK_A receptors which are abundant in the periphery and more relevant for the regulation of food intake (Noble et al., 1999). In addition, CCK action in the brain was connected to anxiety and cognitive functions, but not directly to the control of satiety. The idea that a compensatory upregulation of CCK release and therefore increased satiety signaling accounts for the smaller size of cKO mice therefore does not hold.

After considering potential off-target effects of neuronal DG ablation, the notion that behavioral deficits arise from the loss of CCK-positive terminals on pyramidal cells emerges as a plausible possibility. As CCK-positive interneurons make up around half of all basket cells, dysfunctional neurotransmission from CCK-positive cells would be expected to have a dramatic impact on cognition and behavior (Whissell et al., 2015). Indeed, essential functions of CCK-positive interneurons in synaptic plasticity and for network activity were described (Bartos and Elgueta, 2012). Whether disruption of neurotransmission from CCK-positive terminals causes the reduced body size by social rejection in competition with littermates in the home cage or whether the phenotype arises from intrinsic causes remains to be determined. To address this question, DG cKO and control mice should be separated at birth or at the time of weaning and their development monitored. If the deficits in physical constitution persist despite genotypical separation, social rejection could be excluded as the sole cause. Still, intrinsic factors might be attributed to dysfunctional neurotransmission from CCK-positive basket cells or to other, nonspecific deficits, or to a combination thereof.

NEX-Cre DG cKO mice as a model to study function of CCK-positive interneurons

The specific and complete loss of immunohistochemical markers and the reduced inhibitory drive in pyramidal cells of DG cKO mice point towards the dysfunction of CCK-positive basket cells. Further physiological and morphological characterization of CCK-positive basket cells in DG cKO mice will have to be carried out to confirm the completeness of this loss-of-function. If subsequent studies validate this notion, NEX-Cre DG cKO mice represent a powerful model to study the contribution of CCK-positive basket cells to brain function.

Various roles were ascribed to CCK-positive basket cells in cortical neuronal circuits, many of which are connected to the interneuron class-defining proteins that are exclusively expressed by this cell type. For instance, the presence of VGluT3 in CCK-positive terminals is unique among GABAergic interneurons and is thought to serve the corelease of glutamate with GABA (Somogyi et al., 2004; Stensrud et al., 2013; Stensrud et al., 2015). The terminal release of CCK is another speciality of CCK-positive basket cells, and has far-reaching implications for the activity of neighboring PV-

positive cells (Lee and Soltesz, 2011). The impact of the lost CCK-positive terminals could be tested by examining compensatory changes of CCK_B receptors on PV-positive basket cells, for instance.

The presence of CB1 receptors on axon terminals of CCK-positive basket cells is a further defining feature. Disinhibition through endocannabinoids by silencing GABA release from CCK-positive basket cells, known as DSI, is activity-dependent. During gamma activity, which is promoted by exploratory behavior, CCK-positive basket cells fire in a phase-locked manner shortly before the peak of the oscillation (Tukker et al., 2007). When pyramidal cells, acting as place cells, increase action potential frequency, this might trigger the release of endocannabinoids and locally lead to DSI (Leutgeb et al., 2007). The resulting disinhibition from CCK-positive terminals might cause place cells to fire in a phase-shifted rhythm, relative to surrounding pyramidal cells. This process, which is likely to play an important role in spatial navigation, is predicted to be disrupted in DG cKO mice. Behavioral testing as well as correlating pyramidal cell activity to population activity in the hippocampus of DG cKO mice might elucidate the dependence of this mechanism on CCK-positive interneurons.

Oscillatory activity patterns correlate with distinct behaviors and interneuron firing patterns, including those from CCK-positive basket cells, are aligned with oscillations *in vivo* (Klausberger et al., 2005; Klausberger and Somogyi, 2008). Therefore, there is a large interest in identifying the cell types and physiological processes that generate oscillations. The mechanisms underlying generation of theta oscillations in different subfields of the hippocampus are still controversial, but there is evidence suggesting a crucial role of CCK-positive basket cells. PV-positive basket cells seem to be heavily involved in generation of rhythmic activity patterns, especially in CA3 (Gulyas et al., 2010; Amilhon et al., 2015). However, theta oscillations induced by the AChR agonist CCh are sensitive to DSI, which is mediated by activation of CB1 receptors (Pitler and Alger, 1992). Furthermore, CCh-induced neuronal firing in CA1 is strongly attenuated by CB1 agonists, showing the dependence of this rhythmic activity on CB1-containing terminals more directly (Wyeth et al., 2010). Along the same lines, only optogenetic inhibition of CCK-positive but not of PV-positive basket cell activity resulted in the loss of CCh-induced oscillatory activity (Nagode et al., 2014). The finding that, in contrast to control mice, sIPSC frequency could not be increased by CCh application in DG cKO mice, confirms therefore that CCK-positive terminal function is disrupted in DG cKO mice. Conversely, this finding also highlights that NEX-Cre DG cKO mice represent a unique opportunity to study the contribution of CCK-positive basket cells to theta oscillations *in vivo*, without the need for pharmaceutical manipulations. Therefore, spectral analysis of surface electroencephalogram or local field potential recordings in DG cKO mice might reveal clues about the role of CCK-positive basket cells in generation of oscillatory activity patterns.

Clinical implications of DG-CCK-positive basket cell interconnection

Conditional ablation of DG in principal neurons of the forebrain represents an unphysiological manipulation, which does not directly correspond to any known disease. However, by unraveling the importance of DG for CCK-positive terminals, the results of this experimental approach are likely to shed light on the neuronal circuits that are compromised in patients with genetic defects in DGC components.

The partly severe ID exhibited by muscular dystrophy patients without associated brain malformations indicates that neuronal DG serves essential functions for normal cognition. DG T190M KI mice are a model for dystroglycanopathy patients carrying the DG T192M mutation (Hara et al., 2011). Since these patients suffer from severe ID despite lacking gross neuroanatomical alterations, the DG T190M KI mice might represent the disease model most closely resembling the situation in DG cKO mice (Dincer et al., 2003). The integrity of CCK-positive terminals in KI mice was therefore unexpected. However, the presence of immunohistochemical markers does not exclude the possibility that CCK-positive terminals are dysfunctional in this model. DG binding to an unknown presynaptic molecule, important for maintenance of CCK-positive terminals, might be intact in T190M KI mice. Still, it is conceivable that, in addition, neurexin binding is necessary for normal neurotransmission from CCK-positive terminals, leading to cognitive dysfunctions. Electrophysiological characterization of pyramidal cells in T190M KI mice, with a focus on inhibitory input received from basket cells, might therefore serve as a starting point in the search for the physiological basis of ID in this group of patients.

It is likely that the DG-CCK interconnection is also relevant in the etiology of ID in dystrophinopathies. A reduction in CB1 and VGluT3 immunoreactivity was found in mdx mice, hinting at a role for dystrophin in trans-synaptic signaling (Krasowska et al., 2014). In this context, it will be instructive to examine the integrity of CCK-positive terminals in DG βcyt/βcyt mice, which lack the intracellular part of DG (Satz et al., 2010). If deficits in CCK-positive basket cell markers in mdx mice and in brain biopsies of DMD patients confirm a role for dystrophin in this signaling pathway, brain alterations associated with DMD might have to be reinterpreted in the light of this new role. For instance, an increase in choline-containing compounds was reported in DMD patients and in mdx mice (Kato et al., 1997; Parames et al., 2014). These differences might represent compensatory changes in response to altered function or abundance of CCK-positive basket cells. This hypothesis is especially compelling considering the importance of cholinergic activation of CCK-positive interneurons for generating theta oscillations (Cea-del Rio et al., 2010). Thus, special emphasis should be put on spectral power analyses of population recordings in dystrophinopathy patients and animal models.

DG and synArfGEF serve independent functions

Their biochemical interaction, colocalization and lack of knowledge of their functional role in the GABAergic PSD was part of the rationale to study the DGC and synArfGEF in parallel (Fukaya et al., 2011). A role for both proteins in subcellular domain-specific regulation of GABAergic PSDs was suggested by the following observations. First, the DGC displays a preferentially perisomatic distribution in pyramidal cells. Secondly, in $GABA_AR$ α2 subunit KO mice, NL2 clustering is compromised only in dendritic but not in somatic regions (Panzanelli et al., 2011). Together with the report of a specific requirement of NL2 in CA1 pyramidal layer for GABAergic PSD clustering (Poulopoulos et al., 2009), these findings suggested a common role for the DGC, NL2 and possibly synArfGEF in regulation of perisomatic GABAergic PSDs. This notion was further strengthened by experiments demonstrating that the scaffolding protein S-SCAM can bind to DG, NL2 and synArfGEF (Sumita et al., 2007; Fukaya et al., 2011). Finally, synArfGEF expression is induced by the transcription factor NPAS4, which regulates GABAergic PSD clustering in a layer-specific manner in the hippocampus (Bloodgood et al., 2013).

Under the premise that synArfGEF builds part of an extended DGC at perisomatic GABAergic synapses, synArfGEF clustering was examined in DG cKO mice. The unexpected result that synArfGEF clustering in CA1 pyramidal layer was not substantially different in cKO mice, demonstrates that the dystrophin-synArfGEF interaction is not necessary for synaptic targeting of synArfGEF. The detailed study of synArfGEF colocalization with GABAergic markers revealed that gephyrin immunolabeling was most thoroughly overlapping with the synArfGEF staining pattern (Sakagami et al., 2013). Biochemical interaction with gephyrin might therefore be essential for postsynaptic clustering of synArfGEF. Indeed, in primary hippocampal cultures, gephyrin downregulation was paralleled by a drastic reduction of synArfGEF clustering (Um et al., 2016).

The initial description of synArfGEF-dystrophin colocalization was based on the immunocytochemical analysis of low-density dissociated hippocampal cultures (Fukaya et al., 2011). In this preparation, where neurons are separated from an astrocyte feeder layer, the neuronal DGC is present in large perisomatic clusters (Brunig et al., 2002; Levi et al., 2002). However, in mixed high-density hippocampal cultures, as used for synArfGEF experiments in this thesis, immunolabeling of DGC components was extremely sparse and generally restricted peripheral areas, which were not covered by astrocytes completely (unpublished observation). For this reason, the function of synArfGEF in regulation of mismatched GABAergic PSDs is likely independent of the DGC. The observation that mutation of the dystrophin-interaction motif in synArfGEF did not affect synArfGEF distribution further supports this assumption.

Still, the presence of a WW domain interaction motif in synArfGEF, together with the colocalization in low-density cultures, argues that interaction with dystrophin serves a physiological function in the GABAergic PSD. Dystrophin interaction might substitute the binding of synArfGEF to S-SCAM in

synapses containing the DGC. Whether interaction with dystrophin has an inhibitory or inducing effect on synArfGEF catalytic function is unknown. However, it is tempting to speculate that in synapses of CCK-positive terminals, there is a necessity to dampen synArfGEF activity, due to the putative corelease of glutamate and the subsequent increase in intracellular Ca^{2+} concentrations, which would otherwise lead to excessive synArfGEF activity.

Selectivity for GABAergic proteins in regulation of PSD apposition by synArfGEF

The results of overexpression and ablation experiments demonstrated a role for synArfGEF in the regulation of GABAergic PSD proteins which are mismatched with glutamatergic presynaptic terminals. Neither correctly apposed GABAergic PSD proteins nor glutamatergic PSD proteins were affected by manipulation of synArfGEF expression levels. The specificity of this regulation provides clues about the mechanism of synArfGEF-mediated regulation of PSD proteins.

Sec7 mutant overexpression did not affect the density of correctly apposed GABAergic PSDs. Assuming that overexpression of this mutant resulted in the complete blocking of synArfGEF catalytic activity, this finding suggests that under physiological conditions, synArfGEF is catalytically inactive in correctly apposed GABAergic PSDs or that catalytic activity does not impact clustering of PSD proteins in these synapses. Two scenarios are conceivable to explain the selectivity of synArfGEF function to mismatched GABAergic PSDs. A factor exclusively located at correctly matched PSDs might inhibit synArfGEF or its effectors. Alternatively, signaling or proteins specific to mismatched GABAergic PSDs are necessary for synArfGEF function. Because neuronal activity is crucial for transmitter-specific alignment of synaptic structures, any such factor is likely to undergo activity-dependent modulation (Anderson et al., 2004; Cesa et al., 2008). Glutamate release at mismatched GABAergic PSDs might activate extrasynaptic NMDA receptors, presumably leading to high Ca^{2+} concentrations during neuronal activity. Since calmodulin binds to synArfGEF specifically in low Ca^{2+} concentrations, calmodulin represents a likely candidate to take the role of an activity-dependent modulator of synArfGEF function.

Thus, to induce synArfGEF catalytic activity at synaptic sites, two conditions might have to be met. First, gephyrin has to be present in the PSD. This conclusion is inferred from the finding that synArfGEF catalytic activity does not affect PSD-95 apposition and from the observation that gephyrin downregulation interferes with synArfGEF clustering (Um et al., 2016). Whether gephyrin serves only to accumulate synArfGEF at GABAergic PSDs or whether gephyrin binding itself is necessary for activation of synArfGEF remains unclear. To address this question, a Sec7 mutant construct lacking the N-terminal CC domain should be examined for the capacity to increase the density of mismatched GABAergic PSDs, similar to the Sec7 mutant construct. Secondly, Ca^{2+} influx due to glutamate release at mismatched gephyrin-containing PSDs might lead to the dissociation of

calmodulin and synArfGEF, thereby facilitating synArfGEF catalytic activity. In addition, increases in Ca^{2+} concentration might lead to the activation of other Ca^{2+}-dependent enzymes.

A model in which both the presence of gephyrin and the Ca^{2+}-dependent unbinding of calmodulin are crucial for synArfGEF function is complicated by evidence suggesting that synArfGEF might bind to these proteins in a competitive manner. The gephyrin binding site on synArfGEF is in close proximity to the IQ motif, which was found to be essential for apocalmodulin binding. Furthermore, deletion of the N-terminal CC domain, which has a putative role in synArfGEF dimerization (Myers et al., 2012), revealed that synArfGEF binding to gephyrin and to calmodulin might represent different conformational states. The ΔN construct exhibited weaker interaction with gephyrin, whereas the binding to calmodulin was enhanced by deletion of the N-terminus. The existence of an inactive synArfGEF-gephyrin-apocalmodulin complex therefore seems unlikely. Rather, experimental evidence points to a dimeric gephyrin-interacting state and a monomeric apocalmodulin-interacting state.

If release of calmodulin from synArfGEF is sufficient to induce synArfGEF catalytic activity, then the IQ mutant, which lacks calmodulin binding capacity, would be predicted to act as a constitutively active mutant. However, overexpression of the IQ mutant did not lead to a reduction of mismatched GABAergic PSDs. Under the assumption that this result is not due to intrinsic properties of the neuronal cultures examined or due to technical artifacts (setting a lower limit on the density of mismatched synapses, for instance because of technical limitations such as the resolution of confocal microscopy), this finding suggests that additional steps are necessary to induce the catalytic function of synArfGEF in mismatched GABAergic PSDs. Residues on synArfGEF which are accessible for posttranslational modification only if calmodulin is not bound might represent such a switch to activate synArfGEF catalytic function after release of calmodulin. Strikingly, S348 was identified as a phosphorylation site and because of the proximity to the IQ motif, the dependence of modification of this site on calmodulin release is plausible (Trinidad et al., 2006). The kinases catalyzing phosphorylation of S348 in synArfGEF were not yet identified and thus pharmacological approaches to test the relevance of this PTM are tedious. However, overexpression of S348 point-mutated constructs in primary hippocampal neurons will reveal whether modification of this site is essential for regulation of mismatched GABAergic PSDs by synArfGEF.

Molecular mechanisms underlying synArfGEF-mediated GABAergic PSD regulation

The Sec7 mutation is expected to abrogate catalytic activity of synArfGEF, based on experiments which systematically tested the effect of mutations on catalytic activity in proteins containing a highly homologous Sec7 domain (Beraud-Dufour et al., 1998; Cherfils et al., 1998; Myers et al., 2012). However, conflicting results were reported for the specificity of synArfGEF to Arf1 or to Arf6. While

human synArfGEF was found to display specificity to Arf1, specific catalytic activity for Arf6 was demonstrated for the rat isoform (Hattori et al., 2007; Fukaya et al., 2011). Besides the fact that the rat isoform was used for overexpression experiments, there is additional evidence to suggest that the regulation of mismatched GABAergic PSDs by synArfGEF is mediated by Arf6. First, overexpression of Arf6 mutants recapitulated the increase in density of mismatched GABAergic PSDs found with overexpression of the Sec7 mutant. Secondly, IQSEC1 and IQSEC2, the closest synArfGEF homologs, exhibit strongest catalytic activity for Arf6 (Someya et al., 2001; Sakagami et al., 2008; Moravec et al., 2012). Finally, Arf6 is the only member of Arf GTPases which cycles between a plasma membrane-bound and a endosome-bound form (Peters et al., 1995; D'Souza-Schorey and Chavrier, 2006). Other Arf members are predominantly located in ER or Golgi compartments. Therefore, Arf6 is predestined to act at synapses due to its subcellular localization.

Neuronal morphology is controlled by Arf6 through two basic, interconnected mechanisms. On one hand, Arf6 regulates membrane trafficking by directly activating phospholipase D (PLD) and phosphatidylinositol-4-phosphate 5-kinases (PIP5K). This leads to an increase in phosphatidic acid (PA) and phosphatidylinositol bisphosphate (PIP2) production. PIP2, in turn, promotes clathrin-dependent endocytosis by recruiting AP2 as well as clathrin-independent endocytosis (Brown et al., 2001; Krauss et al., 2003; Paleotti et al., 2005). On the other hand, Arf6 is involved in regulation of actin dynamics. The actin cytoskeleton is impacted by Arf6 activity because of the rise in PIP2, which regulates actin dynamics, but also due to the ability of Arf6 to activate the GTPase Rac1 (Radhakrishna et al., 1999; Yin and Janmey, 2003; Santy et al., 2005). Determining whether Arf6 activity mainly affects membrane trafficking or actin dynamics in a given context is difficult, because both processes are interdependent. Not only is PIP2 involved in regulation of actin polymerization, but actin plays an important role in endocytosis as well.

SynArfGEF-mediated Arf6 activation might thus regulate mismatched GABAergic PSDs by modulating actin dynamics or by promoting membrane internalization. Since the actin cytoskeleton is not necessary for gephyrin clustering in mature neurons, this regulation is unlikely to rely solely on modulation of actin dynamics (Allison et al., 2000). Therefore, the involvement of membrane internalization, possibly by $GABA_AR$ endocytosis, should be examined. This hypothesis could be tested by distinct labeling of cell surface and intracellular pools of $GABA_AR$ subunits in primary neurons overexpressing wildtype or Sec7 mutant synArfGEF (van Rijnsoever et al., 2005). Furthermore, viral overexpression or ablation of synArfGEF in primary neuronal cultures in combination with surface biotinylation and immunoblotting of transmembrane proteins might reveal differences in the fraction of $GABA_ARs$ located at the cell membrane. This approach also allows to screen for other transmembrane proteins which are potentially targeted for internalization by synArfGEF.

If synArfGEF-induced activation of Arf6 leads to endocytosis of transmembrane proteins at mismatched GABAergic PSDs, the question how specificity for these proteins is ensured remains. The

interaction and colocalization of gephyrin with profilin 2A might serve as a starting point to address this question (Mammoto et al., 1998; Giesemann et al., 2003). Profilins bind to proteins regulating endocytosis, such as clathrin and dynamin, in the mouse brain, and in addition serve important functions in actin polymerization (Witke et al., 1998; Birbach, 2008). The idea that profilin 2A might accumulate proteins in the GABAergic PSD which play a role in synArfGEF-mediated endocytosis of GABAergic transmembrane proteins is further supported by the finding that neuronal activity promotes the synaptic localization of this protein (Murk et al., 2012).

Putative physiological functions of synArfGEF

The extensive and specific expression of synArfGEF in the CNS, association with important GABAergic PSD proteins and the function of close homologs in glutamate receptor subtype-specific regulation of synaptic strength suggest that synArfGEF serves important functions in the brain. The mechanisms preventing the formation of mismatched GABAergic PSDs *in vivo* were not explored to date, possibly due to the lack of mutants exhibiting such a phenotype. However, because synaptic structures are more densely packed in intact neural tissue than in dissociated neuronal cultures, the conclusive demonstration of synaptic misalignment *in vivo* is substantially more laborious. The fact that mismatched GABAergic PSDs were not yet described in intact brain tissue might thus be caused be these technical difficulties, which hampered the systematic search for mismatched synapses. GABAergic presynaptic structures were observed on glutamatergic postsynaptic structures such as spines *in vivo*, under blockade of neuronal activity (Cesa et al., 2008). Together with the newly uncovered role of synArfGEF in regulation of mismatched GABAergic PSDs, these findings urge the investigation of potential molecular mechanisms underlying mismatched GABAergic PSDs in the brain. To study the putative role of synArfGEF in alignment of GABAergic postsynaptic proteins with presynaptic terminals *in vivo*, synArfGEF KO mouse models will be instrumental. In addition, overexpression of synArfGEF mutations during development might be employed to unravel the functions of individual domains in this process.

Transcriptomic analysis of cortical tissue revealed that synArfGEF is one of only two genes which is downregulated in schizophrenia, autism and bipolar disorder patients in comparison to control groups (Ellis et al., 2016). Even if these changes represent compensatory alterations rather than a common etiology of these neuropsychiatric disorders, this striking finding points towards a physiological role of synArfGEF in the human brain. Mutations in IQSEC2, for which a function in GluA1-specific internalization of AMPA receptors and in LTD was demonstrated, were implicated in X-linked ID (Morleo et al., 2008; Shoubridge et al., 2010; Myers et al., 2012; Tran Mau-Them et al., 2014; Brown et al., 2016a). These mutations were located to the Sec7 domain and IQ motif, indicating that activity-dependent removal of AMPA receptors plays a role in the etiology of cognitive impairment in these patients. It might therefore be instructive to explore the occurrence of missense mutations in the corresponding regions in synArfGEF in patients suffering from neuropsychiatric disorders.

Conclusions

In the search for the molecular determinants of synaptic specificity, the role of a postsynaptic complex containing DG and synArfGEF was analyzed. The study of DG function, primarily based on the conditional ablation of DG *in vivo*, revealed that this complex is essential for synaptic specificity within the GABAergic neurotransmitter system. Furthermore, a novel role for the DGC in trans-synaptic signaling was suggested by the requirement for DG in synaptic maintenance. Molecular analysis of synArfGEF function *in vitro* and in cell culture uncovered an unexpected role in regulation of mismatched GABAergic PSDs, thus conferring specificity between neurotransmitter systems. The regulatory role of synArfGEF did not extend to correctly matched GABAergic PSDs or to glutamatergic proteins, highlighting that both pre- and postsynaptic structures restrict synArfGEF function. Together, these findings demonstrate that the postsynaptic molecular heterogeneity reflects the presynaptic cell type and neurochemical diversity and that GABAergic postsynaptic proteins can mediate synaptic specificity. Due to the far-reaching implications for neuronal connectivity, these newly identified mechanisms will provide a framework for the understanding and treatment of clinical manifestations of synaptic defects.

REFERENCES

Allison DW, Chervin AS, Gelfand VI, Craig AM (2000) Postsynaptic scaffolds of excitatory and inhibitory synapses in hippocampal neurons: maintenance of core components independent of actin filaments and microtubules. J Neurosci 20:4545-4554.

Amilhon B, Huh CY, Manseau F, Ducharme G, Nichol H, Adamantidis A, Williams S (2015) Parvalbumin Interneurons of Hippocampus Tune Population Activity at Theta Frequency. Neuron 86:1277-1289.

Anderson JL, Head SI, Morley JW (2012) Duchenne muscular dystrophy and brain function. In: Muscular dystrophy (Hegde M, ed): InTech.

Anderson TR, Shah PA, Benson DL (2004) Maturation of glutamatergic and GABAergic synapse composition in hippocampal neurons. Neuropharmacology 47:694-705.

Ascoli GA et al. (2008) Petilla terminology: nomenclature of features of GABAergic interneurons of the cerebral cortex. Nat Rev Neurosci 9:557-568.

Azevedo FA, Carvalho LR, Grinberg LT, Farfel JM, Ferretti RE, Leite RE, Jacob Filho W, Lent R, Herculano-Houzel S (2009) Equal numbers of neuronal and nonneuronal cells make the human brain an isometrically scaled-up primate brain. J Comp Neurol 513:532-541.

Balic E, Rudolph U, Fritschy JM, Mohler H, Benke D (2009) The alpha5(H105R) mutation impairs alpha5 selective binding properties by altered positioning of the alpha5 subunit in GABAA receptors containing two distinct types of alpha subunits. J Neurochem 110:244-254.

Barresi R, Campbell KP (2006) Dystroglycan: from biosynthesis to pathogenesis of human disease. J Cell Sci 119:199-207.

Bartholoma A, Nave KA (1994) NEX-1: a novel brain-specific helix-loop-helix protein with autoregulation and sustained expression in mature cortical neurons. Mech Dev 48:217-228.

Bartos M, Elgueta C (2012) Functional characteristics of parvalbumin- and cholecystokinin-expressing basket cells. J Physiol 590:669-681.

Baudouin S, Scheiffele P (2010) SnapShot: Neuroligin-neurexin complexes. Cell 141:908, 908 e901.

Bemben MA, Shipman SL, Nicoll RA, Roche KW (2015) The cellular and molecular landscape of neuroligins. Trends Neurosci 38:496-505.

Ben-Ari Y, Gaiarsa JL, Tyzio R, Khazipov R (2007) GABA: a pioneer transmitter that excites immature neurons and generates primitive oscillations. Physiol Rev 87:1215-1284.

Benke D, Fakitsas P, Roggenmoser C, Michel C, Rudolph U, Mohler H (2004) Analysis of the presence and abundance of GABAA receptors containing two different types of alpha subunits in murine brain using point-mutated alpha subunits. J Biol Chem 279:43654-43660.

Beraud-Dufour S, Robineau S, Chardin P, Paris S, Chabre M, Cherfils J, Antonny B (1998) A glutamic finger in the guanine nucleotide exchange factor ARNO displaces Mg2+ and the beta-phosphate to destabilize GDP on ARF1. Embo J 17:3651-3659.

Biederer T, Sara Y, Mozhayeva M, Atasoy D, Liu X, Kavalali ET, Sudhof TC (2002) SynCAM, a synaptic adhesion molecule that drives synapse assembly. Science 297:1525-1531.

Birbach A (2008) Profilin, a multi-modal regulator of neuronal plasticity. Bioessays 30:994-1002.

Bloodgood BL, Sharma N, Browne HA, Trepman AZ, Greenberg ME (2013) The activity-dependent transcription factor NPAS4 regulates domain-specific inhibition. Nature 503:121-125.

Bock O (2013) Cajal, Golgi, Nansen, Schafer and the neuron doctrine. Endeavour 37:228-234.

Bortone D, Polleux F (2009) KCC2 expression promotes the termination of cortical interneuron migration in a voltage-sensitive calcium-dependent manner. Neuron 62:53-71.

Boucard AA, Chubykin AA, Comoletti D, Taylor P, Sudhof TC (2005) A splice code for trans-synaptic cell adhesion mediated by binding of neuroligin 1 to alpha- and beta-neurexins. Neuron 48:229-236.

Brown FD, Rozelle AL, Yin HL, Balla T, Donaldson JG (2001) Phosphatidylinositol 4,5-bisphosphate and Arf6-regulated membrane traffic. J Cell Biol 154:1007-1017.

Brown JC, Petersen A, Zhong L, Himelright ML, Murphy JA, Walikonis RS, Gerges NZ (2016a) Bidirectional regulation of synaptic transmission by BRAG1/IQSEC2 and its requirement in long-term depression. Nat Commun 7:11080.

Brown LE, Nicholson MW, Arama JE, Mercer A, Thomson AM, Jovanovic JN (2016b) gamma-Aminobutyric Acid Type A (GABAA) Receptor Subunits Play a Direct Structural Role in Synaptic Contact Formation via Their N-terminal Extracellular Domains. J Biol Chem 291:13926-13942.

Brunig I, Suter A, Knuesel I, Luscher B, Fritschy JM (2002) GABAergic terminals are required for postsynaptic clustering of dystrophin but not of GABA(A) receptors and gephyrin. J Neurosci 22:4805-4813.

Budreck EC, Scheiffele P (2007) Neuroligin-3 is a neuronal adhesion protein at GABAergic and glutamatergic synapses. Eur J Neurosci 26:1738-1748.

Butt SJ, Sousa VH, Fuccillo MV, Hjerling-Leffler J, Miyoshi G, Kimura S, Fishell G (2008) The requirement of Nkx2-1 in the temporal specification of cortical interneuron subtypes. Neuron 59:722-732.

Campbell KP, Kahl SD (1989) Association of dystrophin and an integral membrane glycoprotein. Nature 338:259-262.

Caroni P, Chowdhury A, Lahr M (2014) Synapse rearrangements upon learning: from divergent-sparse connectivity to dedicated sub-circuits. Trends Neurosci 37:604-614.

Cea-del Rio CA, Lawrence JJ, Tricoire L, Erdelyi F, Szabo G, McBain CJ (2010) M3 muscarinic acetylcholine receptor expression confers differential cholinergic modulation to neurochemically distinct hippocampal basket cell subtypes. J Neurosci 30:6011-6024.

Cesa R, Morando L, Strata P (2008) Transmitter-receptor mismatch in GABAergic synapses in the absence of activity. Proc Natl Acad Sci U S A 105:18988-18993.

Chamberlain JS, Pearlman JA, Muzny DM, Gibbs RA, Ranier JE, Caskey CT, Reeves AA (1988) Expression of the murine Duchenne muscular dystrophy gene in muscle and brain. Science 239:1416-1418.

Chelly J, Kaplan JC, Maire P, Gautron S, Kahn A (1988) Transcription of the dystrophin gene in human muscle and non-muscle tissue. Nature 333:858-860.

Chen JL, Villa KL, Cha JW, So PT, Kubota Y, Nedivi E (2012) Clustered dynamics of inhibitory synapses and dendritic spines in the adult neocortex. Neuron 74:361-373.

Cherfils J, Menetrey J, Mathieu M, Le Bras G, Robineau S, Beraud-Dufour S, Antonny B, Chardin P (1998) Structure of the Sec7 domain of the Arf exchange factor ARNO. Nature 392:101-105.

Chih B, Engelman H, Scheiffele P (2005) Control of excitatory and inhibitory synapse formation by neuroligins. Science 307:1324-1328.

Chih B, Gollan L, Scheiffele P (2006) Alternative splicing controls selective trans-synaptic interactions of the neuroligin-neurexin complex. Neuron 51:171-178.

Christie SB, Miralles CP, De Blas AL (2002) GABAergic innervation organizes synaptic and extrasynaptic GABAA receptor clustering in cultured hippocampal neurons. J Neurosci 22:684-697.

Chung WS, Clarke LE, Wang GX, Stafford BK, Sher A, Chakraborty C, Joung J, Foo LC, Thompson A, Chen C, Smith SJ, Barres BA (2013) Astrocytes mediate synapse elimination through MEGF10 and MERTK pathways. Nature 504:394-400.

Clements JD, Lester RA, Tong G, Jahr CE, Westbrook GL (1992) The time course of glutamate in the synaptic cleft. Science 258:1498-1501.

Cohen EJ, Quarta E, Fulgenzi G, Minciacchi D (2015) Acetylcholine, GABA and neuronal networks: a working hypothesis for compensations in the dystrophic brain. Brain Res Bull 110:1-13.

Cotton S, Voudouris NJ, Greenwood KM (2001) Intelligence and Duchenne muscular dystrophy: full-scale, verbal, and performance intelligence quotients. Dev Med Child Neurol 43:497-501.

Cotton SM, Voudouris NJ, Greenwood KM (2005) Association between intellectual functioning and age in children and young adults with Duchenne muscular dystrophy: further results from a meta-analysis. Dev Med Child Neurol 47:257-265.

Cowan WM, Kandel ER (2001) A brief history of synapses and synaptic transmission. In: Synapses (Cowan WM, Südhof TC, Stevens CF, eds), pp 1-87. Baltimore: The Johns Hopkins University Press.

Cox R, Mason-Gamer RJ, Jackson CL, Segev N (2004) Phylogenetic analysis of Sec7-domain-containing Arf nucleotide exchangers. Mol Biol Cell 15:1487-1505.

Crestani F, Low K, Keist R, Mandelli M, Mohler H, Rudolph U (2001) Molecular targets for the myorelaxant action of diazepam. Mol Pharmacol 59:442-445.

Crestani F, Keist R, Fritschy JM, Benke D, Vogt K, Prut L, Bluthmann H, Mohler H, Rudolph U (2002) Trace fear conditioning involves hippocampal alpha5 GABA(A) receptors. Proc Natl Acad Sci U S A 99:8980-8985.

Cuzon VC, Yeh PW, Cheng Q, Yeh HH (2006) Ambient GABA promotes cortical entry of tangentially migrating cells derived from the medial ganglionic eminence. Cereb Cortex 16:1377-1388.

D'Souza-Schorey C, Chavrier P (2006) ARF proteins: roles in membrane traffic and beyond. Nat Rev Mol Cell Biol 7:347-358.

Daniels MP (2012) The role of agrin in synaptic development, plasticity and signaling in the central nervous system. Neurochem Int 61:848-853.

De Groot-Ebeling CR (2014) Molecular determinants of collybistin function in GABAergic synapses: In vitro and in vivo analysis. PhD thesis. Zentralbibliothek Zürich: Mathematisch-naturwissenschaftliche Fakultät, University of Zurich.

Del Tongo C, Carretta D, Fulgenzi G, Catini C, Minciacchi D (2009) Parvalbumin-positive GABAergic interneurons are increased in the dorsal hippocampus of the dystrophic mdx mouse. Acta Neuropathol 118:803-812.

Dincer P, Balci B, Yuva Y, Talim B, Brockington M, Dincel D, Torelli S, Brown S, Kale G, Haliloglu G, Gerceker FO, Atalay RC, Yakicier C, Longman C, Muntoni F, Topaloglu H (2003) A novel form of recessive limb girdle muscular dystrophy with mental retardation and abnormal expression of alpha-dystroglycan. Neuromuscul Disord 13:771-778.

Du J, Reznikov LR, Price MP, Zha XM, Lu Y, Moninger TO, Wemmie JA, Welsh MJ (2014) Protons are a neurotransmitter that regulates synaptic plasticity in the lateral amygdala. Proc Natl Acad Sci U S A 111:8961-8966.

Duchenne de Boulogne G-B (1861) De l'électrisation localisée et de son application à la physiologie, à la pathologie et à la thérapeutique (2e édition). Paris: J.-B. Baillière et fils.

Elliott TR (1905) The action of adrenalin. J Physiol 32:401-467.

Ellis SE, Panitch R, West AB, Arking DE (2016) Transcriptome analysis of cortical tissue reveals shared sets of downregulated genes in autism and schizophrenia. Transl Psychiatry 6:e817.

Ervasti JM, Campbell KP (1991) Membrane organization of the dystrophin-glycoprotein complex. Cell 66:1121-1131.

Ervasti JM, Ohlendieck K, Kahl SD, Gaver MG, Campbell KP (1990) Deficiency of a glycoprotein component of the dystrophin complex in dystrophic muscle. Nature 345:315-319.

Fang C, Deng L, Keller CA, Fukata M, Fukata Y, Chen G, Luscher B (2006) GODZ-mediated palmitoylation of GABA(A) receptors is required for normal assembly and function of GABAergic inhibitory synapses. J Neurosci 26:12758-12768.

Farach-Carson MC, Warren CR, Harrington DA, Carson DD (2014) Border patrol: insights into the unique role of perlecan/heparan sulfate proteoglycan 2 at cell and tissue borders. Matrix Biol 34:64-79.

Fishell G, Rudy B (2011) Mechanisms of inhibition within the telencephalon: "where the wild things are". Annu Rev Neurosci 34:535-567.

Fiumelli H, Woodin MA (2007) Role of activity-dependent regulation of neuronal chloride homeostasis in development. Curr Opin Neurobiol 17:81-86.

Flames N, Long JE, Garratt AN, Fischer TM, Gassmann M, Birchmeier C, Lai C, Rubenstein JL, Marin O (2004) Short- and long-range attraction of cortical GABAergic interneurons by neuregulin-1. Neuron 44:251-261.

Flores CE, Nikonenko I, Mendez P, Fritschy JM, Tyagarajan SK, Muller D (2015) Activity-dependent inhibitory synapse remodeling through gephyrin phosphorylation. Proc Natl Acad Sci U S A 112:E65-72.

Freund TF, Katona I (2007) Perisomatic inhibition. Neuron 56:33-42.

Fritschy JM, Mohler H (1995) GABAA-receptor heterogeneity in the adult rat brain: differential regional and cellular distribution of seven major subunits. J Comp Neurol 359:154-194.

Fritschy JM, Panzanelli P (2014) GABAA receptors and plasticity of inhibitory neurotransmission in the central nervous system. Eur J Neurosci 39:1845-1865.

Fritschy JM, Harvey RJ, Schwarz G (2008) Gephyrin: where do we stand, where do we go? Trends Neurosci 31:257-264.

Fuccillo MV, Foldy C, Gokce O, Rothwell PE, Sun GL, Malenka RC, Sudhof TC (2015) Single-Cell mRNA Profiling Reveals Cell-Type-Specific Expression of Neurexin Isoforms. Neuron 87:326-340.

Fuchs C, Abitbol K, Burden JJ, Mercer A, Brown L, Iball J, Anne Stephenson F, Thomson AM, Jovanovic JN (2013) GABA(A) receptors can initiate the formation of functional inhibitory GABAergic synapses. Eur J Neurosci 38:3146-3158.

Fukaya M, Kamata A, Hara Y, Tamaki H, Katsumata O, Ito N, Takeda S, Hata Y, Suzuki T, Watanabe M, Harvey RJ, Sakagami H (2011) SynArfGEF is a guanine nucleotide exchange factor for Arf6 and localizes preferentially at post-synaptic specializations of inhibitory synapses. J Neurochem 116:1122-1137.

Fukuda T, Kosaka T (2000) Gap junctions linking the dendritic network of GABAergic interneurons in the hippocampus. J Neurosci 20:1519-1528.

Fukuda T, Kosaka T, Singer W, Galuske RA (2006) Gap junctions among dendrites of cortical GABAergic neurons establish a dense and widespread intercolumnar network. J Neurosci 26:3434-3443.

Giesemann T, Schwarz G, Nawrotzki R, Berhorster K, Rothkegel M, Schluter K, Schrader N, Schindelin H, Mendel RR, Kirsch J, Jockusch BM (2003) Complex formation between the postsynaptic scaffolding protein gephyrin, profilin, and Mena: a possible link to the microfilament system. J Neurosci 23:8330-8339.

Godfrey C et al. (2007) Refining genotype phenotype correlations in muscular dystrophies with defective glycosylation of dystroglycan. Brain 130:2725-2735.

Goebbels S, Bormuth I, Bode U, Hermanson O, Schwab MH, Nave KA (2006) Genetic targeting of principal neurons in neocortex and hippocampus of NEX-Cre mice. Genesis 44:611-621.

Gorecki DC, Monaco AP, Derry JM, Walker AP, Barnard EA, Barnard PJ (1992) Expression of four alternative dystrophin transcripts in brain regions regulated by different promoters. Hum Mol Genet 1:505-510.

Graciotti L, Minelli A, Minciacchi D, Procopio A, Fulgenzi G (2008) GABAergic miniature spontaneous activity is increased in the CA1 hippocampal region of dystrophic mdx mice. Neuromuscul Disord 18:220-226.

Graf ER, Zhang X, Jin SX, Linhoff MW, Craig AM (2004) Neurexins induce differentiation of GABA and glutamate postsynaptic specializations via neuroligins. Cell 119:1013-1026.

Gulyas AI, Szabo GG, Ulbert I, Holderith N, Monyer H, Erdelyi F, Szabo G, Freund TF, Hajos N (2010) Parvalbumin-containing fast-spiking basket cells generate the field potential oscillations induced by cholinergic receptor activation in the hippocampus. J Neurosci 30:15134-15145.

Haas JS, Greenwald CM, Pereda AE (2016) Activity-dependent plasticity of electrical synapses: increasing evidence for its presence and functional roles in the mammalian brain. BMC Cell Biol 17 Suppl 1:14.

Hammond C (2008) The metabotropic GABAB receptors. In: Cellular and molecular neurophysiology, pp 232-255: Elsevier.

Hara Y, Balci-Hayta B, Yoshida-Moriguchi T, Kanagawa M, Beltran-Valero de Bernabe D, Gundesli H, Willer T, Satz JS, Crawford RW, Burden SJ, Kunz S, Oldstone MB, Accardi A, Talim B, Muntoni F, Topaloglu H, Dincer P, Campbell KP (2011) A dystroglycan mutation associated with limb-girdle muscular dystrophy. N Engl J Med 364:939-946.

Harvey K, Duguid IC, Alldred MJ, Beatty SE, Ward H, Keep NH, Lingenfelter SE, Pearce BR, Lundgren J, Owen MJ, Smart TG, Luscher B, Rees MI, Harvey RJ (2004) The GDP-GTP exchange factor collybistin: an essential determinant of neuronal gephyrin clustering. J Neurosci 24:5816-5826.

Hattori Y, Ohta S, Hamada K, Yamada-Okabe H, Kanemura Y, Matsuzaki Y, Okano H, Kawakami Y, Toda M (2007) Identification of a neuron-specific human gene, KIAA1110, that is a guanine nucleotide exchange factor for ARF1. Biochem Biophys Res Commun 364:737-742.

Hernandez-Deviez DJ, Casanova JE, Wilson JM (2002) Regulation of dendritic development by the ARF exchange factor ARNO. Nat Neurosci 5:623-624.

Hernandez-Deviez DJ, Roth MG, Casanova JE, Wilson JM (2004) ARNO and ARF6 regulate axonal elongation and branching through downstream activation of phosphatidylinositol 4-phosphate 5-kinase alpha. Mol Biol Cell 15:111-120.

Herweg J, Schwarz G (2012) Splice-specific glycine receptor binding, folding, and phosphorylation of the scaffolding protein gephyrin. J Biol Chem 287:12645-12656.

Hoffman EP, Hudecki MS, Rosenberg PA, Pollina CM, Kunkel LM (1988) Cell and fiber-type distribution of dystrophin. Neuron 1:411-420.

Hong S, Dissing-Olesen L, Stevens B (2016) New insights on the role of microglia in synaptic pruning in health and disease. Curr Opin Neurobiol 36:128-134.

Hoon M, Soykan T, Falkenburger B, Hammer M, Patrizi A, Schmidt KF, Sassoe-Pognetto M, Lowel S, Moser T, Taschenberger H, Brose N, Varoqueaux F (2011) Neuroligin-4 is localized to glycinergic postsynapses and regulates inhibition in the retina. Proc Natl Acad Sci U S A 108:3053-3058.

Ibraghimov-Beskrovnaya O, Ervasti JM, Leveille CJ, Slaughter CA, Sernett SW, Campbell KP (1992) Primary structure of dystrophin-associated glycoproteins linking dystrophin to the extracellular matrix. Nature 355:696-702.

Inaba Y, Tian QB, Okano A, Zhang JP, Sakagami H, Miyazawa S, Li W, Komiyama A, Inokuchi K, Kondo H, Suzuki T (2004) Brain-specific potential guanine nucleotide exchange factor for Arf, synArfGEF (Po), is localized to postsynaptic density. J Neurochem 89:1347-1357.

Incontro S, Asensio CS, Edwards RH, Nicoll RA (2014) Efficient, complete deletion of synaptic proteins using CRISPR. Neuron 83:1051-1057.

Jacob TC, Moss SJ, Jurd R (2008) GABA(A) receptor trafficking and its role in the dynamic modulation of neuronal inhibition. Nat Rev Neurosci 9:331-343.

Jacob TC, Michels G, Silayeva L, Haydon J, Succol F, Moss SJ (2012) Benzodiazepine treatment induces subtype-specific changes in GABA(A) receptor trafficking and decreases synaptic inhibition. Proc Natl Acad Sci U S A 109:18595-18600.

Jaworski J (2007) ARF6 in the nervous system. Eur J Cell Biol 86:513-524.

Jayasinha V, Nguyen HH, Xia B, Kammesheidt A, Hoyte K, Martin PT (2003) Inhibition of dystroglycan cleavage causes muscular dystrophy in transgenic mice. Neuromuscul Disord 13:365-375.

Jucker M, Tian M, Norton DD, Sherman C, Kusiak JW (1996) Laminin alpha 2 is a component of brain capillary basement membrane: reduced expression in dystrophic dy mice. Neuroscience 71:1153-1161.

Kaczmarek L, Lapinska-Dzwonek J, Szymczak S (2002) Matrix metalloproteinases in the adult brain physiology: a link between c-Fos, AP-1 and remodeling of neuronal connections? Embo J 21:6643-6648.

Kanatani S, Yozu M, Tabata H, Nakajima K (2008) COUP-TFII is preferentially expressed in the caudal ganglionic eminence and is involved in the caudal migratory stream. J Neurosci 28:13582-13591.

Kasugai Y, Swinny JD, Roberts JD, Dalezios Y, Fukazawa Y, Sieghart W, Shigemoto R, Somogyi P (2010) Quantitative localisation of synaptic and extrasynaptic GABAA receptor subunits on hippocampal pyramidal cells by freeze-fracture replica immunolabelling. Eur J Neurosci 32:1868-1888.

Kato T, Nishina M, Matsushita K, Hori E, Akaboshi S, Takashima S (1997) Increased cerebral choline-compounds in Duchenne muscular dystrophy. Neuroreport 8:1435-1437.

Katsumaru H, Kosaka T, Heizmann CW, Hama K (1988) Gap junctions on GABAergic neurons containing the calcium-binding protein parvalbumin in the rat hippocampus (CA1 region). Exp Brain Res 72:363-370.

Khazipov R, Esclapez M, Caillard O, Bernard C, Khalilov I, Tyzio R, Hirsch J, Dzhala V, Berger B, Ben-Ari Y (2001) Early development of neuronal activity in the primate hippocampus in utero. J Neurosci 21:9770-9781.

Kikuno R, Nagase T, Ishikawa K, Hirosawa M, Miyajima N, Tanaka A, Kotani H, Nomura N, Ohara O (1999) Prediction of the coding sequences of unidentified human genes. XIV. The complete sequences of 100 new cDNA clones from brain which code for large proteins in vitro. DNA Res 6:197-205.

Kins S, Betz H, Kirsch J (2000) Collybistin, a newly identified brain-specific GEF, induces submembrane clustering of gephyrin. Nat Neurosci 3:22-29.

Kirsch J, Langosch D, Prior P, Littauer UZ, Schmitt B, Betz H (1991) The 93-kDa glycine receptor-associated protein binds to tubulin. J Biol Chem 266:22242-22245.

Klausberger T, Somogyi P (2008) Neuronal diversity and temporal dynamics: the unity of hippocampal circuit operations. Science 321:53-57.

Klausberger T, Marton LF, O'Neill J, Huck JH, Dalezios Y, Fuentealba P, Suen WY, Papp E, Kaneko T, Watanabe M, Csicsvari J, Somogyi P (2005) Complementary roles of cholecystokinin- and parvalbumin-expressing GABAergic neurons in hippocampal network oscillations. J Neurosci 25:9782-9793.

Knuesel I, Mastrocola M, Zuellig RA, Bornhauser B, Schaub MC, Fritschy JM (1999) Short communication: altered synaptic clustering of GABAA receptors in mice lacking dystrophin (mdx mice). Eur J Neurosci 11:4457-4462.

Koenig M, Hoffman EP, Bertelson CJ, Monaco AP, Feener C, Kunkel LM (1987) Complete cloning of the Duchenne muscular dystrophy (DMD) cDNA and preliminary genomic organization of the DMD gene in normal and affected individuals. Cell 50:509-517.

Korber C, Richter A, Kaiser M, Schlicksupp A, Mukusch S, Kuner T, Kirsch J, Kuhse J (2012) Effects of distinct collybistin isoforms on the formation of GABAergic synapses in hippocampal neurons. Mol Cell Neurosci 50:250-259.

Kothmann WW, Trexler EB, Whitaker CM, Li W, Massey SC, O'Brien J (2012) Nonsynaptic NMDA receptors mediate activity-dependent plasticity of gap junctional coupling in the AII amacrine cell network. J Neurosci 32:6747-6759.

Kowalczyk S, Winkelmann A, Smolinsky B, Forstera B, Neundorf I, Schwarz G, Meier JC (2013) Direct binding of GABAA receptor beta2 and beta3 subunits to gephyrin. Eur J Neurosci 37:544-554.

Krasowska E, Zablocki K, Gorecki DC, Swinny JD (2014) Aberrant location of inhibitory synaptic marker proteins in the hippocampus of dystrophin-deficient mice: implications for cognitive impairment in duchenne muscular dystrophy. PLoS One 9:e108364.

Krauss M, Kinuta M, Wenk MR, De Camilli P, Takei K, Haucke V (2003) ARF6 stimulates clathrin/AP-2 recruitment to synaptic membranes by activating phosphatidylinositol phosphate kinase type Igamma. J Cell Biol 162:113-124.

Krueger DD, Tuffy LP, Papadopoulos T, Brose N (2012) The role of neurexins and neuroligins in the formation, maturation, and function of vertebrate synapses. Curr Opin Neurobiol 22:412-422.

Krylova O, Herreros J, Cleverley KE, Ehler E, Henriquez JP, Hughes SM, Salinas PC (2002) WNT-3, expressed by motoneurons, regulates terminal arborization of neurotrophin-3-responsive spinal sensory neurons. Neuron 35:1043-1056.

Kuhse J, Kalbouneh H, Schlicksupp A, Mukusch S, Nawrotzki R, Kirsch J (2012) Phosphorylation of gephyrin in hippocampal neurons by cyclin-dependent kinase CDK5 at Ser-270 is dependent on collybistin. J Biol Chem 287:30952-30966.

Le Magueresse C, Monyer H (2013) GABAergic interneurons shape the functional maturation of the cortex. Neuron 77:388-405.

Lee K, Kim Y, Lee SJ, Qiang Y, Lee D, Lee HW, Kim H, Je HS, Sudhof TC, Ko J (2013) MDGAs interact selectively with neuroligin-2 but not other neuroligins to regulate inhibitory synapse development. Proc Natl Acad Sci U S A 110:336-341.

Lee SY, Soltesz I (2011) Cholecystokinin: a multi-functional molecular switch of neuronal circuits. Dev Neurobiol 71:83-91.

Leutgeb JK, Leutgeb S, Moser MB, Moser EI (2007) Pattern separation in the dentate gyrus and CA3 of the hippocampus. Science 315:961-966.

Levi S, Grady RM, Henry MD, Campbell KP, Sanes JR, Craig AM (2002) Dystroglycan is selectively associated with inhibitory GABAergic synapses but is dispensable for their differentiation. J Neurosci 22:4274-4285.

Li M, De Blas AL (1997) Coexistence of two beta subunit isoforms in the same gamma-aminobutyric acid type A receptor. J Biol Chem 272:16564-16569.

Liang J, Xu W, Hsu YT, Yee AX, Chen L, Sudhof TC (2015) Conditional neuroligin-2 knockout in adult medial prefrontal cortex links chronic changes in synaptic inhibition to cognitive impairments. Mol Psychiatry 20:850-859.

Lidov HG, Byers TJ, Kunkel LM (1993) The distribution of dystrophin in the murine central nervous system: an immunocytochemical study. Neuroscience 54:167-187.

Lidov HG, Byers TJ, Watkins SC, Kunkel LM (1990) Localization of dystrophin to postsynaptic regions of central nervous system cortical neurons. Nature 348:725-728.

Lodato S, Shetty AS, Arlotta P (2015) Cerebral cortex assembly: generating and reprogramming projection neuron diversity. Trends Neurosci 38:117-125.

Loewi O (1924) Über humorale Übertragbarkeit der Herznervenwirkung. Pflüger's Archiv für die gesamte Physiologie des Menschen und der Tiere:629-640.

Love DR, Bloomfield JF, Kenwrick SJ, Yates JR, Davies KE (1990) Physical mapping distal to the DMD locus. Genomics 8:106-112.

Low K, Crestani F, Keist R, Benke D, Brunig I, Benson JA, Fritschy JM, Rulicke T, Bluethmann H, Mohler H, Rudolph U (2000) Molecular and neuronal substrate for the selective attenuation of anxiety. Science 290:131-134.

Luscher B, Fuchs T, Kilpatrick CL (2011) GABAA receptor trafficking-mediated plasticity of inhibitory synapses. Neuron 70:385-409.

Luscher C, Malenka RC (2012) NMDA receptor-dependent long-term potentiation and long-term depression (LTP/LTD). Cold Spring Harb Perspect Biol 4.

Maher BJ, McGinley MJ, Westbrook GL (2009) Experience-dependent maturation of the glomerular microcircuit. Proc Natl Acad Sci U S A 106:16865-16870.

Mammoto A, Sasaki T, Asakura T, Hotta I, Imamura H, Takahashi K, Matsuura Y, Shirao T, Takai Y (1998) Interactions of drebrin and gephyrin with profilin. Biochem Biophys Res Commun 243:86-89.

Manent JB, Jorquera I, Ben-Ari Y, Aniksztejn L, Represa A (2006) Glutamate acting on AMPA but not NMDA receptors modulates the migration of hippocampal interneurons. J Neurosci 26:5901-5909.

Maric HM, Mukherjee J, Tretter V, Moss SJ, Schindelin H (2011) Gephyrin-mediated gamma-aminobutyric acid type A and glycine receptor clustering relies on a common binding site. J Biol Chem 286:42105-42114.

Marin O, Yaron A, Bagri A, Tessier-Lavigne M, Rubenstein JL (2001) Sorting of striatal and cortical interneurons regulated by semaphorin-neuropilin interactions. Science 293:872-875.

Marsden KC, Beattie JB, Friedenthal J, Carroll RC (2007) NMDA receptor activation potentiates inhibitory transmission through GABA receptor-associated protein-dependent exocytosis of GABA(A) receptors. J Neurosci 27:14326-14337.

Martini FJ, Valiente M, Lopez Bendito G, Szabo G, Moya F, Valdeolmillos M, Marin O (2009) Biased selection of leading process branches mediates chemotaxis during tangential neuronal migration. Development 136:41-50.

McKernan RM et al. (2000) Sedative but not anxiolytic properties of benzodiazepines are mediated by the GABA(A) receptor alpha1 subtype. Nat Neurosci 3:587-592.

McNally EM, Pytel P (2007) Muscle diseases: the muscular dystrophies. Annu Rev Pathol 2:87-109.

Michaluk P, Kolodziej L, Mioduszewska B, Wilczynski GM, Dzwonek J, Jaworski J, Gorecki DC, Ottersen OP, Kaczmarek L (2007) Beta-dystroglycan as a target for MMP-9, in response to enhanced neuronal activity. J Biol Chem 282:16036-16041.

Miike T, Miyatake M, Zhao J, Yoshioka K, Uchino M (1989) Immunohistochemical dystrophin reaction in synaptic regions. Brain Dev 11:344-346.

Miranda R, Sebrie C, Degrouard J, Gillet B, Jaillard D, Laroche S, Vaillend C (2009) Reorganization of inhibitory synapses and increased PSD length of perforated excitatory synapses in hippocampal area CA1 of dystrophin-deficient mdx mice. Cereb Cortex 19:876-888.

Missler M, Sudhof TC (1998) Neurexophilins form a conserved family of neuropeptide-like glycoproteins. J Neurosci 18:3630-3638.

Missler M, Hammer RE, Sudhof TC (1998) Neurexophilin binding to alpha-neurexins. A single LNS domain functions as an independently folding ligand-binding unit. J Biol Chem 273:34716-34723.

Missler M, Sudhof TC, Biederer T (2012) Synaptic cell adhesion. Cold Spring Harb Perspect Biol 4:a005694.

Miyazaki H, Yamazaki M, Watanabe H, Maehama T, Yokozeki T, Kanaho Y (2005) The small GTPase ADP-ribosylation factor 6 negatively regulates dendritic spine formation. FEBS Lett 579:6834-6838.

Mizokami A, Kanematsu T, Ishibashi H, Yamaguchi T, Tanida I, Takenaka K, Nakayama KI, Fukami K, Takenawa T, Kominami E, Moss SJ, Yamamoto T, Nabekura J, Hirata M (2007) Phospholipase C-related inactive protein is involved in trafficking of gamma2 subunit-containing GABA(A) receptors to the cell surface. J Neurosci 27:1692-1701.

Moore SA, Saito F, Chen J, Michele DE, Henry MD, Messing A, Cohn RD, Ross-Barta SE, Westra S, Williamson RA, Hoshi T, Campbell KP (2002) Deletion of brain dystroglycan recapitulates aspects of congenital muscular dystrophy. Nature 418:422-425.

Moravec R, Conger KK, D'Souza R, Allison AB, Casanova JE (2012) BRAG2/GEP100/IQSec1 interacts with clathrin and regulates alpha5beta1 integrin endocytosis through activation of ADP ribosylation factor 5 (Arf5). J Biol Chem 287:31138-31147.

Morleo M, Iaconis D, Chitayat D, Peluso I, Marzella R, Renieri A, Mari F, Franco B (2008) Disruption of the IQSEC2 transcript in a female with X;autosome translocation t(X;20)(p11.2;q11.2) and a phenotype resembling X-linked infantile spasms (ISSX) syndrome. Mol Med Rep 1:33-39.

Murk K, Wittenmayer N, Michaelsen-Preusse K, Dresbach T, Schoenenberger CA, Korte M, Jockusch BM, Rothkegel M (2012) Neuronal profilin isoforms are addressed by different signalling pathways. PLoS One 7:e34167.

Myers KR, Wang G, Sheng Y, Conger KK, Casanova JE, Zhu JJ (2012) Arf6-GEF BRAG1 regulates JNK-mediated synaptic removal of GluA1-containing AMPA receptors: a new mechanism for nonsyndromic X-linked mental disorder. J Neurosci 32:11716-11726.

Nagerl UV, Eberhorn N, Cambridge SB, Bonhoeffer T (2004) Bidirectional activity-dependent morphological plasticity in hippocampal neurons. Neuron 44:759-767.

Nagode DA, Tang AH, Yang K, Alger BE (2014) Optogenetic identification of an intrinsic cholinergically driven inhibitory oscillator sensitive to cannabinoids and opioids in hippocampal CA1. J Physiol 592:103-123.

Noble F, Wank SA, Crawley JN, Bradwejn J, Seroogy KB, Hamon M, Roques BP (1999) International Union of Pharmacology. XXI. Structure, distribution, and functions of cholecystokinin receptors. Pharmacol Rev 51:745-781.

Notter T, Panzanelli P, Pfister S, Mircsof D, Fritschy JM (2014) A protocol for concurrent high-quality immunohistochemical and biochemical analyses in adult mouse central nervous system. Eur J Neurosci 39:165-175.

Nyiri G, Freund TF, Somogyi P (2001) Input-dependent synaptic targeting of alpha(2)-subunit-containing GABA(A) receptors in synapses of hippocampal pyramidal cells of the rat. Eur J Neurosci 13:428-442.

O'Brien R, Xu D, Mi R, Tang X, Hopf C, Worley P (2002) Synaptically targeted narp plays an essential role in the aggregation of AMPA receptors at excitatory synapses in cultured spinal neurons. J Neurosci 22:4487-4498.

O'Brien RJ, Xu D, Petralia RS, Steward O, Huganir RL, Worley P (1999) Synaptic clustering of AMPA receptors by the extracellular immediate-early gene product Narp. Neuron 23:309-323.

O'Sullivan GA, Kneussel M, Elazar Z, Betz H (2005) GABARAP is not essential for GABA receptor targeting to the synapse. Eur J Neurosci 22:2644-2648.

Olsen RW, Sieghart W (2008) International Union of Pharmacology. LXX. Subtypes of gamma-aminobutyric acid(A) receptors: classification on the basis of subunit composition, pharmacology, and function. Update. Pharmacol Rev 60:243-260.

Omori Y, Araki F, Chaya T, Kajimura N, Irie S, Terada K, Muranishi Y, Tsujii T, Ueno S, Koyasu T, Tamaki Y, Kondo M, Amano S, Furukawa T (2012) Presynaptic dystroglycan-pikachurin complex regulates the proper synaptic connection between retinal photoreceptor and bipolar cells. J Neurosci 32:6126-6137.

Osada N, Hida M, Kusuda J, Tanuma R, Iseki K, Hirata M, Suto Y, Hirai M, Terao K, Suzuki Y, Sugano S, Hashimoto K (2001) Assignment of 118 novel cDNAs of cynomolgus monkey brain to human chromosomes. Gene 275:31-37.

Ozawa E, Mizuno Y, Hagiwara Y, Sasaoka T, Yoshida M (2005) Molecular and cell biology of the sarcoglycan complex. Muscle Nerve 32:563-576.

Paleotti O, Macia E, Luton F, Klein S, Partisani M, Chardin P, Kirchhausen T, Franco M (2005) The small G-protein Arf6GTP recruits the AP-2 adaptor complex to membranes. J Biol Chem 280:21661-21666.

Panzanelli P, Gunn BG, Schlatter MC, Benke D, Tyagarajan SK, Scheiffele P, Belelli D, Lambert JJ, Rudolph U, Fritschy JM (2011) Distinct mechanisms regulate GABAA receptor and gephyrin clustering at perisomatic and axo-axonic synapses on CA1 pyramidal cells. J Physiol 589:4959-4980.

Papadopoulos T, Eulenburg V, Reddy-Alla S, Mansuy IM, Li Y, Betz H (2008) Collybistin is required for both the formation and maintenance of GABAergic postsynapses in the hippocampus. Mol Cell Neurosci 39:161-169.

Papadopoulos T, Korte M, Eulenburg V, Kubota H, Retiounskaia M, Harvey RJ, Harvey K, O'Sullivan GA, Laube B, Hulsmann S, Geiger JR, Betz H (2007) Impaired GABAergic transmission and altered hippocampal synaptic plasticity in collybistin-deficient mice. Embo J 26:3888-3899.

Parames SF, Coletta-Yudice ED, Nogueira FM, Nering de Sousa MB, Hayashi MA, Lima-Landman MT, Lapa AJ, Souccar C (2014) Altered acetylcholine release in the hippocampus of dystrophin-deficient mice. Neuroscience 269:173-183.

Pereda AE (2014) Electrical synapses and their functional interactions with chemical synapses. Nat Rev Neurosci 15:250-263.

Peters PJ, Hsu VW, Ooi CE, Finazzi D, Teal SB, Oorschot V, Donaldson JG, Klausner RD (1995) Overexpression of wild-type and mutant ARF1 and ARF6: distinct perturbations of nonoverlapping membrane compartments. J Cell Biol 128:1003-1017.

Petrenko AG, Ullrich B, Missler M, Krasnoperov V, Rosahl TW, Sudhof TC (1996) Structure and evolution of neurexophilin. J Neurosci 16:4360-4369.

Pettem KL, Yokomaku D, Takahashi H, Ge Y, Craig AM (2013) Interaction between autism-linked MDGAs and neuroligins suppresses inhibitory synapse development. J Cell Biol 200:321-336.

Pfeiffer F, Graham D, Betz H (1982) Purification by affinity chromatography of the glycine receptor of rat spinal cord. J Biol Chem 257:9389-9393.

Pitler TA, Alger BE (1992) Postsynaptic spike firing reduces synaptic GABAA responses in hippocampal pyramidal cells. J Neurosci 12:4122-4132.

Poulopoulos A, Aramuni G, Meyer G, Soykan T, Hoon M, Papadopoulos T, Zhang M, Paarmann I, Fuchs C, Harvey K, Jedlicka P, Schwarzacher SW, Betz H, Harvey RJ, Brose N, Zhang W, Varoqueaux F (2009) Neuroligin 2 drives postsynaptic assembly at perisomatic inhibitory synapses through gephyrin and collybistin. Neuron 63:628-642.

Pribiag H, Peng H, Shah WA, Stellwagen D, Carbonetto S (2014) Dystroglycan mediates homeostatic synaptic plasticity at GABAergic synapses. Proc Natl Acad Sci U S A 111:6810-6815.

Purves D (2012) Neuroscience: Sinauer Associates.

Radhakrishna H, Al-Awar O, Khachikian Z, Donaldson JG (1999) ARF6 requirement for Rac ruffling suggests a role for membrane trafficking in cortical actin rearrangements. J Cell Sci 112 (Pt 6):855-866.

Ralvenius WT, Benke D, Acuna MA, Rudolph U, Zeilhofer HU (2015) Analgesia and unwanted benzodiazepine effects in point-mutated mice expressing only one benzodiazepine-sensitive GABAA receptor subtype. Nat Commun 6:6803.

Rao A, Cha EM, Craig AM (2000) Mismatched appositions of presynaptic and postsynaptic components in isolated hippocampal neurons. J Neurosci 20:8344-8353.

Reissner C, Stahn J, Breuer D, Klose M, Pohlentz G, Mormann M, Missler M (2014) Dystroglycan binding to alpha-neurexin competes with neurexophilin-1 and neuroligin in the brain. J Biol Chem 289:27585-27603.

Rudolph U, Knoflach F (2011) Beyond classical benzodiazepines: novel therapeutic potential of GABAA receptor subtypes. Nat Rev Drug Discov 10:685-697.

Rudolph U, Crestani F, Benke D, Brunig I, Benson JA, Fritschy JM, Martin JR, Bluethmann H, Mohler H (1999) Benzodiazepine actions mediated by specific gamma-aminobutyric acid(A) receptor subtypes. Nature 401:796-800.

Rudy B, Fishell G, Lee S, Hjerling-Leffler J (2011) Three groups of interneurons account for nearly 100% of neocortical GABAergic neurons. Dev Neurobiol 71:45-61.

Saiepour L, Fuchs C, Patrizi A, Sassoe-Pognetto M, Harvey RJ, Harvey K (2010) Complex role of collybistin and gephyrin in GABAA receptor clustering. J Biol Chem 285:29623-29631.

Saiyed T, Paarmann I, Schmitt B, Haeger S, Sola M, Schmalzing G, Weissenhorn W, Betz H (2007) Molecular basis of gephyrin clustering at inhibitory synapses: role of G- and E-domain interactions. J Biol Chem 282:5625-5632.

Sakagami H, Katsumata O, Hara Y, Tamaki H, Watanabe M, Harvey RJ, Fukaya M (2013) Distinct synaptic localization patterns of brefeldin A-resistant guanine nucleotide exchange factors BRAG2 and BRAG3 in the mouse retina. J Comp Neurol 521:860-876.

Sakagami H, Sanda M, Fukaya M, Miyazaki T, Sukegawa J, Yanagisawa T, Suzuki T, Fukunaga K, Watanabe M, Kondo H (2008) IQ-ArfGEF/BRAG1 is a guanine nucleotide exchange factor for Arf6 that interacts with PSD-95 at postsynaptic density of excitatory synapses. Neurosci Res 60:199-212.

Santy LC, Ravichandran KS, Casanova JE (2005) The DOCK180/Elmo complex couples ARNO-mediated Arf6 activation to the downstream activation of Rac1. Curr Biol 15:1749-1754.

Sassoe-Pognetto M, Panzanelli P, Sieghart W, Fritschy JM (2000) Colocalization of multiple GABA(A) receptor subtypes with gephyrin at postsynaptic sites. J Comp Neurol 420:481-498.

Sassoe-Pognetto M, Kirsch J, Grunert U, Greferath U, Fritschy JM, Mohler H, Betz H, Wassle H (1995) Colocalization of gephyrin and GABAA-receptor subunits in the rat retina. J Comp Neurol 357:1-14.

Sato S, Omori Y, Katoh K, Kondo M, Kanagawa M, Miyata K, Funabiki K, Koyasu T, Kajimura N, Miyoshi T, Sawai H, Kobayashi K, Tani A, Toda T, Usukura J, Tano Y, Fujikado T, Furukawa T (2008) Pikachurin, a dystroglycan ligand, is essential for photoreceptor ribbon synapse formation. Nat Neurosci 11:923-931.

Satz JS, Ostendorf AP, Hou S, Turner A, Kusano H, Lee JC, Turk R, Nguyen H, Ross-Barta SE, Westra S, Hoshi T, Moore SA, Campbell KP (2010) Distinct functions of glial and neuronal dystroglycan in the developing and adult mouse brain. J Neurosci 30:14560-14572.

Schafer MK, Varoqui H, Defamie N, Weihe E, Erickson JD (2002) Molecular cloning and functional identification of mouse vesicular glutamate transporter 3 and its expression in subsets of novel excitatory neurons. J Biol Chem 277:50734-50748.

Scholz R, Berberich S, Rathgeber L, Kolleker A, Kohr G, Kornau HC (2010) AMPA receptor signaling through BRAG2 and Arf6 critical for long-term synaptic depression. Neuron 66:768-780.

Schrader N, Kim EY, Winking J, Paulukat J, Schindelin H, Schwarz G (2004) Biochemical characterization of the high affinity binding between the glycine receptor and gephyrin. J Biol Chem 279:18733-18741.

Schuz A, Palm G (1989) Density of neurons and synapses in the cerebral cortex of the mouse. J Comp Neurol 286:442-455.

Schwab MH, Druffel-Augustin S, Gass P, Jung M, Klugmann M, Bartholomae A, Rossner MJ, Nave KA (1998) Neuronal basic helix-loop-helix proteins (NEX, neuroD, NDRF): spatiotemporal expression and targeted disruption of the NEX gene in transgenic mice. J Neurosci 18:1408-1418.

Schwarz G, Schrader N, Mendel RR, Hecht HJ, Schindelin H (2001) Crystal structures of human gephyrin and plant Cnx1 G domains: comparative analysis and functional implications. J Mol Biol 312:405-418.

Sekiguchi M, Zushida K, Yoshida M, Maekawa M, Kamichi S, Sahara Y, Yuasa S, Takeda S, Wada K (2009) A deficit of brain dystrophin impairs specific amygdala GABAergic transmission and enhances defensive behaviour in mice. Brain 132:124-135.

Serwanski DR, Miralles CP, Christie SB, Mehta AK, Li X, De Blas AL (2006) Synaptic and nonsynaptic localization of GABAA receptors containing the alpha5 subunit in the rat brain. J Comp Neurol 499:458-470.

Shepherd GM (2009) Symposium overview and historical perspective: dendrodendritic synapses: past, present, and future. Ann N Y Acad Sci 1170:215-223.

Shi L, Fu AK, Ip NY (2012) Molecular mechanisms underlying maturation and maintenance of the vertebrate neuromuscular junction. Trends Neurosci 35:441-453.

Shoubridge C et al. (2010) Mutations in the guanine nucleotide exchange factor gene IQSEC2 cause nonsyndromic intellectual disability. Nat Genet 42:486-488.

Simon J, Wakimoto H, Fujita N, Lalande M, Barnard EA (2004) Analysis of the set of GABA(A) receptor genes in the human genome. J Biol Chem 279:41422-41435.

Sola M, Kneussel M, Heck IS, Betz H, Weissenhorn W (2001) X-ray crystal structure of the trimeric N-terminal domain of gephyrin. J Biol Chem 276:25294-25301.

Sola M, Bavro VN, Timmins J, Franz T, Ricard-Blum S, Schoehn G, Ruigrok RW, Paarmann I, Saiyed T, O'Sullivan GA, Schmitt B, Betz H, Weissenhorn W (2004) Structural basis of dynamic glycine receptor clustering by gephyrin. Embo J 23:2510-2519.

Someya A, Sata M, Takeda K, Pacheco-Rodriguez G, Ferrans VJ, Moss J, Vaughan M (2001) ARF-GEP(100), a guanine nucleotide-exchange protein for ADP-ribosylation factor 6. Proc Natl Acad Sci U S A 98:2413-2418.

Somogyi J, Baude A, Omori Y, Shimizu H, El Mestikawy S, Fukaya M, Shigemoto R, Watanabe M, Somogyi P (2004) GABAergic basket cells expressing cholecystokinin contain vesicular glutamate transporter type 3 (VGLUT3) in their synaptic terminals in hippocampus and isocortex of the rat. Eur J Neurosci 19:552-569.

Specht CG, Izeddin I, Rodriguez PC, El Beheiry M, Rostaing P, Darzacq X, Dahan M, Triller A (2013) Quantitative Nanoscopy of Inhibitory Synapses: Counting Gephyrin Molecules and Receptor Binding Sites. Neuron 79:308-321.

Stensrud MJ, Sogn CJ, Gundersen V (2015) Immunogold characteristics of VGLUT3-positive GABAergic nerve terminals suggest corelease of glutamate. J Comp Neurol 523:2698-2713.

Stensrud MJ, Chaudhry FA, Leergaard TB, Bjaalie JG, Gundersen V (2013) Vesicular glutamate transporter-3 in the rodent brain: vesicular colocalization with vesicular gamma-aminobutyric acid transporter. J Comp Neurol 521:3042-3056.

Sugita S, Saito F, Tang J, Satz J, Campbell K, Sudhof TC (2001) A stoichiometric complex of neurexins and dystroglycan in brain. J Cell Biol 154:435-445.

Sugiyama J, Bowen DC, Hall ZW (1994) Dystroglycan binds nerve and muscle agrin. Neuron 13:103-115.

Sumita K, Sato Y, Iida J, Kawata A, Hamano M, Hirabayashi S, Ohno K, Peles E, Hata Y (2007) Synaptic scaffolding molecule (S-SCAM) membrane-associated guanylate kinase with inverted organization (MAGI)-2 is associated with cell adhesion molecules at inhibitory synapses in rat hippocampal neurons. J Neurochem 100:154-166.

Taniguchi H, He M, Wu P, Kim S, Paik R, Sugino K, Kvitsiani D, Fu Y, Lu J, Lin Y, Miyoshi G, Shima Y, Fishell G, Nelson SB, Huang ZJ (2011) A resource of Cre driver lines for genetic targeting of GABAergic neurons in cerebral cortex. Neuron 71:995-1013.

Taylor PJ, Betts GA, Maroulis S, Gilissen C, Pedersen RL, Mowat DR, Johnston HM, Buckley MF (2010) Dystrophin gene mutation location and the risk of cognitive impairment in Duchenne muscular dystrophy. PLoS One 5:e8803.

Tian M, Jacobson C, Gee SH, Campbell KP, Carbonetto S, Jucker M (1996) Dystroglycan in the cerebellum is a laminin alpha 2-chain binding protein at the glial-vascular interface and is expressed in Purkinje cells. Eur J Neurosci 8:2739-2747.

Tissir F, Bar I, Jossin Y, De Backer O, Goffinet AM (2005) Protocadherin Celsr3 is crucial in axonal tract development. Nat Neurosci 8:451-457.

Tran Mau-Them F, Willems M, Albrecht B, Sanchez E, Puechberty J, Endele S, Schneider A, Ruiz Pallares N, Missirian C, Rivier F, Girard M, Holder M, Manouvrier S, Touitou I, Lefort G, Sarda P, Moncla A, Drunat S, Wieczorek D, Genevieve D (2014) Expanding the phenotype of IQSEC2 mutations: truncating mutations in severe intellectual disability. Eur J Hum Genet 22:289-292.

Traunmuller L, Gomez AM, Nguyen TM, Scheiffele P (2016) Control of neuronal synapse specification by a highly dedicated alternative splicing program. Science 352:982-986.

Trinidad JC, Specht CG, Thalhammer A, Schoepfer R, Burlingame AL (2006) Comprehensive identification of phosphorylation sites in postsynaptic density preparations. Mol Cell Proteomics 5:914-922.

Tukker JJ, Fuentealba P, Hartwich K, Somogyi P, Klausberger T (2007) Cell type-specific tuning of hippocampal interneuron firing during gamma oscillations in vivo. J Neurosci 27:8184-8189.

Tyagarajan SK, Fritschy JM (2014) Gephyrin: a master regulator of neuronal function? Nat Rev Neurosci 15:141-156.

Tyagarajan SK, Ghosh H, Yevenes GE, Imanishi SY, Zeilhofer HU, Gerrits B, Fritschy JM (2013) Extracellular signal-regulated kinase and glycogen synthase kinase 3beta regulate gephyrin postsynaptic aggregation and GABAergic synaptic function in a calpain-dependent mechanism. J Biol Chem 288:9634-9647.

Tyagarajan SK, Ghosh H, Yevenes GE, Nikonenko I, Ebeling C, Schwerdel C, Sidler C, Zeilhofer HU, Gerrits B, Muller D, Fritschy JM (2011) Regulation of GABAergic synapse formation and plasticity by GSK3beta-dependent phosphorylation of gephyrin. Proc Natl Acad Sci U S A 108:379-384.

Tyzio R, Represa A, Jorquera I, Ben-Ari Y, Gozlan H, Aniksztejn L (1999) The establishment of GABAergic and glutamatergic synapses on CA1 pyramidal neurons is sequential and correlates with the development of the apical dendrite. J Neurosci 19:10372-10382.

Um JW, Choii G, Park D, Kim D, Jeon S, Kang H, Mori T, Papadopoulos T, Yoo T, Lee Y, Kim E, Tabuchi K, Ko J (2016) IQ Motif and SEC7 Domain-containing Protein 3 (IQSEC3) Interacts with Gephyrin to Promote Inhibitory Synapse Formation. J Biol Chem 291:10119-10130.

Umemori H, Linhoff MW, Ornitz DM, Sanes JR (2004) FGF22 and its close relatives are presynaptic organizing molecules in the mammalian brain. Cell 118:257-270.

Vaillend C, Perronnet C, Ros C, Gruszczynski C, Goyenvalle A, Laroche S, Danos O, Garcia L, Peltekian E (2010) Rescue of a dystrophin-like protein by exon skipping in vivo restores GABAA-receptor clustering in the hippocampus of the mdx mouse. Mol Ther 18:1683-1688.

van Rijnsoever C, Sidler C, Fritschy JM (2005) Internalized GABA-receptor subunits are transferred to an intracellular pool associated with the postsynaptic density. Eur J Neurosci 21:327-338.

van Versendaal D, Rajendran R, Saiepour MH, Klooster J, Smit-Rigter L, Sommeijer JP, De Zeeuw CI, Hofer SB, Heimel JA, Levelt CN (2012) Elimination of inhibitory synapses is a major component of adult ocular dominance plasticity. Neuron 74:374-383.

Varoqueaux F, Aramuni G, Rawson RL, Mohrmann R, Missler M, Gottmann K, Zhang W, Sudhof TC, Brose N (2006) Neuroligins determine synapse maturation and function. Neuron 51:741-754.

Verhage M, Maia AS, Plomp JJ, Brussaard AB, Heeroma JH, Vermeer H, Toonen RF, Hammer RE, van den Berg TK, Missler M, Geuze HJ, Sudhof TC (2000) Synaptic assembly of the brain in the absence of neurotransmitter secretion. Science 287:864-869.

Waite A, Brown SC, Blake DJ (2012) The dystrophin-glycoprotein complex in brain development and disease. Trends Neurosci 35:487-496.

Whissell PD, Cajanding JD, Fogel N, Kim JC (2015) Comparative density of CCK- and PV-GABA cells within the cortex and hippocampus. Front Neuroanat 9:124.

Wierenga CJ, Becker N, Bonhoeffer T (2008) GABAergic synapses are formed without the involvement of dendritic protrusions. Nat Neurosci 11:1044-1052.

Williamson RA, Henry MD, Daniels KJ, Hrstka RF, Lee JC, Sunada Y, Ibraghimov-Beskrovnaya O, Campbell KP (1997) Dystroglycan is essential for early embryonic development: disruption of Reichert's membrane in Dag1-null mice. Hum Mol Genet 6:831-841.

Witke W, Podtelejnikov AV, Di Nardo A, Sutherland JD, Gurniak CB, Dotti C, Mann M (1998) In mouse brain profilin I and profilin II associate with regulators of the endocytic pathway and actin assembly. Embo J 17:967-976.

Woo J, Kwon SK, Nam J, Choi S, Takahashi H, Krueger D, Park J, Lee Y, Bae JY, Lee D, Ko J, Kim H, Kim MH, Bae YC, Chang S, Craig AM, Kim E (2013) The adhesion protein IgSF9b is coupled to neuroligin 2 via S-SCAM to promote inhibitory synapse development. J Cell Biol 201:929-944.

Wright KM, Lyon K, Ginty D (2015) Dystroglycan is a critical regulator of forebrain connectivity. Int J Devl Neuroscience 47:117.

Wright KM, Lyon KA, Leung H, Leahy DJ, Ma L, Ginty DD (2012) Dystroglycan organizes axon guidance cue localization and axonal pathfinding. Neuron 76:931-944.

Wyeth MS, Zhang N, Mody I, Houser CR (2010) Selective reduction of cholecystokinin-positive basket cell innervation in a model of temporal lobe epilepsy. J Neurosci 30:8993-9006.

Yamada H, Saito F, Fukuta-Ohi H, Zhong D, Hase A, Arai K, Okuyama A, Maekawa R, Shimizu T, Matsumura K (2001) Processing of beta-dystroglycan by matrix metalloproteinase disrupts the link between the extracellular matrix and cell membrane via the dystroglycan complex. Hum Mol Genet 10:1563-1569.

Yang XD, Korn H, Faber DS (1990) Long-term potentiation of electrotonic coupling at mixed synapses. Nature 348:542-545.

Yao Y, Chen ZL, Norris EH, Strickland S (2014) Astrocytic laminin regulates pericyte differentiation and maintains blood brain barrier integrity. Nat Commun 5:3413.

Yin HL, Janmey PA (2003) Phosphoinositide regulation of the actin cytoskeleton. Annu Rev Physiol 65:761-789.

Yu YC, He S, Chen S, Fu Y, Brown KN, Yao XH, Ma J, Gao KP, Sosinsky GE, Huang K, Shi SH (2012) Preferential electrical coupling regulates neocortical lineage-dependent microcircuit assembly. Nature 486:113-117.

Zaccaria ML, Di Tommaso F, Brancaccio A, Paggi P, Petrucci TC (2001) Dystroglycan distribution in adult mouse brain: a light and electron microscopy study. Neuroscience 104:311-324.

Zhou L, Bar I, Achouri Y, Campbell K, De Backer O, Hebert JM, Jones K, Kessaris N, de Rouvroit CL, O'Leary D, Richardson WD, Goffinet AM, Tissir F (2008) Early forebrain wiring: genetic dissection using conditional Celsr3 mutant mice. Science 320:946-949.

APPENDIX

Abbreviations

5-HT3aR	5-hydroxytryptamine 3a receptor
AAV	adeno-associated virus
ACSF	artificial cerebrospinal fluid
AMPA	α-amino-3-hydroxy-5-methyl-4-isoxazolepropionic acid
AP2	adaptor protein 2
Arf	ADP ribosylation factor
BRAG	brefeldin A-resistant Arf-GEF
CA	constitutively active
CA1	cornu ammonis 1
CaMKII	Ca^{2+}/calmodulin-dependent protein kinase II
CB1	cannabinoid receptor 1
CCh	carbachol
CCK	cholecystokinin
Celsr3	cadherin EGF LAG seven-pass G-type receptor 3
CGE	caudal ganglionic eminence
cKO	conditional knock-out
CMD	congenital muscular dystrophy
CNS	central nervous system
DG	dystroglycan
DGC	dystrophin-glycoprotein complex
DMD	Duchenne muscular dystrophy
DN	dominant negative
DSI	depolarization-induced suppression of inhibition
ECM	extracellular matrix
eGFP	enhanced green fluorescent protein
ER	endoplasmic reticulum
ERK1	extracellular signal-regulated kinase 1
FISH	fluorescence *in situ* hybridization
GABA	γ-aminobutyric acid
$GABA_AR$	GABA type A receptor
GABARAP	$GABA_A$R-associated protein
GAD	glutamic acid decarboxylase
GAP	GTPase activating protein

GEF	guanine nucleotide exchange factor
GFAP	glial fibrillary acidic protein
GlyR	glycine receptor
GODZ	Golgi-specific DHHC zinc finger protein
GSK3β	glycogen synthase kinase 3β
GTP	guanosine triphosphate
HEK293	human embryonic kidney 293
ID	intellectual disability
IgSF9b	immunoglobulin superfamily member 9b
IP	immunoprecipitation
IQSEC	IQ motif and Sec7 domain
kDa	kilodalton
KI	knock-in
KO	knock-out
LARGE	like-acetylglucosaminyltransferase
LFP	local field potential
LNS	laminin-alpha, neurexin and sex hormone-binding globulin
LTD	long-term depression
LTP	long-term potentiation
mAChR	muscarinic acetylcholine receptor
MDGA	MAM domain-containing GPI anchor protein
MGE	medial ganglionic eminence
MOR	μ-opioid receptor
mRNA	messenger RNA
nAChR	nicotinic acetylcholine receptor
NL	neuroligin
NMDA	N-methyl-D-aspartate
NMJ	neuromuscular junction
NPAS4	neuronal PAS domain protein 4
PBS	phosphate-buffered saline
PCR	polymerase chain reaction
PIP2	phosphatidylinositol bisphosphate
PKA	protein kinase A
PKC	protein kinase C
PNS	peripheral nervous system
PRIP1/2	phospholipase C-related catalytically inactive proteins 1 and 2
PSD	postsynaptic density

PSD-95	postsynaptic density protein 95
PTM	post-translational modification
PV	parvalbumin
qPCR	quantitative PCR
Rac1	Ras-related C3 botulinum toxin substrate 1
RGC	radial glial cell
SH3	Src homology 3
sIPSC	spontaneous inhibitory postsynaptic current
SLM	Sam68-like mammalian protein
SS	splice site
SST	somatostatin
S-SCAM	synaptic scaffolding molecule
SUMO	small ubiquitin-like modifier
VGAT	vesicular GABA transporter
VGluT	vesicular glutamate transporter
VIP	vasoactive intestinal polypeptide

Curriculum vitae

Last name:	Früh
First name:	Simon
Date of birth:	September 24, 1985
Place of birth:	Frauenfeld, Switzerland
Home address:	Schaffhauserstrasse 408, 8050 Zürich
Nationality:	Swiss

Education:

2000 – 2004	**Matura** Kantonsschule Frauenfeld (biological/chemical curriculum)
2005 – 2009	**Bachelor of Science UZH in Biology**
2009 – 2011	**Master of Science UZH in Biology, Neurosciences** Institute of Molecular Life Sciences, UZH Thesis: *Excitatory Amino Acid Transporters in the Zebrafish Retina* (Supervisor: Prof. Stephan Neuhauss)
2012 – 2016	**PhD thesis** Institute of Pharmacology and Toxicology, UZH (Supervisor: Prof. Jean-Marc Fritschy) Recipient of the UZH Candoc Forschungskredit grant (2012)

Teaching:

November – December 2013	Supervision of research project of Daniela Bürgisser Pharmaceutical Sciences, ETH
February – August 2014	Supervision of Master thesis of Daniela Bürgisser Pharmaceutical Sciences, ETH Thesis: *Role of the dystrophin-glycoprotein complex for regulation of GABAergic synapses in the mouse hippocampus*

Administrative academic positions:

2010 – 2011	Representative of Master students at the Institute of Molecular Life Sciences, UZH

Publications

Peer-reviewed original articles

Früh S, Romanos J, Panzanelli P, Bürgisser D, Tyagarajan SK, Campbell KP, Santello M, Fritschy JM (2016) Neuronal dystroglycan is necessary for formation and maintenance of functional CCK-positive basket cell terminals on pyramidal cells. J Neurosci, accepted.

Früh S, Tyagarajan SK, Bosshard G, Fritschy JM (2016) The catalytic function of the gephyrin-binding protein synArfGEF regulates neurotransmitter-specific matching of pre- and postsynaptic structures in primary hippocampal cultures. In preparation.

Panzanelli P, Früh S, Fritschy JM (2016) Differential role of $GABA_A$ receptors and neuroligin 2 for perisomatic postsynaptic density formation in the hippocampus. In preparation.

Abstracts for posters

Panzanelli P, Früh S, Tyagarajan SK, Fritschy JM (2012) Impaired clustering of the dystrophin-protein complex at GABAergic synapses of CA1 pyramidal cells in neuroligin-2 deficient mice. 42nd Annual Meeting of the Society for Neuroscience, New Orleans, LA, USA.

Früh S, Panzanelli P, Tyagarajan SK, Fritschy JM (2013) The role of dystrophin-associated proteins in GABAergic synapse formation and plasticity. 17th Annual Meeting of the Swiss Society for Neuroscience, Geneva, Switzerland.

Früh S, Panzanelli P, Tyagarajan SK, Fritschy JM (2013) The role of dystrophin-associated proteins in GABAergic synapse formation and plasticity. Mechanisms of GABAergic synaptic plasticity, Chexbres, Switzerland.

Früh S, Panzanelli P, Tyagarajan SK, Fritschy JM (2013) The role of dystrophin-associated proteins in GABAergic synapse formation and plasticity. Gordon Research Conference, Les Diablerets, Switzerland.

Früh S, Bürgisser D, Panzanelli P, Tyagarajan SK, Fritschy JM (2014) The role of dystrophin-associated proteins in GABAergic synapse formation and plasticity. 9th FENS Forum of Neuroscience, Milan, Italy.

Früh S, Bürgisser D, Panzanelli P, Tyagarajan SK, Fritschy JM (2014) The role of dystrophin-associated proteins in GABAergic synapse formation and plasticity. 17th ZNZ Symposium, Zürich, Switzerland.

Früh S, Bürgisser D, Panzanelli P, Tyagarajan SK, Fritschy JM (2015) The role of dystrophin-associated proteins in GABAergic synapse formation and plasticity. 19th Annual Meeting of the Swiss Society for Neuroscience, Fribourg, Switzerland.

Früh S, Tyagarajan SK, Fritschy JM (2015) The gephyrin-interacting protein synArfGEF regulates mismatched GABAergic synapses in primary hippocampal neurons. 18th ZNZ Symposium, Zürich, Switzerland.

Früh S, Tyagarajan SK, Fritschy JM (2015) The gephyrin-interacting protein synArfGEF regulates mismatched GABAergic synapses in primary hippocampal neurons. 45th Annual Meeting of the Society for Neuroscience, Chicago, IL, USA.

Früh S, Tyagarajan SK, Fritschy JM (2016) The gephyrin-interacting protein synArfGEF regulates mismatched GABAergic synapses in primary hippocampal neurons. 20th Annual Meeting of the Swiss Society for Neuroscience, Lausanne, Switzerland.

Declaration of originality

University of Zurich[UZH]

Institute of Pharmacology and Toxicology

Declaration of originality

The signed declaration of originality is a component of every Master's thesis, PhD thesis and any other degree paper undertaken during the course of studies, including the respective electronic versions.

Lecturers may also require a declaration of originality for other written papers compiled for their courses.

I hereby confirm that I am the sole author of the written work here enclosed and that I have compiled it in my own words. Parts excepted are corrections of form and content by the supervisor.

Title of work (in block letters):

Postsynaptic molecular determinants of synapse specificity in the GABAergic neurotransmitter system

Authored by (in block letters):

For papers written by groups the names of all authors are required.

Name(s):	**First name(s):**
Früh	Simon

With my signature I confirm that

- I have committed none of the forms of plagiarism described in the information sheet issued on 30 April 2007 by the Teaching Committee of the University of Zurich.
- I have documented all methods, data and processes truthfully.
- I have not manipulated any data.
- I have mentioned all persons who were significant facilitators of the work.

I am aware that the work may be screened electronically for plagiarism.

Place, date	**Signature(s)**
Zürich, 5.9.2016	

Adapted from the Declaration of originality of the ETH Zürich

For papers written by groups the names of all authors are required. Their signatures collectively guarantee the entire content of the written paper.

Acknowledgements

I would like to thank everybody who helped me successfully accomplish my PhD.

I thank Prof. Dr. Jean-Marc Fritschy for his supervision, support and for giving me the opportunity to perform my PhD in his research unit at the Institute of Pharmacology and Toxicology. When I applied for a PhD student position in your lab, the lack of an open position did not hinder you from supporting me in my ambitions. You offered me the opportunity to write a research proposal for the Candoc Forschungskredit grant in your lab, which would finance the first year of my PhD. Even before we received the news that the application was successful, you decided to employ me as a doctoral student. This trust was inspiring and motivating for me until the end of the thesis. I would like to thank you for the continuous support, supervision and guidance throughout my thesis. Your style of supervision, guiding my PhD thesis while still granting me scientific freedom, was very motivating and a great lesson for me in learning how to lead a project. I am thankful to have learned many things about science, the work in a lab and about leading a group from you.

I thank the additional members of my PhD thesis committee, Prof. Dr. Stephan Neuhauss and Prof. Dr. Peter Scheiffele. Your critical feedback about my projects inspired many crucial experiments and helped guiding my PhD thesis.

I thank Dr. Shiva Tyagarajan for support, help and critical feedback throughout my PhD. You introduced me to many techniques used in the lab and helped guiding my projects. Your input about molecular aspects of my projects was especially crucial. Furthermore, I would like to thank you for sharing your knowledge and offering ideas in the Journal Club, and for always being open to my questions.

I am grateful to Daniela Bürgisser, who performed an excellent Master thesis on a project related to my PhD thesis. Supervising you was a great pleasure and your work was very important to my PhD and for being able to publish our data.

Further, I would like to thank Dr. Patrizia Panzanelli for support, collaboration and scientific discussions. Your support and generous help was crucial to my thesis and collaborating with you was a great pleasure.

I would like to thank Dr. Mirko Santello and Jennifer Romanos for a fantastic collaboration. You agreed to collaborate on my project although we had limited time until publication of the data. I

learned many things from your crucial experiments but also from your kind support of my project as well as from your way of working together.

I am grateful to Dr. Tatjana Haenggi, Dr. Nicole Wildner-Verhey and Cornelia Schwerdel for genotyping and support during my PhD thesis.

I would like to thank Giovanna Bosshard, who has contributed greatly to many experiments by preparing primary cultures and by further supporting the lab.

I would like to thank all former and present students in the lab for their help and support. Especially, I would like to thank Dr. Dennis Mircsof, Dr. Claire de Groot, Dr. Francine Deprez, Dr. Tina Notter and Dr. Sandra Pfister for help during the beginning of my PhD and Tilo Gschwind for help with stereotactic injections.

I am thankful to Christina Köster-Hegmann, Tim Gfeller, Dr. Lukas Rambousek, Dr. Tatjana Haenggi and Dr. Edith Schneider-Gasser for their great company in the office and for scientific discussions.

Finally, I would like to thank my loved ones, especially my parents, who were part of the inspiration to do a PhD.